

**PATHOGENESIS OF GLOMERULAR SCLEROSIS
IN THE FAWN-HOODED RAT**

PATHOGENESE VAN GLOMERULAIRE SCLEROSE
IN DE FAWN-HOODED RAT

PATHOGENESIS OF GLOMERULAR SCLEROSIS IN THE FAWN-HOODED RAT

PATHOGENESE VAN GLOMERULAIRE SCLEROSE
IN DE FAWN-HOODED RAT

PROEFSCHRIFT

ter verkrijging van de graad van doctor
aan de Erasmus Universiteit Rotterdam
op gezag van de rector magnificus
Prof. Dr. P.W.C. Akkermans M.A.
en volgens het besluit van het College voor Promoties.
De openbare verdediging zal plaats vinden op
woensdag 21 december 1994 om 15.45 uur.

door

JACOB LEVIE SIMONS

geboren te Rotterdam

PROMOTIECOMMISSIE

Promotor: Prof. Dr. J.C. Molenaar

Co-promotor: Dr. A.P. Provoost

Overige leden: Prof. Dr. M.A.D.H. Schalekamp

Prof. Dr. H.A. Koomans, Universiteit van Utrecht

Prof. Dr. J.J. Weening, Universiteit van Amsterdam

The studies presented in this thesis were financially supported by the Dutch Kidney Foundation (Grant C88.804 and C90.95.957A) and the National Institutes of Health (DK P01-40839, DK-08720 and DK-41641).

The publication of this thesis was financially supported by the Dutch Kidney Foundation.

This thesis was printed by PASMANS Offsetdrukkerij bv, Den Haag.

Aan Mama, Papa, Enikö, Bram, Philip en Louis.

CONTENTS

PART I: GENERAL INTRODUCTION

1	INTRODUCTION	
1.1	Progression of Renal Disease	1
1.2	Focal and Segmental Glomerular Sclerosis	1
1.3	Experimental Models	2
2	THE FAWN-HOODED RAT	
2.1	Origin	5
2.2	Glomerular Sclerosis and Proteinuria	5
2.3	Systemic Hypertension	11
2.4	Bleeding Diathesis	13
2.5	Pulmonary Hypertension and Vessel Wall Abnormalities	14
2.6	Behavioral and Neuropharmacologic Characteristics	14
2.7	Conclusions	15
2.8	Specific Aims and Study Design	16

PART II: MATERIALS AND METHODS

3	TECHNIQUES	
3.1	Experimental Animals	21
3.2	Nephrectomy	21
3.3	Functional Studies	21
3.4	Glomerular Hemodynamics	22
3.4.1	Animal Preparation and Microcirculatory Studies	22
3.4.2	Analytic Procedures	26
3.5	Experimental Histopathology of the Kidney	26
3.6	Glomerular Permselectivity	28
3.6.1	Fractional Clearance Measurements	28
3.6.2	Calculation of Sieving Coefficients	28
3.6.3	Sieving Data Analysis	29
3.6.4	Calculation of r^* for the Lognormal plus Shunt Model	30
3.6.5	Estimation of Glomerular Hydraulic Pressure from Sieving Data	31
4	EVALUATION APPLIED TECHNIQUES	
4.1	Micropuncture	33
4.2	Glomerular Morphology	38

4.2.1	Glomerular Sclerosis	38
4.2.2	Glomerular Tuft Volume	39
4.2.3	Stereology	41
4.3	Glomerular Permselectivity	44

PART III: EXPERIMENTS

5	Pathogenesis of Glomerular Injury in the Fawn-Hooded Rat: Early Glomerular Capillary Hypertension Predicts Glomerular Sclerosis <i>Adapted from: J Am Soc Nephrol 3:1775-1782, 1993</i>	51
6	Pathogenesis of Glomerular Injury in the Fawn-Hooded Rat: Effect of Unilateral Nephrectomy <i>Adapted from: J Am Soc Nephrol 4:1362-1370, 1993</i>	65
7	Modulation of Glomerular Hypertension Defines Susceptibility to Progressive Glomerular Injury <i>Adapted from: Kidney Int 46:396-404, 1994</i>	77
8	Proteinuria and Impaired Glomerular Permselectivity in Uninephrectomized Fawn-Hooded Rats <i>Adapted from: Am J Physiol 1994 (in press)</i>	93
9	Estimation of Glomerular Transcapillary Hydraulic Pressure in the Rat from Sieving Curves <i>Manuscript in Preparation</i>	109
10	Ultrastructural Observations in Glomeruli of Fawn-Hooded (FHH) Rats	123

PART IV: GENERAL DISCUSSION

11	Summary	135
12	General Discussion and Conclusions	137
13	Summary in Dutch (Samenvatting)	145
14	References	147
15	Dankwoord	177
16	Curriculum Vitae	179

ABBREVIATIONS

ACEI	angiotensin I converting enzyme inhibition
\bar{A}_G	mean glomerular random cross-sectional area
Ang II	angiotensin II
Å	angstrom (10^{-10} m)
BP	blood pressure
bw	body weight
C_A	afferent arteriolar plasma protein concentration
C_E	efferent arteriolar plasma protein concentration
C_{SF}	systemic arterial plasma protein concentration during \bar{P}_{SF} measurement
CON	untreated control animal group
CRF	chronic renal failure
DM	diabetes mellitus
EABF	efferent arteriolar blood flow
ENA	rats treated with enalapril, an ACEI
ERBF	effective renal blood flow
ERPF	effective renal plasma flow
ESRD	end stage renal disease
FF	filtration fraction
FH	fawn-hooded rat strain
FHH	fawn-hooded rat substrain with highest susceptibility for progressive glomerular injury, proteinuria and elevation of blood pressure
FHL	fawn-hooded rat substrain with lowest susceptibility for progressive glomerular injury, proteinuria and elevation of blood pressure
FSA	total available glomerular filtration surface area for an organism or whole kidney
FSGS	focal and segmental glomerular sclerosis
GBF	blood flow rate per single afferent arteriole
GBM	glomerular basement membrane
GFR	glomerular filtration rate
Hct	hematocrit
HRP	horseradish peroxidase
ip	intraperitoneal
iv	intravenous
k	effective hydraulic permeability of the glomerular capillary wall
k_0	true hydraulic permeability of the glomerular capillary wall

K_f	glomerular capillary ultrafiltration coefficient ($= k \cdot S$)
K_F	total available K_f for an organism or whole kidney $K_f (= k \cdot FSA)$
kw	kidney weight
MAP	mean arterial blood pressure
MHS	Milan hypertensive rat strain
MNS	Milan normotensive rat strain
MW	Munich-Wistar rat strain
MWF/Ztm	Munich-Wistar Fromter rat strain
NAME	rats treated with N^W -nitro L-arginine methyl ester, a NO synthase inhibitor
NO	nitric oxide
NPX	renal ablation resulting in a remnant kidney
NX	uninephrectomy (removal of a single kidney)
PAH	para-aminohippurate
PAS	periodic acid-Schiff reagent
$\overline{\Delta P}$	mean glomerular transcapillary hydraulic pressure
$\overline{P_E}$	mean efferent arteriolar hydraulic pressure
$\overline{P_{GC}}$	mean glomerular capillary hydraulic pressure
$\overline{P_{SF}}$	mean proximal tubular hydraulic stop-flow pressure
$\overline{P_T}$	mean proximal free-flow tubular hydraulic pressure
$\overline{P_{UF}}$	net mean local ultrafiltration pressure
$\overline{P_{UF-A}}$	afferent net ultrafiltration pressure
$\overline{P_{UF-E}}$	efferent net ultrafiltration pressure
Q_A	initial glomerular capillary plasma flow rate
R_A	resistance per single afferent arteriole
R_E	resistance per single efferent arteriole
r_s	Stokes-Einstein radius (\AA)
$r^* (1\%)$	pore size such that 1% of the filtrate passes through the pores with $r > r^*$
R_T	total arteriolar resistance for a single pre- to post- glomerular vascular unit
RVR	whole kidney renal vascular resistance
S	surface area available for filtration in a single glomerulus
SBP _e	experimental systolic arterial pressure
SBP _{tc}	awake systolic blood pressure assessed by indirect tail-cuff plethysmography
SD	Sprague-Dawley rat strain
SHR	spontaneously hypertensive rat strain
SN	single nephron
SNFF	single nephron filtration fraction
SNGFR	single nephron glomerular filtration rate

TGF	tubuloglomerular-feedback
TxA ₂	thromboxane
2K	two kidney rat or "intact" rat
U _a V	urinary albumin excretion per 24h
U _p V	urinary protein excretion per 24h
\bar{V}_G	mean glomerular tuft volume
WAG	Wistar Albino Glaxo rat strain
WK	whole kidney
WKY	Wistar-Kyoto rat strain
Θ	sieving coefficient
π_A	afferent arteriolar oncotic pressure
π_T	tubular oncotic pressure
π_E	efferent arteriolar oncotic pressure
ω_0	shunt parameter

PART I:
GENERAL INTRODUCTION

1 INTRODUCTION

1.1 Progression of Renal Disease

Loss of functioning nephron units is often followed by further loss of renal function even when the initial injurious agent has been removed. Not infrequently chronic renal failure (CRF) is the final outcome. In this process, focal and segmental glomerular sclerosis (FSGS) was recognized and described by various authors (63, 118, 172, 421, 435). Glomerulosclerosis was found to be associated with aging (117, 181, 202, 203, 272, 273), hypertension (196), and minimal change disease or lipid nephrosis (168, 372). Today, FSGS is interpreted as a rather nonspecific renal response to injury and is clinically manifested by hypertension, nephrotic syndrome with relatively nonselective proteinuria, microscopic hematuria, frequent corticosteroid resistance, and progressive CRF (168, 297, 318, 365, 418). Although the lesion is rather nonspecific, it stands at the center of the concept that regardless of the etiology of the initial renal insult, the primary loss of functioning nephrons leads to further loss of renal function over time (51, 365). In this response, various risk factors have been identified including reduction in nephron number, either congenital (216, 271, 380) or acquired (162, 233, 327, 375, 469), renal transplantation (52, 57, 64, 77, 245, 334), high protein diet (56), diabetes mellitus (270), hypertension (65, 82, 374), and genetic factors (123, 417) among others (297, 364, 365). The experimental identification of mechanisms involved in this vicious cycle has resulted in improvement in patient management and prognosis (218, 246).

1.2 Focal and Segmental Glomerular Sclerosis

The early and distinctive structural features of FSGS include scarring in some but not all the glomeruli (focal) and in only a portion of the glomerular tuft (segmental) (297, 318, 362, 365, 397). As glomerular injury progresses, the lesion eventually affects the tuft globally. The so called "classic" glomerular scar in FSGS consists of collapsed glomerular capillaries with a relative sparseness of normal cell elements, adhesions between the glomerular capillary tuft and the capsule of Bowman, and hyaline and lipid deposits. By light microscopy, the apparently uninvolved areas of the glomerular tuft are usually described as relatively normal. Additional nondiagnostic light microscopic changes may include segmental and global mesangial hypercellularity, endocapillary foam cells, vascular sclerosis, and tubulointerstitial disease with tubule atrophy and nonspecific interstitial inflammatory cell infiltration. Although obvious proliferative changes are not observed, hypertrophy of podocytes can often be appreciated. An additional important histological finding in progressive renal disease is the heterogeneity among nephrons in size and in apparent functional histologic integrity (365).

The earliest changes of FSGS can best be detected with the use of electron microscopy (169). With this device, separation of endothelial cells from the glomerular basement membrane, platelet thrombi formation, hyalinosis, epithelial foot process fusion and bleb formation with separation of these cells from the glomerular basement membrane, increased mesangial matrix, and microaneurysm formation can be seen. The visceral epithelial cells, the podocytes, invariably show degenerative changes (364).

1.3 Experimental Models

Investigators in the first half of this century used different diets to induce a so called "chronic nephritis" in experimental animals, and identified the renal damaging effect of dietary protein in intact animals (41, 274, 307, 393), rats with surgically reduced renal mass (3, 290), and in rats with induced nephrotoxic nephritis (120). Chanutin and Ferris showed that surgical removal of three fourths of the renal mass in rats led to a syndrome of albuminuria, hypertension, polyuria and progressive glomerular sclerosis which resulted in uremic death (75). Renal functional studies revealed the marked acute and chronic renal vasodilatory response to dietary protein, which was not observed with fats or carbohydrates (241, 400, 457). In animals with reduced renal mass, a similar vasodilatory state with whole kidney and single-nephron hyperfiltration was observed (3, 61, 92, 150, 166, 167, 293, 294, 335, 413, 438), in which the degree of hyperfiltration correlated with the amount of renal tissue removed (206). This led to the formulation that single-nephron hyperfiltration might be responsible for progressive renal injury in both experimental and human conditions of CRF (293, 294, 401). Brenner and coworkers further explored the hemodynamic basis of glomerular injury, and isolated glomerular capillary hypertension as a prerequisite for progressive glomerular injury in numerous experimental models (51, 56). Studies were performed in Munich-Wistar (MW) rats, a unique strain with glomeruli situated on the renal cortical surface accessible for direct micropuncture of the glomerular capillary tuft lumina (58). The examined models included various degrees of renal ablation (11, 13, 92, 179, 277), desoxycorticosterone-salt (112) or glucocorticoid induced hypertension (138, 139), streptozotocin induced diabetes mellitus in intact (14, 180, 464, 466) and in uninephrectomized rats (12), variation in hematocrit (137, 235), and experimental glomerulonephritis and nephrosis (9, 99, 249).

Low protein diet (178, 179, 277) and angiotensin I converting enzyme inhibition (ACEI) (11-13, 138, 139, 276, 464, 466) in several of the above mentioned models showed that progressive proteinuria and CRF can be delayed and often prevented. The protective action of these therapies is through lowering the mean intraglomerular capillary hydraulic pressure (\bar{P}_{GC}) (11-13, 138, 139, 179, 276, 464, 466) probably by modulating angiotensin II (Ang II) activity (234, 269, 328, 379, 406). The glomerular and systemic

hemodynamic effects of Ang II have been studied in detail and support the above concept of glomerular injury and proteinuria (44, 186, 289, 463). Chronic studies on the influence of dietary protein on the renin-angiotensin system further exemplify the link between protein feeding, glomerular hypertension and injury (32, 378, 406, 426, 457), as have studies of that system in diabetes (10).

Age-dependent progressive glomerulosclerosis has been described in various rat strains including the Wistar and Sprague-Dawley (SD) rat (5, 34, 41, 47, 79, 81, 114, 151, 152, 448), and in other non-human species (157, 195). On the other hand, a remarkable resistance to develop FSGS has been observed in several rat strains, including the Wistar Kyoto (WKY) rat (39, 121, 122, 451), the normotensive PVG/c rat (155), and the ACI/NMs rat (265), as was reviewed recently (440, 448). In susceptible strains, a male preponderance to develop FSGS is frequently present and has been linked with different functional and pathogenetic mechanisms (467). In this respect, a defective glomerular protein permeability and single-nephron hyperfiltration (359), reduced glomerular density and single-nephron hyperfiltration (163), lower total vascular resistance per glomerulus (296), loss of fixed glomerular polyanion (27), increased glomerular mRNA for procollagen $\alpha 1(\text{IV})$ (247), and the effects of sex hormones (387) have been described.

The association between systemic hypertension and renal failure was observed over a century ago (259) and numerous animal models with either spontaneous or induced hypertension have been studied to date (262). It is thought that systemic hypertension only results in glomerular injury if the high pressure reaches the glomerular capillary network (305). This was recently demonstrated in a Wistar Kyoto (WKY) rat remnant kidney model (39). Aging Milan normotensive (MNS) rats but not Milan hypertensive (MHS) rats have progressive FSGS and proteinuria, probably because of higher afferent arteriolar resistance in the MHS rats due to structurally different interlobular arteries (50) and a higher sensitivity of the tubuloglomerular feedback (330). Spontaneously hypertensive (SHR) rats develop renal lesions and proteinuria only with advanced age (121, 122). This process is accelerated after uninephrectomy as a result of increased \overline{P}_{GC} (108). Antihypertensive therapy, protein restriction, or a low salt diet protect the remaining kidney after such a procedure (33, 108, 109, 111). Subtotal renal ablation combined with a high salt diet induce malignant hypertension with rapidly progressive glomerular injury in these animals (205). In young Dahl-salt-sensitive rats, a high salt diet elevates systemic blood pressure and aggravates the genetic renal disease (410). Renal ablation in this strain magnifies the genetic predisposition for hypertension and glomerular injury (38), which is prevented by therapy with an ACEI (420). Hypertensive and normotensive WKY rats have similar values for \overline{P}_{GC} and glomerular scarring because of high arteriolar resistance's in the hypertensive animals (24). Hypertension, proteinuria and glomerular injury induced by

desoxycorticosterone acetate injection with dietary salt supplementation and renal ablation is not halted when glomerular hypertension persists (110). Various models of renal artery clip induced hypertension and renal injury have been reported including the two-kidney two-clip hypertension model with removal of one of the clips at different time intervals (302), the two-kidney one-clip model (23, 398, 408), and a modification of the latter, the aortic ligature model (376). The glomeruli in the clipped kidney are generally protected from hypertension (398) and FSGS (320), and to a great extent from the damaging effects of superimposed diabetes (266, 456), glomerulonephritis (170, 262), and puromycin aminonucleoside nephrosis (6). ACEI in these Goldblatt models invariably results in lowering of \overline{P}_{GC} and in renal protection (171, 283). An alternative to these renal artery clipping methods is renal micro-sphere embolization resulting in focal glomerular ischemia (288). The differences in glomerular hemodynamic and histologic responses to renal surgical ablation vs. infarction have been described (154, 278), as has the potential role of renal ischemia on renal disease progression (291). Chronic blockade of endothelial-derived relaxing factor results in systemic and glomerular hypertension and progressive FSGS in previously normal rats (28), which can be aggravated by additional renal ablation (134) and dietary salt overload (135).

Other models include the obese and non-obese Zucker rat (204, 396), and adriamycin (153) and puromycin aminonucleoside (9, 148) induced glomerulopathy.

In several of the above mentioned experimental models it has been observed that damage to or altered behavior of certain glomerular cell populations or glomerular compartments is associated with the initiation and progression of the scarring process. Changes in the interaction of glomerular cells with the extracellular matrix have been implicated in this process (124, 453). Primary epithelial cell stress resulting in hypertrophy, injury and failure with possible focal podocyte detachments from the GBM (132, 201, 214, 224, 298, 363), mesangial (164, 223, 349) or endothelial changes (412, 427), macrophage activation (149) and other immune related responses (113), GBM expansion (225) and altered GBM deposition and composition (373) have been mentioned. Involvement of the tubulointerstitial compartment in progressive glomerular injury (99, 321) in addition to lipid abnormalities (98, 149), alterations in intraglomerular coagulation (35, 199, 322, 382, 468), and changes in the hormonal environment (119, 275, 422, 458) have all been studied. Glomerular growth and hypertrophy have been associated with progressive glomerular injury, and indicators of growth and growth factors are being investigated to further unravel the scarring process (125-128, 190, 232, 364). Modifications of the complex anatomical relationship within the glomerular tuft (80, 299, 309, 347), glomerular macromolecular permselectivity changes (358, 360) and the damaging effects of proteinuria have been studied (455).

2 THE FAWN-HOODED RAT

2.1 Origin

The fawn-hooded rat appeared as a mutant from unplanned cross breeding of various populations of laboratory rats of uncertain genealogy at the Department of Psychology of the University of Michigan, Ann Arbor (256, 350, 425). The German-brown rat, the white Lashley rat, and the Wistar and Long-Evans rat strains have been mentioned as putative ancestors (31, 419, 425). The fawn color is the result of color change induced by an autosomal recessive red-eyed dilution gene on an agouti background (337), and not the product of a specific fawn color gene (243). The origin, generation of various strains, and genealogy of the FH rat were reviewed recently (226, 256, 338, 341). The original FH strain from the University of Michigan was introduced by W. Jean Dodds into the animal breeding facilities of the New York State Department of Health in the early 1970's and has been maintained as an inbred strain by brother-sister mating (FH/Wjd) (256, 350, 428). The original FH strain from the University of Michigan was also transferred to the American Museum of National History in New York at about the same time and remained randomly bred. Tschopp introduced the FH strain from the National History Museum in Europe and this strain was kept outbred at the Institute for Biological and Medical Research, Fullinsdorf, Switzerland. This Swiss colony provided the breeding nucleus for the colony kept at Unilever Research Laboratories, Vlaardingem, The Netherlands, where this strain was maintained outbred until 1990 (FH/URL). Spontaneous systemic hypertension was noted in the FH/URL rats in 1981 (227). Subsequently, two strains of inbred FH/URL rats were developed based on differences in awake blood pressure and urinary protein excretion (341). These strains were transferred to the animal facilities of Erasmus University, Rotterdam (EUR), The Netherlands in 1990 and named FHH/EUR for the strain with the highest values for blood pressure and proteinuria and FHL/EUR for the strain with the lowest values for blood pressure and proteinuria (341). FHH/EUR rats showed fastest development of chronic renal failure. Genetic homogeneity within each strain regarding the histocompatibility haplotype was confirmed in the 15th generation by skin transplantation tests. The FHH/EUR and FHL/EUR rats were bred by brother-sister mating. For convenience, FHH/EUR and FHL/EUR rat strains are referred to as FHH and FHL in the subsequent chapters.

2.2 Glomerular Sclerosis and Proteinuria

As discussed previously in Section 1.3, various rat strains develop FSGS and proteinuria spontaneously. However, the rate of progression of these lesions varies greatly among strains. FH rats present with FSGS and proteinuria early in life, and these increase

further in a progressive fashion with aging. Detailed structural studies were done by: Kreisberg and Karnovsky (222), Urizar *et al.* (428), and Kuijpers and Gruys (228).

The first to describe FSGS in FH rats were Kreisberg and Karnovsky in 1978 in the FH/Wjd strain. (222). They observed a marked difference in the development of the lesion between male and female rats. Fifty percent of four month old males had proteinuria (U_pV) in excess of 10 mg per 24 hours, whereas none of the females had significant U_pV (mean: 0.6 mg/24h). At age 12 months, all males excreted more than 45 mg protein per 24 hours (mean: 69 mg/24h) while females had only mild U_pV (mean: 7 mg/24h). Other observations included a normal blood urea nitrogen (BUN) level, absence of hematuria, and heart weights similar to controls (Charles River CD rats). Light microscopy showed no established FSGS up to six months of age. At that time, a mild increase in mesangial periodic acid-Schiff reagent (PAS) positive material was seen, and some tubules contained luminal protein casts. Kidneys from 12 month old male rats revealed > 70% FSGS involving two or more lobules, and some sclerotic areas adherent to Bowman's capsule. An interstitial mononuclear cell infiltrate was seen in some areas and tubular protein casts were common. Glomeruli with FSGS were randomly distributed in the renal cortex, with no preferential localization to the juxtamedullary area. Histochemical staining for amyloid was negative. In contrast to male rats, female rats did not show marked pathologic changes up to age 12 months, the end-point of the study. Electron microscopic examination revealed loss of interdigitating glomerular epithelial cell foot processes and replacement by flattened epithelial cytoplasm. This was the first morphological change and was present in all six month old male rats. Concomitantly, large cytoplasmic vacuoles were seen in the podocytes with electron-lucent or electron-dense material. Denuded areas of glomerular basement membrane (GBM) were occasionally present adjacent to such a large cytoplasmic vacuole in an overlying epithelial cell. They observed that with a greater degree of podocyte injury the amount of U_pV increased. Thickening, folding, and whorling of the GBM was seen. At age 12 months, lesions were more advanced in male rats, and denudation of the GBM was pronounced. Intra- and extracellular lipid inclusions were seen in areas of sclerosis. Female rats with proteinuria at 12 months of age showed fusion of visceral epithelial foot processes only. Colloidal iron staining of glomerular polyanion was done by the method of Nicolson (308). Superficial glomerular capillaries were selected from the tissue blocks to avoid false negative staining, and penetration of the stain was confirmed by the presence of iron stained erythrocytes. Focal loss of glomerular polyanion from the endothelium, GBM, and podocyte glycocalyx was seen at six months in male rats, which correlated positively with the amount of U_pV . Loss of charge was sometimes observed even before fusion of epithelial foot processes. Positive mesangial immunofluorescent staining for IgG, IgM, and

sometimes C3 was seen at six months of age, and at 12 months of age these deposits were seen in areas of sclerosis. This positive staining at 12 months of age was accompanied by positive immune staining for albumin and fibrinogen. These observations suggested that nonspecific trapping of proteins was the most likely cause of the positive immunofluorescent staining and not the result of an *in vivo* immune mediated response. This conclusion was further supported by the morphological observation that electron-dense material was only rarely seen in mesangial areas, and that subepithelial dense-deposits were never present. IgA staining was absent, and serum examined for circulating immune complexes was negative in 6 and 12 month old rats. This led to the general conclusion that glomerular epithelial cell injury is the key to progressive glomerular injury and proteinuria in FH rats.

Urizar and coworkers performed detailed structural studies and showed that the congenital hemostatic abnormalities (discussed in Section 2.4) did not change with age (428). Studies were done in male and female FH/Wjd rats. Light microscopy in young (two to four months old) FH rats showed segmental mesangial hyperplasia with increased argyrophilia, peripheral expansion, patent lumens, and normal GBM. Older FH rats (more than one year old) exhibited greater argyrophilia and thickened, wrinkled and laminated GBM. Hyalinized glomeruli adherent to the Bowman's capsule, and nonhyalinized enlarged glomeruli with peripheral mesangial interposition and distended capillary lumina were seen. Interstitial and periarteriolar mononuclear and polymorphonuclear inflammatory infiltrates, and tubular atrophy with cystic like change of the tubules were appreciated. Diffuse segmental granular mesangial and hilar deposits of IgM were seen, and in older FH animals IgG staining was increased. Staining for C3 was minimal or absent, and fibrinogen-fibrin appeared in the glomerular mesangium and hili at low intensity in a granular or non descript pattern. Interstitial infiltrates stained positively for IgM and occasionally for IgG. Positive staining for factor VIII:Ag (von Willebrand factor: vWF) was seen in all FH rat specimens at mild intensity in a clumpy nodular mesangial and capillary pattern in young animals. This antigen was seen in capillary endothelium and occasionally in the extracapillary spaces, presumably the podocytes. Older animals showed brighter clumps of fluorescence in mesangial lesions and a smeared nodular fluorescence along capillary walls. This pattern correlated with the areas with argyrophilic aggregates and electron densities on electron microscopy. Endothelial lining of the peritubular capillaries and the arterioles stained positive for vWF. Immunofluorescence for fibronectin stained predominantly the glomerular capillaries, Bowman's capsule and tubular basement membranes in both FH and Wistar controls. Segmental glomerular fluorescence of fibronectin was seen in older FH rats, which correlated with the histopathological changes of FSGS. When glomeruli were completely sclerosed, fibronectin became less intense or

negative. Electron microscopy showed swollen, spongy endothelial and epithelial cells, which occluded many capillaries and showed foot process fusion, respectively. The subendothelial spaces were loosely packed with granular electron dense material, which resulted in separation of the cells from the GBM. These lesions advanced with age in FH rats, and mesangial expansion and glomerular sclerosis were maximal at 12 to 16 months of age. Patchy tubulointerstitial nephritis, some cystic structures, and thickened collagenized tubular basement membranes were seen. The GBM thickness increased with age (200-225 nm at two to six months and \pm 400 nm at 12 to 16 months; Wistar control: 285 nm at all ages), and structurally became ragged, folded, duplicated, or laminated. These investigators thought that the early mesangial lesions were significant for the development of FSGS in FH rats. It should be stated however that the earliest microscopic evaluation was at two to four months of age. At that time mesangial hyperplasia and epithelial foot process fusion were seen concomitantly. Independent of age and sex, rat immunoglobulins (mainly IgG and IgM) were seen in a granular and nodular pattern. The intensity of immunofluorescence staining was related directly to the severity of lesions in aged rats. The increased mesangial deposits of fibrinogen-fibrin, vWF, fibronectin, IgG and IgM in diseased glomeruli were thought to indicate a persistent low-grade inflammation leading to progressive glomerulopathy. In addition, they suggested that deposition of these molecules enhanced the sclerotic process by coagulation activation. Reasons for the activation included GBM alterations with collagen exposure. Why these immunoglobulins were seen in young animals without changes compatible with FSGS was explained by simple trapping of proteins. Thus, the final route of glomerular injury and subsequent FSGS proposed by Urizar *et al.* consisted of early functional and/or structural mesangial and GBM lesions with exposure of collagen, Hageman factor and coagulation activation, causing deposition of molecules observed by immunofluorescence. However, the cause of the early mesangial and GBM lesions remained unsolved. A few animals had circulating immune complexes. The glomerular lesions however did not resemble that of immune complex mediated disease, and these complexes were thought to be probably not significant for the observed glomerular injury. They speculated that the platelet serotonin release defect could be part of a more generalized metabolic disorder involving behavior, renin release, kallikrein production, blood pressure control, and the progressive glomerulopathy. The difference between female and male rats of the FH/Wjd strain for susceptibility to develop FSGS could not be explained by such a metabolic disarray. The authors suggested therefore a protective effect of estrogens or, alternatively an injurious role for androgens. The exposed collagen as seen on ultrastructural examination can explain the increased immunofluorescence staining for C3 and vWF through activation of the usual pathways of coagulation, kinin, and complement systems (194). The endothelium appeared spongy with

many vacuoles and occlusions of the capillary lumina. Alterations in the endothelium may promote vWF expression, platelet aggregation, and coagulation. The podocytes had a similar vacuolated appearance with foot process fusion. Thus, although not specifically indicated by Urizar *et al.*, relative failure of the endothelium and epithelium were probably present in these rats. It remains to be solved whether those changes were due to altered glomerular hemodynamics or that hereditary factors are responsible. The latter option is certainly possible in this strain. The congenital bleeding diathesis which is related to a deficiency of platelet dense granules is similar as found in the Chediak-Higashi syndrome (37, 282). In this syndrome varying additional deficiencies are present which are due to cellular lysosomal defects. To explain the pronounced difference in progression of glomerular lesions between male and female FH rats by such a lysosomal defect is difficult because the hereditary platelet defect is present in both sexes. Since platelets are defective in FH rats, fibrin clot formation is probably less optimal. However, the platelet lesion does not preclude that fibrin deposition may be important in the development of FSGS in these animals. This view is supported by a recent study by Magro *et al.* who showed that FH platelets with defective ATP secretion aggregate and generate thromboxane (TxB₂) upon stimulation with collagen in plasma, but not as effectively as platelets from control Wistar rats (255). When collagen-stimulated in whole blood, FH platelet function improves significantly. An incidental finding was the relatively high base line TxB₂ production in FH platelets when studied in a whole blood assay. The FH/Wjd rats studied were three to four months old. Von Willebrand factor is known to be produced by vascular endothelium and megakaryocytes. Whether the observed deposition of vWF is due to platelet adhesion, increased binding of circulating vWF, or due to local production and matrix deposition by the endothelium is not clear. It is known that increasing subendothelial vWF concentrations improve adhesion of platelets (212, 386). The result of the vWF immunofluorescent staining may therefore imply the presence of an active platelet adhesion process to the injured endothelium or to the extracellular matrix.

Kuijpers and Gruys noted early FSGS with occasional hyalinosis in two month old FH/URL rats, whereas three to five week old animals were free of such light microscopic lesions (228). These outbred FH/URL rats were the direct ancestors of the inbred FHH/EUR and FHL/EUR rat strains used in the experiments described in this thesis. Electron microscopy, first done at two months of age, showed increased mesangial matrix, thickening and occasional splitting of the GBM, and local or diffuse epithelial foot process loss. In some areas, numerous electron-dense granules were seen in both podocytes and mesangial cells. These granules corresponded with the PAS and phosphotungstic acid-hematoxylin (PTAH) positive hyaline droplets seen on light microscopy, thus probably representing carbohydrates and fibrin, respectively. Electron-dense deposits suggestive of

immune complex accumulation were not found. At three weeks of age no positive immunofluorescent staining was seen, and at five weeks of age a fine granular deposition of IgA and IgG in the mesangium of some glomeruli was noted. In older animals great variations in the immune staining pattern were seen. Fibrinogen, IgG, IgA, IgM, C3 were found in a segmental pattern along the capillary walls and/or mesangial areas. End-stage kidneys showed glomerular deposits and tubular casts with immunoglobulins, C3 and fibrinogen, indicative of plasma leakage. The authors concluded that mesangial cell dysfunction and increased permeability of the glomerular capillary wall were probably present in FH rats, and suggested that these alterations played some role in the pathogenesis of FSGS in these animals. FH rat serum tested for anti-ds-DNA antibodies was negative.

De Keijzer, Provoost and Molenaar were the first to study renal function along with the spontaneous proteinuria. They found that GFR was significantly higher in 12 week old FH/URL rats compared with age and weight matched control Wistar rats, whereas ERPF was similar among groups (209). The number of glomeruli in FH rats ($32,598 \pm 3,799$) was comparable to that in Wistar rats ($32,729 \pm 5,971$). Glomerular count was assessed by injecting India ink into the aorta and counting five 50 μ l aliquots of macerated kidney under a microscope. These observations indicated that the average GFR per glomerulus in FH rats was 33% higher than in Wistar animals, and suggested that in FH rats hyperfiltration was present on single-nephron level. The increased urinary protein excretion together with the glomerular hyperfiltration were thought to be the result of glomerular capillary hypertension. De Keijzer *et al.* noted that the level of U_pV at 10 weeks of age determined the subsequent development of renal failure, i.e. the greater the amount of U_pV at that age, the faster the decline in GFR with time (210). Life long feeding of a low (12%) protein diet attenuated the development of U_pV and renal failure in FH/URL rats, but did not prevent it (207). High (36%) protein diet caused a marked increase in U_pV and initially higher GFR. After one year however, GFR declined progressively and animals died early of renal failure (mean survival time in weeks: 81 ± 20 with the 36% protein diet vs. 102 ± 21 with the 12% protein diet). Of note, approximately 40 weeks after the initiation of the various diets the systemic hypertension was higher in animals on the protein restricted diet. Uninephrectomy was found to greatly accelerate renal functional deterioration in FH/URL rats (208).

The occurrence of FSGS and U_pV in two-kidney (2K) and uninephrectomized (NX, at age four months) outbred FH/URL rats was described by Westenend *et al.* (450). Proteinuria in 2K animals remained in the 100 mg/24h range over a seven month follow-up period whereas NX animals had progressive increases in U_pV up to a final level in the 500 to 600 mg/24h range. The incidence of FSGS (expressed in % of total population of

glomeruli) was increased in NX rats (2K vs. NX: 5 ± 3 vs. 37 ± 16), whereas SBP_{IC} (2K vs. NX: 130 ± 6 vs. 126 ± 13 mm Hg) and direct measured MAP (2K vs. NX: 143 ± 8 vs. 135 ± 9 mm Hg) were similar among groups. Sclerotic lesions were evenly distributed throughout the renal cortex. Kidney weight (2K vs. NX: 0.38 ± 0.05 vs. 0.52 ± 0.05 g/100 g bw) and glomerular volume calculated from the glomerular radius were increased after NX (2K vs. NX: 1.39 ± 0.25 vs. $1.86 \pm 0.25 \times 10^6 \mu\text{m}^3$). Renal functional studies showed whole kidney hyperfiltration (2K vs. NX: 0.28 ± 0.09 vs. 0.40 ± 0.07 ml/min/100 g bw) after NX with no alterations in RPF (2K vs. NX: 1.36 ± 0.44 vs. 1.65 ± 0.47 ml/min/100 g bw) and FF (2K vs. NX: 0.21 ± 0.07 vs. 0.25 ± 0.05). Values for urinary excretion of noradrenaline, dopamine and kallikrein were not different among groups. These investigators also studied the effects of long-term angiotensin I converting enzyme inhibition (ACEI) with captopril in 2K FH/URL rats and noted preservation of renal function with protection from FSGS (442, 449). Treatment with the serotonin receptor blocker ketanserin did not lower systemic hypertension, U_pV, and FSGS in FH rats, whereas GFR was increased by this drug (443). Glomerular tuft volume was unaltered by captopril or ketanserin.

An abnormal urinary eicosanoid excretion was noted which consisted of increases in urinary TxB₂, 6-keto-prostaglandin F_{1α} and prostaglandin-E₂ (211). A shift in the pattern of excretion from vasodilatory to vasoconstrictor eicosanoids was observed over time, which was accompanied by progressive proteinuria (211).

2.3 Systemic Hypertension

The spontaneous development of systemic hypertension has been reported in outbred FH/URL (227) and inbred FH/Wjd rats (381). The hypertension in FH/URL rats was not the result of selective inbreeding. Blood pressure in FH/URL animals was already increased at five weeks of age, increased steeply between ages five and seven months and a final level of approximately 200 mm Hg systolic was observed at one year of age (229). The ultimate level of systemic hypertension varied among animal litters and the level of U_pV varied in parallel. Thus rats with the highest blood pressure and U_pV (> 100 mg/24h) could be identified from those with lower levels for these parameters (231). Animals with the highest level of systemic hypertension had a higher mean daily water intake which could not be explained by increased food intake. Urine output was also higher in these rats. This increased daily water turnover was present around 7 to 11 weeks of age, the period during which systemic hypertension developed (229). Animal body weights were similar among groups. The level of systemic hypertension correlated positively with the weights of the heart, spleen, liver, kidney, and adrenal glands. Plasma renin activity correlated

positively only with heart weight (226). In a subsequent study, Kuijpers and De Jong demonstrated significant positive relationships between severity of FSGS and blood pressure ($r = 0.41$), severity of tubular protein casts and blood pressure ($r = 0.59$), and FSGS and tubular casts ($r = 0.62$), over a 48 week age range (230). Correlations calculated for the lesions present at the study end point showed r values for these associations of 0.65, 0.63, and 0.83, respectively.

The precise cause of the systemic hypertension remains speculative. Various abnormalities in FH rats have been described and may contribute. In 1982, Magro and Rudofsky reported the spontaneous decline in plasma renin activity at three to four months of age in male FH/Wjd rats (257). This occurred prior to the development of severe FSGS at six to eight months of age, and global sclerosis at 9 to 10 months of age. A similar but less accelerated pattern of renin decrease and development of FSGS over time was observed in female FH rats. Wistar rats served as controls and together with the data from the FH rats indicated a strong correlation between rate of decrease in plasma renin activity and development of FSGS with age. Renal renin activity declined around five to seven months of age in male FH rats, after the decline in plasma renin activity. Because specific β -adrenergic stimulation of renal renin release was diminished in male FH rats, the authors concluded that with adequate kidney stores of renin a decrease in secretory capacity of the chromaffin cells of the juxtaglomerular apparatus was the most likely reason for the decline in plasma renin activity. Ultrastructural studies of the juxta-glomerular apparatus were not done, but the demonstrated secretory abnormalities of platelets (350, 414, 425) and mast cells (254) in FH/Wjd rats supported the hypothesis of a cellular secretory disarray.

Others found a low urinary kallikrein excretion (145, 450), and an increased urinary catecholamine output (258, 450). Modulation of urinary kallikrein and plasma renin activity by low- and high salt diets did not alter systemic hypertension in 3.5 to 4.5 month old male FH/Wjd rats (146). Plasma renin activity and angiotensin II showed the usual responses to changes in salt intake. Proteinuria was increased by high salt diet (7 mg/24h), and lowered to similar levels as in non proteinuric control Wistar rats by low salt feeding (2 mg/24h) (146). Lithium clearance studies indicated that the fractional reabsorption of sodium and water in the proximal tubules is higher in FH/URL rats. Because the distal tubules compensated for the increased proximal sodium retention, the fractional excretion of sodium in the urine was similar as in controls (340).

Although glomerular counts are normal in FH/URL, FHH/EUR, and FHL/EUR rats (209, 341), a renal abnormality may be the cause of the hypertension. Transplant studies in FH rats have not been performed to date, but such studies in other rat strains clearly indicate that hypertension is transferable (36, 129, 221, 368, 369). Strong evidence for a renal genetic defect in SHR rats to account for the systemic hypertension was recently

reported (389). A kidney with an abnormal glomerular filtration membrane requires increased perfusion pressure to maintain homeostasis for volume and electrolytes (158-160, 215). It is thought that the kidney is a major determinant of systemic blood pressure over long term by regulating the total available glomerular filtration surface area (FSA) (55, 158-160, 215). Nephron number in humans correlates with mean arterial blood pressure, i.e. the lower the count the higher the pressure (55, 165).

2.4 Bleeding Diathesis

A congenital hemorrhagic diathesis was the first major abnormality described in FH rats. The abnormal bleeding was observed during brain surgery experiments and affected both sexes (425). A defective platelet release pool of ATP, ADP and serotonin has been found to be associated with an abnormal bleeding time (425), and resembles the platelet defect observed with storage pool deficiency in humans (175, 176). Under normal conditions, this pool is released during platelet adhesion and aggregation. The defect was present in platelets emerging from the bone marrow several days after irradiation, possibly indicating that the platelet defect was not the result of premature release of the storage contents during their circulation in the blood (424). Kuijpers and Gruys reported the platelet disorder in approximately one month old weanling FH rats (226). Platelet counts, platelet volume, clot retraction and ADP-induced aggregation are normal while collagen-induced aggregation is disturbed. Stimulated release of ATP, ADP and serotonin is greatly reduced. Further description of the complex bleeding disorder was done by Raymond and Dodds (350). *In vivo* and *in vitro* defective platelet adhesion and adhesion induced aggregation is present similar as in patients with storage pool disease (423). Both the platelet uptake and release of serotonin are reduced (419). A platelet membrane glycoprotein defect possibly contributes to the bleeding diathesis (217), and a defective serotonin uptake in both platelets and cerebral cortex of fawn hooded rats has been described (17, 106, 411). Release of histamine from mast cells of FH rats is abnormal (254). Infusion of a liposome based platelet substitute could partially reduce the bleeding diathesis (385). The bleeding diathesis and the fawn color are pleiotropic effects of an autosomal recessive red-eyed dilution gene (337, 419). Lack of ATP secretion is associated with homozygosity of the red-eyed dilution gene (255).

In conclusion, a hereditary functional defect of platelets is present in these animals. This defect is most apparent when platelets are studied in plasma assays and stimulated with weak agents. Ultrastructural studies on the platelets of FH rats have been done by Sweeney and Needleman (414). These investigators observed dense-granule like structures by electron microscopy. According to these authors, the primary defect in FH rat platelets

involves defective serotonin storage and defective release of serotonin and ADP which is independent of arachidonic acid metabolism.

2.5 Pulmonary Hypertension and Vessel Wall Abnormalities

Spontaneous pulmonary hypertension was documented in 4 to 13 week old male and female FH rats, before the onset of systemic hypertension (213, 390). The marked pulmonary vascular remodeling was partly due to the environmental conditions associated with high altitude, since chronic administration of supplemental oxygen prevented the pulmonary abnormalities (391). Pulmonary hypertension could be transferred to offspring from cross breeding with Wistar Kyoto rats (391). Differences in the relative concentrations of platelet-derived mediators such as ADP and serotonin, as well as abnormal responses of the aortic and pulmonary artery walls to these mediators were found to promote systemic and pulmonary hypertension (19). Increased lung endothelin-1 production was demonstrated, but the stimulus and the cell responsible for the altered synthesis were not identified (409). A possible site of such a local endothelin-1 producer, the neuroepithelial body, has been identified in the airway of the FH rat (248). These densely innervated corpuscles can act as both endocrine gland and sensory receptor.

Wey *et al.* reported on the abnormal low conversion of arachidonic acid to 6-keto-prostaglandin- $F_{1\alpha}$ by FH rat aorta, which was stimulated by cholesterol feeding. Arachidonic acid induced aggregation of platelet rich plasma from FH rats was stimulated by cholesterol feeding, whereas collagen induced aggregation remained absent despite high cholesterol intake (452).

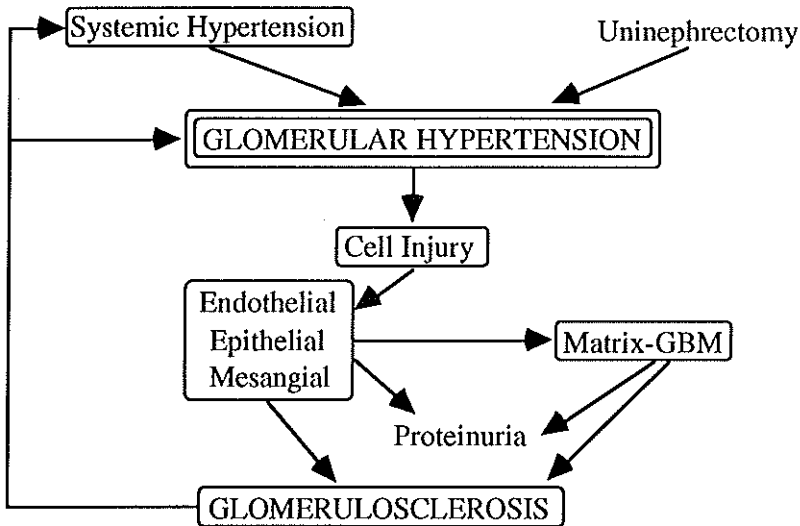
2.6 Behavioral and Neuropharmacologic Characteristics

An unusual docile nature and lower excitability have been observed in the FH rats. Abnormal brain serotonin and tryptophan metabolism have been suggested to explain this behavior (31, 197). The number of regional brain serotonin receptors, the activity of these receptors, and the affinity of serotonin uptake binding sites are all abnormal in FH rats (182, 183). This strain is used as a genetic model for some neuropsychiatric disorders in which a serotonergic dysfunction is thought to be present. These include depression (22, 324), and eating and alcohol intake dysregulation (86, 323, 324, 370, 371, 394, 395). The 5-hydroxytryptamine $_{1C}$ receptor is subsensitive to clonidine induced growth hormone (GH) release, but the base line GH levels in FH rats are similar to those in control Wistar rats (21). These findings might indicate that the FH rat is unable to regulate GH levels normally. Whether the occasionally observed increased body growth at a young age can be explained by this possible GH dysregulation or is due to other neurological or metabolic

abnormalities is unknown. Since GH levels are normal in FH rats, the latter options are more likely.

2.7 Conclusions

The FH rat has several lesions which appear at young age. The strong association between systemic blood pressure, U_pV , and subsequent FSGS indicates an important route for glomerular injury. Modulation of systemic blood pressure has been proven to alter the progression of CRF. Contributory or associated lesions include an abnormal prostaglandin balance, present in blood platelets, vessel walls, and reflected in urinary excretion. The abnormal platelet function may shift the balance of a normal fibrin-fibrinolysis system and may be associated with lysosomal defects in various other cell populations. The abnormal serotonin metabolism may reflect altered endothelial function and vessel wall reactivity. Alterations in the kinin-bradykinin system may promote tissue injury. However, these latter mentioned mechanisms do not explain for the rapid and early sclerosis of glomeruli, the specific structural and functional changes seen by various investigators, and the important differences among sexes in development of FSGS and U_pV in FH rats. Therefore, the pathway shown in the figure below is proposed. The key initiator in the cascade is glomerular capillary hypertension, which has been associated with glomerular injury (305, 364). In this plot, changes in the glomerular filtration barrier may contribute to systemic hypertension and uninephrectomy can increase mean glomerular capillary hydraulic pressure (\bar{P}_{GC}).



2.8 Specific Aims and Study Design

De Keijzer *et al.* showed that FH rats exhibit whole kidney hyperfiltration accompanied by normal effective renal plasma flow and a normal number of glomeruli (209). These authors postulated the presence of elevated \bar{P}_{GC} as the predominant cause of the hyperfiltration, U_pV and glomerular damage (209). In this thesis, we planned to establish the spontaneous occurrence of glomerular hypertension in FH rats. Therefore, we determined single glomerular pressures and flows, including \bar{P}_{GC} , single-nephron GFR, glomerular capillary ultrafiltration coefficient (K_f), and afferent (R_A) and efferent (R_E) arteriolar resistances in inbred FHH and FHL rats. Apart from basal conditions, glomerular hemodynamics were varied experimentally to further delineate the relationship between glomerular hemodynamics and injury. As glomerular size alterations and growth have been associated with the pathogenesis of FSGS, we measured glomerular tuft volume. To explain the early proteinuria in FHH rats, the permselectivity of the filtration barrier was studied. Glomerular electron microscopic studies were done in FHH rats to illustrate and discuss possible associations between alterations in ultrastructure, function and injury.

Experiment 1 (Chapter 5) was performed to test the hypothesis that FH rats have spontaneous glomerular hypertension. Wistar (WAG) rats, not prone to develop renal failure, were used as control animals (173). Different age and weight matched groups were created since at young age FHH animals were found to grow faster than FHL and WAG animals. The outcome of this experiment served as basis for further study.

The marked increases in U_pV and rate of decline in renal function over time after uninephrectomy (NX) were associated with increased whole kidney GFR (208). To further assess the glomerular microcirculatory and morphologic responses to NX in FHH rats, Experiment 2 (Chapter 6) was performed.

In Experiment 3 (Chapter 7) we modulated systemic blood pressure in NX FHH rats, in an attempt to alter \bar{P}_{GC} . Uninephrectomy was chosen to heighten the hemodynamic stresses on the glomeruli and, since ablation frequently induces glomerular growth, to further assess the importance of glomerular tuft size increases as a moderator in progressive FSGS in FHH rats.

In Experiment 4 (Chapter 8), we studied glomerular permselectivity in FHH rats to find an explanation for the early proteinuria observed in this strain. The results of these sieving experiments were used in Experiment 5 (Chapter 9) to analyze the potential value of such measurements to predict the transmembrane glomerular filtration pressure.

Electron microscopic views of FHH rat glomeruli from the various experimental groups were obtained. The ultrastructural findings were integrated with the results of the

previously performed experiments and possible routes contributing to glomerular injury were discussed (Chapter 10).

Before presenting the results of the different experiments, we first introduce the various applied materials and methods (Chapter 3) followed by an evaluation of these techniques (Chapter 4).

PART II:
MATERIALS AND METHODS

3 **TECHNIQUES**

3.1 **Experimental Animals**

Details on animal breeding are provided in Chapter 2.1. FHH and FHL rats generated during the 16th through 18th inbreeding cycle were used. Experimentation was performed at the Laboratory for Kidney and Electrolyte Physiology at the Brigham and Women's Hospital, Boston, Massachusetts, USA, except for the long-term functional studies described in Experiment 2 which were done at the Laboratory for Surgery at Erasmus University, Rotterdam, The Netherlands. Animals were shipped to Boston by plane at three to four weeks of age, and were allowed two to three weeks for adaptation before any experimental or functional study was performed. Animals were fed a similar *ad libitum* 24% protein rat chow as was provided in The Netherlands and received tap water *ad libitum*. Up to the time of final experimentation, chow and water were available for the animals. All animals were tested for parasites and viruses as required at the animal facilities of Erasmus University and Brigham and Women's Hospital. Infections were not identified. Animals were kept in a virus, parasite, and pathogen free over-flow air room. Inbred Wistar (WAG: Wistar Albino Glaxo strain) animals used in Experiment 1 were purchased from Harlan Sprague-Dawley, Zeist, The Netherlands. These animals develop only very minimal FSGS with aging [$< 2\%$ of glomeruli at 30 months of age (173)]. After arrival at Erasmus University, these control animals were treated similar as the FH rats, and after shipment to Boston, handled as described above for FH rats.

3.2 **Nephrectomy**

Uninephrectomized (NX) FHH rats were used in Experiments 2, 3, 4, 5, and 6. These animals were compared with sham operated controls with two-kidneys (2K). Surgery was performed with ethyl ether anesthesia. A midline abdominal incision was made, and the right kidney was removed after careful separation from the adrenal gland and associated connective tissue. In sham operated rats, the right kidney was gently manipulated but otherwise left intact.

3.3 **Functional Studies**

Indirect tail-cuff plethysmography was used to measure the systolic blood pressure (SBP_{tc}) in awake restrained animals. Urine was collected from individual rats in metabolic cages for one 24 hour period. Total urinary protein concentration was measured colorimetrically by precipitation with 3% sulfosalicylic acid (49). This protocol was followed for all U_pV measurements except for the assessment done in the long-term study

in Experiment 2. In that study, U_pV was estimated by collecting urine from individual rats during two successive 24 hour periods and measuring colorimetrically the concentration of a pyrogallol red molybdate complex (439). In that same study, GFR and effective RPF (ERPF) were determined in awake rats. This was done by measuring the plasma clearance of [^{51}Cr]-EDTA and [^{125}I]-iodohippurate, respectively, which was determined every six weeks. The method has been described in detail elsewhere (343). Briefly, from pentobarbital-anesthetized rats (60 mg/kg, ip), a single, timed blood sample was obtained 60 minutes after the iv injection of precounted amounts of the radioactive markers. The method allows for repeated measurements within the same animal. In plasma samples obtained during GFR measurement, the creatinine (P_{Cr}) and urea (P_{Ur}) levels were assessed by standard clinical chemical techniques as additional parameters for renal function. In Experiment 4, assessment of urinary albumin was measured by immunodiffusion (261).

3.4 Glomerular Hemodynamics

3.4.1 Animal Preparation and Micropuncture Studies

Rats were prepared and studies performed in the standard fashion for micropuncture (11). Therefore, after anesthesia was induced with ethyl ether, rats were placed on a temperature-regulated micropuncture table and subsequently given 5-sec-butyl-5-ethyl-2-thiobarbituric acid (Inactin) (BYK, Konstanz, Federal Republic of Germany) (100 mg/kg bw, ip). Temperature was monitored rectally and maintained at $37.0 \pm 0.5^{\circ}\text{C}$. After tracheostomy with a size 250 polyethylene catheter (PE-250; Clay Adams, Parsippany, New Jersey, USA), a left femoral artery catheter (PE-50; Clay Adams) was inserted to directly monitor arterial blood pressure and to obtain blood samples. Direct femoral mean arterial pressure (MAP) and experimental systolic arterial pressure (SBP_e) were monitored by means of a transducer (Statham Instruments; Model P23AA) connected to a direct-writing recorder (Hewlett-Packard Co.; Model 7702B). After a baseline blood sample was collected, the right jugular vein was cannulated (PE-50) for the infusion of plasma, inulin, and para-aminohippurate (PAH). For the studies described in Experiment 4, tritiated Ficoll was infused through an additional left jugular vein catheter (PE-50). The plasma volume of rats prepared for micropuncture is reduced by approximately 20% (252). In order to study the rats in an euolemic state, isoncotic plasma obtained from normal adult Sprague-Dawley rats was infused iv at a rate of 0.1 ml/min to a total amount equal to 1% of the bw. Thereafter, plasma infusion was continued at a rate of 0.58 ml/h, to maintain the hematocrit (Hct) stable. Inulin (10 g/dl for rats with two kidneys (2K), and 5 g/dl for uninephrectomized (NX) rats) in 0.9% NaCl, and PAH (0.8 g/dl for 2K rats, and 0.4 g/dl

for NX rats) in 0.9% NaCl was infused iv at a rate of 1.2 ml/h. The bladder was drained only in 2K rats (PE-50). The left kidney was exposed and suspended on a Lucite holder, with its surface illuminated and kept moist with isotonic saline. The left ureter was cannulated (PE-10; Clay Adams). A 60 minute equilibration period was allowed after completion of the 1% bw plasma infusion. Generally 20 to 30 minutes after the initiation of the plasma infusion, surgery was completed and a stable blood pressure was observed approximately 15 to 20 minutes before the end of the equilibration period and start of experimental sampling. Studies were usually completed within 2.5 to 3 hours after induction of anesthesia.

Micropuncture was performed under stereo microscopic control (x210). All sampling micropipettes were coated with silicon. For calculation of single-nephron (SN) GFR, four to six exactly timed (45 seconds to 2 minutes) samples of fluid were collected from superficial proximal tubules for the determination of flow rate and inulin concentration. Sharpened glass micropipettes with tip diameters of 8 to 12 μm were used. After injection of a three to four tubule diameters in length column of blue pigmented polymer oil into the lumen of a well functioning tubule segment, gentle controlled suction was applied to collect fluid and to maintain the oil in a relatively constant position just distal to the site of puncture (53, 54). Three to six efferent arteriolar blood samples were obtained from superficial star vessels for determination of protein concentration. These star vessels are surface vessels with relatively large diameters ($\sim 20 \mu\text{m}$) from which a typical radiating network of branching capillaries could readily be identified. Sharpened micropipettes with an outer tip diameter of 10 to 14 μm were introduced into the first-order branch of the efferent arteriole and then advanced to the center of the welling point. The welling point is the most superficial aspect of the efferent arteriole and is found just before first-order branches take off. A small amount of clear polymer oil was subsequently injected to block the first-order branches, and then blood was collected by applying gentle suction in order to keep the oil block stable. Coincident with these collections and the hydraulic pressure measurements, arterial blood samples (100 μl) were obtained for the determination of Hct and plasma concentrations of inulin, PAH, and total protein, and 10 to 20 minute urine collections from the left kidney were obtained for the determination of urinary flow rate, inulin, and PAH concentrations. These measurements permitted calculation of GFR, effective renal plasma flow rate (ERPF), filtration fraction (FF), effective renal blood flow (ERBF), and whole kidney renal vascular resistance (RVR) by standard formulae.

To assess glomerular hemodynamic pressures we used a continuous recording servo-null micropipette transducer system (Instrumentation for Physiology and Medicine, San Diego, California, USA; Model 5A) with 2 M NaCl containing sharpened micropipettes as the sensing arm of the Wheatstone bridge (outer tip diameters of 2 to 3

μm). Hydraulic output from the linear motor of the servo-null system was coupled electronically to a second channel of the Hewlett Packard recorder by means of a pressure transducer (P23Db; Statham Instruments). The servo-null system adjusts to very rapid changes in microvascular pressures and allows direct on-line recording of mean as well as pulsatile pressures (454). Accuracy, frequency response and stability features of this servo-null system as applied to the renal microcirculation have been described in detail by Brenner *et al.* (59). Since FH and WAG rats lack superficial glomeruli, time-averaged hydraulic pressures were measured in superficial proximal tubules under stop-flow conditions (\bar{P}_{SF}) as first described by Gertz *et al.* (143), and modified by Baylis *et al.* (26). The measurement of \bar{P}_{SF} allows for indirect calculation of the mean glomerular capillary hydraulic pressure (\bar{P}_{GC}). After interrupting the flow of filtrate in a tubule, glomerular filtration continues for approximately 30 to 40 seconds and then a new equilibrium of filtration forces is reached with zero net filtration. It is assumed that reabsorption of fluid in the blocked segment ceases, because stop-flow pressure in Bowman's space and proximal tubule were found to be equal (143). This suggests that there is no active filtration under blocked conditions. The Starling equation for glomerular ultrafiltration can now be solved:

$$SNGFR = K_f (\bar{P}_{GC} - \bar{P}_T) - (\pi_A - \pi_T) \quad (1)$$

Where \bar{P}_T is the mean free-flow tubular or mean Bowman's space pressure. Under stop-flow conditions \bar{P}_T becomes \bar{P}_{SF} . The calculation of \bar{P}_{GC} assumes tubular fluid to be protein-free and thus the oncotic pressure (π_T) is 0. Stop-flow indicates $SNGFR = 0$, and the glomerular capillary ultrafiltration coefficient (K_f) is equal to 1 with net zero filtration. π_A during stop-flow conditions was designated π_{SF} . Thus Equation 1 becomes:

$$0 = \bar{P}_{GC} - (\bar{P}_{SF} + \pi_{SF}) \quad (2)$$

and finally:

$$\bar{P}_{GC} = \bar{P}_{SF} + \pi_{SF} \quad (3)$$

Stop-flow conditions in proximal tubules were obtained by the injection of bone wax (W-31G; Ethicon) by means of a sharpened micropipette (outer tip diameter of 12 to 14 μm) connected to a hydraulic wax-blocking device (Research Instruments & Mfg., Corvallis, Oregon, USA). Obtained wax blocks were generally three to four tubular diameters in length. Blocked tubules were readily identified as they acquired a so called silver-shine appearance. Although some dilatation of blocked tubules generally occurred, those tubules with obvious ballooning were not used to assess \bar{P}_{SF} . Variations in pulsatile pressures in the blocked tubules were synchronous with those in the femoral arterial blood pressure tracings. This observation helped to ascertain that the \bar{P}_{SF} recordings were accurate, and if erroneous micropipette positioning occurred it was noted relatively early and corrected easily. At least three to four \bar{P}_{SF} recordings in different nephrons, with a minimum

duration of 2 to 4 minutes each, were obtained during each experiment and mean values were recorded. The mean transcapillary hydraulic pressure difference ($\Delta \bar{P}$) was calculated as:

$$\Delta \bar{P} = \bar{P}_{GC} - \bar{P}_T \quad (4)$$

where \bar{P}_T is the mean proximal free-flow tubular pressure as measured in four to six non obstructed proximal tubules. In addition, mean pressures were assessed directly in four to six efferent arterioles (\bar{P}_E) (59). These recordings were obtained by positioning the pressure pipette tip in the welling center of non obstructed efferent arterioles.

The colloid osmotic pressure of plasma entering and leaving glomerular capillaries was estimated from values for protein concentration in femoral arterial (representing afferent arteriolar) and efferent arteriolar plasma. Estimation of pre- (C_A) and post glomerular (C_E) protein concentration permit the calculation of single-nephron filtration fraction (SNFF):

$$SNFF = 1 - (C_A / C_E) \quad (5)$$

Femoral arterial plasma protein concentrations were measured separately during microsampling (C_A) and during micropressure measurement (C_{SP}). Afferent and efferent arteriolar resistances (R_A and R_E), glomerular capillary ultrafiltration coefficient (K_f), and initial glomerular capillary plasma flow rate (Q_A) were calculated by equations described by Deen *et al.* (97). Resistance per single afferent arteriole was:

$$R_A = [(MAP - \bar{P}_{GC}) / GBF] \cdot (7.962 \cdot 10^{10}) \quad (6)$$

where the factor $7.962 \cdot 10^{10}$ is used to give resistance in $\text{dyn} \cdot \text{s} \cdot \text{cm}^{-5}$ when MAP and \bar{P}_{GC} are expressed in mm Hg and blood flow rate per single afferent arteriole (GBF) in nl/min .

Resistance per single efferent arteriole was:

$$R_E = [(\bar{P}_{GC} - \bar{P}_E) / EABF] \cdot (7.962 \cdot 10^{10}) \quad (7)$$

Total arteriolar resistance for a single pre- to post glomerular vascular unit was:

$$R_T = R_A + R_E \quad (8)$$

Initial glomerular capillary plasma flow rate was:

$$Q_A = \text{SNGFR} / \text{SNFF} \quad (9)$$

Blood flow rate per single afferent arteriole was:

$$\text{GBF} = Q_A / (1 - \text{Hct}) \quad (10)$$

where Hct is taken from femoral arterial hematocrit and is assumed equal to afferent arteriolar blood Hct.

Efferent arteriolar blood flow rate was:

$$\text{EABF} = \text{GBF} - \text{SNGFR} \quad (11)$$

The K_f is the product of the effective hydraulic permeability of the glomerular capillary wall (k) and the surface area available for filtration in an individual glomerulus (S). K_f can be assessed by various techniques (251). By glomerular hemodynamic

assessment, K_f can be calculated using a differential equation which gives the rate of change of protein concentration (C) with distance (x) along an idealized glomerular capillary (97). The derivation of this equation (93) treats the glomerular capillary network as a rigid cylindrical tube of equivalent total surface area, impermeable to plasma proteins, and with Q_A and C dependent only on the axial coordinate x . Thus:

$$dC^*/dx^* = FC^{*2} (1 - A_1C^* - A_2C^{*2}) \quad (12)$$

where $C^* = C / C_A$, $0 \leq x^2 \leq 1$, and $F = K_f \cdot (\overline{\Delta P} / Q_A)$. F , A_1 , and A_2 are dimensionless parameters, and A_1 and A_2 are defined by $\overline{\Delta P}$ and C_A . K_f was then calculated on a single-nephron basis from group mean values of SNGFR, Q_A , C_A , and $\overline{\Delta P}$ (93).

3.4.2 Analytic Procedures

The volume of fluid collected from individual proximal tubules was estimated from the length of the fluid column in a constant bore capillary tube of known internal diameter. The tubule fluid inulin concentration was measured by a micro-fluorescence method (436). All microassays for the determination of SNGFR were performed within 48 hours after sample collection. SNGFR was calculated as:

$$SNGFR = (TF/P)_{In} \cdot V_{TF} \quad (13)$$

where $(TF/P)_{In}$ and V_{TF} refer to transtubular inulin concentration ratio and tubule fluid flow rate, respectively. Inulin concentrations in plasma and urine were measured using a macro-anthrone method (88, 133). PAH concentrations in plasma and urine were measured by the method of Chasis *et al.* (76). Protein concentrations (C) in efferent arteriolar blood samples and arterial blood were determined using a fluorometric method (433). Processing of these samples for determination of C were completed within 24 hours after collection. Protein oncotic pressures (π) were calculated with the equation:

$$\pi = 1.629 \cdot C + 0.2935 \cdot C^2 \quad (29, 93) \quad (14)$$

where C is in units of g/dl (valid over the range 4 to 10 g/dl) and π is in mm Hg.

3.5 Experimental Histopathology of the Kidney.

Animals designated for histopathologic evaluation were either anesthetized with inactin (100 mg/kg bw) during previous microcirculatory studies or acutely with sodium pentobarbital (50 mg/kg bw ip). Prior to this, the systolic blood pressure was measured either directly immediately before kidney perfusion during final micropuncture experimentation, or zero to two days prior to kidney perfusion by indirect tail-cuff plethysmography in animals in which no glomerular hemodynamics were assessed. Kidneys were perfusion fixed at the measured systolic arterial blood pressure for two to three minutes with 1.25% glutaraldehyde in 0.1 M sodium cacodylate buffer (pH 7.4). For

this, the abdominal aorta was cannulated at a point just cranial to the bifurcation of the common iliac vessels with a sharpened glass pipette of similar diameter as the aorta. A route of egress for the infused substances and blood was created by cutting the inferior vena cava immediately prior to start of fixation. Flow of fixative fluid into the thoracic aorta and main gastrointestinal vessels was prevented by placement of a silk tie around the aorta between the orifices of the superior mesenteric artery and the renal arteries. This ligature was tied off concurrently with the start of fixative perfusion. After in situ fixation, the kidney(s) were removed and kidney weight(s) noted after careful removal of excess soft tissue elements. The non-fixed heart was removed and its weight recorded. Two midcoronal slices, one of each kidney in rats with two kidneys (2K) and two from the left kidney in uninephrectomized (NX) animals, of 2 to 3 mm thickness, were processed for light microscopic examination.

The extend of glomerular damage was determined on paraffin sections (3 μm thick) stained with hematoxylin and eosin, and with periodic acid-Schiff reagent (PAS). On average 400 to 500 glomeruli were counted per animal, and these measurements included glomeruli over the entire thickness of the cortex. Glomerulosclerosis was defined as glomerular profiles with segmental or global collapse of capillaries, with or without associated hyalin deposition and adhesion of the tuft to Bowman's capsule. The extent of FSGS was expressed as the percentage of glomeruli with sclerotic lesions.

The average glomerular tuft volume (\bar{V}_G) for each animal was determined by the procedure described by Weibel (446). For this purpose, the mean glomerular random cross-sectional area (\bar{A}_G) was determined on approximately 50 systematically sampled glomerular tuft profiles by point counting at a final magnification of x200 with a 361-point ocular grid covering a 369,664 μm^2 microscopic field. \bar{V}_G was then calculated as $\bar{V}_G = (\beta/k)(\bar{A}_G)^{3/2}$, where $\beta = 1.38$ is the shape coefficient for spheres, the idealized shape of the glomerular tuft, and $k = 1.1$, is a size distribution coefficient (174, 446). The measurements were performed on all glomerular profiles present in several 2 μm thick Toluidine blue stained epoxy sections through the entire thickness of the renal cortex, insuring a balanced representation of cortical and juxtamedullary nephrons. Completely collapsed glomeruli were excluded from morphometric evaluation. The Toluidine blue stained plastic sections (2 μm) were used to obtain micrographs of representative glomeruli in Experiment 3 (Chapter 7).

For transmission electron microscopic evaluation, small pieces of perfusion fixed kidneys were postfixed in osmium tetroxide. Transmission electron microscopy was done following standard techniques described previously (441). At least four glomeruli were studied per animal with a final magnification ranging from 5,800x to 25,000x.

3.6 Glomerular Permselectivity

3.6.1 Fractional Clearance Measurements

An isotonic saline solution of tritiated Ficoll of broad molecular size distribution was prepared from unlabelled Ficoll (Pharmacia Fine Chemicals, Piscataway, New Jersey, USA) as previously described (315). The solution had a Ficoll concentration < 700 mg/dl and a specific activity of ~ 110 μ Ci/ml.

Immediately after completion of the micropuncture measurements, a 0.4 ml bolus of the tritiated Ficoll solution was infused iv over 1.5 minutes, followed immediately by a constant infusion of the same solution at a rate of 1.2 ml/hr. Ten to 15 minutes after the priming bolus, a continuous arterial blood collection was begun at a rate of 24 μ l/min for 15 - 20 minutes using a withdrawal pump (Harvard Apparatus Co., Millis, Massachusetts, USA; model 941). Urine collection from a ureteral catheter was initiated and terminated 1.5 minutes after the arterial blood collections to allow for the transit time from Bowman's space to the tip of the ureteral catheter.

The arterial sample was spun at 3000 revolutions/min in a refrigerated centrifuge (DuPont, Wilmington, Delaware, USA ; Sorvall model RT6000B) to remove cells, and 25- to 75- μ l aliquots of the supernatant were added to 1 ml of 2 mg/100 ml blue dextran (Sigma Chemical Co., St. Louis, Missouri, USA). Aliquots, 50 - 100 μ l, of urine were likewise added to blue dextran.

Labeled plasma or urine samples were drawn into a syringe. The empty vial was rinsed twice with a volume of 0.5 ml distilled water, and the rinsings were added to the sample. The total 2-ml volume was fractionated on a Sephacryl S-300 HR column (Pharmacia), which had been calibrated with narrow-molecular-weight Ficoll standards as described previously (315). The eluent buffer was 0.05 M ammonium acetate at pH 7. The samples were fractionated into 3-ml aliquots, each corresponding to a particular value of Stokes-Einstein radius (r_s) as determined by the calibration. Two milliliters from each aliquot was mixed with 4 ml of scintillation fluid (Packard Instrument Co., Inc., Downers Grove, Illinois, USA; Ultima Gold). Activity was measured in a scintillation counter (Packard Instrument Co.; Tri-Carb model 4530). On the basis of an analysis of the minimum significant activity above background, rates below 120 counts/min were rejected.

3.6.2 Calculation of Sieving Coefficients

The sieving coefficient (Θ) of a given molecule is the ratio of its concentration in Bowman's space to its concentration in arterial plasma water. Sieving coefficients for Ficoll were equivalent to fractional clearances, calculated as:

$$\Theta = [(U/P)_{\text{cpm}} / (U/P)_{\text{inulin}}] \times f \quad (1)$$

$$f = - 0.007895 \cdot C_A + 0.9916 \quad (2)$$

where $(U/P)_{\text{cpm}}$ is the urine-to-plasma ratio of scintillation counts per unit volume of sample, $(U/P)_{\text{inulin}}$ is the urine-to-plasma ratio of inulin concentration, and f is a plasma volume correction factor that accounts for the fact that the inulin plasma concentrations were measured in protein-free plasma water, whereas the labeled plasma samples contained protein. A typical value for f was 0.95. Finally, Θ was calculated at integer values of r_s by interpolation of the raw data (4).

3.6.3 Sieving Data Analysis

Membrane parameters were calculated from the sieving coefficients and hemodynamic data using a mathematical model previously described (91). In this model, the glomerular tuft is represented as a number of identical capillaries in parallel, and steady-state differential mass balance equations are used to describe the variations in plasma flow rate and solute concentration with axial position along a capillary. The capillary wall is assumed to be perforated by pores which allow the passage of water and solutes into Bowman's space. The sieving characteristics of the test molecule and capillary wall are described by the theory of hindered transport for ideal, spherical molecules passing through long, cylindrical membrane pores. The governing equations were formulated to accommodate any hypothetical pore-size distribution. Three alternative distributions were used to analyze the group-mean Ficoll sieving data.

The simplest pore-size used here envisions the glomerular barrier as consisting of many identical pores of radius r_0 along with a few pores of effectively infinite size that behave as a nonselective "shunt" through the barrier. The parameter ω_0 is the fraction of filtrate volume which would pass through the shunt in a hypothetical state of zero colloid osmotic pressure. This is termed the isoporous-plus-shunt model. In the second approach, the lognormal model, the pore radius (r) is assumed to follow a lognormal probability distribution (91, 352) with parameters u and s . The mean pore radius is u and the pore-size distribution has a standard deviation equal to $\ln(s)$. The third approach, the lognormal-plus-shunt model, assumes a lognormal distribution in parallel with a nonselective shunt and is described by the parameters u , s , and ω_0 (315).

The pore-size parameters were computed by fitting the theoretical model to the sieving data, using an approximate method for integrating the mass balance equations (91). Powell's method (336) was used to minimize the value of χ^2 , defined as:

$$\chi^2 = \sum_{i=1}^m ((\Theta_{i,\text{exp}} - \Theta_{i,\text{calc}})/\sigma_{i,\text{exp}})^2 \quad (3)$$

where m is the number of data points; $\Theta_{i,\text{exp}}$ and $\Theta_{i,\text{calc}}$ are the experimental and calculated sieving coefficients, respectively, for molecular size i ; and $\sigma_{i,\text{exp}}$ is the standard error of $\Theta_{i,\text{exp}}$. Standard errors for each fitted parameter were estimated from the covariance matrix of the fit, as described previously (315).

Statistical comparisons were made using one-way analysis of variance (ANOVA), with Scheffe's test used to determine significant differences (1). The Pearson correlation coefficient was used to measure correlation between parameters (1).

3.6.4 Calculation of r^* for the Lognormal-plus-Shunt Model

The usual equation for calculation of r^* requires a slight modification for the lognormal-plus-shunt model, since by definition a small fraction of the filtrate always passes through the shunt. In the absence of a shunt, r^* (1%) is defined by (352):

$$\frac{\int_{r^*}^{\infty} r^4 g(r) dr}{\int_0^{\infty} r^4 g(r) dr} = 0.01 \quad (4)$$

where $g(r)$ is the pore-size distribution function, equal to the fraction of pores with radii between r and $r + dr$. The flow rate through a single pore of radius r is proportional to r^4 . For the *lognormal* model $g(r)$ is given by:

$$g(r) = \frac{1}{\sqrt{2\pi} r \ln s} \exp\left(-\frac{1}{2} \left[\frac{\ln(r/u)}{\ln s}\right]^2\right) \quad (5)$$

For a distribution including a shunt, Equation 4 was modified to:

$$(1 - \langle\omega\rangle) \left[\frac{\int_{r^*}^{\infty} r^4 g(r) dr}{\int_0^{\infty} r^4 g(r) dr} \right] + \langle\omega\rangle = 0.01 \quad (6)$$

where $\langle\omega\rangle$ is the fraction of the filtrate that passes through the shunt, averaged over the length of a capillary. This value was calculated from ω_0 as shown by Deen *et al.* (91). In

most instances the difference between r^* (1%) values calculated from Equations 4 and 6 was less than 1 Å.

3.6.5 Estimation of Glomerular Hydraulic Pressure from Sieving Data

Pore size parameters plus $\Delta\bar{P}$ were fitted simultaneously to sieving data using the χ^2 criterion described in Chapter 3.6.3. Both data from the individual rats and averaged data for the experimental groups were used. The group mean sieving coefficients, as derived in the sieving experiments, were fitted using the appropriate hemodynamic parameters from the same studies. For fits to individual rat sieving curves, data was used only from animals on which both micropuncture and sieving studies were performed. When data from a single rat was fitted, the standard error $\sigma_{i,\text{exp}}$ was set equal to $\Theta_{i,\text{exp}}$ in Equation 3 of Chapter 3.6.3.

Either Powell's method or the downhill simplex method was used to determine the best-fit set of parameters (336). Pearson's correlation coefficient was used to determine the significance of correlation between parameters.

4 EVALUATION APPLIED TECHNIQUES

4.1 Micropuncture

In all presented acute micropuncture animal studies in this thesis, a 1% bw iv isoncotic plasma infusion was given. This protocol is routinely used in comparable micropuncture experimentation in rats. The reason to administer such an amount of plasma is to restore fluid balance to conditions thought to be present in awake intact animals. Furthermore, the plasma infusion serves to keep the hematocrit (Hct) constant. This is necessary since alterations in the Hct result in shifts in glomerular hemodynamics, notably \bar{P}_{GC} (280). In the following text we shall discuss the effects of fluid balance on glomerular hemodynamics, the use of the direct and indirect stop-flow techniques to assess \bar{P}_{GC} under different plasma volume conditions, and provide information on the reliability of the stop-flow technique.

In 1977, Maddox *et al.* reported that Munich-Wistar (MW) rats prepared for micropuncture have an approximately 20% reduction of circulating plasma volume, relative to values in conscious animals, and are thus acutely volume-depleted (252). Ichikawa *et al.* compared the hemodynamic data provided by Maddox *et al.* for hydropenic rats (252) with values obtained in MW rats in which the euvoletic state was restored by the iv infusion of plasma (188). Plasma infusion ($\pm 1\%$ bw) resulted in higher values for GFR (1.30 ± 0.08 vs. 0.85 ± 0.06 ml/min), SNGFR (42.8 ± 2.6 vs. 28.0 ± 1.8 nl/min), Q_A (134 ± 7 vs. 76 ± 6 nl/min), in lower values for Hct (45.5 ± 0.6 vs. 50 ± 1 vol %), SNFF (0.32 ± 0.03 vs. 0.37 ± 0.01), R_A (2.2 ± 0.1 vs. $4.1 \pm 0.3 \times 10^{10}$ dyn·s·cm⁻⁵) and R_E (1.7 ± 0.1 vs. $2.4 \pm 0.2 \times 10^{10}$ dyn·s·cm⁻⁵), whereas values for MAP were unchanged (113 ± 3 vs. 113 ± 2 mm Hg). Values for Hct in awake, non-operated intact anesthetized, and in euvoletic MW rats were similar (188), and comparable with those in FH and WAG rats documented in this thesis. Slightly higher values for \bar{P}_{GC} (48.1 ± 0.5 vs. 43.7 ± 0.7 mm Hg), \bar{P}_T (13.6 ± 0.3 vs. 11.8 ± 0.4 mm Hg), and $\Delta\bar{P}$ (34.4 ± 0.4 vs. 31.9 ± 0.7 mm Hg) were seen in euvoletic rats as compared to hydropenic animals (188). Because the values for \bar{P}_{GC} obtained by Maddox *et al.* for hydropenic rats were somewhat lower than usually observed under such conditions, Ichikawa *et al.* concluded that the observed differences were of little significance or importance (188). The results of Ichikawa were in agreement with previous observations done by Brenner *et al.* who studied the effects of 2.5% bw plasma expansion and 10% bw Ringer infusion (60). While plasma infusion kept \bar{P}_{GC} unaltered, Ringer infusion depressed \bar{P}_{GC} compared to hydropenic controls. They observed that SNGFR was entirely determined by Q_A , $\Delta\bar{P}$, and C_A under conditions of filtration pressure equilibrium. More recently, Blantz *et al.* studied glomerular hemodynamics in salt depleted MW rats after 0.8% bw plasma infusion and in the same

animals after an additional 2.5% bw plasma expansion (40). Changes in single-nephron pressures and flows were similar to those documented by Brenner and Ichikawa, and in agreement with the analysis of selected data from various studies provided by Maddox, Deen, and Brenner and summarized below in Table 1 (250, 251). We compared glomerular hemodynamic studies obtained in hydropenic, euvolemic, and volume expanded, non-fasted mature male MW rats (250, 251). The average values for \overline{P}_{GC} are 46.8, 49.9, and 50.7 mm Hg, and 33.8, 35.6, and 36.0 mm Hg for $\Delta\overline{P}$, under hydropenic, euvolemic, and volume expanded conditions, respectively. Thus, intravascular fluid status affects several microcirculatory parameters, whereas \overline{P}_{GC} and $\Delta\overline{P}$ are relatively constant. The most impressive changes are the increases in Q_A and SNGFR as a result of decreases in R_A and R_E . Concomitantly, minimum values for K_f increase, and indicate that parallel to the rise in Q_A , a greater area of the glomerular tuft is involved in net fluid filtration. This change in K_f contributes to the rise in SNGFR. With further plasma volume restoration, Q_A is increased to such extent that the perfused blood can only be partially filtered. This results in a small decline in C_E and thus π_E . The net mean local ultrafiltration pressure (\overline{P}_{UF} ; defined as: $\overline{P}_{UF} = \Delta\overline{P} - \Delta\pi$), near the efferent arteriole (\overline{P}_{UF-E}) increases due to the increased $\Delta\overline{P}$ and decreased $\Delta\pi$. When $\pi_E/\Delta\overline{P} < 1$, unique values for K_f can be calculated, since the total glomerular surface available for filtration is involved in net ultrafiltration of blood and an exact $\Delta\pi$ profile can be derived (97). Generally, when $Q_A \leq 130$ nl/min, filtration pressure equilibrium is present ($\pi_E/\Delta\pi \geq 1$), and when $Q_A > 130$ nl/min, filtration pressure disequilibrium ($\pi_E/\Delta\overline{P} < 1$) is nearly always found (251). It should be noted that under physiological conditions the actual filtration in a single glomerular network is probably heterogeneously distributed, with some areas operating at filtration pressure equilibrium and others at disequilibrium (353-355). In such a network, K_f is approximately 30% higher than in the uniform model. Concentration polarization of protein within the capillary lumen results in a higher protein concentration at the periphery along the wall than at the midline axis. The experimentally obtained effective hydraulic permeability of the filtration membrane (k) is therefore lower than the true hydraulic permeability of the capillary wall (k_0), since filtration of water is more restricted by the relatively higher $\Delta\pi$ along the wall. Generally, k_0 and actual $\Delta\pi$ are 10% higher than can be estimated by the used micropuncture techniques (94).

Table 1 indicates that the \overline{P}_{GC} and $\Delta\overline{P}$ are not only fairly similar in MW rats despite changes in volume status, but in various other rat strains as well. Because \overline{P}_{GC} in those strains was assessed with the indirect stop-flow method, it is possible that the nephron under zero net flow conditions can not respond to plasma-volume alterations with a change in \overline{P}_{GC} . Analysis of reported values for \overline{P}_{GC} in MW rats obtained with both direct and

indirect stop-flow techniques under hypotensive, euvolemic, and volume expanded conditions show that the nephron is able to change \bar{P}_{SF} and thus \bar{P}_{GC} (Table 2). MW rats with chronic Goldblatt hypertension (one clip-two kidney model) had increased \bar{P}_{SF} as compared to non-clipped hypotensive controls, and similar values for \bar{P}_{GC} with both techniques (23). In this induced model of renovascular hypertension, plasma volume is presumably unaltered (333).

Table 1. Hemodynamic parameters for hypotensive, euvolemic, and plasma expanded, fed adult male Munich-Wistar rats and other rat strains.

	\bar{P}_{GC}	$\Delta\bar{P}$	π_A	π_E	\bar{P}_{UF-A}	\bar{P}_{UF-E}	K_f	Q_A	SNGFR
	----- mm Hg -----						nl/(min·mm Hg)	--- nl/min ---	
MW-hy	47	34	17	34	17	0	≥ 0.059	77	28
MW-eu	50	36	19	33	17	3	≥ 0.091	154	44
MW-ex	51	36	18	32	18	4	0.088	170	47
WKY-hy	52	39	16	26	23	13	0.041	186	45
WKY-eu	57	44	17	28	27	15	0.021	89	26
WKY-ex	46	34	10	17	24	17	0.040	167	50
SD-hy	54	41	18	34	23	7	≥ 0.054	140	44
SD-eu	55	40	18	32	22	8	0.050	140	42
SHR-hy	51	40	14	26	26	14	0.030	100	36
SHR-eu	57	44	19	36	25	8	0.032	83	28
SHR-ex	49	38	9	16	29	22	0.033	142	51

\bar{P}_{GC} , mean glomerular capillary hydraulic pressure as determined with direct puncture in Munich-Wistar rats and with an indirect (stop-flow) technique in the other rat strains; $\Delta\bar{P}$, mean transcapillary hydraulic pressure difference; π_A and π_E , afferent and efferent arteriolar oncotic pressure; \bar{P}_{UF-A} and \bar{P}_{UF-E} , afferent and efferent net ultrafiltration pressure; K_f , glomerular ultrafiltration coefficient (When filtration disequilibrium is not present, only minimal values for K_f are provided and indicated by \geq); Q_A , initial glomerular plasma flow rate; SNGFR, single-nephron glomerular filtration rate; MW, Munich-Wistar (251); WKY, Wistar-Kyoto (16, 24, 100, 101); SD, Sprague-Dawley (15, 242, 284, 285, 301); SHR, Spontaneous Hypertensive Rat (16, 100, 101, 108); hy, hypotensive; eu, euvolemic; ex, volume expanded.

The validation studies summarized in Table 2 indicate that in approximately two out of every three reports, differences between direct and indirect measured \bar{P}_{GC} were found. Of the in Table 2 included studies, seven showed overestimation and three underestimation

for indirect vs. direct measurements (251). Five studies revealed identical values for the two techniques (251). Notably, the study by Azar *et al.* did not indicate any difference between these methods, under both hydropenic and euvolemic conditions (23).

Table 2. Mean glomerular capillary hydraulic pressure (\bar{P}_{GC}) assessed both with direct and indirect (stop-flow) techniques in the same experimental animal, and compared among animals with different volume status.

Volume status	\bar{P}_{GC} (direct)	\bar{P}_{GC} (stop-flow)	Studies
	----- mm Hg -----		N
hydropenic	46.5	48.3	11
euvolemic	53.0	55.0	2
expanded	63.0	62.0	1
eu* (hy)	53.6 (44.7)	53.8 (44.5)	1

N, number of studies included in analysis; eu*, one clip-two-kidney experimental model of hypertension (Values between parentheses were recorded in the same study in normal intact Munich-Wistar control rats, and these values are included in the average provided for hydropenic animals) (23).

The reason why some studies report dissimilarities, whereas others do not, is not clear. One reason might be that the altered macula densa control of the afferent arteriole under zero net flow conditions results in too high values for \bar{P}_{SF} . Differences in the activity and sensitivity of the tubuloglomerular-feedback (TGF) system among animals, either inborn or due to animal preparation (399), may be responsible for differences between direct and indirect obtained values for \bar{P}_{GC} . Variability among rat strains in the sensitivity of the TGF-loop to nephron blockage may explain differences in \bar{P}_{SF} and thus \bar{P}_{GC} . Perssen *et al.* reported on the differences in TGF-feedback responses between the Milan normotensive (MNS) and hypertensive (MHS) strains (330). In contrast to MNS and Sprague-Dawley (SD) rats, MHS animals did not show a significant change in the TGF sensitivity after volume expansion with saline or after ureteral obstruction. Several studies have demonstrated that activation of the TGF, induced by changes in the loop of Henle flow, result in parallel changes in \bar{P}_{SF} and directly measured \bar{P}_{GC} , thereby confirming that differences in \bar{P}_{SF} do reflect differences in \bar{P}_{GC} (30, 62, 331). Salmond and Seney observed that unilateral nephrectomy and 5/6 renal ablation result in step-wise increases in \bar{P}_{SF} equal to those reported for MW rats by others (11, 92, 179, 388). Animals were studied seven days after surgery under hydropenic conditions. Loop microperfusion resulted in similar maximal decrements in \bar{P}_{SF} of 8 to 9 mm Hg in all three groups. The

rate of loop perfusion required to obtain the TGF-response curve increased proportional to the amount of ablated renal tissue, which according to the authors was most likely due to reduction of the responsiveness of the TGF sensor (388).

During the collection of fluid from the proximal tubule to measure SNGFR, the distal nephron does not receive its normal fluid load. The vasoconstrictor effect of the TGF on the afferent arteriole is minimal under such blocked conditions, and consequently values for SNGFR are maximal (48). Differences in values for SNGFR assessed from proximal and distal nephron segments in blocked nephrons are not routinely reported however. Only when flow to the distal nephron is restored are differences between proximally and distally measured SNGFR noted (292). A dissimilarity in blocked nephrons was not observed in plasma loaded (2% bw) MW rats, three weeks after uninephrectomy (253), and in chronically volume expanded rats (161). Varying volume status of the experimental animals among studies may thus be an explanation, since modification of plasma volume generally changes the responsiveness of the TGF. When plasma volume is expanded, the TGF responsiveness is decreased and SNGFR remains high (48, 292). Renal ablation alters the TGF setting but does not alter the absolute difference between proximally and distally measured SNGFR (388).

Other variables may influence the outcome of a micropuncture experiment as well. Besides possible technical limitations, variability and error (130, 312, 351), changes in animal physiology due to circadian and spontaneous alterations in blood pressure and GFR, and oscillations in vasomotion or TGF activity (177) have been mentioned. Brenner and Daugharty showed that the methodological influence on the determination of SNGFR resulting from different suction technique, sample variability, and repuncturing of tubules were all negligible (53, 54). Values obtained by the standard SNGFR technique and by calculation of SNGFR by measuring efferent arteriolar plasma flow and hematocrit were similar (54). Drumond and Deen analyzed the effects of the pulsatile quality on glomerular ultrafiltration and concluded that the usual steady-state assumption is valid and introduces negligible errors in calculating glomerular membrane parameters such as K_f (102).

We would like to emphasize that interpretation of the data shown in Table 1 and 2 has some limitations since variables within and among studies may have been present and possibly resulted in bias. The reason to provide these tables is to support the following conclusions: 1- With changing plasma volume status, \bar{P}_{GC} remains relatively stable; 2- If \bar{P}_{GC} changes as a result of an alternating volume status, such change is picked up by the stop-flow-method; 3- The stop-flow method may infer too high or too low values for \bar{P}_{GC} . The observed differences in the validation studies were usually small, and alternations in values for direct \bar{P}_{GC} resulting from experimental manipulation were reflected in similar changes in \bar{P}_{SF} .

4.2 Glomerular Morphology

4.2.1 Glomerular Sclerosis

FSGS was assessed by counting glomerular capillary collapse with or without concomitant hyalin deposition and adhesion of the damaged glomerular tuft to Bowman's capsule. Capillary collapse is thought to represent the key histopathologic feature of this otherwise rather nonspecific process (362, 365). Although the criteria to assess FSGS vary among researchers, most of the reported methods include some aspect of the capillary obsolescence. Microaneurysm and podocyte bleb formation, microthrombosis, mesangial expansion, and hyalin accumulation are all used in this respect, since these changes are believed to represent intermediary or contributory steps in the evolution of the final capillary lesion (364). These latter changes are nonspecific and their presence does not indicate FSGS. Information on other changes associated with FSGS is sometimes provided. Among these are glomerular macrophage influx or other glomerular cellular adaptations, vascular sclerosis, interstitial inflammatory cell infiltration, and tubular casts and atrophy (236).

To assess the total incidence and severity of FSGS in a kidney one could look at the complete tuft of all glomeruli. This is impractical and for the purpose of most experiments not necessary because of available statistical tools. We used a method which eliminates bias as a result of selection of glomeruli in an individual animal, provides information derived from relatively large numbers of animals, and is still feasible. Remuzzi *et al.* have criticized one aspect of this method: the estimation of the incidence of FSGS based on a single random cortical section (356). They showed that in rats with only mild FSGS, counting of 50 glomeruli on a single section reveals only approximately one third of the real incidence of sclerosis. A multi section approach in which 30 to 50 glomerular tufts are completely assessed in 3-dimensions was advocated by these authors. Such a technique is probably very time consuming and this might explain for the low number of rats per experimental group in their report. In the method employed in our studies, 400 to 500 different glomeruli were counted on cross section per animal and approximately seven to nine animals per experimental group were assessed. The average diameter of a rat glomerulus is approximately 120 μm . Complete examination in 3 μm sections of one glomerulus therefore requires ± 40 sections. The currently used technique resulted in the estimation of FSGS based on approximately 50% of the sections used in Remuzzi's method. This method is not limited to a random selection of tufts present on a cross section since all glomeruli seen on such a cross section are included. In addition, information from relatively large groups of animals is obtained.

As an alternative from the total incidence method, some investigators use a semiquantitative injury scoring system (349, 459). The severity of the lesion seen in each

glomerulus is graded on a scale of 0 to 4+ according to the percentage of glomerular involvement. Briefly, if 25% of the glomerulus is affected, a score of 1+ is adjudged, 50% is scored as 2+, 75% as 3+ and 100% as 4+. The ultimate score is then obtained by multiplying the degree of change by the percentage of glomeruli with the same degree of injury and additions of these scores. Again, as with the technique described by Remuzzi *et al.*, a limited number of glomeruli are usually assessed and may result in bias. Otherwise, this technique provides a grading of the severity of the lesion and may reveal more subtle differences among experimental groups. Van Goor *et al.* examined the relationship between the semiquantitative injury score (349) and the incidence of FSGS in rats after renal ablation (149). Despite the broad variation of FSGS among animals, a highly significant positive correlation was found between values obtained with these techniques ($r = 0.98$, $p < 0.001$).

4.2.2 Glomerular Tuft Volume

Increase in glomerular tuft size is thought to represent glomerular growth. Such growth occurs in normal maturation of an organism, after renal ablation, and in association with glomerular disease. Whether glomerular growth by itself results in more progressive deterioration of renal function in glomerular illnesses, that such size alterations may cause glomerular failure by its own nature, or that such size changes are rather coincidental and not causally linked with FSGS is controversial (465). Aspects related with preparation of the tissue for tuft analysis, several techniques at hand for the study of the size, and a discussion on 3-dimensional interpretation of cross sections is provided.

In nondiseased *ex vivo* perfused rat glomeruli, a S-shaped curve, a straight line, or a curvilinear plot best describes the relationship between proximal intraglomerular perfusion pressure and the glomerular volume (80, 373). In such normal glomeruli the most impressive change in glomerular volume is seen when perfusion pressure is increased from zero to 120 to 150 mm Hg (equal to a range in \bar{P}_{GC} from zero to 60 to 75 mm Hg), which results in an average 30 to 60% increase in size. This perfusion pressure range lies within the range of pressures reported in conditions associated with progressive glomerular injury. For example, over a pathophysiologically relevant range of a \bar{P}_{GC} increase from 31 to 52 mm Hg, the glomerular tuft increases on average 16% (373). Larger glomeruli at zero pressure have greater compliance and expand significantly more with increasing pressure than initially smaller corpuscles. In whole kidney specimens, perfusion pressure dramatically affects final glomerular size, and this is similar in magnitude to *ex vivo* glomeruli (287, 373). When perfusion is done with significantly higher pressures (165 mm Hg) than mean blood pressure (114 mm Hg) outcome is, surprisingly, not affected. This suggests that antihypertensive therapy does not affect final tuft size between treated and

untreated specimens as a result of the technique of acute perfusion fixation of tissue. Since alterations in the compliance of the capillary tuft to increasing pressure may be present in diseased glomeruli, one should be careful in assuming no effect of perfusion pressure on tuft size and therefore perfuse kidneys at previously assessed systemic blood pressure. As recently indicated by Kriz *et al.*, the nondiseased glomerular tuft is a highly dynamic elastic structure and the GBM can greatly expand with different perfusion pressures and added vasodilators (225). These authors suggested to monitor glomerular capillary pressure not only before, but also during the perfusion fixation of kidneys used for morphologic studies. Such an approach would ideally eliminate altered \bar{P}_{GC} as a source for morphologic misinterpretation of the "in vivo glomerulus", which remains unknown to us.

Immersion fixation may result in collapse of the capillary tuft and reduction in Bowman's space volume. Again, as noted above, nondiseased and diseased glomeruli may react differently to any fixation technique. In the case of immersion fixation it is possible that sclerosed glomeruli or glomeruli with early wall injury do not collapse as easily as normal tufts. Thus immersion fixation may selectively allow diseased glomeruli to appear larger on glomerular tuft size measurements. These "large" glomeruli indicate that there is a structural abnormality and may be interpreted as a signal of a severe underlying disease which has not fully shown its true nature. Clearly, more study is needed to confirm these suggestions.

An alternative method is the in situ fixation of a kidney by dripping fixative on the surface (193, 317). In Munich-Wistar rats this technique is useful to selectively study the superficial glomeruli. In such an in situ fixation study, acute elevation of the mean systemic blood pressure by angiotensin II infusion with 45 mm Hg did not significantly increase the glomerular tuft volume (317). However, capillary lumina and extracellular mesangial matrix did significantly expand.

Use of different fixatives and embedding media may contribute to variability. Characteristics of a fixative itself, concentration of the fixative, osmolality of the vehicle, pH of the solution, and choice of buffer system all influence the ultra- and light microscopic structure of cells and tissues (268). The type of perfusion method used may alter the tissue to some extent (267). Embedding in paraffin results in shrinkage of tissue as compared to epoxy treated sections (287).

Examination of glomerular casts by scanning electron microscopy allows detailed description of the capillary tuft (244, 347). One can estimate tuft size, pattern of capillary loop branching and tortuosity, and the contour of these loops such as the presence of intracapillary narrowing or interruptions and the occurrence of aneurysmal dilatations. Distention of mesangial areas, irregularities of the endothelial lining, and morphology of the afferent and efferent arterioles can be studied. This technique is mentioned here to

indicate that one can perform morphological studies of the glomerular tuft with alternative techniques, with each technique providing an unique view of the glomerular adaptations to injury.

Change in glomerular tuft size is an example of how glomeruli can structurally react to various stimuli. Different architectural modifications can explain an increased tuft or may occur without such tuft size changes (299). For example change in length of individual capillary loops of the glomerular tuft has been described (309). The stresses in a such capillaries increases, for short cylinders resist compression and distortion better than long structures (437). As a cylindrical element grows, its strength and stiffness increase with its cross-sectional area, which is directly proportional to the square of its radius. A small structure cannot grow into a large one without changing the proportions or material stiffness of its supportive elements (434, 437). The stiffness of an element against pressure and flow are dependent on rigid material such as fibers, and the complex interaction in the structure which results from the basic shape of the structure and placement of fibers within it. The glomerular capillary is a structure supported at the circumference by means of an exoskeleton. This design is guided by the beam theory, which implies that the most economical means of stiffening a cylinder is to place the stiffest material as far away from the axis as possible. Placement of abundant supportive material at the periphery results in decreasing flexibility of the structure itself, and may contribute to increased stresses within the structure. The Laplace law (after Pierre Simon Laplace, a French mathematician and astronomer, 1749-1827) is occasionally mentioned to explain for increased stresses on the glomerular capillary wall when capillary radius increases. From the above one has to conclude that many different pathways are probably operational in the adapting tuft. Even when glomerular tuft size does not change, other disturbances in the delicate architecture of this structure may provide or represent routes for continuing glomerular damage.

4.2.3 Stereology

Various methods have been reported for the assessment of the size of the glomerular tuft from cross sections (236, 310). Several of these techniques are derived from formulations developed in stereology. Stereology means the knowledge of space and when applied to histology the 3-dimensional interpretation by mathematical methods of 2-dimensional images from sections or projections (445, 446). Thus, by sending some probes into tissue which pick out a sample of the interior we try to gain insight from the architecture of the tissue. The Delesse principle on which some of these measurements are based was first introduced by the French geologist Delesse in 1847. It states that the areal density of profiles on a section is, on average, equal to the volume fraction of the component. This relation can be used to estimate volumes of structures by planimetry of the

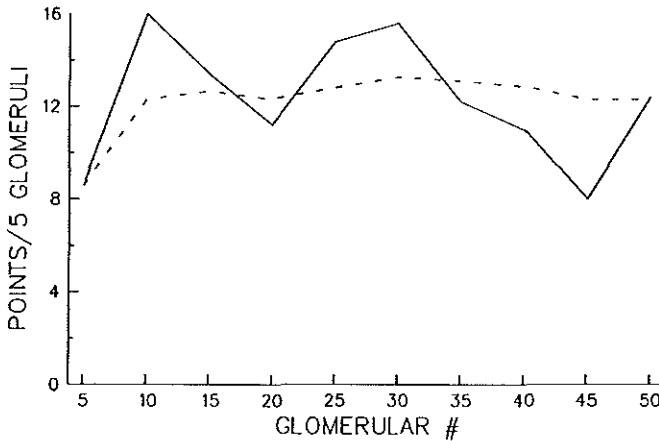
combined area of all profiles divided by the enclosed test area. This can be done by applying a point grid to a microscopic field and counting all points enclosed in a profile or outline of a structure with a computer assisted planimetric device.

The stereological principles for assessment of volume from 2-dimensional information are based on the assumption that the tissue sections are true 2-dimensional sections and hence have no thickness whatsoever. A histological slide with a certain thickness results in too large projection of opaque, and too small estimation of translucent structures, the Holmes effect (116, 447). When estimating mean volume of a structure by stereological means, several basic conditions must be met. The particles must all be of similar shape and may vary only in size, the shape must be known, and the shape must be such that a random plane can intersect each particle only once. In addition, there must be random orientation of the particles in the section plane and an even dispersion of particles must be present to such an extent that representative samples can be defined. The glomerulus is an irregular spheroid or oblate ellipsoid and is not randomly oriented in space (2, 115). Differences in shape are small however, since the equatorial diameter is approximately 5% larger than the polar diameter. The elimination of this geometrical aberration is not possible in biopsy specimens (83). If the range of diameters of glomeruli in a tissue section or biopsy are small, the sample size is usually sufficient to be representative. However, when as in renal disease a widening of the range in diameters occurs or a new population of different sized glomeruli emerges, then the problem of representatively becomes very important (83).

The smaller a profile is on cross-section, the greater the likelihood of being missed. Thus, often the profile size distribution is incomplete in the smallest size region, and may be corrected by extrapolation of the distribution pattern toward zero. Stereological methods therefore tend to overestimate mean particle size, unless corrected. Such correction can be done by applying the distribution curves provided by Elias *et al.* (115, 116). Briefly, the investigator has to construct a histogram for the size distribution of observed sectional circles and fit it in one of the curves. Then, the size distribution of spheres can be assessed. In a randomly dispersed population of spheres of varying normally distributed size, the chance of being cut in the plane of counting is proportional to size. The degree of overestimation of the true diameter depends on the standard deviation of the distribution pattern of the sizes. Thus a correction factor is needed. Various computer assisted methods for \bar{V}_G estimation are currently available and correct for this error.

After these considerations, the next step is to ascertain random tissue sampling and the estimation of the sample size. This is a rather complex stereological theoretical problem (444, 446). For practical purposes it is accepted to find the number of samples needed by

calculating cumulative means of the measured surfaces or volumes. We experienced that after approximately 40 to 60 counts, the variability was leveled off. Sample size required for each animal in each experimental group was evaluated by this method, either by manual point counting (Figure) or with a computer assisted planimetry method.



Real mean (solid line) vs. cumulative mean (dotted line) for estimation of sample size and glomerular tuft volume in an individual animal by manual point counting.

The method used in this thesis for assessment of \bar{V}_G was originally described by Weibel and Gomez for the measurement of constant shape particles (446). In this approach measurement of a surface is translated into a volume through using a dimensionless shape coefficient β :

$$N = \frac{1}{\beta} \cdot \frac{N_A}{V_V} \quad (1)$$

β is defined by the dimensionless relationship between the particle volume v and its mean cross-sectional area \bar{a} :

$$v = \beta \cdot \bar{a} \quad (2)$$

Thus values for β depend on the particle shape, and for a sphere is equal to 1.38.

Stereological techniques are useful tools in assessing glomerular volume when various criteria are met. The method employed in the current study is based on assumptions for shape and size distribution. Since we determined sample size for the individual rats, corrected for possible size-distribution errors, used thin plastic sections, and assessed mean glomerular volume through the full thickness of the renal cortex, bias was most likely limited.

4.3 Glomerular Permselectivity

The normal glomerular capillary wall provides an effective permselective barrier to plasma proteins with very little resistance to the filtration of water and small solutes. Study of these permselectivity characteristics is usually done by assessing the filtration of a marker molecule and calculating its fractional clearance. The fractional clearance is defined as the urinary clearance of a solute divided by the GFR. If the test molecule is not reabsorbed or secreted its fractional clearance will equal its Bowman's space-to-plasma ratio. This ratio, termed sieving coefficient (Θ) is calculated as $\Theta = C_B/C_A$, where C_B is the average concentration of the solute in Bowman's space and C_A is its concentration in systemic plasma, assumed to be representative of afferent arteriolar plasma.

Effective molecular radius, molecular configuration, and charge have been established as determinants of the permeability of the normal glomerular capillary wall to macromolecules (200, 251, 318). Since intrinsic plasma proteins are heterogeneous in regard to these variables and reabsorption of filtered proteins by the tubules is difficult to accurately estimate or predict, exogenous polymers have been developed in which these parameters can be individually studied in a quantitative fashion. Applied agents include dextran, polyvinylpyrrolidone, polyethylene glycol, horseradish peroxidase, and Ficoll. These markers have been used in numerous experiments to estimate the size-selectivity of the filtration barrier. This is generally done by studying the fractional clearance of a marker over a wide range of different molecular sizes. As an estimate of molecular size, the Stokes-Einstein molecular radius (r_s) is used which is a measure of frictional interactions between the polymer and the solvent. The value for r_s represents the radius of a hypothetical sphere that would have the same diffusion coefficient in bulk solution as the actual test macromolecule. It does not correlate directly with real dimensions of the molecule, but provides a basis for comparing results and offers the advantage of allowing data to be interpreted more readily in terms of apparent membrane pore radii.

Dextran molecules, frequently used to assess glomerular permselectivity, have characteristics which result in too high fractional filtration by the glomeruli and thus in under estimation of the true size-selectivity of the filtration membrane (315, 367). Diffusion studies of dextrans have indicated that these polymers in solution behave as random coils, enabling them to permeate in an end-on fashion through membranes by virtue of their shape and deformability (46, 87). This process is called reptation, and is probably responsible for the high Θ for neutral dextrans. Ficoll and horseradish peroxidase molecules are globular spheres and behave more ideally as test agents. Oliver *et al.* recently showed that the fractional clearance of Ficoll in normal euvoletic Munich-Wistar rats over a wide range of molecular sizes (r_s : 19 - 65 Å) is less than that for uncharged dextran (315). For $r_s > 30$ Å, Θ for dextran was approximately 10 times that for Ficoll. The values of Θ for Ficoll

approximated previously reported values for uncharged horseradish peroxidase (367). Since there is poor understanding of the mechanistic effects of molecular configuration on macromolecular filtration (251), the use of Ficoll, a molecule with a nearly spherical rigid configuration bypasses these current shortcomings. Tubular handling is inert giving this molecule an advantage as compared to horseradish peroxidase. Furthermore, horseradish peroxidase is not available over a broad spectrum of molecular sizes as is Ficoll. Although Θ for Ficoll at $r_s = 35 \text{ \AA}$, the approximate size of albumin, was much smaller than the corresponding value for dextran, it was still about 30 times greater than the typical values of the filtrate-to-plasma ratio reported for serum albumin in the rat (315). This agrees with the concept that in addition to size-selectivity, charge-selectivity plays an important role in the prevention of albuminuria. The charge results from fixed glomerular anionic sites, which have been demonstrated by light and electron microscopy using cationic probes and biochemically in isolated glomerular basement membranes (441). Charge-selectivity as a determinant for molecular filtration has been established by studies with charged tracer molecules (42, 44, 72, 96, 286, 319). Such studies indicated that for any given molecular size the passage of the anionic derivative was reduced and that of the cationic derivative was enhanced relative to that of uncharged molecules (42, 96, 251, 366, 441). Charged derivatives of Ficoll are not yet available to directly compare the role of charge-selectivity with macromolecules having more desirable sieving characteristics.

Next to the characteristics of the test molecules, intrinsic properties of the glomerular filtration barrier and hemodynamic variables such as plasma flow rate and glomerular pressure determine permselectivity as well. Mathematical models of glomerular macromolecule sieving describe relationships between quantities that are measurable in clearance and micropuncture experiments, and membrane parameters that determine the functional properties of the glomerular barrier. The pioneering theoretical and experimental work which lay the foundation for modeling restricted transport in pores was done by Pappenheimer, Renkin, and Borrero in the 1950's (325, 326, 361). The application of these early models was somewhat limited in respect to glomerular filtration because the intra- and extravascular spaces were each assumed to be well mixed reservoirs. Chang, Robertson, Brenner and Deen subsequently developed cross-flow filtration models in which the dependence of molecular transport on afferent arteriolar plasma flow rate and on the gradients of concentration, flux, and osmotic pressure in the capillary tuft were considered (73, 93). In the simplest of these models, the isoporous solid-sphere model, the glomerular capillary wall is assumed to be perforated by right cylindrical pores. Cross-flow filtration is assumed to be conducted through these pores of radius r_p and length l . Renal plasma flow is parallel to the inner surface of the wall. Filtration is governed by opposing hydraulic ($\Delta\bar{P}$) and osmotic ($\Delta\pi$) pressure differences, resulting in the net flux of both

solvent (J_v) and solute (J_s) into Bowman's space. For a mathematical description of the model the reader is referred to Chang *et al.* (73). This model predicts a sharp cutoff of Θ at $r_s = r_0$. Typical values for r_0 are 45 - 50 Å in the rat. However, small but significant filtration of macromolecules with $r_s \geq 60$ Å occurs (91). Development of heteroporous models by Deen and coworkers has resulted in two somewhat different approaches to solve the cutoff problem. These are a continuous lognormal distribution of pore sizes and the so-called isoporous-plus-shunt distribution, which postulates a small number of infinitely-sized pores in parallel with the isoporous membrane. Both of these models require two parameters to describe membrane size-selectivity, as opposed to the one-parameter isoporous membrane. Finally, the lognormal-plus-shunt model, a logical extension of the previous two, assumes a small number of infinitely large pores in conjunction with a lognormal distribution. This model uses three parameters for its description. A full description of the various models of glomerular permselectivity is presented by Oliver *et al.* (315).

Sieving data and the theoretical models described above allow the intrinsic selectivity of the glomerular filtration barrier to be described in terms of specific membrane properties. The assumption that this barrier is functionally equivalent to a single membrane perforated by a population of cylindrical pores, allows expression of the size-selectivity in terms of an effective pore radius (r_0). If K_f is known from measurements of glomerular pressures and flow rates or alternatively K_F from whole kidney functional and systemic parameters, this radius can be estimated from the value of Θ measured for any uncharged macromolecule of known r_s . With this method, effective pore radii of glomerular capillaries in normal rats have been reported ranging from 46 to 54 Å (44, 74, 90, 185, 303, 461-463). The existence of effective pore radii of about 50 Å fails to explain the extent to which larger molecules appear in the filtrate. To account for this, a small fraction of the filtrate passes through large, nonselective pores or "shunts" as indicated above in the various models with a shunt parameter (91). The shunt is expressed as a quantity, ω_0 , relating to the fraction of the filtrate passing through the shunts. This has been reported to average about 1×10^{-4} in normal rats (461-463). Using the newer lognormal and lognormal-plus-shunt models, two parameters, u and s , appear, replacing r_0 . The probability density function has its maximum at a pore radius $r=u$, whereas the breadth of the distribution is determined by s (315).

The various determinants of glomerular filtration affect the sieving of macromolecules (251, 354, 355). For example, an increase in Q_A results in a decrease in Θ (95). However, this is only true when the glomerular network is assumed to be composed of identical capillary loops. In reality, the tuft consists of capillaries of varying length. Correction for this results in a decrease of the effect of Q_A on Θ (355). Since there is a

diffusive component to the flux of a given solute, increasing SNGFR results in lowering of Θ . However, even at constant SNGFR, Θ may vary as a result of alterations in SNFF. This is explained by the fact that high SNFF causes increases in the concentration of the solute in the more distal segments of the capillaries. With increasing $\Delta\bar{P}$, the Θ decreases. This effect is most notable for the smaller sized molecules ($< 36 \text{ \AA}$). Decreasing the length of the capillaries causes modest elevations in Θ . The effects of π_A on Θ are essentially the inverse of those for $\Delta\bar{P}$. An increase in K_f results in increased Θ , independent on molecular size or network structure. Overall, increased capillary length decreases Θ , and thus a heterogeneous network requires smaller pore radii to achieve a given Θ . The above mentioned models, all based on identical capillaries in parallel, therefore tend to overestimate the pore radii calculated from sieving data. In most models, this error is negligible. However, the shunt parameter, ω_0 , is constantly overestimated by approximately 28% (355). Further details on the interaction between permselectivity and hemodynamics is provided in Chapter 9, in the Section: Theoretical Considerations.

Processing of information derived from sieving data for neutral macromolecules has been suggested as a means to estimate glomerular pressures. In particular, in some experimental models and in humans, where direct measurement of glomerular pressure by micropuncture is impossible, such efforts have been made (18, 69, 70, 104, 105, 140-142, 147, 237-240, 279, 281, 332, 430, 431). In the isoporous model it is required that at least two quantities, r_0 and either K_f (or K_F for whole kidney data) or $\Delta\bar{P}$, be derived from the sieving data. This assumes of course, that glomerular plasma flow rate and either systemic protein concentration or oncotic pressure have been measured, in addition to GFR and fractional clearances. Generally, the more information that is extracted from the sieving data, the more severe are the requirements for accuracy in both the data and theory. There have only been very few attempts to compare directly measured values of $\Delta\bar{P}$ with those inferred from sieving data. Chang *et al.* (70, 74) compared direct and estimated pressure data obtained in Munich-Wistar rats. The value of $\Delta\bar{P}$ inferred from the sieving data was generally less than that measured directly. Thus, these indirect estimates do not appear to be highly reliable. Recent uses of dextran sieving data to assess renal hemodynamics in humans have focused largely on estimating directional changes in $\Delta\bar{P}$ (69, 147, 279, 281, 332). However, an extensive study directly comparing measured and estimated pressures and applying newer models of glomerular permselectivity is needed to establish the reliability of such indirect techniques. In Chapter 9 we studied data for dextran sieving and glomerular hemodynamics in various rat models obtained from the literature. In addition, we analyzed the results on Ficoll sieving in FHH rats in an attempt to infer $\Delta\bar{P}$.

PART III:
EXPERIMENTS

Chapter 5: Experiment 1

Adapted from:

JOURNAL of the AMERICAN SOCIETY of NEPHROLOGY, 3:1775-1782, 1993.

PATHOGENESIS OF GLOMERULAR INJURY IN THE FAWN-HOODED RAT: EARLY GLOMERULAR CAPILLARY HYPERTENSION PREDICTS GLOMERULAR SCLEROSIS

Jacob L. Simons^{1,3}, Abraham P. Provoost³, Sharon Anderson¹,
Julia L. Troy¹, Helmut G. Rennke², Deborah J. Sandstrom²,
and Barry M. Brenner¹

Renal Division and Departments of Medicine¹ and Pathology²,
Brigham and Women's Hospital,
The Harvard Center for The Study of Kidney Diseases
Harvard Medical School,
Boston, Massachusetts, USA

and

Department of Pediatric Surgery³,
Erasmus University,
Rotterdam, The Netherlands

Portions of these studies were presented at the 24th Annual Meeting of the American Society of Nephrology (J Am Soc Nephrol 2:691, 1991) and at the 7th Scientific Meeting of the American Society of Hypertension (Am J Hypertens 5:14A, 1992).

ABSTRACT

Fawn-hooded (FH) rats spontaneously develop focal and segmental glomerular sclerosis (FSGS), systemic hypertension and proteinuria (U_pV) at a young age. Micropuncture and morphological studies were performed in two inbred strains of FH rats, FHH and FHL, with different susceptibilities to develop chronic renal failure (CRF). FHH rats have higher values for systolic blood pressure and U_pV and more rapid development of FSGS and subsequent CRF as compared to genetically closely related FHL rats. FHH and FHL strains and a Wistar control strain, WAG, were matched for age and were studied at 16 weeks. FHH, FHL and WAG-old (WAG-O) strains were matched for body weight (bw), the last group studied at 22 weeks. WAG were also matched for bw to a young group of FHH rats (FHH-Y), and these were studied at eight weeks. In comparison with WAG and WAG-O rats, FHH and FHH-Y rats exhibited an increase in mean glomerular capillary hydraulic pressure (\bar{P}_{GC}) (WAG, 52 ± 1 mm Hg; WAG-O, 47 ± 2 mm Hg; FHH, 60 ± 2 mm Hg; FHH-Y, 65 ± 1 mm Hg), whereas values in FHL animals were intermediate (56 ± 2 mm Hg). No significant differences in mean glomerular volume (\bar{V}_G) were found among groups. Moderate FSGS developed in FHH and FHH-Y rats, with values for older FHH rats being significantly greater than those for WAG, WAG-O and FHL animals. Thus, the genetically determined sensitivity to develop proteinuria, FSGS, and CRF in FH rats correlated with early evidence of glomerular capillary hypertension. By contrast, glomerular hypertrophy was not associated with and not a prerequisite for early glomerular injury in FH rats.

For many years, experimental animal models have been studied to elucidate the potential mechanisms causing the progression of renal disease to end-stage chronic renal failure (CRF). In humans, focal and segmental glomerulosclerosis (FSGS) is usually present at the end-stage as is hypertension and non selective proteinuria (365). Animal models described include surgical removal and/or infarction of renal tissue with or without superimposed hypertension and difference in dietary protein content (112, 179), administration of drugs or toxins (9), and induction of a diabetic state (466). In contrast to these induced models, FSGS develops spontaneously in certain rat strains, reflecting a genetic predisposition (114). The fawn-hooded (FH) rat constitutes such a hereditary model. These rats develop FSGS spontaneously, together with systemic hypertension and proteinuria (U_pV) at a young age (222, 228). Systemic hypertension and proteinuria increase further with age, and the progression of sclerosis results in premature death from end-stage renal failure (228). This rat strain therefore constitutes a unique model, because

it may resemble intrinsic human kidney disease more closely than the various models of induced renal injury mentioned above.

We previously reported that FH rats exhibit whole kidney hyperfiltration accompanied by normal effective renal plasma flow (ERPF) and normal total number of glomeruli (209). These findings suggested the presence of single-nephron (SN) hyperfiltration and, because of the non-elevated renal plasma flow rate (RPF) and high filtration fraction (FF), elevated mean glomerular capillary hydraulic pressure (\overline{P}_{GC}) as the predominant cause of the hyperfiltration (209). Maneuvers known to decrease \overline{P}_{GC} in other animal models, such as low protein diet (179) or angiotensin II converting enzyme inhibition (ACEI) (8), minimize glomerular sclerosis and proteinuria and also prolong renal survival in FH rats (207, 449). On the other hand, maneuvers known to further increase \overline{P}_{GC} , such as uninephrectomy (92, 108) or high protein diet (179), accelerate the development of proteinuria and renal failure in FH rats (207, 208). These findings further support the hypothesis that \overline{P}_{GC} is elevated in FH rats.

In this study, we assessed glomerular hemodynamics in FH rats and related the findings to the development of early proteinuria and FSGS. This was performed in combination with renal morphologic studies. Two separate inbred strains of FH rats (341) with different susceptibilities to development of FSGS were used.

MATERIALS AND METHODS

Information on the different animal strains used in this experiment is provided in Chapters 2.1 and 3.1. Thirty-nine male rats were used in five experimental groups. Briefly, we used two groups of FHH rats of different ages together with one group of FHL rats and two groups of normotensive control Wistar (WAG) rats. Groups FHH, FHL, and WAG were matched for age. FHH, FHL, and WAG-Old (WAG-O) animals were matched for body weight (bw), as were WAG and FHH-Young (FHH-Y) rats.

Beginning at the age of 12 weeks, SBP_{tc} and 24h U_pV were monitored in groups FHH, FHL, and WAG, and at age 7 and 21 weeks in groups FHH-Y and WAG-O, respectively. Glomerular hemodynamic and morphologic studies were performed at age 16 weeks in FHH, FHL, and WAG animals and at age 8 and 22 weeks in groups FHH-Y and WAG-O, respectively.

Details on animal preparation, and microcirculatory, analytic, and renal histological studies is provided in Part II of this thesis.

Values were compared by one-way analysis of variance with the Scheffe's F-test for multiple comparison. Statistical significance was defined as $P < 0.05$. All values represent mean \pm SE.

RESULTS

Functional Studies

Figures 1 and 2 summarize the values for SBP_{ct} and U_pV. Moderate systemic hypertension was present in both FHH groups. Values for SBP_{ct} in FHH-Y and FHH groups were significantly higher than in FHL rats and both groups of WAG rats. Significant proteinuria was present in young FHH rats as compared to both WAG groups. In older FHH rats, the level of proteinuria was further increased, the value being significantly higher than in all other groups.

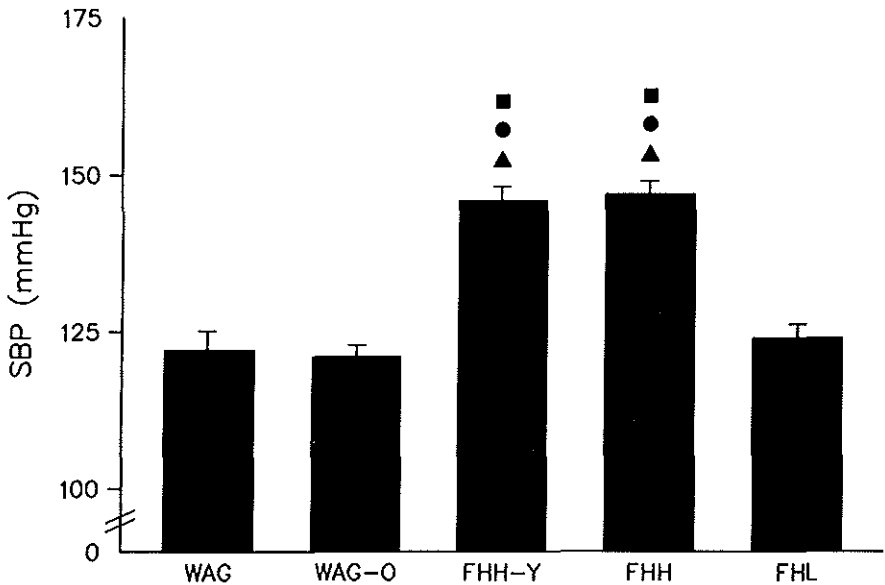


Figure 1. SBP in the awake condition (SBP_{ct}). Values are mean ± SE. (circle) P < 0.05 vs. WAG, (square) P < 0.05 vs. WAG-O and (triangle) P < 0.05 vs. FHL. Moderate systemic hypertension of similar level is present in FHH-Y and FHH rat groups. FHL and Wistar rats are normotensive.

Systemic and Renal Hemodynamic Parameters

Mean values for systemic and renal hemodynamic parameters are summarized in Table 1. Despite numerically higher values for MAP in all FH rat groups as compared to Wistar rats, differences during anesthesia were no longer statistically significant. Hct was similar in all groups. High values for whole kidney GFR were found in FHH and FHH-Y

rats, but only those in FHH animals were significantly higher than those in WAG rats. On the single-nephron (SN) level, GFR was significantly higher in FHH and FHH-Y animals than in WAG rats. FHL and WAG-O animals exhibited intermediate values for SNGFR. SNFF was also highest in FHH and FHH-Y rats, but only values for FHH-Y rats were significantly higher as compared with those for WAG rats. Values for C_A and C_{SF} were identical in all groups, whereas C_E and consequently π_E were significantly higher in FHH rats as compared with WAG-O rats.

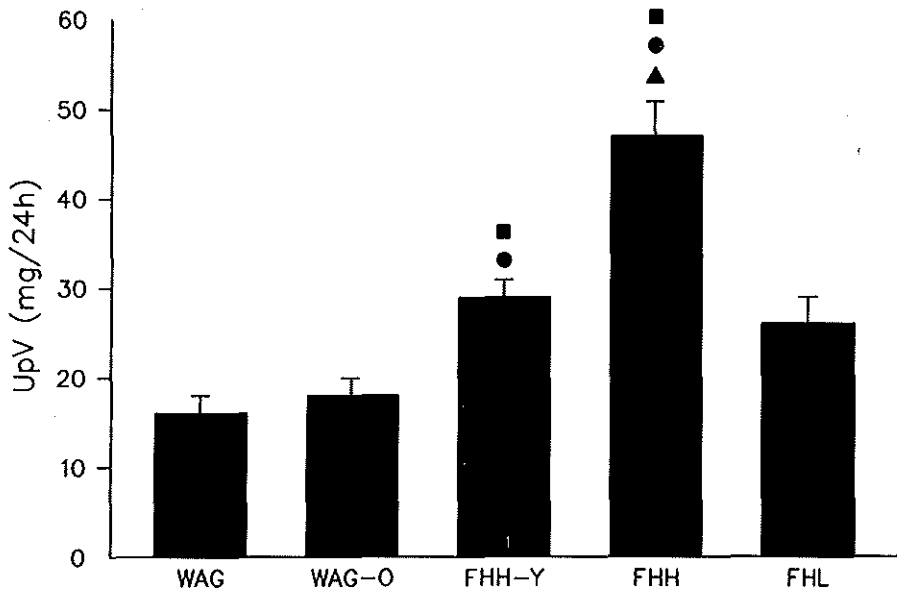


Figure 2. Urinary protein excretion (U_{pV}) during 24 hour collection. Values are mean \pm SE. (square) $P < 0.05$ vs. WAG, (circle) $P < 0.05$ vs. WAG-O and (triangle) $P < 0.05$ vs. FHL. FHH-Y rats exhibited significantly more proteinuria than either WAG group. In older FHH rats, the level of proteinuria was further increased, the value being significantly higher compared to all other groups.

Despite less evident systemic hypertension during anesthesia, measurements of \bar{P}_{GC} revealed the presence of glomerular capillary hypertension in both FHH and FHH-Y animals (Figure 3). Values for \bar{P}_{GC} in FHH-Y rats were on average 5 mm Hg higher than pressures observed in FHH rats; however, this difference was not statistically significant. As a consequence of the increased \bar{P}_{GC} , $\Delta\bar{P}$ was elevated in FHH and FHH-Y rats. $\Delta\bar{P}$

values for FHH rats were on average 12 mm Hg higher than values in WAG-O rats matched for bw. A similar mean elevation of 13 mmHg was found in FHH-Y rats compared with body weight-matched WAG rats. $\Delta\bar{P}$ values for FHL rats were on average 7 mm Hg higher than those for WAG-O rats. This value is intermediate compared with that for FHH and WAG-O animals.

Efferent arteriolar pressures tended to be lower in FHH and FHH-Y rats, but only values in FHH-Y rats were significantly lower compared to FHL, WAG, and WAG-O rats. Values for K_f , Q_A , and R_A did not differ among groups, with the exception of the significantly higher Q_A in FHL rats compared with that in age-matched WAG rats. Values for R_E in FHH rats were twice those found in WAG-O rats and were also higher compared with those in FHL rats. Values for R_E in FHH-Y rats were also increased significantly as compared with those in FHL and WAG-O rats but were only numerically higher compared to body weight-matched WAG rats.

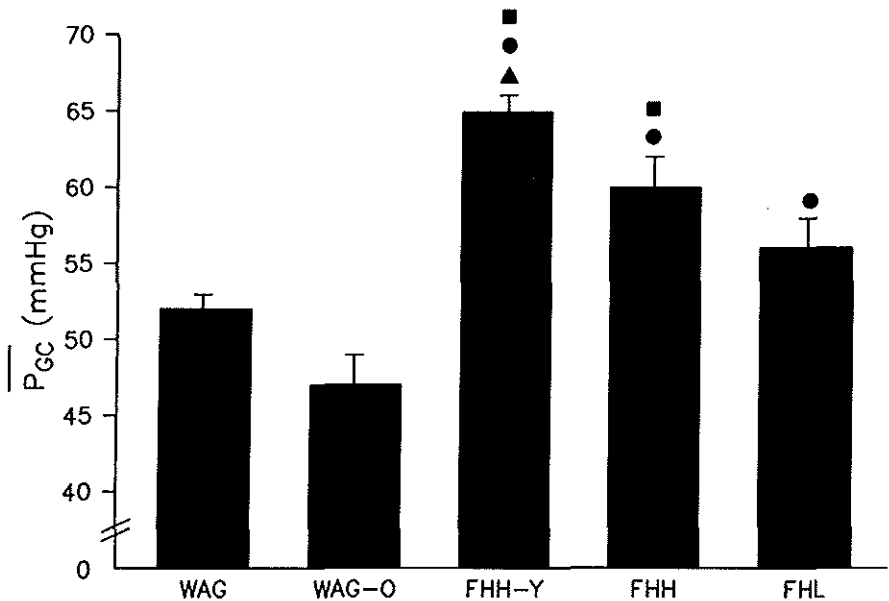


Figure 3. Mean glomerular capillary hydraulic pressure (\bar{P}_{GC}). Values are mean \pm SE. (square) $P < 0.05$ vs. WAG, (circle) $P < 0.05$ vs. WAG-O, (triangle) $P < 0.05$ vs. FHL. Values for \bar{P}_{GC} were elevated in FHH rats of all ages and were significantly higher than those for both WAG groups. FHL rats exhibited slightly increased values for \bar{P}_{GC} , which were only significantly higher as compared to WAG rats matched for body weight.

Table 1.		MAP	Hct	GFR	SNGFR	SNFF
Group	n	mm Hg	%	ml/min	nl/min	
WAG	8	120±3	44±1	1.19±0.06	47±1	0.29±0.02
WAG-O	7	116±2	47±1	1.37±0.06	52±2	0.26±0.03
FHH-Y	8	125±3	44±1	1.41±0.09	63±3	0.36±0.01
FHH	8	123±3	44±1	1.57±0.08	60±4	0.34±0.03
FHL	8	128±2	45±1	1.50±0.08	55±2	0.30±0.01
WAG vs. WAG-O		NS	NS	NS	NS	NS
WAG vs. FHH-Y		NS	NS	NS	*	NS
WAG vs. FHH		NS	NS	*	*	NS
WAG vs. FHL		NS	NS	NS	NS	NS
WAG-O vs. FHH-Y		NS	NS	NS	NS	*
WAG-O vs. FHH		NS	NS	NS	NS	NS
WAG-O vs. FHL		NS	NS	NS	NS	NS
FHH-Y vs. FHH		NS	NS	NS	NS	NS
FHH-Y vs. FHL		NS	NS	NS	NS	NS
FHH vs. FHL		NS	NS	NS	NS	NS

C _A	C _E	C _{SF}	π _A	π _E	π _{SF}	\bar{P}_{SF}	\bar{P}_{GC}	\bar{P}_T	Δ \bar{P}
----- g/dl -----			----- mm Hg -----						
5.2±0.1	7.4±0.2	5.2±0.1	16±1	28±1	16±1	36±1	52±1	13±1	39±1
5.0±0.2	6.8±0.3	4.7±0.3	15±1	25±2	14±1	34±1	47±2	11±1	36±1
5.1±0.1	7.9±0.2	5.2±0.1	16±1	32±1	16±1	49±1	65±1	13±1	52±2
5.4±0.2	8.2±0.3	5.5±0.2	18±1	34±2	18±1	43±1	60±2	12±1	48±2
5.4±0.2	7.5±0.3	5.4±0.2	17±1	29±2	18±1	39±1	56±2	13±1	43±2
NS	NS	NS	NS	NS	NS	NS	NS	NS	NS
NS	NS	NS	NS	NS	NS	*	*	NS	*
NS	NS	NS	NS	NS	NS	*	*	NS	*
NS	NS	NS	NS	NS	NS	NS	NS	NS	NS
NS	NS	NS	NS	NS	NS	*	*	NS	*
NS	*	NS	NS	*	NS	*	*	NS	*
NS	NS	NS	NS	NS	NS	NS	*	NS	NS
NS	NS	NS	NS	NS	NS	*	NS	NS	NS
NS	NS	NS	NS	NS	NS	*	*	NS	*
NS	NS	NS	NS	NS	NS	NS	NS	NS	NS

Continuation Table 1.

\bar{P}_E mm Hg	K_f nl/(s·mm Hg)	Q_A nl/min	R_A --- 10^{10} ·dyn·s·cm ⁻⁵ ---	R_E
16±1	0.048±0.003	160±9	1.93±0.15	1.23±0.08
16±1	0.066±0.011	208±24	1.56±0.20	0.77±0.09
12±1	0.036±0.001	180±12	1.54±0.10	1.70±0.12
14±1	0.045±0.004	182±14	1.66±0.21	1.54±0.18
15±1	0.053±0.010	200±8	1.59±0.08	1.08±0.07
NS	NS	NS	NS	NS
*	NS	NS	NS	NS
NS	NS	NS	NS	NS
NS	NS	*	NS	NS
*	NS	NS	NS	*
NS	NS	NS	NS	*
NS	NS	NS	NS	NS
NS	NS	NS	NS	NS
*	NS	NS	NS	*
NS	NS	NS	NS	*

Values are mean ± SE. * $P < 0.05$ between pairs; NS, $P \geq 0.05$ between pairs. MAP, mean arterial pressure; C_A and C_E , afferent and efferent arteriolar protein concentration; C_{SF} , afferent arteriolar protein concentration during stop-flow measurement; π_A , afferent arteriolar oncotic pressure; π_E , efferent arteriolar oncotic pressure; π_{SF} , afferent arteriolar oncotic pressure during stop flow measurement; \bar{P}_{SF} , mean stop-flow pressure; \bar{P}_{GC} , mean glomerular capillary hydraulic pressure; \bar{P}_T , mean intratubular hydraulic pressure; $\Delta\bar{P}$, mean glomerular transcapillary hydraulic pressure difference; \bar{P}_E , mean efferent arteriolar hydraulic pressure; K_f , glomerular capillary ultrafiltration coefficient; Q_A , glomerular capillary plasma flow rate; R_A , afferent arteriolar resistance; R_E , efferent arteriolar resistance.

Morphologic Parameters

Data for morphologic studies are presented in Table 2. Kidney weight was significantly higher in FHH and FHL rats as compared with that in WAG rats of similar age. However, when compared with that in WAG-O rats of similar weight, no significant difference was found. The heart weight reflected the level of awake systolic blood pressure in the various strains and was greatest in FHH and FHL rats. Values for \bar{V}_G were not significantly different among groups (Figure 4) and remained in the normal range (236). The percentages of glomeruli affected by sclerosis were highest in FHH and FHH-Y animals, but only values in FHH rats were significantly higher than those in both groups of WAG and FHL rats.

Table 2. Morphologic parameters.

Group	n	age wk	body weight ----- g	kidney weight ----- g	heart weight ----- g	\bar{V}_G $10^6 \mu\text{m}^3$	FSGS %
WAG	8	16	282±5	2.75±0.08	0.82±0.02	1.39±0.07	0.2±0.1
WAG-O	7	22	340±3	3.14±0.10	0.95±0.02	1.58±0.03	0.3±0.2
FHH-Y	8	8	253±9	3.21±0.10	0.96±0.03	1.62±0.04	4.1±1.0
FHH	8	16	322±5	3.64±0.19	1.23±0.09	1.65±0.07	5.5±2.1
FHL	8	16	327±14	3.45±0.14	1.14±0.04	1.55±0.07	1.4±0.3
WAG vs. WAG-O			*	NS	NS	NS	NS
WAG vs. FHH-Y			NS	NS	NS	NS	NS
WAG vs. FHH			*	*	*	NS	*
WAG vs. FHL			*	*	*	NS	NS
WAG-O vs. FHH-Y			*	NS	NS	NS	NS
WAG-O vs. FHH			NS	NS	*	NS	*
WAG-O vs. FHL			NS	NS	NS	NS	NS
FHH-Y vs. FHH			*	NS	*	NS	NS
FHH-Y vs. FHL			*	NS	NS	NS	NS
FHH vs. FHL			NS	NS	NS	NS	*

Values are mean ± SE. *, $P < 0.05$ between pairs; NS, $P \geq 0.05$ between pairs.

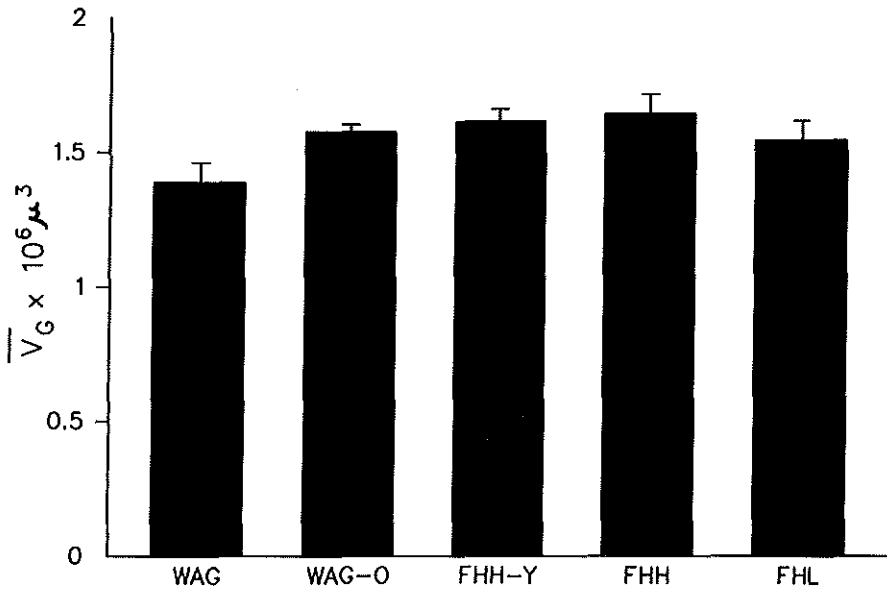


Figure 4. Average glomerular tuft volume (\bar{V}_G). Values are mean \pm SE. No significant differences in glomerular volume were found among groups.

DISCUSSION

In this study, we have examined glomerular hemodynamics as well as renal morphology in two strains of FH rats with different susceptibilities to develop systemic hypertension, proteinuria, FSGS, and subsequent CRF. The FHH strain is characterized by high values for SBP, SNGFR, \bar{P}_{GC} , R_E , and proteinuria. These parameters were found to define susceptibility to progressive glomerular sclerosis, because they were not abnormally elevated in control WAG and WAG-O rats. Values were intermediate in the FHL strain, as were degrees of glomerular sclerosis and proteinuria. Values for glomerular volume were similar in all groups and remained far below those reported in rats with diabetes and remnant kidneys (236), thereby failing to support a pathophysiologic role for hypertrophy in the pathogenesis of FSGS in FHH rats. Because rats were studied before the development of severe sclerosis, we feel confident that we did not underestimate the true value of hypertrophy as a consequence of retraction and scarring.

As in human essential hypertension, the precise cause of the spontaneous development of systemic hypertension in FH rats is not well understood. It has been

reported that FH rats have low plasma and intrarenal renin (145, 257), low urinary kallikrein excretion and renal kallikrein content (145), increased urinary output of dopamine, norepinephrine and homovanillic acid (258), altered urinary eicosanoid excretion (211), and altered volume homeostasis (340).

Because of absence of surface glomeruli in FH rats, \bar{P}_{GC} can not be evaluated by direct techniques and the indirect stop-flow technique had to be used. Debate regarding the equality of the \bar{P}_{GC} values estimated by the two approaches has been extensive. Data obtained from indirect stop-flow technique may slightly overestimate values obtained by direct measurement. The differences between stop-flow and free-flow measurements are due to a TGF response to the blockade of the flow in the loop of Henle. However, differences are usually small and present only in approximately one half of the studies (251). Activation of the TGF induced by changes in the loop of Henle flow resulted in parallel changes in directly measured \bar{P}_{GC} and \bar{P}_{SF} , confirming that differences in \bar{P}_{SF} do reflect differences in \bar{P}_{GC} (62). However, it could be argued that the significantly higher \bar{P}_{SF} values in FHH and FHH-Y rats when compared with values in weight- and age-matched WAG controls, are only present under stop-flow conditions. Without fluid delivery, there is complete suppression of the TGF and \bar{P}_{GC} and \bar{P}_{SF} reach maximal values. The observed difference could disappear under free-flow conditions if the TGF system were more active in FHH than in WAG rats. A comparison of the TGF response between both strains is needed to settle this argument.

A number of studies have used the stop-flow technique in strains of rats that do not have surface glomeruli (251), among them another hypertensive strain, the spontaneously hypertensive rat (SHR). Comparison of SHR with the normotensive Wistar-Kyoto (WKY) rat revealed no significant differences in \bar{P}_{GC} between these strains (16, 100). Thus, the SHR differs from the FHH with regard to the regulation of their glomerular hemodynamics. The presence of a normal \bar{P}_{GC} in SHR might explain the finding that, in contrast to mildly hypertensive FH rats, SHR with a markedly higher blood pressure level do not develop proteinuria and renal lesions at young age (122). The glomeruli in young SHR rats appear to be protected from high SBP by afferent vasoconstriction. However, when uninephrectomy is performed (108) or older SHR are studied (377), afferent vascular tone decreases, \bar{P}_{GC} rises, and progressive FSGS and CRF ensue.

The glomerular capillary hypertension present in FHH rats results from increased efferent arteriolar resistance in the absence of increased afferent vascular tone. The moderate systemic hypertension is thus transmitted into the glomerular capillaries and because of the high R_E , the pressure is retained in this network. The differences in SBP measured between animal groups in the awake condition were largely dissipated under anesthesia during the micropuncture experiments. It is therefore likely that \bar{P}_{GC} values are

even higher in non anesthetized FH animals. Evidence for a fundamental role of glomerular capillary hypertension in the progression of renal disease has been established in various other animal models (8, 9, 108, 112, 179, 466). This study suggests that this hemodynamic maladaptation also contributes to the development of FSGS in FHH rats.

Only a few studies in rats with spontaneous development of proteinuria and FSGS, which may represent human progressive renal disease more closely than intervention models, have been reported. Remuzzi and coworkers recently described the spontaneous development of proteinuria, FSGS, and hypertension in the male MW-Fromter rat (358). \bar{P}_{GC} was elevated, suggesting that it may have again been the main factor responsible for these pathological changes. Selective reduction of this pressure by converting enzyme inhibition resulted in protection against glomerular damage, restoration of glomerular permselectivity, and increased hydraulic membrane permeability (358). Brandis and colleagues suggested that, in rats of the Milan normotensive strain (MNS), proteinuria and FSGS occur as a consequence of alterations in intrarenal hemodynamics, in particular elevation of \bar{P}_{GC} (50). Genetically similar animals of the Milan hypertensive strain (MHS) are protected from glomerular capillary hypertension and consequent glomerulosclerosis, possibly because of thickening of the interlobular arteries, which increases R_A and thereby prevents the transmission of systemic hypertension into the glomeruli.

Kreisberg and Karnovsky first described the spontaneous occurrence of FSGS in FH rats (222). Affected glomeruli were randomly distributed in the renal cortex, with no preferential localization to the juxtamedullary area. The earliest morphologic changes were noted at the age of 6 months and consisted of extensive changes in glomerular epithelium, including foot process fusion, vacuolization, bleb formation, and focal detachment from the glomerular basement membrane. The degree of epithelial cell damage and loss of glomerular polyanion correlated with the amount of proteinuria observed. Antibody-mediated injury was not present. These authors concluded that epithelial cell damage initiates a cascade of glomerular damage and proteinuria, eventually resulting in FSGS. The importance of an intact podocyte population for the maintenance of glomerular function was emphasized by Fries and coworkers (132). In a model of progressive glomerulosclerosis induced by adriamycin and renal ablation, the degree of FSGS and proteinuria was to a great extent directly related to epithelial cell injury and density. Kriz and coworkers suggested that glomerular capillary hypertension may cause distention of capillary loops when the system responsible for the creation of counteracting wall tension fails (223). The resulting capillary dilation is then thought to reduce the relative density of visceral epithelial cells. According to this formulation, epithelial cells eventually fail and the resulting denuded portion of glomerular basement membrane creates an area for increased protein convection, which results in further glomerular damage and eventually glomerulosclerosis.

Because in the FHH rat we find that elevated glomerular hydraulic pressure predicts the subsequent development of FSGS whereas significant increase of the glomerular tuft volume does not, epithelial cell damage must result from factors other than simple stretching of podocytes over an expanded glomerular tuft area.

In conclusion, this study establishes the presence of glomerular capillary hypertension, hyperfiltration and exaggerated post-glomerular resistance as early occurrences in FHH rats. Furthermore, we were able to demonstrate that these adaptations predict the genetically determined propensity to develop proteinuria, FSGS, and CRF. FHH and FHL rat strains thus constitute a new model for progressive CRF caused by glomerular hypertension, the latter attributable directly to enhanced efferent arteriolar resistance. The basis for this early postglomerular vascular abnormality, whether structural, functional, or both, and whether genetically predetermined, merits further study.

ACKNOWLEDGMENTS

These studies were supported by a grant from the Dutch Kidney Foundation (C90.957A, A.P. Provoost), and by a grant from the NIH (DK P01-40839 to B.M. Brenner). All animal experimentation was conducted in accord with the NIH Guide for the Care and Use of Laboratory Animals. The authors are grateful to Miguel A. Zayas, Sandra J. Downes, and Myriam Lee for expert technical assistance.

Chapter 6: Experiment 2

Adapted from:

JOURNAL of the AMERICAN SOCIETY of NEPHROLOGY 4:1362-1370, 1993.

PATHOGENESIS OF GLOMERULAR INJURY IN THE FAWN-HOODED RAT: EFFECT OF UNILATERAL NEPHRECTOMY

Jacob L. Simons^{1,3}, Abraham P. Provoost³, Marinus H. De Keijzer³,
Sharon Anderson¹, Helmut G. Rennke², and Barry M. Brenner¹

With the technical assistance of:

Julia L. Troy¹, Miguel A. Zayas¹, Myriam Lee¹, Sandra J. Downes¹,
Deborah J. Sandstrom², and Matthijs van Aken³

Renal Division and Departments of Medicine¹ and Pathology²
Brigham and Women's Hospital
The Harvard Center for The Study of Kidney Diseases
Harvard Medical School, Boston, Massachusetts, USA

and

Department of Pediatric Surgery³
Erasmus University
Rotterdam, The Netherlands

Portions of these studies were presented at the 40th Scientific Meeting of the Dutch Society of Nephrology, Groningen, The Netherlands, October 27, 1990, and were published in abstract form (Kidney Int 39:1051, 1991).

ABSTRACT

Fawn-hooded (FH) rats with congenital proteinuria and systemic and glomerular hypertension are very susceptible to renal damage at a young age. In this study, the effects of unilateral nephrectomy (NX) on the function and structure of the remaining kidney in the FHH substrain were assessed. A long-term study was performed to determine the changes in systemic blood pressure, renal function, and proteinuria during the development of chronic renal failure in NX FHH and two-kidney (2K) FHH rats. Renal micropuncture and morphologic studies were performed at four weeks after surgery. The long-term study showed that, after NX, systolic blood pressure did not differ significantly from that of 2K FHH rats. After NX, there was compensatory hyperfiltration, at about 70% of the 2K level, that could be maintained for 12 weeks only. The subsequent fall in GFR was preceded by severe proteinuria. The mean survival time of NX FHH rats was only 35 weeks. Micropuncture studies showed that the high mean glomerular capillary hydraulic pressure (\bar{P}_{GC}) of 2K FHH rats was further elevated after NX. The glomerular capillary ultrafiltration coefficient (K_f) did not differ significantly between NX FHH and 2K FHH rats. The weight of the remaining kidney and the mean glomerular tuft volume (\bar{V}_G) in NX FHH were, on average, 36 and 31% greater than in 2K rats. The results indicate that the FHH rat is extremely vulnerable to the adverse renal effects of NX. A comparison of the hemodynamic and structural data of this study with those reported for other rat strains indicated that the severe glomerular hypertension, but not the degree of glomerular hypertrophy, underlies the high susceptibility to renal damage in NX FHH rats.

The rate of development of chronic renal failure (CRF) in renal ablation models varies directly with the amount of excised and/or infarcted kidney tissue (166, 206) and with the corresponding maladaptive increase in mean glomerular capillary hydraulic pressure (\bar{P}_{GC}) (11, 51, 108, 112, 179). In general, after a variable period of compensatory glomerular hyperfiltration, nephron loss results in progressive focal and segmental glomerular sclerosis (FSGS) and CRF. However, marked differences have been described in the susceptibility of different rat strains to the development of long-term sequelae after ablation (155, 339, 440, 451), suggesting that genetic factors also influence the rate of progression of CRF in such models.

The fawn-hooded (FH) rat exhibits a remarkable susceptibility to develop FSGS spontaneously at a young age (222, 228). This is associated with moderate systemic hypertension (228, 231), increased proteinuria (U_pV) (209, 210, 222, 228, 231),

glomerular hypertension (404) and glomerular hyperfiltration (209, 210). FSGS and proteinuria progress, and eventually, animals die as a result of end stage renal disease (ESRD) (210, 228). We recently detected the spontaneous occurrence of glomerular capillary hypertension and hyperfiltration in two inbred substrains of FH rats and were able to predict the development of FSGS according to the level of \overline{P}_{GC} (404). Excessive efferent arteriolar resistance in association with elevated systemic blood pressure proved to be responsible for the observed glomerular capillary hypertension. For inbreeding, FH rats were selected on the basis of differences in values for awake systolic blood pressure (SBP_{tC}) (341). Rats with the highest values for SBP_{tC} were designated FHH, and those with lowest were designated FHL. FHH rats were shown to have higher values for U_pV , \overline{P}_{GC} , and single-nephron (SN) and whole kidney GFR and more rapid development of FSGS and CRF than FHL animals (210, 341, 404).

The purpose of this study was to assess the effects of unilateral nephrectomy (NX) on the structure and function of the remaining kidney of the FHH substrain. A long-term study was done to determine the changes in renal function, proteinuria, and systemic blood pressure during the development of CRF in both NX and two-kidney (2K) FHH rats. At four weeks after surgery, renal micropuncture studies were also performed to ascertain the magnitude of changes in glomerular hemodynamics induced by the NX state. Morphologic studies were done in kidney tissue from rats used for these microcirculatory studies.

MATERIALS AND METHODS

Animal preparation, and functional, micropuncture, analytical and morphologic studies were done as described previously in Part II of this thesis.

For long-term experimentation, twenty-eight weight matched male FHH rats were operated on at the age of four to five weeks (2K, $n = 14$; NX, $n = 14$). After surgery, body weight (bw) and SBP_{tC} were monitored every two weeks. GFR and ERPF were determined as the plasma clearance of $[^{51}Cr]$ -EDTA and $[^{125}I]$ -iodohippurate, respectively, and were determined every six weeks. The method for estimation of GFR and ERPF in awake animals is further detailed in Chapter 3.3.

All data are given as means \pm SE. A t test was applied to detect differences between the mean values of 2K and NX rats in the long-term, the microcirculatory, and the morphologic studies. Statistical significance was defined as $P < 0.05$.

RESULTS

Long-term Studies

SBP_{tC} increased in both 2K and NX rats, but no significant differences were found between groups at any time point (Figure 1).

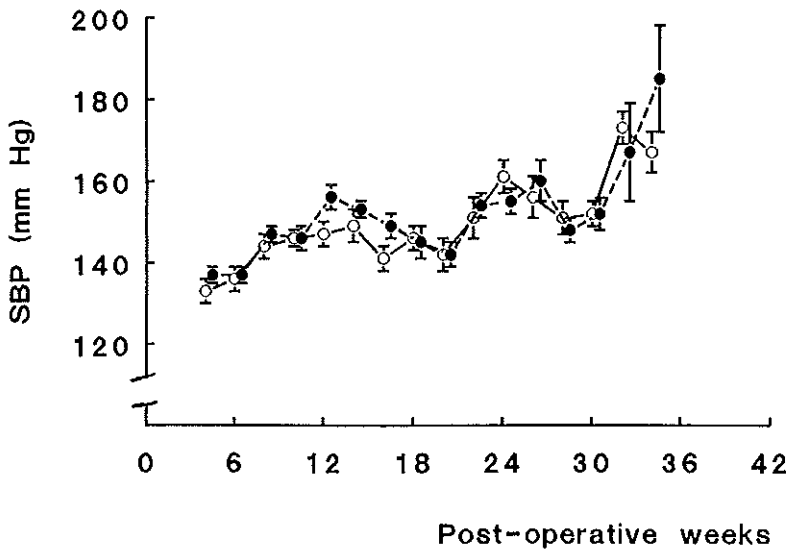


Figure 1. Long-term changes in the SBP_{TC} of 2K and NX FHH rats. Open circles, 2K rats; closed circles, NX rats. Mean \pm SE. No significant differences between 2K and NX rats.

Initially, values for GFR and ERPF in NX animals showed a compensatory rise of 40% and 60%, respectively, as compared with single-kidney values in 2K rats (Figure 2). However, from weeks 12 onwards, GFR and ERPF showed a rapid decline, and eventually all NX animals died as a result of end-stage renal failure. Mean survival time was 35 ± 7 weeks (median, 34 weeks) post-NX.

NX initially resulted in slightly higher values for P_{Cr} and P_{ur} compared with those found in 2K rats (Table 1). Values for P_{Cr} and P_{ur} increased steadily from week 12 onwards in the NX animals, whereas values for these parameters remained unaltered in 2K rats during the complete follow-up period.

In NX rats, the declines in GFR and ERPF were accompanied by a marked increase in U_pV (Figure 3). Proteinuria was also present in 2K rats, but to a much lower degree. Because of the marked reduction in GFR of NX rats after week 24, there was a slight decrease in the level of proteinuria.

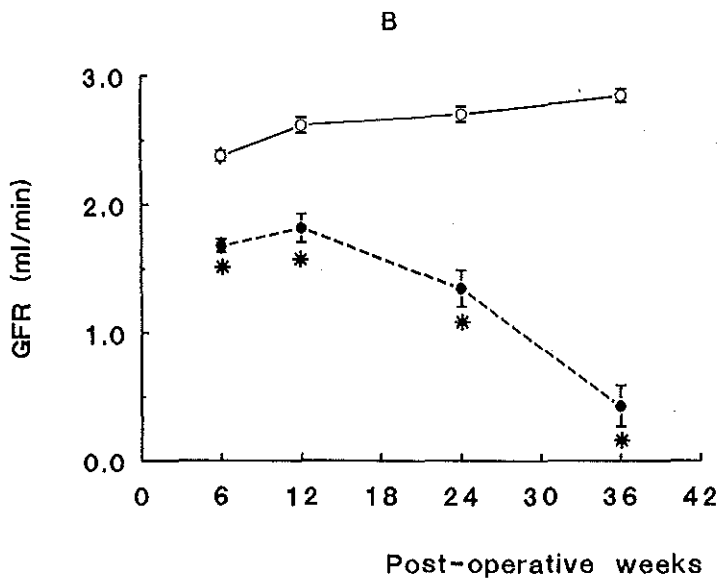
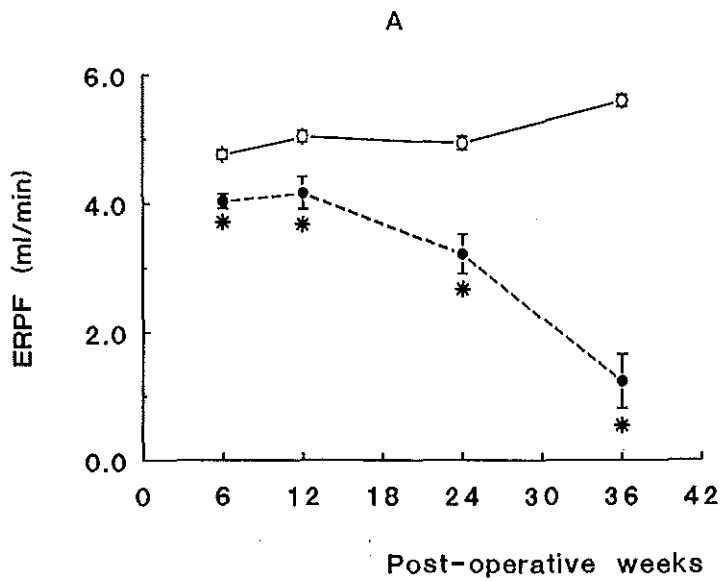


Figure 2. Long-term changes in ERPF (A) and GFR (B) of 2K and NX FHH rats. Open circles, 2K rats; closed circles, NX rats. Mean \pm SE. * $P < 0.01$ vs. 2K rats.

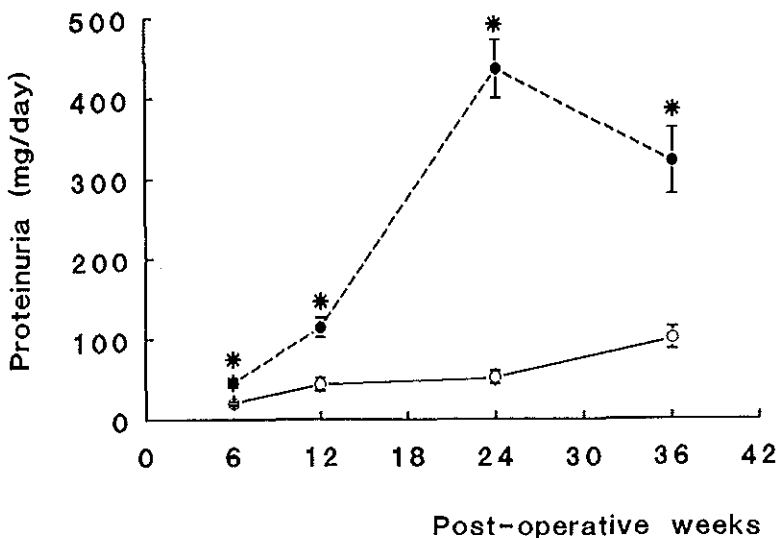


Figure 3. Long-term changes in U_pV of 2K and NX FHH rats. Open circles, 2K rats; closed circles, NX rats. Mean \pm SE. * $P < 0.01$ vs. 2K rats.

Table 1. Body weight, P_{Cr} , and P_{Ur} in the long-term study.

wk	Body weight				P_{Ur}		P_{Cr}	
	----- g -----				--- mmol/L ---		--- μ mol/L ---	
	2K	NX	2K	NX	2K	NX	2K	NX
6	252 \pm 4 (14)	237 \pm 5 (14)	4.9 \pm 0.1	6.5 \pm 0.2	33 \pm 1	39 \pm 1		
12	297 \pm 4 (14)	280 \pm 4 (14)	4.0 \pm 0.2	5.1 \pm 0.2	42 \pm 2	50 \pm 4		
24	348 \pm 4 (14)	319 \pm 5 (1/13)	5.0 \pm 0.2	12.0 \pm 1.4	35 \pm 2	55 \pm 4		
36	373 \pm 5 (14)	322 \pm 6 (7/7)	5.5 \pm 0.2	26.5 \pm 5.3	40 \pm 1	144 \pm 28		

Values are mean \pm SE. Values in parentheses, number of rats; values in parentheses with shilling construction, number of rats dead due to CRF/number of rats measured. Throughout the study, the data for body weight, P_{Ur} , and P_{Cr} of NX rats were significantly different from those of 2K rats.

Micropuncture Studies

Results are summarized in Table 2. One week before the acute micropuncture study, U_{pV} was elevated in NX as compared with 2K animals, averaging 65 ± 13 and 26 ± 3 mg/24h, respectively ($P < 0.05$). Values for SBP_e and mean arterial pressure (MAP) were not statistically different, and SBP_e values for both groups were comparable to values

Table 2. Summary data of micropuncture study.

Group	U_{pV}	SBP_e	MAP	Hct	SNGFR	SNFF	C_A	
n	mg/24h	- - mm Hg - -		%	- nl/min -		g/dl	
2K	8	26±3	159±4	122±4	44±1	62.6±2.8	0.34±0.01	5.2±0.1
NX	7	65±13*	160±4	130±3	45±1	92.1±6.4*	0.31±0.01	5.2±0.1

Continuation Table 2.

C_E	C_{SF}	π_A	π_E	π_{SF}	\bar{P}_{SF}	\bar{P}_{GC}	\bar{P}_T	$\Delta\bar{P}$
---- g/dl ----		----- mm Hg -----						
7.9±0.2	5.2±0.1	16±1	31±1	16±1	45±1	62±1	13±1	49±1
7.5±0.2	5.1±0.1	16±1	29±2	16±1	51±1*	67±1*	11±1*	56±1*

\bar{P}_E	K_f	Q_A	R_A	R_E	R_T
	nl/s.mm Hg	nl/min	----- 10^{10} ·dyn·s·cm ⁻⁵ ----		
13±1	0.041±0.002	182±9	1.50±0.11	1.51±0.10	3.01±0.19
12±1	0.045±0.003	300±19*	0.94±0.10*	0.97±0.05*	1.92±0.14*

Values are means \pm SE. * $P < 0.05$ vs. 2K rats. n, number of rats; MAP, mean arterial blood pressure; Hct, hematocrit; C_A and C_E , afferent and efferent arteriolar protein concentration; C_{SF} , afferent arteriolar protein concentration during stop-flow measurement; π_A and π_E , afferent and efferent arteriolar oncotic pressure; π_{SF} , afferent arteriolar protein oncotic pressure during stop-flow measurement; \bar{P}_T , mean intratubular hydraulic pressure; \bar{P}_E , mean efferent arteriolar hydraulic pressure; R_T , sum of R_A and R_E . See text for definitions of other abbreviations.

for SBP_{tc} found in the long-term study. SNGRF increased approximately 47% and FF tended to decrease, as a consequence of NX. No significant differences were found for C_A , C_E , and C_{SF} among groups. \bar{P}_{SF} , \bar{P}_{GC} , and $\Delta\bar{P}$ were high in 2K rats, averaging 45 ± 0.8 , 62 ± 1.0 and 49 ± 1.2 mm Hg, respectively. NX caused a significant further increase in these parameters, averaging 51 ± 1.3 , 67 ± 1.4 and 56 ± 1.5 mm Hg, respectively ($P <$

0.05). Filtration pressure disequilibrium (where $\pi_E < \Delta\bar{P}$) was present in all rats studied, and unique values for the glomerular capillary ultrafiltration coefficient (K_f) were calculated. K_f averaged 0.041 ± 0.002 and 0.045 ± 0.003 (nl / (s-mm Hg)) for 2K and NX groups, respectively, and were not statistically different. Values for initial Q_A in NX rats increased by approximately 65% compared with that in 2K rats. Despite a significant decrease in values for R_A and R_E (36 - 37%), the abnormal balance between afferent and efferent arteriolar resistance's, already present in 2K FHH rats (404), was not altered as a consequence of NX.

Renal Morphology

Results are summarized in Table 3. Left kidney weight and mean glomerular tuft volume in NX rats were, on average, 36 and 31% greater, respectively, than in 2K rats ($P < 0.05$). Values for FSGS were only numerically higher in NX rats at age 12 weeks.

Table 3. Summary of morphologic parameters.

Group	bw	left kw	total kw	\bar{V}_G	FSGS	
n	----- g -----			$10^6 \mu\text{m}^3$	%	
2K	8	278±8	1.73±0.10	3.43±0.20	1.64±0.04	3.8±0.7
NX	7	262±8	2.35±0.07*	2.35±0.07*	2.15±0.11*	10.1±2.9

Values are \pm SE. * $P < 0.05$ vs. 2K rats. n, number of rats; bw, body weight; kw, kidney weight; \bar{V}_G , mean glomerular tuft volume; FSGS, focal and segmental glomerular sclerosis.

DISCUSSION

This study demonstrates the remarkable susceptibility of the remaining kidney in NX FHH rats to progress rapidly to end-stage renal failure. The mean survival time post-NX of 35 weeks in these animals is approximately one third of that observed in a normotensive strain (WAG) submitted to NX (342). A stable GFR post-NX in WAG rats is present for 48 weeks, but this period of stability is reduced to only 12 weeks in FHH rats. A rate of decline in GFR could not be estimated for individual rats in this study, because more frequent measurements are required for such calculations. However, the changes in the mean GFR in NX FHH rats indicate a rate of decline of approximately 0.7 ml/min per 12-week period, about three times faster than reported by us in NX WAG (342). The amount of proteinuria post-NX was also much higher in FHH than in WAG animals. In NX FHH, the highest value for U_pV , more than 400 mg/day, was obtained at

24 weeks post-NX, whereas the maximum value for U_pV in NX WAG was 250 mg/day at 72 weeks post-NX (342). In accord with previous studies, NX did not increase blood pressure. However, at four weeks post-NX, the glomerular hemodynamics, already altered in 2K FHH rats with a normal number of nephrons (341), became further abnormal. The average increase in SNGFR in NX FHH animals of 47% was comparable to the increase in total GFR found in the long-term study group. The $\Delta\bar{P}$ was increased on average by 7 mm Hg, to 56 ± 1.5 mm Hg. Values found for K_f were similar in both 2K and NX groups. The \bar{V}_G can be used as a rough indicator of glomerular tuft area available for filtration. Because \bar{V}_G increased and K_f remained the same after NX, pore parameters defining molecular membrane conductivity, must have been altered. A decrease in pore density and/or an increase in pore length could explain the unaltered K_f . Values for R_A and R_E decreased proportionally as a consequence of NX. Therefore, the anomalous balance between preglomerular and postglomerular resistance, present in 2K FHH animals, remained unmodified.

Various mechanisms of glomerular adaptation to initial injury have been proposed as important in the cause and/or mediation of progressive CRF. Brenner and coworkers have postulated that intraglomerular circulatory adaptation to nephron loss and/or injury, notably an increase in \bar{P}_{GC} , is the main driving force for continuous glomerular damage (51). This hypothesis has been confirmed in numerous experimental studies of renal ablation (11, 51, 179) as well as in other experimental models. In these models, \bar{P}_{GC} is increased from the onset of the disease, and maneuvers that lower \bar{P}_{GC} protect the kidney from FSGS. Recently, the congenital occurrence of glomerular capillary hypertension in FH rats was found to predict the subsequent development of increased U_pV , FSGS, and CRF. Therefore, even if an animal has a normal number of nephrons, glomerular capillary hypertension can be present and this inborn glomerular hypertensive state can lead to progressive CRF (404). In recent years, others have surmised that growth promoters cause glomerular hypertrophy and mesangial matrix accumulation (127, 219) and may play a role in the progressive destruction of glomerular ultrastructure and function. Finally, an altered permeability of the glomerular capillary membrane to macromolecules has been postulated to contribute to glomerulosclerosis (360).

In this study, we did not compare FHH animals with a strain that is less susceptible to develop FSGS and CRF. Previous studies have established variability among rat strains in susceptibility to develop FSGS (108, 155, 451). However, none of these studies assessed both glomerular hemodynamics and morphologic parameters. We are aware that comparison with data reported from other laboratories might be speculative. Nevertheless,

we will do so in order to reveal potential differences in the responses of FHH and other less-susceptible rat strains to NX.

At four weeks post-NX, FHH rats developed a marked degree of glomerular capillary hypertension. The \overline{P}_{GC} value of 67 mm Hg in these animals is much higher than those reported for NX Munich-Wistar (MW) rats (92, 112, 179) or Wistar Kyoto (WKY) rats (108), which range from 50 to 55 mm Hg. Both strains are not very susceptible to the development of renal damage in the remaining kidney post-NX (108, 132, 178, 451). The level of glomerular hypertension in NX FHH, however, is comparable to that reported for MW rats with remnant kidneys (11, 132, 179), in which renal damage typically progresses rapidly.

At four weeks post-NX, the degree of hyperfiltration at the whole kidney level in NX FHH amounted to about 140% of the single-kidney value in 2K rats. The magnitude of the compensatory increase in FHH rats is therefore not substantially different from the increase reported for many other rat strains (92, 108, 155, 451) that are less susceptible to FSGS and CRF post-NX than are FHH rats. Consequently, the magnitude of the relative increase in GFR post-NX can not explain the differences in susceptibility to renal damage. However, the absolute level of glomerular hyperfiltration post-NX may be higher in FHH than in other strains. The value found in this study, 92 ± 6 nl/min (Table 2), is indeed much higher than usually reported for NX rats of other strains (92, 108, 112). Similarly, a Q_A value of 300 ± 19 nl/min for NX FHH (Table 2) is higher than that reported for other strains. Like the values for \overline{P}_{GC} , those for SNGFR and Q_A determined in NX FHH are closer to those reported for glomeruli remaining after three-fourths or five-sixths nephrectomy in MW rats (11, 132) than to those of NX MW rats (92, 112).

The magnitude of weight change of the remaining kidney at four weeks post-NX in FHH is comparable with values previously reported for WAG rats (344). The 40% average increase in kidney weight is similar to values reported in other strains (92, 155, 451). Therefore, whole kidney hypertrophy does not explain the increased susceptibility of the FHH strain to develop renal damage post-NX. On the glomerular level, increases in both \overline{V}_G and absolute values for \overline{V}_G post-NX in FHH were similar to those reported in other strains post-NX (155, 451). Thus, glomerular hypertrophy appears to be unimportant when accounting for differences in susceptibility between strains.

The question still remains unsolved whether compensatory glomerular growth promoters or hemodynamic alterations cause glomerular volume to increase post-NX. Hemodynamic adaptation occurs immediately post-NX, as demonstrated by the increase in both whole kidney (344, 402) and SN GFR (402) even before the increase in kidney weight is apparent. Furthermore, an early specific growth response of glomeruli is doubtful because the gene expression of growth-related proteins and extracellular matrix constituents

was unaltered in isolated glomeruli during the first week post-NX (300). However, because gene expression in total renal cortex was increased in a specific time-related fashion, this study confirmed earlier findings that renal growth post-NX consists predominantly of hypertrophy of renal tubules, rather than of glomeruli (429). Finally, a morphologic study indicated that the glomerular lesions induced by NX, i.e., the formation of irregular and giant capillary loops, were not the result of normal or compensatory growth but were secondary to failure of the mesangium (299). An increased wall tension, caused by hemodynamic changes, may initiate and maintain this capillary expansion. It may be of note that a 31% increase in \bar{V}_G , as induced by NX in this study, can be explained by just a 10% increase in capillary diameter.

Comparison of the hemodynamic and structural changes of various rat strains after NX strongly suggests the conclusion that the high susceptibility to develop renal damage in the NX FHH rat compared with other strains is defined by the level of glomerular hypertension, hyperfiltration, and hyperperfusion, but not the degree of increase in glomerular size. The question remains whether these persistent adaptive hemodynamic changes in NX FHH account solely for the high susceptibility, or whether there is an additional role for altered permeability to macromolecules in the progressive renal damage. An increased permeability due to changes in size selective and charge selective properties of the glomerular capillary wall has been reported following NX (66) and extreme ablation of renal mass (319). Proteinuria is a prominent feature in FHH rats. It is unclear whether this is solely the result of the elevated glomerular filtration pressure, flow, and filtration present in these animals, or whether alterations in size selective and/or charge selective properties of the glomerular wall and/or altered tubular handling of proteins are contributory. Substrains of FH rats with differences in U_pV also differ in rate of renal deterioration (210). The highest values for U_pV and \bar{P}_{GC} were coincident in FHH animals, whereas in FHL rats, the lowest values for these parameters were linked (404). In FHH animals, the increased proteinuria is almost exclusively due to increased urinary albumin excretion (A.P. Provoost, unpublished observation). This excludes a prominent role for an impaired tubular handling of filtered proteins and might indicate a specific alteration in charge-selective properties of the filtration barrier. Studies of the permeability of the capillary wall of FHH rats to macromolecules are needed to determine a role for size selectivity and/or charge selectivity defects in the glomeruli of FHH rats. Preliminary data from such a study indicate that 2K FHH rats have higher fractional clearances of polydisperse Ficoll, with a Stokes radius less than 50 Å, than those reported for MW rats (313, 315). In NX FHH, there was no further change in size selectivity in the 20 to 40 Å range, suggesting that the

more pronounced albuminuria post-NX results from additional defects in charge selectivity (313).

Systemic hypertension in spontaneously hypertensive rats (SHR) is much higher than in FHH animals at a similar age. The hypertension in SHR is not transmitted in the glomerular capillary network, and FSGS and renal failure are not early findings in this rat strain. However, when renal mass is reduced, the R_A decreases in SHR and allows the transmission of systemic hypertension into the glomerular capillary network (108). Subsequent renal damage, as evidenced by significant proteinuria, was present at age 23 week in NX SHR rats, at 18 weeks post-NX (108). Dworkin and Feiner used the WKY rat as a control strain for the SHR. The WKY is resistant to renal damage during aging, even post-NX. \overline{P}_{GC} in NX WKY animals remains at a level similar to that in 2K SHR rats (108). In the study presented here, we found that 2K FHH rats with relatively mild systemic hypertension have elevated values for \overline{P}_{GC} , and NX causes a further increase in this parameter. An abnormal balance in R_A and R_E is present in intact FHH rats and is not altered by NX. Renal vascular regulation of glomerular filtration might be genetically determined and thereby predispose to renal failure if \overline{P}_{GC} or $\Delta\overline{P}$ is excessive. Recent studies in humans have identified genetic factors as an important independent risk factor for the development of ESRD, secondary to hypertension and diabetes (123, 417). The different animal strains available for renal pathophysiologic studies in reference to FSGS and CRF may allow us to identify such genetic determinants, as has been the case in rats with congenital hypertension (192).

In conclusion, after NX, the FHH rat rapidly develops renal damage and this damage correlates with adaptive increases in glomerular pressure, plasma flow, and filtration rate, as well as in the size of the glomerulus. In our view, the hemodynamic changes, rather than the structural adaptation of the glomeruli, appear to underlie the high susceptibility to develop renal damage after NX in FHH rats compared as with other rat strains.

ACKNOWLEDGMENTS

These studies were supported by Grants C 88.804 and C 90.95.957A from the Dutch Kidney Foundation (to A.P. Provoost) and by a grant DK P01-40839 from the NIH (to B.M. Brenner). All animal experimentation described in the manuscript was conducted according to Dutch Law and the NIH Guide for the Care and Use of Laboratory Animals.

Chapter 7: Experiment 3

Adapted from: KIDNEY INTERNATIONAL 46:396-404, 1994.

MODULATION OF GLOMERULAR HYPERTENSION DEFINES SUSCEPTIBILITY TO PROGRESSIVE GLOMERULAR INJURY

Jacob L. Simons^{1,3}, Abraham P. Provoost³, Sharon Anderson¹,
Helmut G. Rennke², Julia L. Troy¹, and Barry M. Brenner¹

Renal Division¹ and Department of Pathology²,
Brigham and Women's Hospital,
The Harvard Center for The Study of Kidney Diseases,
Harvard Medical School,
Boston, Massachusetts, USA

and

Department of Pediatric Surgery³,
Erasmus University,
Rotterdam, The Netherlands

ABSTRACT

The fawn-hooded rat constitutes a spontaneous model for chronic renal failure with early systemic and glomerular hypertension, proteinuria (U_pV) and high susceptibility to development of focal and segmental glomerular sclerosis (FSGS). It has been argued that uninephrectomy (NX) accelerates the development of glomerular injury by aggravation of glomerular hypertension and by an independent effect to promote glomerular enlargement. The present study was performed to further delineate the importance of these parameters for the development of FSGS. At the age of eight weeks male rats were NX and randomly assigned to either control (CON), enalapril (ENA) or N^W-nitro L-arginine methyl ester (NAME) treatment. In all groups glomerular hemodynamic studies were performed four weeks post-NX. Systemic blood pressure and U_pV were monitored for 4 to 12 weeks post-NX. Kidneys were then prepared for morphologic study. ENA treatment achieved control of both systemic and glomerular hypertension, maintenance of glomerular hyperfiltration and hyperperfusion, increased ultrafiltration coefficient (K_f), and long-term protection against U_pV and FSGS. NAME rats showed aggravation of both systemic and glomerular hypertension, decreased renal perfusion and filtration with reduced K_f , and high filtration fraction. The incidence of FSGS in NAME and CON groups was similar at 8 and 12 weeks post-NX, respectively. Glomerular enlargement was present in CON and ENA rats, but did not correlate with injury, while glomerular tuft size was lowest in NAME rats, which displayed prominent glomerular injury. Systemic blood pressure correlated strongly with glomerular capillary pressure. We conclude that systemic and glomerular hypertension govern the development of U_pV and FSGS. Renal protection with converting enzyme inhibition is achieved by controlling glomerular hypertension in this highly susceptible model.

Nephron function loss, from any cause, is followed by compensatory glomerular hemodynamic and structural adaptations. Over time these changes are believed to be maladaptive and result in further deterioration of renal excretory function (51). In rat models of renal injury associated with permanent nephron loss, high glomerular capillary hydraulic pressure was found to constitute a major driving force for continuous glomerular injury with resulting focal and segmental glomerular sclerosis (FSGS) and progressive chronic renal failure (CRF) (11, 137, 179). Amelioration of the glomerular hypertensive state resulted in long term protection against glomerular injury (11, 107), even when initial glomerular damage has already occurred (276). The beneficial effect of angiotensin I

converting enzyme inhibitors (ACEI) to achieve renal protection in these studies has been attributed to the specific property of this class of drug to reduce glomerular capillary hypertension (11, 107, 276). This hemodynamic theory on progressive renal disease has been reviewed recently (306).

It has been proposed that glomerular hypertrophy, expressed as an increase in glomerular tuft size in response to renal injury or ablation predisposes to further glomerular malfunction over the long-term. This may occur as a result of increased glomerular capillary diameter with subsequent altered wall tension, according to the Laplace law, or from glomerular pressure effects on glomerular cell subpopulations or matrix (85, 289, 459).

The fawn-hooded (FH) rat is a spontaneous model for CRF, as these animals develop the major stigmata of renal disease early in life. These include moderate systemic hypertension, proteinuria (U_pV) and FSGS (222, 341). Sclerosis and U_pV progress and animals eventually die due to uremia at a relatively young age. In previous studies we detected the early occurrence of glomerular capillary hypertension and hyperfiltration in these animals, and were able to predict the development of FSGS according to the level of glomerular capillary hydraulic pressure (\overline{P}_{GC}) in two inbred substrains of FH rats (404). For inbreeding, these rats were selected based upon difference in awake tail-cuff systolic blood pressure (SBP_{tc}) level. Rats with highest values for SBP_{tc} were designated FHH, and those with lowest, FHL. FHH rats also exhibit the highest values for U_pV , \overline{P}_{GC} , and fastest development of FSGS and CRF, as compared to FHL (341, 404). In the current study we focused our interest on this FHH substrain.

We previously reported on the marked acceleration of the development of proteinuria and CRF in FHH rats after uninephrectomy (NX). The high susceptibility of FHH rats to NX was thought to be related to further increases in \overline{P}_{GC} (405). In that study, a specific role for changes in glomerular capillary tuft size as an independent risk factor for accelerated CRF could not be fully assessed. In the present study we further investigated and delineated the pathophysiological properties of glomerular hemodynamic and morphologic changes in progressive CRF. We therefore modulated systemic blood pressure (BP) in NX FHH rats with the use of either ACEI or nitric oxide (NO) synthase inhibition. Administration of ACEI in experimental models of renal disease generally results in lowering of systemic BP and \overline{P}_{GC} , and protection from renal damage (11, 107, 276). On the other hand, NO synthase inhibition induces systemic and glomerular hypertension with subsequent FSGS (28, 135). With the use of these pharmacological interventions we modulated systemic BP and studied renal hemodynamics, function and morphology.

MATERIALS AND METHODS

Forty-nine male FHH rats entered the study and were NX at eight weeks of age, and were then randomly assigned to one of three groups. Control (CON) rats were untreated. A second group received enalapril (ENA) (Merck Sharp & Dohme, West Point, Pennsylvania, USA) 250 mg/liter and a third group N^w-nitro L-arginine methyl ester (NAME) (Sigma Chemical Co., St. Louis, Missouri, USA) 50 mg/liter, both administered in the drinking water. Half the rats in each group underwent whole kidney and glomerular micropuncture hemodynamic studies four weeks post-NX. The remainder of each group was followed for long-term functional and morphologic assessment up to 12 weeks. Preliminary studies revealed that NAME rats would not survive for these 12 weeks, and accordingly were sacrificed earlier, at eight weeks post-NX. Rats were fed *ad libitum* with standard rat chow (24% protein) and received tap water with added drugs as indicated up to the time of micropuncture experiment or kidney perfusion.

For the long-term functional and histopathological studies, body weight (bw), awake systolic blood pressure (SBP_{TC}), and urinary protein excretion (U_pV) were determined before NX and every four weeks thereafter to time of kidney perfusion. Animal preparation, and functional, micropuncture, analytical, and morphological studies were done as previously described in Chapter 3. The amount of protein excreted in the urine relative to the GFR (mg/liter) was calculated as: (U_pV)/(GFR·1.44). The 24 hour U_pV, determined a few days before the micropuncture study was used in these calculations.

Values were compared by one way analysis of variance with the Scheffe's F-test for multiple comparisons. Statistical significance was defined as P < 0.05. All values represent means ± SEM. Linear regression analysis was performed for correlation between \overline{P}_{GC} and MAP, both obtained at the time of micropuncture.

RESULTS

Functional Studies

Long-term values for SBP_{TC} and U_pV are summarized in Figures 1 and 2. Before NX all animals showed similar levels for both SBP_{TC} and U_pV. After NX and initiation of therapy, control animals exhibited a moderate increase in SBP_{TC} over time, which was similar to that previously found in intact 2K FHH rats at corresponding ages (341, 405). ENA treated animals exhibited control of systemic hypertension over the duration of the study, with values for SBP_{TC} in the normotensive range. Animals in the NAME group exhibited further elevation of SBP_{TC}, with values of approximately 200 mm Hg.

As shown in Figure 2, proteinuria was increased in both CON and NAME groups, whereas ENA animals showed minimal U_pV throughout the duration of the study. U_pV in

these ENA rats was also lower than that generally observed in two-kidney FHH rats at similar ages (341).

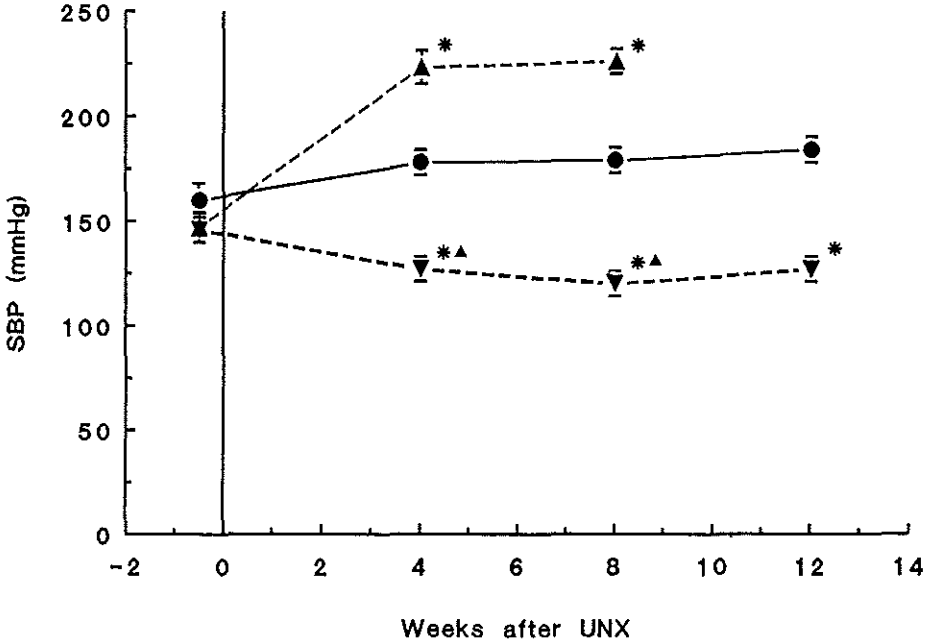


Figure 1: Systolic blood pressure (SBP_{tc}) in awake rats over long-term. Symbols are: circles, CON (n = 7); triangles tip down, ENA (n = 9); triangles tip up, NAME (n = 7). * P < 0.05 vs. CON; P < 0.05 vs. NAME.

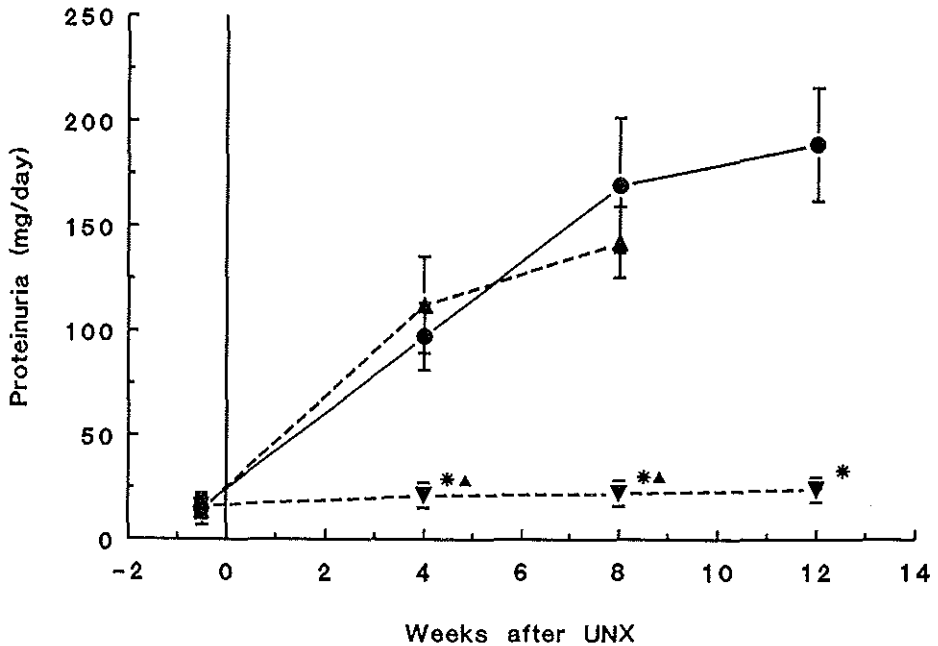


Figure 2: Urinary protein excretion (U_pV) over long-term. Symbols are: circles, CON (n = 7); triangles tip down, ENA (n = 9); triangles tip up, NAME (n = 7).

* P < 0.05 vs. CON; P < 0.05 vs. NAME.

Systemic and Renal Hemodynamic Parameters

Values for systemic and renal hemodynamic parameters at four weeks post-NX are summarized in Tables 1 and 2. Compared to CON rats, values for SBP_{TC} , SBP_E , and MAP were reduced to normotensive levels in ENA treated rats, while they were further increased in the NAME group (Table 1). Hct was significantly higher in NAME treated rats as compared to the other groups. Despite the differences in BP between CON and ENA treated rats, GFR, ERPF, and ERBF were not significantly different. On the other hand, the severely hypertensive NAME rats showed a significant decrease in GFR, ERPF, and ERBF resulting in a marked increase in FF as compared to CON and ENA. Compared to CON rats, U_pV and U_pV/GFR were reduced in ENA rats. NAME treated animals exhibited a similar level of U_pV as CON rats, but when corrected for GFR, protein excretion was significantly increased (Table 1).

Table 1. Summary whole body and kidney function parameters in rats used for micropuncture studies at 4 weeks post-NX.

	n	SBP _{tc} ----- mm Hg -----	SBP _e	MAP	Hct %	GFR ----- ml/min -----	ERPF
CON	9	169±3	161±3	129±2	45±1	1.98±0.12	6.89±0.31
ENA	8	120±4 ^a	118±2 ^a	96±3 ^a	45±1	1.86±0.18	6.42±0.51
NAME	9	219±6 ^{ab}	199±6 ^{ab}	168±6 ^{ab}	50±1 ^{ab}	1.05±0.14 ^{ab}	3.05±0.66 ^{ab}

Continuation Table 1.

FF	ERBF ml/min	RVR mm Hg/(ml/min)	U _p V mg/24h	U _p V/GFR mg/l
0.29±0.02	12.68±0.5	10.4±0.5	57±11	20.1±3.7
0.29±0.01	11.6±1.0	8.6±0.6	18±2 ^a	7.0±0.7
0.38±0.02 ^{ab}	5.9±1.1 ^{ab}	36.0±5.9 ^{ab}	52±7 ^b	41.3±8.7 ^{ab}

Values are means ± SEM. Abbreviations: SBP_{tc}, awake systolic blood pressure measured by tail-cuff; SBP_e, direct systolic blood pressure during micropuncture experiment; MAP, mean arterial pressure during micropuncture experiment; Hct, hematocrit; GFR, glomerular filtration rate; ERPF, effective renal plasma flow rate; FF, filtration fraction; ERBF, effective renal blood flow rate; RVR, whole kidney renal vascular resistance; U_pV, urinary protein excretion during 24 hours; U_pV/GFR, protein excretion corrected for the amount of glomerular filtrate.

^a P < 0.05 vs. CON

^b P < 0.05 vs. ENA.

The differences in whole kidney hemodynamics were also present at the single-nephron level (Table 2). The levels of SNGFR, Q_A, and SNFF were not significantly different between CON and ENA treated rats. Values for C_A and C_E and thus π_A and π_E were also comparable. Compared to the high hydraulic pressures obtained in CON rats, ENA treatment resulted in a significant reduction of \bar{P}_{SF} , \bar{P}_{GC} and $\Delta\bar{P}$. Absolute values for \bar{P}_{GC} in the ENA rats were comparable with those reported for normal euvolemic two-kidney Munich-Wistar (MW) rats, as determined with direct and indirect stop-flow techniques, and for other rat strains measured with stop-flow only (251). In contrast, NAME rats showed significantly lower levels of SNGFR and Q_A, and an increase in SNFF as compared to CON and ENA rats. However, NAME rats had markedly increased values for \bar{P}_{SF} , \bar{P}_{GC} and $\Delta\bar{P}$. Values for \bar{P}_{GC} in ENA rats were on average 12 mm Hg

lower than in CON rats, while these values in NAME rats were on average 14 mm Hg higher than in the CON animals. Values for R_A , R_E and R_T were only numerically lower in ENA animals as compared to CON rats. Values for R_T were increased, with R_A and R_E increased proportionally, in NAME rats as compared to CON and ENA rats.

Table 2. Summary glomerular hemodynamics at 4 weeks post-NX.

		SNGFR	SNFF	C_A	C_E	π_A	π_E
	n	nl/min		--- mg/ml ---		--- mm Hg ---	
CON	9	89.6±5.3	0.30±0.01	5.2±0.1	7.5±0.2	16±1	29±1
ENA	8	87.1±5.1	0.29±0.01	5.6±0.1	7.8±0.2	18±1	31±1
NAME	9	65.9±5.8 ^{ab}	0.38±0.02 ^{ab}	5.3±0.1	8.7±0.3 ^a	17±1	37±2 ^a

Continuation Table 2.

\bar{P}_{SF}	\bar{P}_{GC}	\bar{P}_T	$\Delta\bar{P}$	\bar{P}_E	K_f	Q_A
----- mm Hg -----					nl/(sec·mm Hg)	nl/min
51±1	67±1	11±1	56±1	13±1	0.044±0.002	296±17
37±1 ^a	55±1 ^a	12±1	44±1 ^a	14±1	0.076±0.003 ^a	304±22
64±2 ^{ab}	81±2 ^{ab}	11±1	70±2 ^{ab}	10±1 ^{ab}	0.026±0.002 ^{ab}	181±24 ^{ab}

Continuation Table 2.

R_A	R_E	R_T
----- x 10 ¹⁰ ·dyn·sec·cm ⁻⁵ -----		
0.94±0.08	0.98±0.16	1.92±0.12
0.62±0.06	0.74±0.07	1.35±0.11
2.35±0.45 ^{ab}	2.37±0.35 ^{ab}	4.71±0.77 ^{ab}

All values are means ± SEM. Abbreviations are: SNGFR, single-nephron glomerular filtration rate; SNFF, single-nephron filtration fraction; C_A , afferent arteriolar protein concentration; C_E , efferent arteriolar protein concentration; π_A , afferent arteriolar oncotic pressure; π_E , efferent arteriolar oncotic pressure; \bar{P}_{SF} , mean stop-flow pressure; \bar{P}_{GC} , mean glomerular capillary hydraulic pressure; \bar{P}_T , mean tubular hydraulic pressure; $\Delta\bar{P}$, mean glomerular transcapillary hydraulic pressure difference; \bar{P}_E , mean efferent arteriolar hydraulic pressure; K_f , glomerular capillary ultrafiltration coefficient; Q_A , initial glomerular capillary plasma flow rate; R_A , afferent arteriolar resistance; R_E , efferent arteriolar resistance; R_T , total arteriolar resistance ($R_A + R_E$).

^a $P < 0.05$ vs. CON

^b $P < 0.05$ vs. ENA

As depicted in Figure 3, a highly significant linear correlation was found between MAP and \bar{P}_{GC} ($n = 26$, $r^2 = 0.827$, $P < 0.001$). The regression equation:

$$\bar{P}_{GC} = 0.33 \cdot \text{MAP} + 25.0$$

indicates that for each mm Hg increase in MAP, \bar{P}_{GC} increases by 0.33 mm Hg.

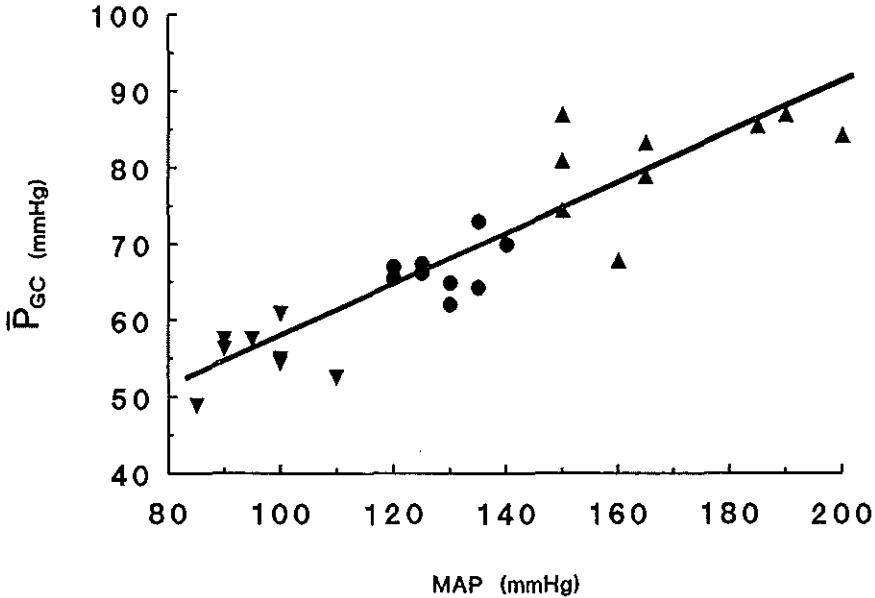


Figure 3: Correlation between mean glomerular capillary pressure (\bar{P}_{GC}) and mean arterial pressure (MAP) at the time of micropuncture. Symbols are: circles, CON; triangles tip down, ENA; triangles tip up, NAME.

Filtration pressure disequilibrium ($\pi_E/\Delta\bar{P} < 1$) was present in all experimental animals and permitted calculation of unique values for K_f . It is clear that in ENA treated rats, with a reduced \bar{P}_{GC} , a high SNGFR could only be maintained by a significant increase in K_f as compared to CON rats. In contrast, NAME treatment resulted in a marked reduction in K_f .

Morphology

Micrographs of representative glomeruli from each of the three treatment groups are given in Figure 4. Glomeruli from CON (Figure 4A, B) and NAME (Figure 4E, F) at 12 and 8 weeks post-NX, respectively, show the typical features of FSGS with segmental mesangial expansion, tuft adhesions, and sclerosis. In contrast, glomeruli from ENA treated rats still show normal glomerular morphology (Figure 4C, D) at 12 weeks post-NX.

The morphometric data are summarized in Table 3. Values for body weight (bw) were similar in CON and ENA groups at 12 weeks post-NX, and higher than those for NAME rats at eight weeks post-NX. Values for left kidney weight (LKW) were highest in CON rats, whereas values for LKW in ENA and NAME groups were comparable. Glomerular tuft size measurements revealed similar values for \bar{V}_G in CON and ENA groups, although those values far exceed \bar{V}_G values in normal two-kidney FHH rats at comparable age (404, 405). \bar{V}_G was significantly lower in NAME rats at eight weeks post-NX compared to CON or ENA at 12 weeks post-NX. Values for \bar{V}_G in NAME rats are very similar to those reported earlier in normal two-kidney FHH rats studied 4 weeks after sham operation at age 12 weeks, and in intact 2K FHH rats at age 8 and 16 weeks (404, 405). Nevertheless, NAME rats had a similar incidence of FSGS as CON rats studied at 12 weeks post-NX. ENA rats at 12 weeks post-NX showed minimal FSGS, with global preservation of the glomerular architecture, as in young two-kidney FHH rats [13].

Table 3. Summary of morphologic parameters.

		Body wt	Left kw	\bar{V}_G	FSGS
	n	----- g -----		10^6 mm^3	%
CON	7	352±6	2.90±0.11	2.52±0.12	55.5±7.8
ENA	9	338±12	2.22±0.11 ^a	2.44±0.12	2.1±0.4 ^a
NAME	7	232±15 ^{ab}	2.23±0.16 ^a	1.76±0.11 ^{ab}	59.1±5.9 ^b

Parameters were estimated at 8 weeks post-NX in NAME rats and at 12 weeks post-NX in CON and ENA rats. All values are means ± SEM. Abbreviations are: kw, kidney weight; \bar{V}_G , mean glomerular tuft volume; FSGS, percentage of glomeruli with focal and segmental glomerular sclerosis. ^a P < 0.05 vs. CON, ^b P < 0.05 vs. ENA.

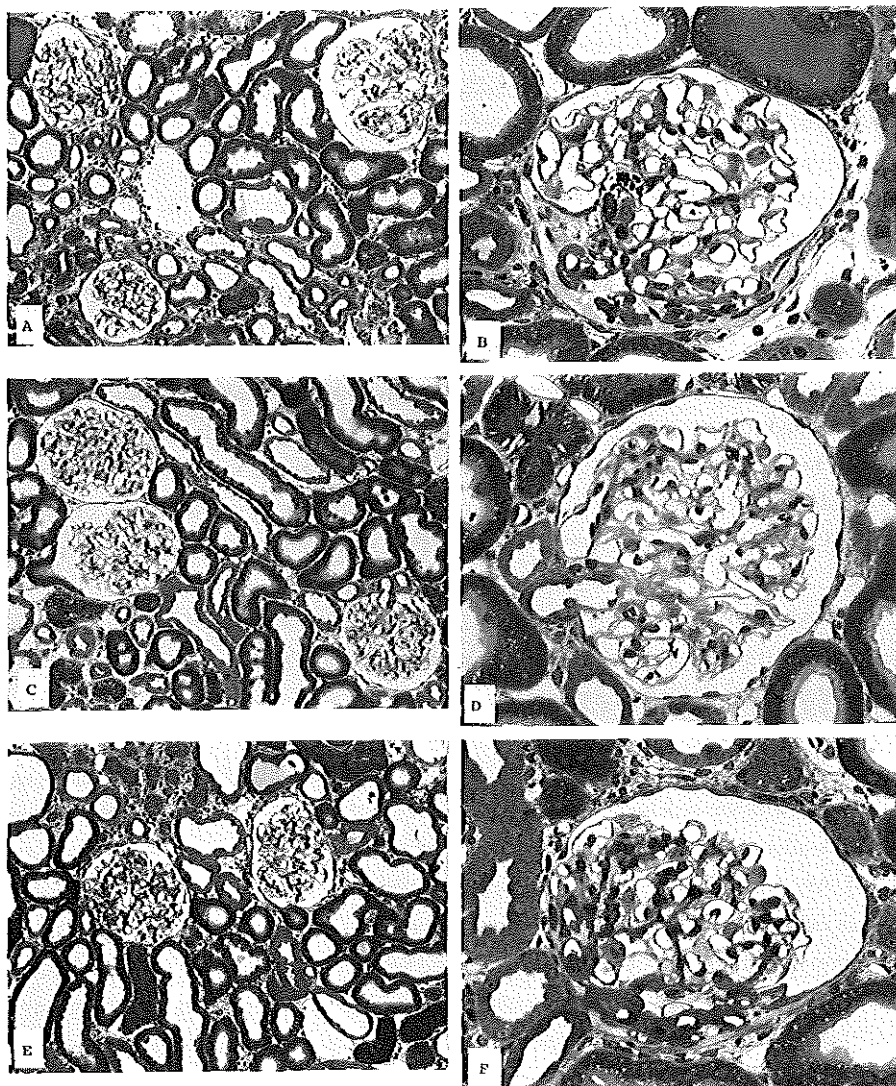


Figure 4 A-F: Representative light micrographs at low and high power magnification of glomeruli in kidneys taken from CON (A, B), and ENA (C, D) rats, at 12 weeks after unilateral nephrectomy, and from NAME (E, F) rats at 8 weeks post-NX. Plastic sections, 2 μm thick were stained with Toluidine Blue. The magnification is 120x for A, C and E, and 350x for B, D and F.

DISCUSSION

The results of the present study indicate that intraglomerular capillary pressure is an important factor in the origin of glomerular injury and sclerosis in this strain. In NX FHH, with high levels of glomerular hyperfiltration and hypertension in addition to glomerular enlargement, we observed that treatment with ACEI prevented the rise of \overline{P}_{GC} but not in glomerular size and abolished the development of renal damage. In contrast, NAME treatment which lowered values for SNGFR and \overline{V}_G but caused a further elevation in \overline{P}_{GC} , did not reduce glomerular damage. On the contrary, FSGS 8 weeks after NX in NAME rats was as severe as 12 weeks after NX in control animals. The values for \overline{P}_{GC} in ENA rats were even lower than those reported by us for young adult two-kidney FHH rats which develop severe proteinuria and early glomerular sclerosis (404), and were similar to values found for normal Munich-Wistar (MW) rats and other strains (251). Furthermore, animal models with high resistance to progressive glomerular injury such as the young two-kidney spontaneously hypertensive rat (SHR) and the uninephrectomized Wistar-Kyoto (WKY) rat, have comparable levels for \overline{P}_{GC} as the ENA group in the current study (108).

Induction of a remnant kidney state (5/6 nephrectomy) or simple NX causes a rise in \overline{P}_{GC} , SNGFR and \overline{V}_G and results in proteinuria and accelerated glomerular injury (179, 405). Glomerular size increases more than threefold after 5/6 nephrectomy (236). Recently, we reported the short- and long-term events occurring after NX in FHH rats (405). We found that both glomerular hemodynamic alterations and glomerular enlargement were associated with the accelerated development of glomerular injury. Similar glomerular size changes after NX in random-bred fawn-hooded rats were reported by Westenend *et al.* (450). Another study by these investigators revealed that ACEI therapy in intact adult rats of this random-bred fawn-hooded strain arrested the progression of glomerular injury and systemic hypertension. Although \overline{V}_G increased in both control and ACEI treated animals over the 7 months follow-up period, such changes were without pathogenic significance in ACEI treated rats (449). Microcirculatory studies were not performed in these two-kidney animals, but whole kidney vasodilatation and reduced urinary protein excretion were noted in ACEI treated rats. Thus, it is likely that ACEI treatment not only reduced systemic blood pressure, but reduced \overline{P}_{GC} as well.

Yoshida *et al.* (459) suggested that glomerular growth is an independent risk factor for progressive glomerular injury, and that the protective effect of ACEI is mainly due to its effect to limit glomerular enlargement. This hypothesis is not supported by our data. Glomerular growth, present in intact random-bred (449) and NX FHH (current study) fawn-hooded rats treated with ACEI, did not result in glomerular damage. Shrinkage of glomeruli in CON rats in the present study is unlikely, since values for \overline{V}_G in this group at

12 weeks after NX were slightly higher than the observed value in 12 weeks old NX FHH at four weeks after ablation (405). A difference in glomerular size between control and ACEI treated animals with reduced renal mass has been reported rarely. In Table 4 data are summarized from several other renal ablation studies in which glomerular hemodynamic and morphologic responses to extrinsic modulation of angiotensin II (Ang II) activity on progressive glomerular sclerosis were assessed. When Ang II formation is chronically inhibited with ACEI or when its receptors are blocked in such models, glomerular hyper-

Table 4. Effects of chronic angiotensin II modulation on glomerular hemodynamics and structure after renal ablation.

<u>Model: + Modulation:</u>	SNGFR	\bar{P}_{GC}	K _f	\bar{V}_G	FSGS	Ref.
	nl/min	mm Hg	nl/(sec.mm Hg)	10 ⁶ μm ³	%	
<u>Ang II inhibition:</u>						
NPX-MW	93±8	69±2	0.05±0.01	2.1±0.1	21±3	11
NPX-MW + ACEI	82±7	54±1 ^a	0.09±0.02 ^a	1.7±0.1 ^a	6±2 ^a	"
NPX-MW	182±37	65±2	0.12±0.03	2.0±0.1	18	107
NPX-MW + ACEI	211±17	54±3 ^a	0.26±0.04 ^a	2.0±0.2	9	"
NPX-MW	118±4	65±1	0.08±0.01	4.0±0.2	41±3	234
NPX-MW + ACEI	112±6	54±2 ^a	0.14±0.03 ^a	3.6±0.2	9±1 ^a	"
NPX-MW + LOS	107±6	56±2 ^a	0.11±0.01	3.8±0.2	9±1 ^a	"
NX-DM-MW	91±7	60±1	0.07±0.01	2.3±0.1	20±3	12
NX-DM-MW + ACEI	90±10	49±2 ^a	0.15±0.04 ^a	2.4±0.3	5±1 ^a	"
NX-FHH	90±5	67±1	0.04±0.01	2.5±0.1	56±8	*
NX-FHH + ACEI	87±5	55±1 ^a	0.08±0.01 ^a	2.4±0.1	2±1 ^a	*
<u>Ang II activation:</u>						
NX-MW	76±6	56±3	0.08±0.01	2.4±0.2	1±1	289
NX-MW + Ang II	72±10	69±6 ^a	0.05±0.01 ^a	2.2±0.2	18±10 ^a	"

Summary of measurements of single-nephron glomerular filtration rate (SNGFR), ultrafiltration coefficient (K_f), mean glomerular capillary hydraulic pressure (\bar{P}_{GC}), mean glomerular tuft volume (\bar{V}_G), and glomerular injury (FSGS) in studies assessing the effects of angiotensin II modulation in renal ablation models. All values are means ± SEM, except (289) providing means ± SD. Abbreviations: NX, uninephrectomy; NPX, remnant after 5/6 nephrectomy; MW, Munich-Wistar; FHH, fawn-hooded; ACEI, chronic angiotensin I converting enzyme inhibition; Ang II, chronic angiotensin II infusion; LOS, chronic angiotensin II receptor blockade with losartan; DM, diabetes mellitus (streptozotocin); *, this study. ^a P < 0.05 vs. untreated.

tension is controlled while glomerular hyperfiltration and enlargement are usually unaffected (11, 12, 234, 276). Invariably, animals are protected for glomerular injury and proteinuria. In contrast, when Ang II activity is increased by chronic infusion, \overline{P}_{GC} , proteinuria and FSGS are further elevated (289) despite no additional change in glomerular size.

The value for \overline{V}_G found in NAME treated rats was similar to those previously reported for intact FHH rats at comparable ages (404, 405), and smaller than the mean value seen in NX rats followed for four weeks (405). The incidence of FSGS in NAME rats eight weeks after NX was similar to that of CON rats after 12 weeks of follow-up. This probably reflects faster progression of glomerular damage in NAME animals. Thus, while glomerular size in NAME treated rats was limited, glomerular injury developed early. Of note in this respect is the possibility that the higher \overline{P}_{GC} in NAME rats may have offset any limitation in glomerular size. Therefore, our data indicate that, although a role for glomerular size changes in progressive glomerular injury in NX FHH rats cannot be completely excluded, the data do indicate that glomerular hypertrophy alone in the absence of glomerular hypertension does not confer risk.

The importance of glomerular hypertension as the driving force for proteinuria in experimental renal disease has been established in several experiments (328, 463). Hyperfiltration and hyperperfusion are maintained in ACEI treated animals (Table 4), indicating that such alterations do not lead to glomerular injury in the absence of glomerular hypertension. The data on K_f in Table 4 and NAME treated rats in the current study also provide further evidence that increased hydraulic permeability is associated with preservation of glomerular structure and function over the long-term. Furthermore, this finding supports the observation that rat strains which respond to renal mass reduction with an increase in K_f , while maintaining a normal \overline{P}_{GC} , are protected against progressive glomerular injury. The WKY rat is an example of such a response. It has been reported that the NX (108) and remnant WKY (39) show compensatory increases in SNGFR, which are mainly due to an increase in K_f , since \overline{P}_{GC} remains at a normal level. Both models of renal ablation in WKY rats are remarkably resistant to development of FSGS (39, 108).

Although still debated, Ang II is thought to act preferentially on the contraction of the post-glomerular vessels in normal circumstances (40, 186, 191). These Ang II actions on the glomerular circulation tend to become more apparent when renal mass is reduced (328). However, in chronic ACEI treated MW rats with reduced renal mass, a reduction of both R_A and R_E has been described (11, 107), whereas in chronic Ang II infusion, both resistances are enhanced (289). Also in ACEI treated rats in our present study, arteriolar resistances in pre- and postglomerular vessels tended to be lower, but no selective decrease

of R_E was found. We think that the reduction of R_A may represent the autoregulatory response to the fall in systemic BP, through a myogenic reflex, in order to maintain glomerular filtration (20). Thus the selective action of Ang II on R_E could not be identified in this NX animal model. This possibility is supported by the observation that in response to a non-pressor dose of Ang II administered via the renal artery, R_A fails to increase, but R_E and \bar{P}_{GC} do (189). Furthermore, when systemic BP is kept unaltered during acute Ang II antagonist infusion, R_E and \bar{P}_{GC} are selectively reduced (470). It is obvious, however, that we cannot exclude other mechanisms such as a structural change in the resistance vessels over long-term. The contractile properties of the mesangium are affected by Ang II, and thus may regulate K_f in vivo (40, 186, 289, 463). Since the reduction of both R_A and R_E was only numerical with ACEI, but K_f was greatly increased, it is suggested that ACEI and thus Ang II in FHH rats act on K_f to regulate glomerular ultrafiltration. In addition, the current observations do not exclude the possibility that actions of ACEI are not limited to effects on Ang II alone, but also relate to effects on other vasoactive substances (470).

Animals treated with the NO synthase blocker exhibited high systemic BP, heavy proteinuria, further elevation of the ultrafiltration pressure with decreased K_f , and high incidence of FSGS after only eight weeks of treatment. Glomerular filtration and perfusion were diminished and SNFF increased. Total RVR was increased threefold, and proportional increases in R_A and R_E were observed. These observations accord well with previous reports in both 2K (28, 135) and remnant MW rats (134). Finally, hematocrit was increased in NAME-treated rats, which may have contributed to the further elevation of systemic and glomerular pressures, vascular resistances and concomitant glomerular injury (137).

We observed that treatment with ACEI in NX FHH rats prevented the development of heavy proteinuria, which is otherwise present in two-kidney FHH rats at comparable ages and, in the current study, in NX CON and NAME rats. The total proteinuria in NAME treated rats did not increase above values found in controls. However, the reduction in GFR may explain the lower U_pV . Indeed, when proteinuria is corrected for GFR, one observes a greatly elevated protein excretion in NAME-treated rats. Thus hydraulic permeability is diminished, while the permeability for protein is increased. Preliminary studies on the glomerular permselectivity indicated that the proteinuria resulted mainly from changes in charge selectivity. Amelioration of glomerular hypertension corrected this defect and abolished proteinuria (313).

During the acute hemodynamic studies, MAP and \bar{P}_{GC} were closely correlated. For each 10 mm Hg increase in MAP, \bar{P}_{GC} increased by 3.3 mm Hg (Figure 3). This is in contrast to values found in two-kidney MW rats and NX SHR rats, in which a 10 mm Hg systemic BP change led to \bar{P}_{GC} changes of 0.5 mm Hg (329) and 1.0 mm Hg (109, 111),

respectively. This may indicate that in NX FHH rats the mechanism to maintain constancy at \overline{P}_{GC} is less effective, exposing the glomerular capillaries directly to systemic BP variations. It remains to be determined, however, whether observed \overline{P}_{GC} differences among groups are to some extent due to suppression of the tubuloglomerular feedback during stop-flow conditions or due to altered autoregulation as a consequence of NX (329). Various reports suggest that the endothelial NO synthase system and the renin-angiotensin system interact as regulators of the glomerular microcirculation (311, 348). Therefore, the NAME and ENA treated groups in our study might represent the extremes of a continuum of activity of these two systems combined. Any disturbance of the delicate balance in the regulation of glomerular ultrafiltration might result in glomerular malfunction.

Taken together, we demonstrated the importance of glomerular hemodynamic alterations for the development of FSGS, progressive proteinuria, and CRF in this highly susceptible NX FHH model. By use of two different modulators of systemic BP and consequently \overline{P}_{GC} , we observed a strong association with glomerular pressure and glomerular injury. Data on \overline{V}_G in the current study indicated that glomeruli in rats treated with ACEI responded to NX with enlargement of the glomerular tuft, but this process did not result in glomerular injury. Rats treated with NAME had a lower \overline{V}_G , but showed a high incidence of sclerosis after a follow-up of only eight weeks. These observations indicate that changes in glomerular tuft size are poorly associated with the formation of FSGS in this model. Since the two-kidney FHH rat develops FSGS and uremia early in life, the 12 week follow-up after NX can be interpreted as a significant time in the life span of a rat from this strain. We therefore believe that with the use of this model in the current study, we allowed all measured pathophysiological mechanisms to be fully expressed. Our results strongly suggest that the high intraglomerular pressure is the predominant cause of proteinuria and FSGS in the NX FHH rat.

ACKNOWLEDGMENTS

These studies were conducted with support from the Dutch Kidney Foundation (C90.95.957A, A.P. Provoost) and the National Institutes of Health (DK P01-40839, B.M. Brenner), and were presented in part at the 8th Scientific Meeting of the American Society of Hypertension (Am J Hypertens 6:5A, 1993) and the 12th International Congress of Nephrology (Abstract book:51, 1993). Enalapril was provided by Charles S. Sweet, Ph.D. (Merck Sharp & Dohme Research Laboratories, West Point, Pennsylvania, USA). The technical assistance of Miguel A. Zayas, Myriam Lee, Sandra T. Downes, and Deborah J. Sandstrom is acknowledged.

Chapter 8: Experiment 4

Adapted from:

AMERICAN JOURNAL of PHYSIOLOGY,
267 (Renal Fluid Electrolyte Physiol. 36) 1994, in press.

PROTEINURIA AND IMPAIRED GLOMERULAR PERMSELECTIVITY IN UNINEPHRECTOMIZED FAWN-HOODED RATS

James D. Oliver III¹, Jacob L. Simons^{2,3}, Julia L. Troy²,
Abraham P. Provoost³, Barry M. Brenner², and William M. Deen¹

Department of Chemical Engineering¹
Massachusetts Institute of Technology
Cambridge, MA 02139

Laboratory of Kidney and Electrolyte Physiology²
Brigham and Women's Hospital
and Harvard Medical School
Boston, MA 02115

Department of Pediatric Surgery³
Erasmus University
Rotterdam, The Netherlands

ABSTRACT

Previous studies of glomerular permselectivity have indicated that both size selectivity and charge selectivity changes play a role in the pathogenesis of proteinuria. In this study, we measured Ficoll sieving coefficients, hemodynamic parameters, and urinary protein excretion rates in the FHH strain of fawn-hooded rats. These animals spontaneously develop systemic and glomerular hypertension, proteinuria, and focal and segmental glomerulosclerosis at a relatively young age. Three groups of FHH rats were studied: two-kidney controls (2K), untreated uninephrectomized rats (CON-NX), and uninephrectomized rats treated with the angiotensin I converting enzyme inhibitor enalapril (ENA-NX). CON-NX rats had higher glomerular transcapillary pressures ($\Delta\bar{P}$) and higher urinary excretion rates of both total protein (U_pV) and albumin (U_aV) than did the 2K rats, whereas treatment with enalapril prevented both glomerular hypertension and the increased proteinuria. Ficoll sieving coefficients were significantly higher in both groups of NX rats compared to 2K rats only for Stokes-Einstein radii (r_s) $\geq 46 \text{ \AA}$. Fits of sieving data to pore models showed a small increase in the number of large, nonselective pores in NX, which was not prevented by enalapril treatment. Total clearances of Ficoll with $r_s = 36 \text{ \AA}$ (the size of albumin) in the CON-NX and ENA-NX groups were unchanged compared to 2K animals. In contrast, U_aV in CON-NX rats was more than six times that of the 2K and ENA-NX rats. Across groups, U_pV , U_aV , and the ratio $(U_aV)/(U_pV)$ all correlated strongly with $\Delta\bar{P}$. The change in pore-size distribution did not significantly contribute to the rise in U_aV ; therefore, the primary cause of albuminuria appears to have been a reduction in the charge barrier to macromolecular filtration. These findings suggest that increased albuminuria in NX fawn-hooded rats results from a specific defect in glomerular charge selectivity, rather than size selectivity, induced by chronic glomerular hypertension, and that enalapril ameliorates albuminuria by preserving glomerular charge-selectivity.

Proteinuria is one of the defining features of chronic renal failure. In both experimental and clinical studies of chronic renal failure, proteinuria has been associated with a loss in the ability of the glomerulus to restrict filtration on the basis of glomerular size (91, 251). Investigators have shown this usually by measuring the sieving coefficient (filtrate-to-plasma concentration ratio, Θ) of neutral dextran covering a wide range of molecular radii and using the results to infer the effective pore radius or pore-size distribution of the glomerular capillary wall. A frequent finding in proteinuric states is that the sieving coefficients of the largest dextran molecules, those with Stokes-Einstein radius (r_s) > 50

\AA , are selectively elevated. This suggests that an increase in the number of large, less restrictive pores augments filtration of proteins. The normal glomerular filtration barrier also exhibits charge-selective properties: anionic macromolecules have lower values of Θ than do neutral macromolecules of equivalent size and configuration, and values of Θ for neutral macromolecules are lower than those for comparable polycations (156, 251, 269). In several animal models of chronic renal disease, the sieving coefficients of anionic macromolecules are increased compared with that of controls, whereas those of cationic macromolecules are decreased (251), such that there is less difference in Θ among molecules of varying charge. Recently, loss of glomerular charge-selectivity has been found to partially explain proteinuria in nephrotic humans (156).

In a recent study (315) we concluded that effective pore sizes calculated from dextran sieving coefficients are overestimates of the true sizes. The transport properties of dextran, a flexible, linear polymer of D-glucopyranose, deviate considerably from those of neutral, solid sphere (46, 87), the theoretical ideal on which the mathematical models for filtration have been based. As evidence of this, dextran sieving coefficients at $r_s = 30 \text{ \AA}$ are approximately seven times that of neutral horseradish peroxidase (HRP), a globular protein of equivalent size (367). It is thus problematic, using data from dextran studies, for one to quantitatively correlate levels of proteinuria to specific changes in pore size. Ficoll, an uncharged cross-linked copolymer of sucrose and epichlorohydrin, is postulated to be a better probe molecule for determining pore size (315). Like dextran, Ficoll is neither secreted nor reabsorbed by the renal tubules, and therefore its sieving coefficient is equal to its fractional clearance (i.e., the ratio of its clearance to that of inulin) (45). Its physical properties are consistent with the solid-sphere assumptions of the theoretical model (45, 46, 87), and Ficoll sieving coefficients are similar to those of neutral globular proteins of the same molecular size (315). Ficoll sieving coefficients are much lower than those for dextran (45, 315), indicating that the glomerular filtration barrier is more size restrictive than has been previously believed.

In this study, we report on Ficoll sieving measurements performed in the FHH substrain of fawn-hooded rats. These animals are genetically predisposed to developing systemic and glomerular hypertension, proteinuria, and focal glomerulosclerosis at a young age (222, 338, 404) and as such may be a more suitable model of human chronic renal failure than experimental models of induced kidney disease. Unilateral nephrectomy of FHH rats results in a further increase of the transmural hydraulic pressure difference ($\Delta \bar{P}$), which accelerates the progression of renal disease (403, 405). Concomitant with the rise in $\Delta \bar{P}$, elevations were observed in whole kidney and single-nephron plasma flows and whole kidney and single-nephron glomerular filtration rates (SNGFR), but these changes

were without pathological significance (403, 405). Proteinuria and glomerulosclerosis can be prevented in nephrectomized rats by treatment with enalapril, an angiotensin I converting enzyme inhibitor (ACEI) (403). In an attempt to further elucidate the mechanism of enhanced protein excretion in FHH rats, we assessed glomerular permselectivity in intact and uninephrectomized (NX) animals, and studied the effect of enalapril treatment on glomerular permselectivity in NX rats.

MATERIALS AND METHODS

Male FHH rats were bred at the animal facilities of the Erasmus University Medical School, Rotterdam, The Netherlands. After weaning they were shipped to the Laboratory of Kidney and Electrolyte Physiology at Brigham and Women's Hospital, Boston, Massachusetts, USA, where the animal studies were performed. Further details on animal characteristics are provided in Chapters 2.1 and 3.1. A total of 30 rats were studied. At eight weeks of age, all rats underwent either right nephrectomy or a sham operation. All micropuncture and sieving studies were performed at 12 weeks of age.

The animals were randomly divided into three groups. The first group (2K, $n = 13$) consisted of normal two-kidney control animals which underwent the sham operation. After the operation, they resumed a diet of *ad libitum* standard rat chow (Wayne Rodent Blox; Allied Mills, Chicago, Illinois, USA) with free access to water. Five of these animals underwent sieving studies only, without micropuncture or measurement of urinary protein excretion; four underwent both micropuncture and sieving studies, without measurement of protein excretion; the remaining four underwent micropuncture and measurement of protein excretion, without sieving studies.

A second group of animals (CON-NX, $n = 9$) underwent NX and remained on the standard diet and drinking water. The third group of rats (ENA-NX, $n = 8$) also underwent NX, but after surgery were given a water supply containing 250 mg/L enalapril (Merck, Sharp & Dohme, West Point, Pennsylvania, USA) in addition to the standard diet. Micropuncture, sieving studies, and measurements of total urinary protein (U_pV) were performed on all rats in the NX groups.

Protocols for nephrectomy, functional studies, whole kidney and glomerular hemodynamic assessment, and sample analysis are provided in Chapter 3.

RESULTS

Hemodynamic Data

The mean values and standard errors of various systemic and whole kidney quantities, as well as single-nephron pressures and flows, are shown for each group in Table 1. The results for the 2K group were not substantially different from those reported

in earlier studies with this strain of rats (404). The hemodynamic data for the NX groups have been discussed previously (403, 405). Briefly, untreated NX resulted in adaptive hyperperfusion and hyperfiltration in the remaining kidney, as values for whole kidney or single-nephron plasma flows, whole kidney or nephron GFR, the K_f , and $\Delta\bar{P}$ were all significantly elevated ($P < 0.05$) in the CON-NX group compared to 2K rats. Filtration fraction (whole kidney or single-nephron) was not different among groups. Treatment of NX rats with enalapril (ENA-NX group) lowered systemic arterial pressure and $\Delta\bar{P}$, although hyperperfusion and hyperfiltration were present to the same extent as in the untreated, NX group. The high filtration rates in the ENA-NX rats, where $\Delta\bar{P}$ was even lower than in the 2K group, resulted from a marked increase in K_f . There was a modest difference in C_A between CON-NX and ENA-NX rats, which was most likely due to chance. This difference had a negligible effect on the calculation of pore-size parameters.

Table 1. Hemodynamic results.

	<u>2K</u> (n = 13)	<u>CON-NX</u> (n = 9)	<u>ENA-NX</u> (n = 8)
Body weight, g	272±8	265±7	260±8
MAP, mm Hg	123±2 ^(E)	129±2 ^(E)	96±3 ^(KC)
Hematocrit	43.3±0.7	45.3±0.5	44.5±0.6
GFR, ml/min/kidney	1.24±0.04 ^(CE)	1.98±0.12 ^(K)	1.86±0.18 ^(K)
RPF, ml/min/kidney	4.94±0.15 ^(CE)	6.89±0.31 ^(K)	6.42±0.51 ^(K)
FF	0.25±0.01	0.28±0.01	0.29±0.01
SNGFR, nl/min	53.3±2.9 ^{(CE)*}	85.6±5.5 ^(K)	87.3±5.0 ^(K)
Q _A , nl/min	171±11 ^{(CE)*}	296±17 ^(K)	304±2 ^(K)
SNFF	0.32±0.01 [*]	0.30±0.01	0.29±0.01
C _A , g/dl	5.3±0.1	5.2±0.1 ^(E)	5.6±0.1 ^(C)
$\Delta\bar{P}$, mm Hg	48.7±1.0 ^{(CE)*}	55.9±1.2 ^(KE)	43.6±1.2 ^(KC)
K _f , nl/min/mm Hg	2.08±0.11 ^{(CE)*}	2.66±0.13 ^(KE)	4.57±0.20 ^(KC)

Values are means ± SE; n, no. of experiments (*n = 8). MAP, mean arterial pressure; GFR, glomerular filtration rate; RPF, renal plasma flow; FF, filtration fraction; SNGFR, single-nephron GFR; Q_A, glomerular plasma flow rate; SNFF, single-nephron FF; C_A, plasma protein concentration; $\Delta\bar{P}$, transmural hydraulic pressure difference; K_f, ultrafiltration coefficient. Groups: 2K, 2-kidney controls; CON-NX, untreated uninephrectomized rats; ENA-NX, enalapril-treated uninephrectomized rats.

Superscripted letters indicate $P < 0.05$: ^K, vs. 2K; ^C, vs. CON-NX; ^E, vs. ENA-NX.

Ficoll Fractional Clearances

Ficoll sieving coefficients for each group are shown in Table 2 and Figure 1. Values were measured over the range $r_s = 20 - 70 \text{ \AA}$, with Θ approximately equal to 0.7 - 0.9 at $r_s = 20 \text{ \AA}$ and Θ approximately equal to $10^{-4} - 10^{-3}$ at $r_s = 70 \text{ \AA}$. The variances in Θ for each group were shown to be unequal by statistical analysis, violating a requirement for ANOVA (220). A logarithmic transformation of the data satisfied this criterion, and therefore one-way ANOVA was performed on the values of $\log \Theta$ to determine significance. No statistical differences were seen between groups for the smaller Ficoll radii, $r_s < 42 \text{ \AA}$. For $r_s \geq 42 \text{ \AA}$, values of Θ for the CON-NX group were significantly higher ($P < 0.05$) than those for the 2K group, by factors of approximately 5 to 13. Sieving coefficients for the ENA-NX rats lay between those of the other two groups for $r_s \geq 42 \text{ \AA}$ and were significantly larger ($P < 0.05$) than the 2K values for $r_s \geq 46 \text{ \AA}$. There was no statistical difference in Θ between the CON-NX and ENA-NX groups at any value of r_s .

Pore-size Parameters

Membrane pore-size parameters were fitted to the sieving data of Table 2 using the single-nephron hemodynamic data of Table 1. The results for the isoporous-plus-shunt, lognormal, and lognormal-plus-shunt models are shown in Table 3. For each group of rats, the lognormal-plus-shunt model gave the best fit to the sieving data, as indicated by the lowest value of χ^2 . The isoporous-plus-shunt and lognormal models were approximately equivalent. The better performance of the lognormal-plus-shunt model is consistent with previous results from Munich-Wistar rats, although in that case the lognormal model was clearly superior to the isoporous-plus-shunt model (315). The improvement in χ^2 by the lognormal-plus-shunt model over either of the two-parameters models was highly significant for all three of the present groups ($p < 0.001$), as judged by an F-test comparison (295). The best-fit sieving curves computed using the lognormal-plus-shunt model are shown in Figure 1.

For any given model there were mostly minor differences among the pore-size parameters computed for the three groups of rats. In the isoporous-plus-shunt model, r_0 was nearly constant, ranging between 47 and 49 \AA among the groups. The shunt parameter ω_0 was increased by more than an order of magnitude in the CON-NX group compared with the 2K group, from 1.5×10^{-4} to 3.2×10^{-3} . The ENA-NX group had a smaller but still substantial increase in ω_0 , to 9.7×10^{-4} . For the lognormal and lognormal-plus-shunt models, the pore-size distributions are most easily compared by calculation of r^* (1%) (352). This is the pore size such that 1% of the filtrate passes through the pores with $r > r^*$. It indicates the relative prominence of larger pores in the distribution: the larger the

Table 2. Ficoll sieving coefficients.

r_s (Å)	2K (n = 9)	CON-NX (n = 9)	ENA-NX (n = 8)
20	$8.51 \times 10^{-1} \pm 9.04 \times 10^{-2}$	$7.36 \times 10^{-1} \pm 7.04 \times 10^{-2}$	$9.34 \times 10^{-1} \pm 9.00 \times 10^{-2}$
22	$7.74 \times 10^{-1} \pm 8.09 \times 10^{-2}$	$6.73 \times 10^{-1} \pm 5.97 \times 10^{-2}$	$8.59 \times 10^{-1} \pm 8.37 \times 10^{-2}$
24	$6.51 \times 10^{-1} \pm 7.02 \times 10^{-2}$	$5.61 \times 10^{-1} \pm 4.89 \times 10^{-2}$	$7.40 \times 10^{-1} \pm 7.13 \times 10^{-2}$
26	$5.03 \times 10^{-1} \pm 5.28 \times 10^{-2}$	$4.47 \times 10^{-1} \pm 3.48 \times 10^{-2}$	$5.91 \times 10^{-1} \pm 5.60 \times 10^{-2}$
28	$3.60 \times 10^{-1} \pm 3.32 \times 10^{-2}$	$3.37 \times 10^{-1} \pm 2.32 \times 10^{-2}$	$4.39 \times 10^{-1} \pm 4.34 \times 10^{-2}$
30	$2.71 \times 10^{-1} \pm 3.75 \times 10^{-2}$	$2.47 \times 10^{-1} \pm 1.76 \times 10^{-2}$	$3.08 \times 10^{-1} \pm 3.25 \times 10^{-2}$
32	$1.70 \times 10^{-1} \pm 1.76 \times 10^{-2}$	$1.76 \times 10^{-1} \pm 1.23 \times 10^{-2}$	$2.16 \times 10^{-1} \pm 2.25 \times 10^{-2}$
34	$1.07 \times 10^{-1} \pm 1.25 \times 10^{-2}$	$1.23 \times 10^{-1} \pm 1.18 \times 10^{-2}$	$1.44 \times 10^{-1} \pm 1.53 \times 10^{-2}$
36	$7.02 \times 10^{-2} \pm 8.15 \times 10^{-3}$	$8.78 \times 10^{-2} \pm 1.01 \times 10^{-2}$	$9.55 \times 10^{-2} \pm 1.13 \times 10^{-2}$
38	$4.24 \times 10^{-2} \pm 4.95 \times 10^{-3}$	$6.10 \times 10^{-2} \pm 8.45 \times 10^{-3}$	$6.36 \times 10^{-2} \pm 8.16 \times 10^{-3}$
40	$2.59 \times 10^{-2} \pm 3.61 \times 10^{-3}$	$4.19 \times 10^{-2} \pm 7.36 \times 10^{-3}$	$4.20 \times 10^{-2} \pm 6.09 \times 10^{-3}$
42	$1.57 \times 10^{-2} \pm 2.44 \times 10^{-3}(C)$	$3.06 \times 10^{-2} \pm 6.12 \times 10^{-3}(K)$	$2.78 \times 10^{-2} \pm 4.55 \times 10^{-3}$
44	$9.51 \times 10^{-3} \pm 1.60 \times 10^{-3}(C)$	$2.22 \times 10^{-2} \pm 5.12 \times 10^{-3}(K)$	$1.87 \times 10^{-2} \pm 3.25 \times 10^{-3}$
46	$5.64 \times 10^{-3} \pm 1.04 \times 10^{-3}(CE)$	$1.64 \times 10^{-2} \pm 4.34 \times 10^{-3}(K)$	$1.31 \times 10^{-2} \pm 2.53 \times 10^{-3}(K)$
48	$3.49 \times 10^{-3} \pm 6.85 \times 10^{-4}(CE)$	$1.24 \times 10^{-2} \pm 3.69 \times 10^{-3}(K)$	$9.39 \times 10^{-2} \pm 2.08 \times 10^{-3}(K)$
50	$2.29 \times 10^{-3} \pm 4.73 \times 10^{-4}(CE)$	$9.79 \times 10^{-3} \pm 3.23 \times 10^{-3}(K)$	$7.15 \times 10^{-3} \pm 1.75 \times 10^{-3}(K)$
52	$1.51 \times 10^{-3} \pm 3.37 \times 10^{-4}(CE)$	$7.97 \times 10^{-3} \pm 2.96 \times 10^{-3}(K)$	$5.48 \times 10^{-3} \pm 1.46 \times 10^{-3}(K)$
54	$1.03 \times 10^{-3} \pm 2.46 \times 10^{-4}(CE)$	$6.59 \times 10^{-3} \pm 2.71 \times 10^{-3}(K)$	$4.28 \times 10^{-3} \pm 1.22 \times 10^{-3}(K)$
56	$7.46 \times 10^{-4} \pm 1.93 \times 10^{-4}(CE)$	$5.52 \times 10^{-3} \pm 2.47 \times 10^{-3}(K)$	$3.31 \times 10^{-3} \pm 9.88 \times 10^{-4}(K)$
58	$5.46 \times 10^{-4} \pm 1.44 \times 10^{-4}(CE)$	$4.67 \times 10^{-3} \pm 2.23 \times 10^{-3}(K)$	$2.68 \times 10^{-3} \pm 8.67 \times 10^{-4}(K)$
60	$4.01 \times 10^{-4} \pm 9.84 \times 10^{-5}(CE)$	$4.00 \times 10^{-3} \pm 2.03 \times 10^{-3}(K)$	$2.19 \times 10^{-3} \pm 7.60 \times 10^{-4}(K)$
62	$3.09 \times 10^{-4} \pm 7.28 \times 10^{-5}(CE)$	$3.43 \times 10^{-3} \pm 1.86 \times 10^{-3}(K)$	$1.80 \times 10^{-3} \pm 6.46 \times 10^{-4}(K)$
64	$2.48 \times 10^{-4} \pm 5.67 \times 10^{-5}(CE)$	$3.00 \times 10^{-3} \pm 1.70 \times 10^{-3}(K)$	$1.49 \times 10^{-3} \pm 5.45 \times 10^{-4}(K)$
66	$2.04 \times 10^{-4} \pm 4.19 \times 10^{-5}(CE)$	$2.65 \times 10^{-3} \pm 1.54 \times 10^{-3}(K)$	$1.24 \times 10^{-3} \pm 4.74 \times 10^{-4}(K)$
68	$1.72 \times 10^{-4} \pm 3.11 \times 10^{-5}(CE)$	$2.32 \times 10^{-3} \pm 1.39 \times 10^{-3}(K)$	$1.05 \times 10^{-3} \pm 4.23 \times 10^{-4}(K)$
70	$1.50 \times 10^{-4} \pm 2.59 \times 10^{-5}(CE)$	$2.03 \times 10^{-3} \pm 1.25 \times 10^{-3}(K)$	$8.92 \times 10^{-4} \pm 3.71 \times 10^{-4}(K)$

Values are means \pm SE. r_s , Stokes-Einstein radius.

Superscripted letters indicate $P < 0.05$: K, vs. 2K; C, vs. CON-NX; E, vs. ENA-NX.

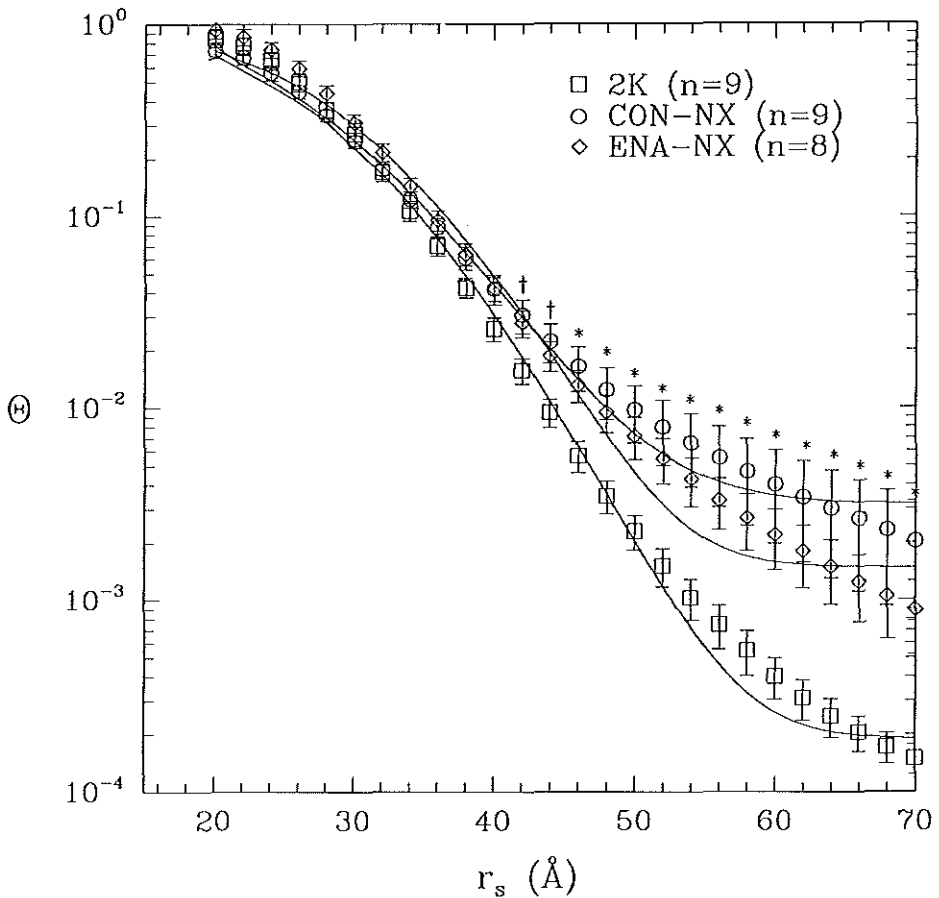


Figure 1. Sieving coefficients (Θ) for Ficoll in fawn-hooded rats as a function of Stokes-Einstein radius (r_s). The symbols and error bars are measured values \pm SE. The curves were calculated from lognormal-plus-shunt model. See Materials and Methods for complete description of groups. $^+$ $P < 0.05$ for CON-NX vs. 2K; * $P < 0.05$ for both CON-NX and ENA-NX vs. 2K.

value of r^* (1%), the greater the contribution of the large pores to transport through the filtration barrier. (The method for calculation of r^* for the lognormal-plus-shunt model is discussed in Section 3.6.4) As shown in Table 3, the values of r^* (1%) for CON-NX and ENA-NX were nearly equal for a given model (62 - 63 Å for the lognormal model, 60 - 61 Å for the lognormal-plus-shunt model) and were approximately 3 - 4 Å larger than the

respective r^* (1%) values for 2K rats. In summary, the pore-size distributions calculated for the NX groups were roughly equivalent, and indicated a small increase in the number of large, non selective pores compared to the 2K group.

Table 3. Membrane-pore parameters.

Model:	Parameter:	2K (n = 9)	CON-NX (n = 9)	ENA-NX (n = 8)
Isoporous plus shunt	$r_0, \text{Å}$	47.1±0.5	48.0±0.3	49.1±0.4
	$\omega_0, \cdot 10^{-3}$	0.148±0.030	3.18±0.58	0.970±0.190
	χ^2	153	37.6	79.4
Lognormal	$u, \text{Å}$	30.7±1.7	28.5±1.1	36.0±2.1
	s	1.23±0.02	1.27±0.02	1.20±0.01
	$r^*(1\%), \text{Å}$	59.0	62.4	62.8
	χ^2	157	36.1	100
Lognormal plus shunt	$u, \text{Å}$	34.2±0.9	30.6±0.6	38.6±1.2
	s	1.19±0.01	1.24±0.09	1.16±0.02
	$\omega_0, 10^{-3}$	0.134±0.016	2.54±0.31	0.854±0.163
	$r^*(1\%), \text{Å}$	57.0	61.0	60.0
	χ^2	44.6	9.86	47.8

Values for pore-size parameters are best-fit values \pm SE. r_0 , radius of pore; r^* (1%), pore size such that 1% of filtrate passes through pores with $r > r^*$; ω_0 , fraction of filtrate volume that would pass through the shunt at zero colloid osmotic pressure; u , mean pore radius. The standard deviation of the pore-size distribution is equal to $\ln(s)$.

Urinary Protein Excretion

Table 4 summarizes the urinary protein excretion data from the three groups. U_pV was significantly increased in CON-NX rats, to approximately three times the 2K rate (40.7 vs. 13.3 mg/24h). Enalapril treatment of NX rats prevented the increase in U_pV , which in the ENA-NX rats remained at the level seen in 2K animals. As shown in Table 4 and illustrated also in Figure 2, the source of the variation in U_pV among groups was the variation in U_aV . The excretion of nonalbumin proteins remained essentially constant, so that the ratio of albumin to total protein excretion, $(U_aV)/(U_pV)$, increased with U_pV . Studies in various other nonproteinuric rat species have reported values of 6 - 13% for this ratio (136). In the 2K rats, this ratio was much higher, i.e., 32%. For CON-NX rats

$(U_aV)/(U_pV)$ was double the 2K value, and for ENA-NX rats this ratio was less than half the 2K value, although the latter difference did not achieve significance.

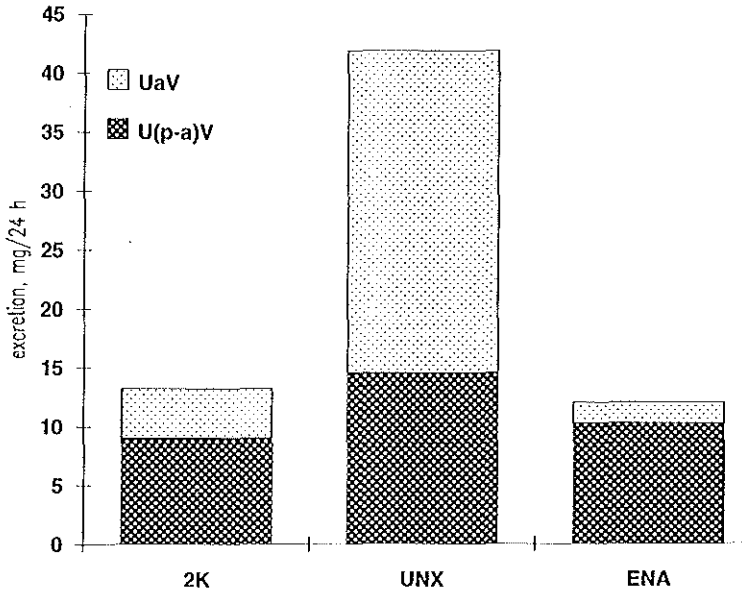


Figure 2. Total rates of urinary protein excretion (U_pV) for the three groups of fawn-hooded rats, measured as albumin (U_aV) or nonalbumin proteins ($U_pV - U_aV$).

The per-kidney clearance of Ficoll of $r_s = 36 \text{ \AA}$ (corresponding to the size of albumin) is shown as $\Theta_{36}\cdot\text{GFR}$ in Table 4. Although the U_aV was increased in only the CON-NX group, the per-kidney clearance of this size of Ficoll was elevated in both CON-NX and ENA-NX rats. The rise in $\Theta_{36}\cdot\text{GFR}$ was entirely attributable to the increase in GFR, as Θ_{36} did not vary significantly among groups. The total clearance of 36 \AA Ficoll, equal to $\Theta_{36}\cdot\text{GFR}$ for the NX animals and twice this value for the 2K animals, was the same for all groups. Thus changes in size selectivity evidently played no role in the increase in U_aV seen in the CON-NX rats. By exclusion, this implies that the primary mechanism for albuminuria was reduced charge barrier. A similar increase in total Ficoll clearance was seen in ENA-NX rats in the absence of a rise in U_aV . Thus treatment with enalapril prevented the increase in U_aV but had no effect on the filtration of Ficoll molecules of the same molecular radius as albumin. Again, this implies that albuminuria did not result from changes in size selectivity.

The extents of the correlations of urinary protein excretion rates with whole kidney or single-nephron hemodynamic parameters, based on the combined data from all three groups, are shown in Table 5. Both U_pV and U_aV were strongly and positively correlated with $\Delta\bar{P}$ ($P < 0.0001$). The fraction of albumin in the excreted urine, $(U_aV)/(U_pV)$, also was highly correlated with $\Delta\bar{P}$ ($P < 0.0001$); $(U_aV)/(U_pV)$ was inversely correlated with K_f . It is noteworthy that neither of the protein excretion rates correlated significantly with GFR. For all molecular sizes studied, the whole kidney clearance of Ficoll (Θ -GFR; not shown) correlated with GFR (as expected) and RPF, but not with $\Delta\bar{P}$, K_f , U_pV , or U_aV . Thus, as already noted, there was a dissociation between the rate of Ficoll excretion and value of U_aV .

Table 4. Urinary protein excretion rates.

	2K (n = 4)	CON-NX (n = 9)	ENA-NX (n = 8)
U_pV , mg/24h	13.3±0.6(C)	40.7±6.9(KE)	12.0±1.8(C)
U_aV , mg/24h	4.2±0.8(C)	27.3±6.2(KE)	1.9±1.0(C)
$(U_aV)/(U_pV)$	0.32±0.06(C)	0.63±0.05(KE)*	0.13±0.05(C)
Θ_{36} -GFR, ml/min/kidney	0.086±0.010(CE)#	0.174±0.024(K)	0.176±0.024(K)

Values are means ± SE; n, no. of experiments (* n = 8, # n = 9). U_pV , urinary excretion of total protein; U_aV , urinary excretion of albumin; Θ_{36} -GFR, per-kidney clearance of Ficoll of $r_s = 36 \text{ \AA}$. $P < 0.05$: K, vs. 2K; C, vs. CON-NX; E, vs. ENA-NX.

Table 5. Pearson coefficients for correlation of urinary protein excretion rates with renal hemodynamic parameters.

	U_pV	U_aV	$(U_aV)/(U_pV)$
GFR	0.364	0.245	- 0.029
SNGFR	0.068	0.055	- 0.044
RPF	0.150	0.045	- 0.054
Q_A	0.333	0.266	0.020
FF	0.495*	0.420	0.050
SNFF	0.140	0.127	0.083
$\Delta\bar{P}$	0.827*	0.812*	0.750*
K_f	- 0.351	- 0.398	- 0.626*

* $P < 0.05$.

DISCUSSION

The present study reports for the first time on the size-selective properties of the glomerular filtration barrier in fawn-hooded rats. These animals are prone to develop proteinuria and glomerular injury early in their life, and the removal of one kidney greatly accelerates these events. Although caution must be taken in comparing sieving data from different rat strains, it is interesting to note that in the three breeds of rats in which Ficoll sieving studies have been performed [FHH, Munich-Wistar (315), and 12-month-old Sprague Dawley (357)], substantial differences in Θ for control rats with intact kidneys are observed only for small-size to moderate-size molecules. Over the range $r_s = 20 - 42 \text{ \AA}$, Ficoll sieving coefficients for the present 2K FHH group were 3 - 10 times larger than values we have previously reported for normal Munich-Wistar rats (315) and approximately three times larger than those reported by Remuzzi *et al.* (357) for aged Sprague-Dawley rats. In contrast, for $r_s > 58 \text{ \AA}$ the 2K values are 0.3 to 0.6 times the Munich-Wistar values and in good agreement with the Sprague-Dawley results. It appears then that, for molecules the size of albumin or smaller, but not for very large molecules, the glomerular capillary wall of fawn-hooded rats exhibits less size-selectivity than that of the other two strains. The values of the pore-size parameters computed for the three strains are consistent with this conclusion. On the basis of previous work, there is reason to believe that 2K-FHH rats also suffer from impaired charge selectivity. Kreisberg and Karnovsky (222) performed structural studies in six month old fawn-hooded rats and described a focal loss of glomerular polyanion. This loss occurred through all layers of the filtration barrier and in some areas even before epithelial foot process fusion was evident. The amount of proteinuria correlated with the degree of loss of fixed negative charge.

The present results suggest that NX induces a loss of size selectivity in the filtration barrier, but only for very large molecules. This defect is evidenced by the "tail" of the sieving curve at large r_s , for the CON-NX rats relative to the 2K group. Treatment of NX rats with enalapril prevented the rise in U_pV and U_aV but had no significant effect on the sieving curve. The defect in size selectivity was not an important determinant of U_aV , because the clearance of Ficoll at $r_s = 36 \text{ \AA}$ was not affected. The sieving coefficients of Ficoll, unlike those of dextran, correspond closely to those of neutral globular proteins and to theoretical predictions for neutral solid spheres. It follows that Ficoll sieving curves and pore parameters based on Ficoll data lend themselves to more quantitative interpretation of the mechanisms of proteinuria. Thus the specific increase in albuminuria in the absence of changes in the total excretion rate of 36 \AA Ficoll strongly suggests an impairment of charge selectivity, in accord with the aforementioned structural results (222). An alternative explanation, which we regard as less likely, is that the increased albuminuria following NX was caused by a decrease in albumin reabsorption by the renal tubules, rather than by an

increase in albumin filtration at the glomerulus. In this case, it would be necessary to postulate that the effect of enalapril was to prevent the decreased tubular reabsorption.

Ficoll is apparently spherical, whereas albumin has been described as a prolate ellipsoid with major and minor axes of approximately 140 and 40 Å, respectively (384). By definition, the Stokes-Einstein radius of albumin $r_s = 36 \text{ Å}$, describes the diffusion behavior of albumin in bulk solution. It is possible, however, that the ellipsoidal shape of the molecule might cause its transport behavior in membrane pores to resemble that of a sphere of some other size, which brings into question the comparison of albumin with a Ficoll of 36 Å radius. One important factor controlling transmembrane transport rates is the partition coefficient (Φ), the ratio of the intrapore concentration of the molecule to that in bulk solution, at equilibrium (91, 251). Accordingly, we calculated Φ for a neutral ellipsoid of the aforementioned dimensions in a cylindrical pore of 50 Å radius, as described by Limbach *et al.* (67). The resulting value of $\Phi = 0.0577$ is the same as that for a neutral sphere of 38 Å radius. Thus, although values of the hemodynamic hindrance factors that also affect transport in pores have not been determined for ellipsoids, it seems likely that the effective radius of albumin in glomerular membrane pores is in the 36 - 38 Å range, or not appreciably different from the Stokes-Einstein value. Even if the effective radius of albumin were as large as 38 Å, our conclusions would be unaffected, because the changes in Θ for Ficoll were not statistically significant at any radius below 42 Å.

In the FHH rats a marked positive correlation was observed between $\Delta\bar{P}$ and U_aV (Table 5). Thus hemodynamic factors might be responsible for the observed alteration in glomerular permselectivity and loss of glomerular charge. The mechanism by which glomerular hypertension might be translated into an alteration of the structure and function of the glomerular barrier is not established. A hypothesis based on the concept of a physically compressed charge barrier does not explain the augmented U_aV . Modeling the filtration barrier as a single equivalent membrane (95), transmural compression of the capillary wall would decrease the effective membrane thickness. If this could be done without altering the pore-size distribution, then the decreased thickness would reduce the resistance to transport of neutral macromolecules, but it would increase the effective membrane charge density and thereby increase the overall resistance to transport of polyanions. Thus transmural passage of albumin would be predicted to be reduced rather than increased by simple compression of the capillary wall. Consequently, we infer that there is actual loss of effective charges on the filtration barrier by as yet unknown process. One may speculate that imposed stretch on the glomerular cells changes gene expression for various signaling and structural proteins, as has been observed in cultured glomerular cells (373).

Daniels *et al.* (84) recently reported on the relative contribution of cells and the glomerular basement membrane to the overall permeability properties of the glomerulus. For larger dextrans, the cellular elements were the major determinants of size selectivity, whereas for smaller dextrans, including those the size of albumin, the presence of native glomerular cells had relatively little effect on Θ . Application of this finding to the FHH sieving data implies that the defect in sieving for larger molecules after NX may result from a cellular defect. Furthermore, the sieving defect seen in all three groups of FHH rats for molecules in the 20 - 40 Å range (compared to Munich-Wistar rats) may reflect damage to the glomerular basement membrane. Further studies are necessary to confirm these hypotheses.

The experimental model of renal ablation has commonly been used to examine the interaction of renal hemodynamics with size selectivity and charge selectivity, but a comprehensive picture of the mechanisms has yet to emerge. Olson *et al.* (319) measured the sieving of neutral dextran, anionic dextran sulfate, and neutral, anionic, and cationic forms of horseradish peroxidase (HRP) in Munich-Wistar rats that had undergone 15/16 nephrectomy. Neutral HRP sieving coefficients and dextran sieving coefficients for $r_s = 16 - 60$ Å were not significantly different from controls. Values of Θ were increased for the anionic HRP and for dextran sulfate (an anionic form of dextran), while those for cationic HRP were decreased. These results imply a specific impairment of charge selectivity rather than size selectivity in response to renal ablation, in concurrence with the results reported here. More recently, Mayer *et al.* (269) measured dextran sieving curves in 5/6 nephrectomized Munich-Wistar rats along with the fractional clearance of a 18-Å dextran sulfate. The reduction in nephron number led to increased U_pV but increased Θ only for large ($r_s > 55$ Å) neutral dextran and for the dextran sulfate. Again, these data imply that a size-selective defect is limited to larger radii and that an alteration in charge selectivity is the primary mechanism for proteinuria in rats subjected to renal ablation. In contrast, Yoshioka *et al.* (463) studied neutral dextran and dextran sulfate clearances in 5/6 nephrectomized Munich-Wistar rats and found a more significant effect on medium-sized molecules, with Θ for $r_s > 36$ Å significantly larger than in 2K controls. Their results indicate a somewhat greater role for the loss of size selectivity in the inducement of proteinuria by partial nephrectomy than do the results of the present study or those of Olsen *et al.* (319) or Mayer *et al.* (269).

In other experimental models of kidney disease, changes in size selectivity appear to be important determinants of proteinuria. For example, in a recent Ficoll sieving study, Remuzzi *et al.* (357) found that streptozotocin-induced diabetes caused increases in Θ from 28 - 60 Å that were of the same order of magnitude as the rise in U_pV . Thus the change in

size selectivity could account for much of the increase in protein excretion. Similarly, the same investigators found significant elevations in Θ of dextran from 26 - 64 Å in proteinuric MWF/Ztm rats (358). U_aV was not measured in those studies, and exogenous charged tracers were not employed, so that it is not known whether or not there were also alterations in charge selectivity.

Modulation of the renin-angiotensin system is recognized as an important method of preventing proteinuria in a number of different rat models (13, 269, 357, 358). The two principal means of counteracting the renin-angiotensin system are with ACEI and with specific angiotensin II (Ang II) receptor antagonists. In the present study we found that treatment of NX rats with enalapril (an ACEI) did not significantly affect the size-selective defect present for the largest Ficoll molecules. An increase in U_aV was not seen in the ENA-NX group, however, indicating that a defect in charge selectivity was prevented by the ACEI. In contrast, Remuzzi *et al.* (358), in MWF/Ztm rats, found that enalapril reduced the sieving coefficients of neutral dextran at all molecular sizes studied. Both the disease model and the macromolecular tracer were different from the present study, which could explain in part the more significant effect of enalapril on size selectivity in the study by Remuzzi *et al.* (358).

Recent studies indicate that ACEIs and Ang II antagonists have different effects on glomerular permselectivity. The ACEIs not only inhibit conversion of Ang I, but also affect other important vasoactive peptides, such as bradykinin, which are hydrolyzed by converting enzyme. Hutchison and Webster (184) demonstrated that enalapril treatment of rats with Heymann nephritis reduced U_aV , whereas treatment with the Ang II receptor antagonist losartan did not. In a study of puromycin aminonucleoside nephrosis, Tanaka *et al.* (415) showed that enalapril, and not an Ang II inhibitor, reduced proteinuria during the first four weeks of nephrosis, and that this antiproteinuric effect could be partially reversed by bradykinin antagonists. These results suggest that enalapril may have a more substantial effect on charge selectivity than do Ang II inhibitors. Only two studies to date have directly examined the effect of Ang II inhibitors on size selectivity. Mayer *et al.* (269) found that treatment of 5/6 nephrectomized rats with MK954 (losartan) decreased $\Delta\bar{P}$ and U_pV and restored the size selectivity as measured with neutral dextran but did not restore the lost charge selectivity as measured with dextran sulfate. Similarly, Remuzzi *et al.* (357) found that treatment of diabetic rats with losartan prevented loss of size selectivity, as assessed with Ficoll. Direct comparisons of ACEI and Ang II inhibition effects on permselectivity, using similar groups of animals and the same test macromolecules, would be helpful in clarifying the different effects of these agents.

In this study we assumed that, in the absence of observable changes in size selectivity at a molecular radius of 36 \AA , the ratio of albumin to total protein in the urine was a measure of the effectiveness of the glomerular barrier to polyanions. In a similar fashion, Di Mario and coworkers (263) have proposed the use of the ratio of anionic immunoglobulin (IgG4) excretion to total IgG excretion as a clinical indicator of charge selectivity. Caution is needed in the use of such indicators, because protein excretion will be influenced by any factors which affect the tubular reabsorption of proteins. A rigorous determination of charge selectivity would require measurement of the sieving coefficient of a charged molecule that, like Ficoll and unlike proteins, undergoes no secretion or reabsorption by the tubules. In the past, dextran sulfate has been used as an anionic tracer. However, the nonideal molecular configuration causes the same inherent difficulties in the quantitative interpretation of sieving data for dextran sulfate as with dextran. Additionally, dextran sulfate has recently been shown to bind to albumin (156, 269), and this must be accounted for in any sieving calculations. Given the more ideal characteristics of Ficoll for sieving studies, the development of a charged derivative of Ficoll is desirable.

In summary, the intact FHH rat appears to have a defect in size selectivity in comparison with the normal Munich-Wistar rat. The increase in U_aV in the FHH rat after NX was found not to be due to an additional defect in size selectivity. This suggests that the increased albuminuria was due to a loss of charge selectivity. Reduction of $\Delta\bar{P}$ by enalapril treatment prevented the increased albuminuria, but did not prevent increases in the sieving coefficients for uncharged Ficoll molecules larger than albumin. Thus, the specific effect of enalapril on glomerular barrier function in these animals appears to have been to preserve its charge selectivity. Further studies are necessary to define the mechanisms by which high glomerular capillary pressure alters the functional properties of the glomerular capillary wall.

ACKNOWLEDGMENTS

The expert technical assistance of Miguel A. Zayas, Myriam Lee, and Sandra T. Downes is gratefully acknowledged. Enalapril was kindly provided by Dr. Charles S. Sweet of Merck Sharp & Dohme Research Laboratories.

These studies were supported by National Institute of Diabetes and Digestive and Kidney Diseases Grants DK-08720, DK-41641, and PO1-DK-40839 and by Dutch Kidney Foundation Grant C90.95.957A.

Portions of this study were presented at the 25th Annual Meeting of the American Society of Nephrology.

Chapter 9: Experiment 5

Manuscript in Preparation.

**ESTIMATION OF GLOMERULAR TRANSCAPILLARY HYDRAULIC PRESSURE
IN THE RAT FROM SIEVING CURVES**

James D. Oliver III¹, Jacob L. Simons^{2,3}, Julia L. Troy²,
Abraham P. Provoost³, Barry M. Brenner², and William M. Deen¹

Department of Chemical Engineering¹
Massachusetts Institute of Technology
Cambridge, MA 02139

Laboratory of Kidney and Electrolyte Physiology²
Brigham and Women's Hospital
and Harvard Medical School
Boston, MA 02115

Department of Pediatric Surgery³
Erasmus University
Rotterdam, The Netherlands

ABSTRACT

Direct in vivo determination of glomerular capillary hydraulic pressure in humans has thus far been impossible. Estimation of filtration pressure from sieving data has been of interest. However, a systematic evaluation of these calculated estimates with direct measured pressure has not been done. Here we report the outcome of comparisons between fitted and measured pressures made retrospectively from nine reported studies in the rat in which both fractional clearances of neutral dextrans were obtained and transcapillary hydraulic pressure ($\Delta\bar{P}$) was measured by micropuncture. In addition, data were analyzed from 25 fawn-hooded rats that had undergone different treatments and had undergone Ficoll sieving studies and micropuncture glomerular pressure measurements. Despite the use of more sophisticated models of glomerular permselectivity and the use of individual and group data, the results indicated that fitted pressures almost uniformly underestimated the actual measured values. Estimation of the change in $\Delta\bar{P}$ between groups was often incorrect. Therefore, it is highly questionable whether estimation of $\Delta\bar{P}$, or directional changes in $\Delta\bar{P}$, from sieving data obtained in humans will be a reliable method.

Numerous experimental studies in rats have shown that elevated glomerular capillary hydraulic pressure (\bar{P}_{GC}) or transcapillary hydraulic pressure ($\Delta\bar{P}$) is associated with a progression of glomerular damage. The models are described in Section 1.3 of this thesis and include renal ablation and infarction (11, 13, 137, 138, 179, 276, 319), desoxycorticosterone-salt hypertension (112), streptozotocin-induced diabetes mellitus (464, 466), unilaterally nephrectomized spontaneously hypertensive rats (108), and the 2-kidney and uninephrectomized fawn-hooded rat (403-405). In all these models $\Delta\bar{P}$ is elevated along with the single-nephron glomerular filtration rate (SNGFR). Therapy in these animals which selectively reduces \bar{P}_{GC} and $\Delta\bar{P}$ without reducing single-nephron hyperfiltration, such as with treatment with an angiotensin I converting enzyme inhibitor (ACEI), slows the progression of glomerular sclerosis. Acute and chronic elevations in $\Delta\bar{P}$ are associated with proteinuria (U_pV) (43, 461, 462).

In humans, \bar{P}_{GC} and $\Delta\bar{P}$ are not known. A method for obtaining values of \bar{P}_{GC} or $\Delta\bar{P}$, or at least determining changes in these values, is required to fully evaluate the importance of the hemodynamic basis of renal damage and the results of therapeutic trials in humans. The estimation of filtration pressure from sieving curve data has been of interest for some time. Early attempts (18, 140, 141, 238, 240, 431) were based on the Pappenheimer-Renkin mathematical model (325, 326) and suffer from its limitations

(discussed in Chapter 4.3). Estimated values for $\Delta\bar{P}$ range from 9 to 30 mm Hg in these various early studies. The differences in the fits principally reflect variations in the method used to calculate the hindrance factors. These estimates were all based on sieving data from dogs and humans, without direct pressure measurements with which to compare (142, 237).

Chang (70), in a retrospective study, used the pore model to fit filtration pressures to dextran sieving literature data for Munich-Wistar rats (71, 74). His fit values for $\Delta\bar{P}$ were consistently lower than the experimental values by 2 to 9 mm Hg, with corresponding higher ultrafiltration coefficient (K_f) values and lower pore size (r_0) values than reported originally. The range of $\Delta\bar{P}$ measured in these studies (34 - 40 mm Hg) was not wide. More recently, Chan *et al.* have used dextran sieving data to estimate $\Delta\bar{P}$ in a clinical study of dietary protein effects (69). Employing the isoporous model, they obtained values for control subjects of $\Delta\bar{P} = 34$ mm Hg and 38 mm Hg in the pre- and postprandial periods, respectively.

In this chapter we will discuss the theoretical basis for estimating $\Delta\bar{P}$ from sieving data, followed by a comprehensive review of fitting isoporous-model pressures to available dextran experimental data. We then examine pressure fitting using recent data with greater ranges in measured filtration pressures, a more optimal exogenous tracer, and newer heteroporous models. The fawn-hooded rat study, presented in Chapters 7 and 8, is one of the few experiments to date in which both micropuncture and sieving measurements were performed and in which substantial alterations in $\Delta\bar{P}$ were achieved. As such, it provides an important new source of data with several advantages pertaining to pressure estimation. Ficoll sieving data were used which are better suited to the theoretical model than that for dextran (315). Through better calibration with Ficoll standards the molecular sizes were more accurately determined than had been previously and a larger range of r_s was used. The animal protocols resulted in a wider range of $\Delta\bar{P}$ than usually reported. Finally, newer and more realistic heteroporous models were employed.

THEORETICAL CONSIDERATIONS

Any method which attempts to determine changes in $\Delta\bar{P}$ from sieving curves must distinguish between those effects due to alterations in permselectivity and those from alterations in hemodynamics. The situation of most interest for deriving pressures is that of $\Delta\bar{P}$ changes at constant SNGFR, since this corresponds to the clinical case where the information on flow rates such as GFR and RPF is at hand while $\Delta\bar{P}$ and K_f are unknown.

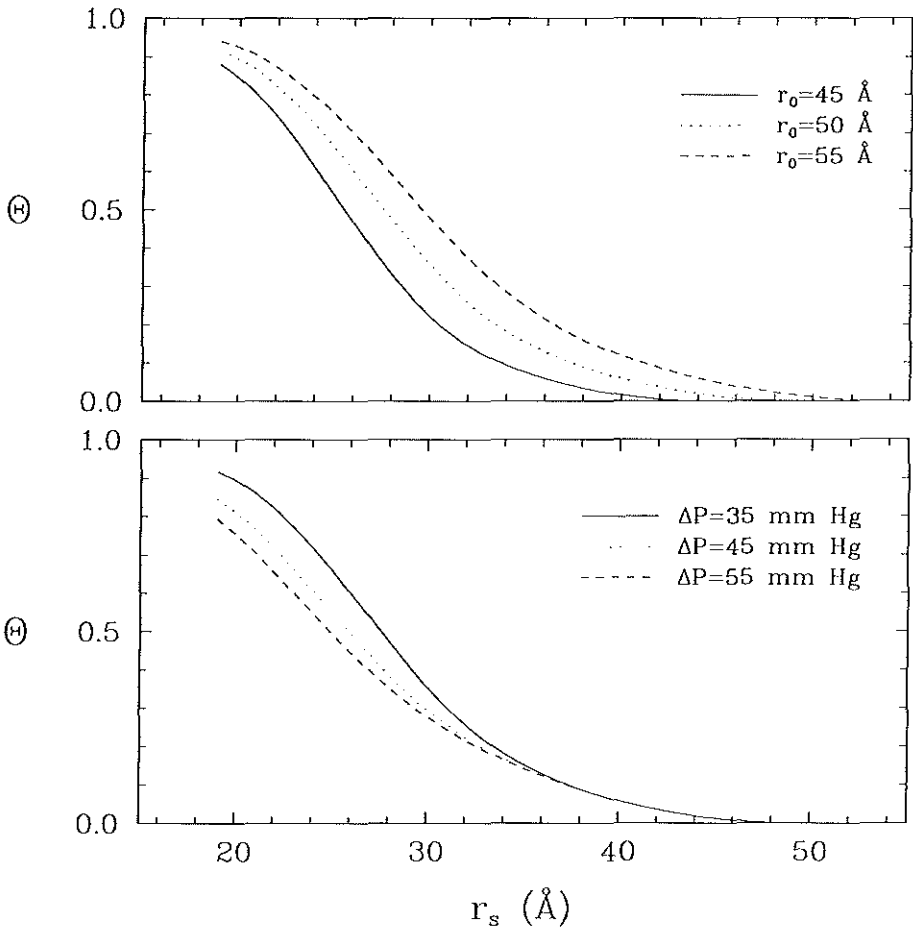


Figure 1. Theoretical effects of changes in isoporous r_0 (top) compared to changes in $\Delta \bar{P}$ (bottom) at constant SNGFR. Unless otherwise shown, input parameters were $r_0 = 50 \text{ \AA}$, SNGFR = 49.8 nl/min, $Q_A = 172 \text{ nl/min}$, $\Delta \bar{P} = 35 \text{ mm Hg}$.

Figure 1 compares the effects of changes in r_0 to those of changes in $\Delta\bar{P}$ at constant SNGFR using the isoporous model. As would be expected, a increase in r_0 is accompanied by a rise in Θ at all values of r_s . The effect is more noticeable at larger sizes. A rise in $\Delta\bar{P}$ increases the net solute clearance but increases GFR to an even greater degree, and therefore the fractional clearance decreases. Decreasing plasma osmotic pressure has essentially a similar effect. In contrast to a change in r_0 , the sieving coefficients for large molecules are all less sensitive to pressure than those for small molecules. Good agreement with this prediction is shown by the findings of Gassee *et al.* (141), where at comparable renal flow rates, sieving curves were generally lower in dogs with higher mean arterial blood pressures, but the curves merged at large solute radius.

As pointed out by DuBois and Stoupel (105), the sieving curves are steeper--the membrane showing greater permselectivity--at lower pressures, where the diffusive forces play a more important role. For large solutes, the sieving curves are relatively independent of pressure, a consequence of convection-domination. Qualitatively, it can therefore be appreciated that permselectivity changes have different effects than hemodynamic changes. The questions remains whether the sensitivity of the measurements or of the models is sufficient to allow $\Delta\bar{P}$ to be inferred.

CALCULATIONS FROM PUBLISHED STUDIES

We retrospectively applied the isoporous, solid-sphere model (Chapter 3.6) to all experimental studies in the rat where both fractional clearances of neutral dextran were obtained and $\Delta\bar{P}$ was measured by micropuncture (44, 71, 74, 185, 286, 461-463). These results are summarized in Table 1. Each of the cases shown involves paired groups of animals; one group serves as a baseline or control group and the other is a group in which some sort of intervention was made. Using the mathematical model, best-fit values of $\Delta\bar{P}$ (along with r_0) were calculated from the data as described in Chapter 3.6.5 and compared to those actually measured. Similarly to Chang (70), fitted values generally underestimate the actual ones. The more central clinical issue of measuring changes in $\Delta\bar{P}$ is shown in Table 1 for the paired groups. The correct direction is calculated in six of the nine cases, but the magnitude of the change is generally lower than measured. The mathematical analysis failed to correspond to the actual results in three cases, for no apparent reason. In summary, while the theory gives reasonable agreement with the data, it is questionable whether the conventional model is a clinically reliable means of estimating $\Delta\bar{P}$, or directional changes in $\Delta\bar{P}$.

Table 1. Comparison of measured and fitted $\Delta \bar{P}$ and of measured and fitted changes in $\Delta \bar{P}$ from published fractional clearance data for dextran in rats using the isoporous solid-sphere model.

	Model	$\Delta \bar{P}$ (mm Hg)			measured/ calculated	Ref:
		measured	diff.	calculated		
1.	normal hydropenia	34.0		33.8	1.01	(44)
	hydropenia + Ang II	43.0	9.0	45.6	11.8	0.94
2.	NSN hydropenia	39.0		29.0	1.34	(71)
	NSN + PVE	40.0	1.0	30.3	1.3	1.32
3.	normal hydropenia	34.0		32.0	1.06	(74)
	normal + PVE	38.0	4.0	27.0	-5.0	1.41
4.	normal euvoemia	33.9		21.9	1.55	(185)
	normal + histamine	39.5	5.6	23.5	1.6	1.68
5.	normal control	39.9		30.7	1.30	(286)
	diabetes	34.5	-5.4	30.8	0.1	1.12
6.	normal euvoemia	33.0		36.8	0.90	(461)
	normal + RVC	42.0	9.0	39.5	2.7	1.06
7.	PHN baseline	40.0		42.5	0.94	(462)
	PHN + Ang II	52.0	12.0	45.6	3.1	1.14
8.	PHN baseline	42.0		49.0	0.85	(462)
	PHN + acetylcholine	35.0	-7.0	50.2	0.8	0.70
9.	NPX	51.9		41.5	1.25	(463)
	NPX + verapamil	34.0	-17.9	35.5	-6.0	0.96

Abbreviations are: diff., calculated difference; NPX, renal ablation; NSN, nephrotoxic serum nephritis; PVE, plasma volume expansion; PHN, passive Heymann nephritis; RVC, renal vein constriction; Ang II, angiotensin II.

FITTING OF $\overline{\Delta P}$ TO FAWN-HOODED RAT DATA

Methods are described in Chapter 3.6. For the data fitting, the results presented in Chapter 8 for two-kidney FHH rats (2K), uninephrectomized FHH rats (CON-NX) and uninephrectomized FHH rats treated with enalapril (ENA-NX) were used. In addition, permselectivity studies were done in uninephrectomized FHH rats treated with a NO synthase inhibitor (N^W-nitro L-arginine methyl ester, Sigma Chemical Co., St. Louis, Missouri, USA: 50 mg/L, NAME-NX). Sieving data and hemodynamic parameters of these NAME-NX rats are presented in Table 2 and 3, respectively. Figure 2 shows the sieving coefficients (Θ) for Ficoll in NAME-NX rats as a function of Stokes-Einstein radius (r_s) calculated using the lognormal-plus-shunt model. In total 25 animals were used for fitting calculations (2K, n = 4; CON-NX, n = 9; ENA-NX, n = 8; and NAME-NX, n = 4). Both micropuncture and sieving studies were performed in each individual animal.

Table 2. Ficoll sieving coefficients for NAME-NX rats (n = 4).

r_s (Å)		r_s (Å)	
20	$8.43 \times 10^{-1} \pm 5.83 \times 10^{-2}$	46	$1.72 \times 10^{-2} \pm 7.47 \times 10^{-3}$
22	$7.93 \times 10^{-1} \pm 6.72 \times 10^{-2}$	48	$1.25 \times 10^{-2} \pm 5.93 \times 10^{-3}$
24	$6.77 \times 10^{-1} \pm 4.57 \times 10^{-2}$	50	$8.94 \times 10^{-3} \pm 4.62 \times 10^{-3}$
26	$5.55 \times 10^{-1} \pm 4.05 \times 10^{-2}$	52	$6.76 \times 10^{-3} \pm 3.72 \times 10^{-3}$
28	$4.30 \times 10^{-1} \pm 3.75 \times 10^{-2}$	54	$5.12 \times 10^{-3} \pm 2.96 \times 10^{-3}$
30	$3.18 \times 10^{-1} \pm 2.65 \times 10^{-2}$	56	$4.15 \times 10^{-3} \pm 2.48 \times 10^{-3}$
32	$2.19 \times 10^{-1} \pm 2.72 \times 10^{-2}$	58	$3.48 \times 10^{-3} \pm 2.18 \times 10^{-3}$
34	$1.56 \times 10^{-1} \pm 2.37 \times 10^{-2}$	60	$2.82 \times 10^{-3} \pm 1.85 \times 10^{-3}$
36	$1.08 \times 10^{-1} \pm 2.08 \times 10^{-2}$	62	$2.22 \times 10^{-3} \pm 1.50 \times 10^{-3}$
38	$7.32 \times 10^{-2} \pm 1.83 \times 10^{-2}$	64	$1.83 \times 10^{-3} \pm 1.26 \times 10^{-3}$
40	$4.95 \times 10^{-2} \pm 1.48 \times 10^{-2}$	66	$1.59 \times 10^{-3} \pm 1.12 \times 10^{-3}$
42	$3.39 \times 10^{-2} \pm 1.22 \times 10^{-2}$	68	$1.38 \times 10^{-3} \pm 9.95 \times 10^{-4}$
44	$2.34 \times 10^{-2} \pm 9.29 \times 10^{-3}$	70	$1.19 \times 10^{-3} \pm 8.72 \times 10^{-4}$

All values are given as mean \pm standard error. Values for NAME-NX rats were not significantly different from all other groups presented in Chapter 8. This was most likely due to the low number of examined animals in the NAME group and the relatively high values for the standard errors for the studies in these rats.

Table 3. Hemodynamic parameters for NAME-NX rats (n = 4).

body weight, g	263±12
MAP, mm Hg	160±4(KCE)
hematocrit	47.0±1.1(K)
GFR, ml/min/kidney	1.47±0.09
RPF, ml/min/kidney	4.54±1.09(C)
FF	0.35±0.04(K)
SNGFR, nl/min	76.5±6.1
Q _A , nl/min	208±40
SNFF	0.38±0.01(KCE)
C _A , g/dl	5.4±0.1
$\Delta\bar{P}$, mm Hg	64.6±3.3(KCE)
K _f , nl/min/mm Hg	1.94±0.07(E)

All values are given as mean ± standard error. Superscripted letters indicate P < 0.05; K, vs. 2K; C, vs. CON-NX; E, vs. ENA-NX. Chapter 8 provides data other rat groups.

To demonstrate the equivalence of using single-nephron versus whole kidney parameters in pressure fits, the four sets of experimental group data were fitted using both the single-nephron and whole kidney hemodynamic data of Table 3. The results are shown in Table 4. Little difference is seen between the results from single-nephron versus whole kidney parameters. Fitted $\Delta\bar{P}$ uniformly underestimated measured values by a considerable amount. None of the models predicted that $\Delta\bar{P}$ for the NAME-NX was substantially higher than the other groups. The isoporos-plus-shunt model gave results closer to those measured, and it correctly demonstrated that pressure in the CON-NX and NAME-NX groups were higher than the 2K and ENA-NX values. Even though they provided better overall fits to the sieving coefficients, the lognormal and lognormal-plus-shunt fits indicated that the pressure in the ENA-NX and NAME-NX groups were either higher than or similar to those of 2K and CON-NX.

Finally, pressures were fitted to the sieving data of each of the 25 rats and compared to the actual micropuncture value. The results for the various glomerular permselectivity models are shown in Figures 3, 4 and 5. Again fitted $\Delta\bar{P}$ tended to underestimate measured $\Delta\bar{P}$. For the isoporos-plus-shunt model, the difference between the fitted and measured pressures averaged -13.6 mm Hg, with a range of +6.7 to -61.4 mm Hg. For the lognormal model, the average was -21.2 mm Hg, with a range of -8.3 to -36.7 mm H, and for the lognormal-plus-shunt model the average was -16.0 mm Hg with a

range of +52.4 to -38.1 mm Hg. None of the correlations between fitted and measured $\Delta\bar{P}$ were significant ($P = 0.733$ for the isoporous-plus-shunt; $P = 0.103$ for the lognormal; $P = 0.312$ for the lognormal-plus-shunt).

Table 4. Fits of pore parameters plus $\Delta\bar{P}$ to group-averaged sieving coefficients.

Group:			2K		NX		ENA		NAME	
$\Delta\bar{P}_{\text{measured}}$ (mm Hg)			48.6±1.2		55.9±1.2		43.6±1.2		64.6±3.3	
Model:			WK	SN	WK	SN	WK	SN	WK	SN
Iso-porous + shunt	r_0	(Å)	46.9	46.8	47.7	47.8	48.6	48.7	49.0	48.7
	ω_0	(10 ⁻⁴)	1.07	1.05	27.4	27.3	7.18	7.23	9.43	8.69
	$\Delta\bar{P}_{\text{fit}}$	(mm Hg)	35.8	37.0	44.8	45.2	37.0	36.9	38.5	40.8
Log-normal	u	(Å)	29.7	29.8	26.6	26.0	32.5	32.5	33.4	33.9
	s		1.26	1.26	1.33	1.34	1.26	1.26	1.25	1.24
	$\Delta\bar{P}_{\text{fit}}$	(mm Hg)	27.2	28.7	29.1	28.8	31.4	31.2	32.1	35.6
Log-normal + shunt	u	(Å)	34.1	35.4	31.9	27.6	35.8	34.5	34.2	35.6
	s		1.21	1.19	1.25	1.31	1.20	1.22	1.23	1.22
	ω_0	(10 ⁻⁴)	0.314	0.415	13.8	4.48	0.905	0.891	1.13	1.31
	$\Delta\bar{P}_{\text{fit}}$	(mm Hg)	27.6	29.7	35.2	28.4	31.1	30.9	31.7	35.6

Abbreviations: WK, whole kidney hemodynamic parameters; SN, single-nephron hemodynamic parameters.

In summary, the results from attempts to fit filtration pressure to sieving data were not encouraging. Neither the use of newer heteroporous models nor fitting of the individual sieving data instead of group means improves the ability of the present models of glomerular permselectivity to infer glomerular hydraulic pressures. It is not clear whether this failure is intrinsic to the model or to the experimental accuracy of the sieving coefficients and hemodynamic data. Further evaluation of the model and the sensitivity of pressure fitting to experimental variance in Θ is necessary to determine whether estimation of $\Delta\bar{P}$ from sieving coefficients is viable. The worst-case scenario is that Θ is not sufficiently sensitive to changes in $\Delta\bar{P}$ to allow for fitting. A more optimistic possibility is that the present mathematical model is simply not advanced enough to enable accurate estimation of $\Delta\bar{P}$.

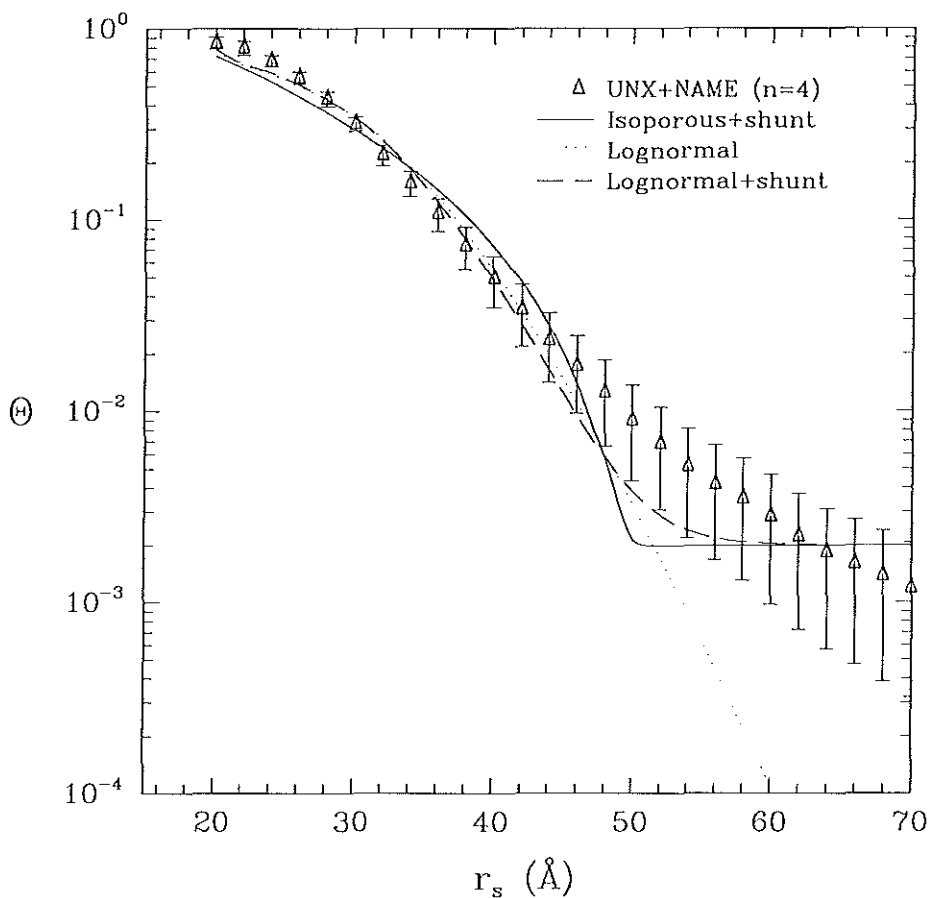


Figure 2. Sieving coefficients (Θ) for Ficoll in NAME-NX rats as a function of Stokes-Einstein radius (r_s). The symbols and error bars represent measured values \pm SE. The curve was calculated using the lognormal-plus-shunt model.

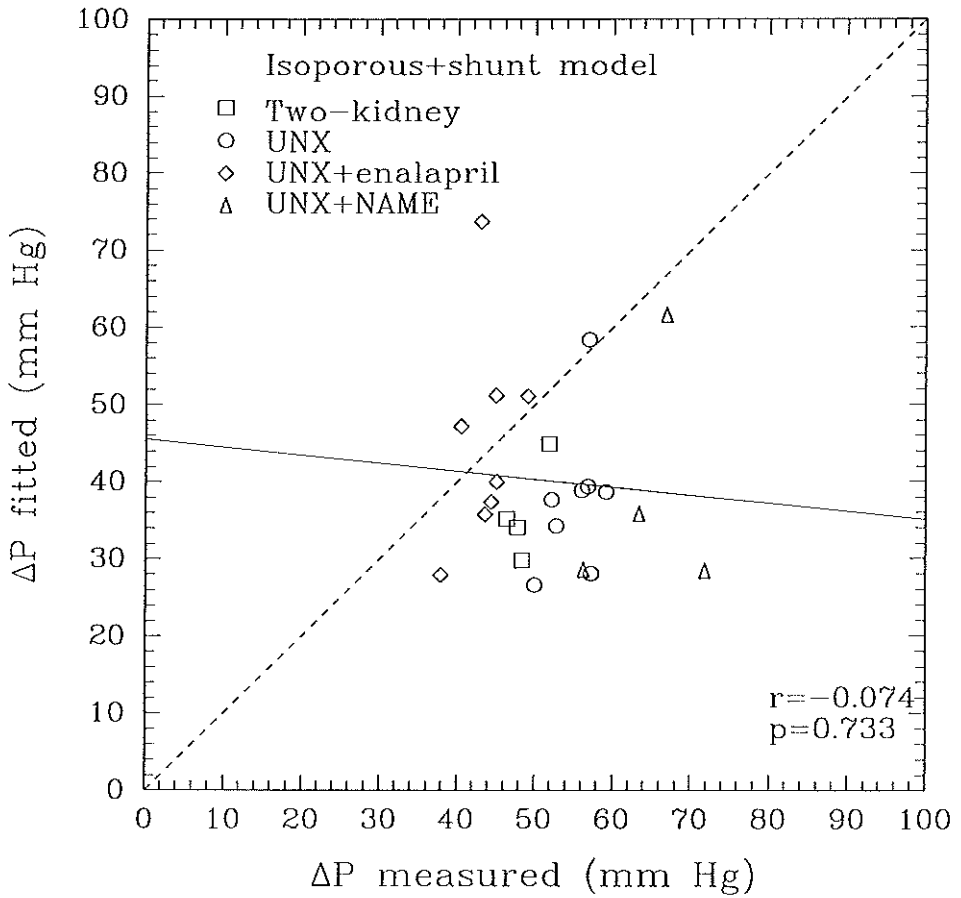


Figure 3. Correlation of measured to fitted $\overline{\Delta P}$ for isoporosis-plus-shunt model. Solid line is a linear fit to the data. Dashed line is $\overline{\Delta P}_{fit} = \overline{\Delta P}_{measured}$.

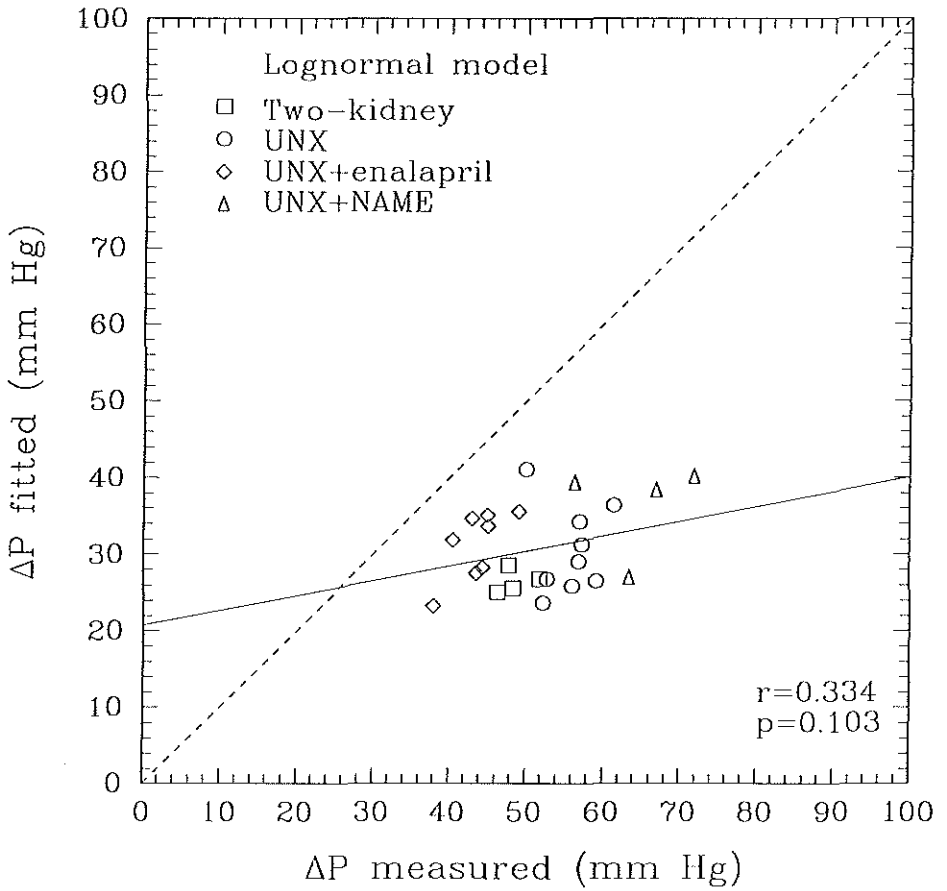


Figure 4. Correlation of measured to fitted $\Delta\bar{P}$ for lognormal model. Solid line is a linear fit to the data. Dashed line is $\Delta\bar{P}_{fit} = \Delta\bar{P}_{measured}$.

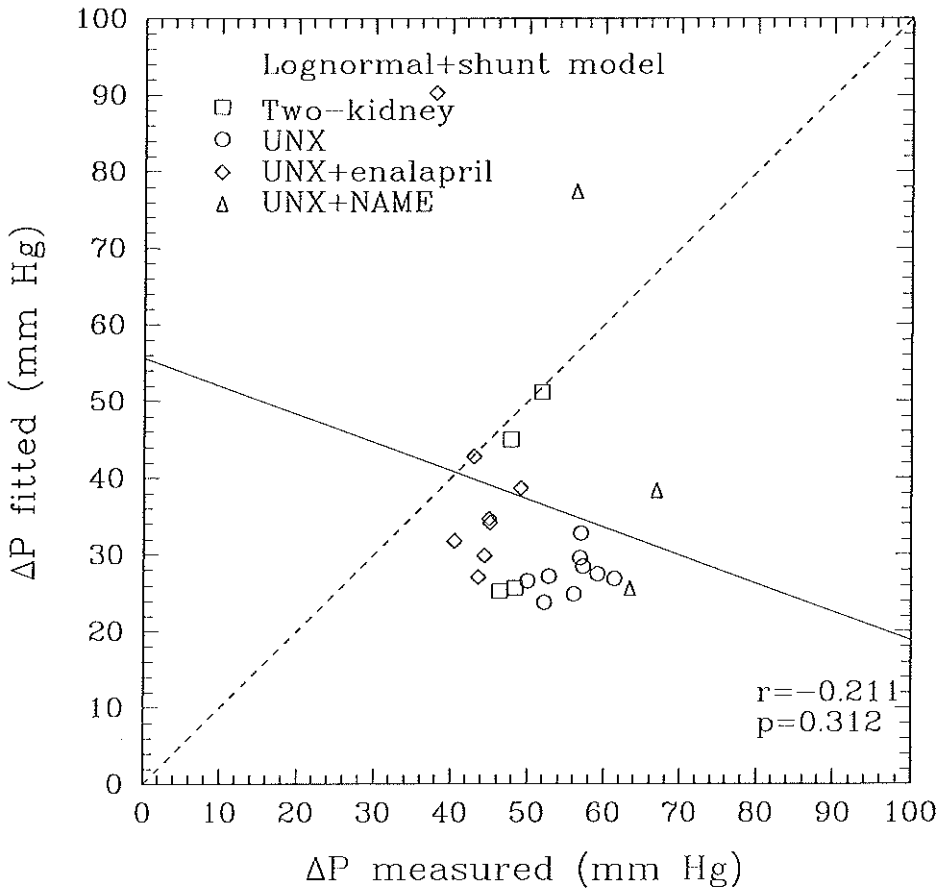


Figure 5. Correlation of measured to fitted $\Delta\bar{P}$ for lognormal-plus-shunt model. Solid line is a linear fit to the data. Dashed line is $\Delta\bar{P}_{fit} = \Delta\bar{P}_{measured}$.

Chapter 10:

ULTRASTRUCTURAL OBSERVATIONS IN GLOMERULI OF
FAWN-HOODED (FHH) RATS

Jacob L. Simons¹, Deborah J. Sandstrom², Abraham P. Provoost¹,
and Helmut G. Rennke²

Department of Pediatric Surgery¹
Erasmus University
Rotterdam, The Netherlands

Department of Pathology²
Brigham and Women's Hospital
Harvard Medical School
Boston, MA

Microcirculatory studies in fawn-hooded (FH) rats have shown a derangement in the glomerular capillary hydraulic pressure (\bar{P}_{GC}), which was associated with subsequent glomerular injury and scarring (404). Removal of one kidney (NX) in FH rats of the FHH substrain resulted in a pronounced acceleration of the progression of chronic renal failure (CRF) to end-stage renal disease (ESRD). Elevated \bar{P}_{GC} was the most significant determinant in this process and values of this parameter were further increased after NX (405). Modulation of this hemodynamic key factor in NX FHH rats was subsequently assessed (403). Those studies revealed that increase of \bar{P}_{GC} resulting from the administration of a NO synthase inhibitor was associated with early FSGS and uremic death. Conversely, animals treated with the angiotensin I converting enzyme inhibitor (ACEI) enalapril had normal values of \bar{P}_{GC} and exhibited long term protection for proteinuria and CRF. Subsequently, permselectivity studies with the tracer macromolecule Ficoll were done (316). FHH rats with 2 kidneys (2K) appeared to have an intrinsic sieving defect in the range of albumin size (36 Å) molecules, rendering the restriction of these molecules more dependent upon anionic charges in the filtration membrane. After NX, an additional permselectivity defect for large size molecules (> 40 Å) was demonstrated. Lowering of \bar{P}_{GC} in NX FHH rats by ACEI therapy did not alter the size-selectivity defects. Indirect evidence for loss of anionic charges after NX due to high \bar{P}_{GC} was also presented. Together, the permselectivity data suggested that FHH rats of the various above mentioned groups have specific defects of the glomerular filtration barrier which are perhaps visible on ultrastructural examination. Recently, Daniels *et al.* showed that relative large size macromolecules (> 40 Å) are mainly restricted by cellular elements of the filtration membrane, whereas permselectivity for smaller molecules (20 - 40 Å) including albumin is more dependent upon the acellular matrix (84). Cells added to the GBM do not greatly improve the permselectivity of the barrier for these small molecules. Interpretation of our sieving data in view of these hypotheses suggested that the defect for large size molecules which appears after NX is the consequence of cellular injury, whereas the intrinsic abnormality in 2K FHH rats is related with a matrix disarray (316). Initial screening studies of the ultrastructure of FHH rat glomeruli were done to allow a better understanding of these mechanisms and possibly test the suggestions as inferred from the work of Daniels *et al.* Electron microscopic studies have been done in several FH rats strains, but not in FHH rats. The reports on those other strains are discussed in Chapter 2.2. The current initial studies therefore also served to possibly identify and compare observations in FHH rats with those of its ancestors.

MATERIALS AND METHODS

Fawn-hooded rats of the FHH substrain were used. A single 22 week old WAG rat with 2 kidneys (2K), part of the study presented in Chapter 5, was added for control. Two young 2K FHH rats were studied, representative for a young FHH rat group also presented in Chapter 5. These rats were 6 to 7 weeks old and had proteinuria in the 25 mg/24h range. Two untreated uninephrectomized (NX) FHH rats were assessed. One of these was NX at age 4 weeks and sacrificed 2 weeks later. Hemodynamic or other parameters were not obtained in this rat. Tissue from this animal served to illustrate and highlight the early glomerular changes in young FHH rats as a consequence of NX. The other NX FHH rat was NX at age 8 weeks and studied 12 weeks later at age 20 weeks. This older animal served to study the effects of NX (Chapter 6), and as control for the pharmacologically treated NX FHH rats (NX-CON) (Chapter 7). The treated rats consisted of one FHH rat NX at age 8 weeks and then treated for 12 weeks with ACEI (enalapril (ENA): 250 mg/L; Merck Sharp & Dohme, West Point, PA), and one FHH rat NX at age 8 weeks and started on a NO synthase inhibitor (N^W-nitro L-arginine methyl ester (NAME): 50 mg/L; Sigma Chemical Co., St. Louis, MO) and sacrificed 8 weeks later. An overview of the studied animals is presented in Table 1 together with the results. The reader is referred to the various chapters for details on the microcirculatory, permselectivity, and light microscopic morphological data. With the exception of the young NX FHH rat indicated above, all animals selected for ultrastructural assessment were part of those studies and thought to be representative for the various groups. Methods for transmission electron microscopy are briefly provided in Chapter 3.5.

RESULTS

The ultrastructural measurements were summarized by a semiquantitative score in Table 1. We would like to stress that these limited studies only served to screen FHH rat glomeruli for lesions rather than to count these to allow for correlations. The low number of rats may have easily resulted in bias.

Young FHH rats showed focal fibrin deposition in capillary loop lumina and in the subendothelium. Some platelet aggregates, with or without concomitant fibrin deposits were present within those lumina or adhered to the endothelium. Overlapping of endothelial cells was seen. Podocytes appeared normal with intact foot processes.

The single 6 week old FHH rat examined 2 weeks after NX showed similar changes as the young FHH rats with 2K. However, the early endothelial lesions were more pronounced and in addition damage of the GBM was seen. Changes included platelet and fibrin adherent to a generally damaged endothelium. Endothelial cells were overlapping and showed regenerative changes. Splitting of the basement membrane was seen with fibrin

deposition within the membrane. Podocytes appeared normal with non-fused foot processes.

Injury of the visceral epithelial cells was seen in rats NX at 8 weeks and studied 12 weeks later. There was marked effacement or fusion of foot processes, with only focal sparing. These screening studies did not reveal platelet aggregation or fibrin deposition, and the endothelium did not appear abnormal. Glomeruli of the single NX FHH rat treated with ACEI showed some attenuation of the cytoplasm of the podocytes and some focal fusion of foot processes. Lesions of the other constituents of the barrier were not apparent in this animal. The tufts of the NX FHH rat treated with NO synthase inhibition revealed extensive damage to all layers of the glomerular capillary wall. The endothelium was swollen and showed subendothelial "fluffy" areas, but was not associated with fibrin or platelet deposition. Extensive foot process fusion was seen together with blebs and lysosomes, indicative of severe podocyte damage.

Table 1. Summary of ultrastructural findings in FHH rats.

	Age wk	bw g	Group	Endo- thelium	GBM	Podocyte	Fibrin	Platelets
FHH	7	235	2K	+	=	=	=	+
FHH	6	210	2K	+	=	=	+	+
FHH	6	148	NX (4)	+	+	=	+	+
FHH	20	344	NX (8) (CON)	+	=	+	=	=
FHH	20	336	NX (8) (ENA)	=	=	±	=	=
FHH	16	240	NX (8) (NAME)	+	+	++	=	=
WAG	22	340	2K	=	=	=	=	=

Values for age and body weight (bw) represent individual values for rats used for ultrastructural assessment. NX, uninephrectomy, with value between parentheses indicating age in weeks at which NX was done; Score for injury: +, present; ±, mild; ++, severe; =, unchanged or not observed.

DISCUSSION

Fawn-hooded rats have an inborn susceptibility to develop FSGS. In previous studies we found that elevated \overline{P}_{GC} was present in young rats and predicted the subsequent development of glomerular injury visible on light microscopy. The current studies showed that these young rats have evidence of endothelial cell damage with fibrin and platelet aggregation, which was more pronounced early after NX. The rat NX and studied at a later

time point showed podocyte injury, which was less severe after ACEI treatment and more pronounced after NO synthase inhibition treatment. In the subsequent sections we shall discuss several lesions which have been described in other rat models of CRF and might perhaps be present and contribute to the progression of CRF in FHH rats as well. Limitations of the current study do not allow definite conclusions on the importance of any of such changes in respect to specific pathophysiological routes of injury in the FHH rat. This study served to identify lesions in the FHH rat and to discuss possible areas of interest for future study.

Glomeruli possess a complex hemostasis system with procoagulant/ antifibrinolytic and anticoagulant/fibrinolytic properties that can act locally on platelet adhesion or aggregation, on the plasma-coagulation pathways, and on fibrinolysis (199). Disturbance of this delicate balance may contribute to glomerular scarring (468). The precise mechanisms through which this may occur are still not well defined. Intraglomerular deposition of fibrin resulting from endothelial cell damage has been reported in the process of glomerulosclerosis (322). Since high pressures and flows dominate the subsequent occurrence of FSGS in young FHH rats, it is conceivable to suggest that this hemodynamic burden may cause some sort of endothelial cell damage. Endothelial cell injury and activation results in release of tissue procoagulant factor, fibrinolytic inhibitors, platelet activating factor, and large multimers of von Willebrand factor (vWF) which all promote fibrin deposition and platelet aggregation (35). Direct endothelial cell injury could expose the GBM which can aggregate platelets (131), or expose the thrombogenic subendothelium which contains procoagulant tissue factor (35).

Evidence of endothelial cell damage, GBM exposure, and coagulation activation in FH/Wjd rats was previously reported by Urizar *et al.* (428). These investigators showed increased glomerular capillary deposition of vWF and complement (C3) in 2 to 4 month old FH/Wjd rats. Kuijpers and Gruys noted increased glomerular fibrin deposition in 2 month old FH/URL rats (228). Although the platelets of the FH rat lack the storage pool, dense granules have been identified in the cytoplasm (414) (current observations). These platelets have a defective ATP and serotonin secretion but do aggregate well and generate thromboxane (TxA₂) upon stimulation with collagen in plasma or whole blood (255). Further studies are needed to define the role of fibrin and platelet aggregation in the progression of FSGS in FHH rats and the relationship of these aggregates with hemodynamic and endothelial abnormalities. In this context, experiments with synthetic peptides containing a recognition site for integrins in several adhesive molecules including fibronectin, fibrinogen, and vWF are of interest. These peptides can inhibit fibrinogen-platelet binding and platelet aggregation (468).

Little is known about the intraglomerular hemostatic properties after renal ablation. Ruedin *et al.* recently reported on the effects of NX and subtotal renal ablation (NPX) on glomerular fibrin deposition and the activity of the intraglomerular procoagulant and fibrinolytic systems (382). Fibrin deposits were only seen after NPX, whereas NX rats had no such lesions as assessed by light and immunofluorescence microscopy. Procoagulant activity was reduced in both NX and NPX rats and fibrinolytic activity was increased in NPX animals only. The latter finding may be due to stimulation by the fibrin deposits which were only present in NPX rats. They concluded that the changes in glomerular hemostatic properties appear adaptive. Administration of the TxA₂ synthase inhibitor OKY 1581 did not alter the glomerular hemostatic balance. Similarly, NX in FHH rats may alter the intraglomerular hemostatic balance, a process which perhaps requires some time to develop its full potency. More studies are needed to confirm this hypothesis.

The role of prostaglandins, notably TxA₂, in the glomerular aggregation of platelets and subsequent sclerosis is somewhat controversial (468). Although glomerular synthesis and urinary excretion of TxA₂ generally increase after removal of nephrons by infarction (25), specific inhibition of the receptor of TxA₂ in ablated rats does not protect for glomerulosclerosis (468). Protection of remnant glomeruli by TxA₂ synthase inhibition probably results from lowering of systemic and glomerular hypertension because of redirection of endoperoxides toward vasodilatory prostaglandins (468). Young FH rats have a high urinary excretion of TxA₂ which gradually increases with age and correlates with level of proteinuria (U_pV) (211). Platelet formation of TxA₂ is abnormally high (255). The effect of NX on TxA₂ excretion and metabolism in FHH rats has not been assessed to date, but there is little reason to believe that the effect would be different from that in other rat strains. Thus, TxA₂ activity probably relates better with glomerular hemodynamics than with fibrin and platelet aggregation per se. The abnormal high platelet synthesis of TxA₂ in FH rats may perhaps influence or contribute to the abnormal glomerular hemodynamics, and indirectly through damage of the endothelium and collagen exposure by high \bar{P}_{GC} relate with fibrin deposition and platelet adherence. Further studies are required.

Ficoll sieving studies in FHH rats suggested an inborn permselectivity defect for size 20 - 40 Å molecules which remains present after NX and additional therapy (316). This defect may render the membrane more dependent upon charge to retain albumin. Most of the size selectivity of the filtration barrier resides in the cells. The contribution of these cellular elements to the overall permselectivity of the glomerulus is most conspicuous at the largest molecular radii (84). The defect for 20 - 40 Å molecules therefore might be the consequence of GBM rather than of cellular disturbances. Dextran sieving studies in patients with thin membrane nephropathy showed increased fractional clearance of neutral

dextran molecules $> 42 \text{ \AA}$ despite the absence of significant proteinuria (416). These subjects have no known cellular membrane defect and normal slit pore counts. The results of the experimental work by Daniels *et al.* (84) and the patient study by Thomas *et al.* therefore appear to be contradictory in respect to the spectrum of the expected sieving defect in the patients. Assumptions of the glomerular hemodynamic status in the patient study may have contributed to this. However, study of the sieving curves presented in the paper by Thomas *et al.* suggests that the defect observed in thin membrane patients in absolute terms is greatest in the smaller molecular spectrum. This is most apparent when comparing the curve of patients with the thin membrane defect with the graph obtained in patients with heavy proteinuria due to membranous nephropathy. Additional studies are needed to more clearly define the possible sieving abnormality in FHH rats. Furthermore, additional experiments need to be done in order to allow more optimal linking of sieving data to structural data.

A structural lesion of the GBM was not apparent in our current observations in the young 2K FHH rats. This is in contrast to observations by Kuijpers and Gruys, who noted thickening and occasional splitting of the GBM in 2 month old 2K FH rats (228). Probably due to small animal number and screening of glomeruli only, did we not observe such changes in our current study. We did identify splitting of the GBM with deposition of fibrin in the defect in the FHH rat NX at age 4 weeks and studied two weeks later. It might well be that this procedure uncovered a potential weakness of the matrix, but this interpretation remains rather speculative. Additional studies of the GBM in FHH rats are required to confirm the above impressions.

Kreisberg and Karnovsky first described the spontaneous development of FSGS in FH rats, and concluded that foot process fusion and epithelial cell injury are important changes contributing to the process of glomerular scarring (222). They studied 6 month old FH rats. Before foot process damage occurred, loss of anionic charges through all layers of the filtration barrier was seen. This loss in charge correlated with the amount of proteinuria, which increased over time in a progressive fashion. More recently, Kriz and coworkers studied the FHH rat strain ($n = 8$) at age 24 weeks (personal communication Dr. Provoost). WAG rats ($n = 7$) served as control. Systemic blood pressure as measured by tail-cuff plethysmography was 141 ± 15 vs. 106 ± 6 mm Hg, and albuminuria measured 36.6 ± 26.1 vs. 1.4 ± 0.5 mg/day/100 g bw for FHH vs. WAG, respectively (all animals with 2K). At this age glomerular damage was seen in all FHH rats, and varied from mild to severe including FSGS. Early lesions consisted of mesangial expansion and capillary ballooning. In more advanced damaged glomeruli the lesions in the podocytes dominated. These changes consisted of simplification of foot processes, flattening of podocyte cell bodies, pseudocyst / bleb formation, and finally detachments of podocytes from the GBM.

Presclerotic lesions consisting of local hyalinosis and thrombosis of glomerular capillaries were always seen in conjunction with tuft adhesions of Bowman's capsule. These authors stated that the early adhesions representing fixation of the tuft to Bowman's capsule is effected by parietal glomerular cells which attach to the GBM of naked capillary loops. Segmental sclerosis was found to exclusively develop in those adherent tuft regions. Mesangial proliferation was locally present but did not appear to contribute decisively to the development of sclerosis.

Podocyte lesions, notably foot process effacement, appeared to relate with level of $\Delta\bar{P}$ among NX FHH groups. Some focal fusion and attenuation of the cytoplasm was still present in the NX FHH rat treated with ACEI. Since glomerular tuft size increased similarly in both untreated and ACEI treated NX FHH rats, it is conceivable to believe that podocytes in these groups underwent a hypertrophic response. This response has been described previously in adriamycin induced nephrosis with (132) and without (441) additional renal ablation. It is thought that in these models stretch and hypertrophy of podocytes occur in an attempt by these cells to cover the GBM completely after an insult. Denudation of the GBM occurs on sites where this attempt has failed. The greater the loss of and damage to podocytes, the more apparent the foot process lesions and GBM denudation (225, 363, 364). These denuded sites are believed to represent the structural defect allowing large ($> 40 \text{ \AA}$) macromolecules to pass into Bowman's space (84, 201, 384, 441). We found a sieving defect for such large molecules in untreated NX FHH and ACEI treated NX FHH rat groups (316). Sieving studies in NX FHH rats treated by NO synthase inhibition involved only 4 animals. Data from those rats showed a similar trend for a defect in the $> 40 \text{ \AA}$ range, but significance was not reached. Thus, although the severity of podocyte injury and foot process fusion varied among groups, a permselective lesion was seen in the two groups indicated above, and was probably present in the latter mentioned group as well. The sieving defect tended to be less marked in ACEI treated rats with lower \bar{P}_{GC} , but remained present. Therefore, it appears that with the currently used tools for the study of permselectivity a graduation in the severity of podocyte injury was not possible. As indicated previously, the current findings are presented only to suggest possible routes of injury in FHH rats and do not identify them as such. For example, a link between level of \bar{P}_{GC} and degree of foot process damage is probably present in this model, but more studies are needed to confirm this.

Level of albuminuria paralleled with the level of $\Delta\bar{P}$ and as indicated above, with the damage to foot processes of the visceral epithelium. Therefore, level of albuminuria might indicate the extent of podocyte damage more precisely than loss of permselectivity for $> 40 \text{ \AA}$ molecules assessed by Ficoll. Olson *et al.* observed a decrement in glomerular fixed negative charge reflecting the extent of epithelial cell detachment in NPX Munich-

Wistar rats (319). In that study, permselectivity for $> 40 \text{ \AA}$ molecules was reduced after ablation, as has been reported in other similar experiments (269). As indicated above, we did not observe a reduction in this size selectivity defect in NX rats treated with ACEI. This is in contrast to many other reports on the effects of Ang II modulation on permselectivity after renal ablation (269). It is likely that the tracer used in the current study, Ficoll, is much more sensitive to identify a lesion in the filtration barrier. Ficoll is a more ideal marker molecule than the frequently used dextrans, since this agent is much more restricted by the normal glomerular barrier than dextran (315). Reversely, when a defect is present in the barrier it will be signalled by this molecule.

Yoshioka *et al.* recently showed that acute albuminuria as a consequence of H_2O_2 administration does not result in any ultrastructural defect, notably podocyte lesions were not seen in this acute setting (460). These findings suggest that podocyte foot process fusion represents damage in a more chronic process rather than resulting from acute changes in the glomerular milieu. Yoshioka *et al.* indicated that hemodynamic aberrations might have been present during the acute proteinuric phase and possibly related with the observed albuminuria. Changes in glomerular pressures and fluxes can alter the convection and diffusion of macromolecules.

Another interesting observation among the various groups is the apparent reciprocal relationship between the value for K_f and $\Delta\bar{P}$. K_f often decreases in rats with more severe podocyte injury and albuminuria. K_f is defined as:

$$K_f = \frac{fS}{l} \cdot \frac{r_0^2}{8\eta}$$

where f denotes the fraction of capillary surface area occupied by small pores, S the total glomerular capillary surface area, l the small pore length, r_0 the pore radius of small pores, and η the viscosity of the filtrate (462). The value for r_0 was essentially similar among groups as assessed by various membrane models (314, 316). The decrement in K_f in NX rats treated by NO synthase inhibition as compared with untreated NX rats therefore must have resulted from a loss in total small pore area (fS), or increase in pore length (l), or a combination of these. Tuft size, a crude indicator of S was not increased after NX in these animals, suggesting that change in pore length and fraction of capillary surface area occupied by small pores were the most important determinants. A reverse process must have occurred in ACEI treated NX rats. These rats increased K_f as compared to untreated NX FHH and 2K FHH animals. The tuft size increase may have contributed to this adaptation. Additional information on podocyte slit process dimensions and total surface

available for filtration among the animal groups is required to allow a better understanding of these preliminary observations.

This limited study on the ultrastructure of FHH rat glomeruli revealed several lesions. The earliest detected damage was seen in the endothelium in 2K young FHH rats, which was associated with fibrin and platelet adhesion. Damage to the GBM was seen in several rats and more studies are needed to define this apparent lesion. Podocyte damage was observed in NX rats, which appeared to reflect degree of albuminuria and the level of \overline{P}_{GC} . Decreased size selectivity for Ficoll molecules $> 40 \text{ \AA}$ appeared to be a marker for the presence of podocyte injury, but probably not for the degree of injury. These initial observations suggest the presence of a possible association between hemodynamic aberrations, morphological changes and permselectivity defects. More studies are required to confirm these suggestions.

PART IV:
GENERAL DISCUSSION

In this thesis, the fawn-hooded rat, a strain with an inborn predisposition to develop glomerular lesions and renal failure early in life, was studied. Details on this strain are provided in Chapter 2. The described experiments are a comprehensive assessment of different pathways previously associated with glomerular obsolescence and renal functional deterioration in other experimental models, illustrated in Chapter 1. These include hemodynamic and structural routes, and alterations in glomerular permselectivity for macromolecules. The various methods used for these studies were described in Chapter 3. In Chapter 4, practical and theoretical aspects of these techniques were provided to support their application and to reveal potential limitations.

In the initial experiment, provided in Chapter 5, the presence of glomerular capillary hypertension acting as a driving mechanism for the initiation and continuation of glomerular injury was established. We found that elevated mean glomerular capillary hydraulic pressure (\bar{P}_{GC}) occurred in young animals, before the development of major structural abnormalities in the filtration units. The level of \bar{P}_{GC} was highest in the fawn-hooded rat substrain characterized by the most progressive renal structural and functional deterioration, the FHH strain. In these rats, high efferent arteriolar vascular resistance resulted in the capture of systemic hypertension in the glomerular tuft. Afferent vasoconstriction could still prevent this from occurring, but was not present. The measurements of the size of the glomerular tuft revealed no differences among studied groups with relatively low values as compared to those previously reported for rats after renal ablation or induced diabetes. It was concluded that tuft size increases are not required for and not associated with the process of FSGS in fawn-hooded rats. Podocyte injury in "intact" fawn-hooded rats with two kidneys therefore does not result from stretch over an increased tuft, but more likely from increased stresses because of high \bar{P}_{GC} .

In the subsequent studies, the FHH substrain was selected because of its remarkable susceptibility for progressive injury and the most marked hemodynamic aberrations. Chapter 6 outlines the effects of uninephrectomy in FHH rats, including renal structural and functional adaptations. A profound acceleration of the renal disease was noted which was associated with a further elevation of \bar{P}_{GC} and hyperfiltration. Also the glomerular tuft was increased in size. We compared the magnitude of the structural and hemodynamic adaptations after NX in FHH rats with those reported in the literature for other rat strains. We concluded that the increased hemodynamic stresses were the most significant changes. The increased glomerular tuft volume was comparable with the response seen in other rat strains, and unlikely to account for the marked differences in the rate of progression of glomerular injury.

In Chapter 7, the importance of glomerular hemodynamic and glomerular hypertrophic responses in CRF were further investigated. Uninephrectomized FHH rats were pharmacologically treated and three groups with different levels of systemic blood pressure were thus created. Mean arterial blood pressure and \bar{P}_{GC} were closely correlated. This illustrated the poor regulatory capacity of FHH rat glomeruli to maintain constancy at \bar{P}_{GC} , thus exposing the capillaries to systemic blood pressure variations. Level of \bar{P}_{GC} among groups predicted the development of subsequent FSGS. Induction of glomerular growth by uninephrectomy did not significantly alter the course of this process. A summary of studies from the literature was provided to show the chronic effects of angiotensin II (Ang II) modulation on glomerular hemodynamics and structure after renal ablation. Concluded was that increases in glomerular tuft size which occur after ablation do not lead to progressive glomerular injury. Control of glomerular hypertension is essential to maintain renal function over long-term.

In Chapter 8, the permselective properties of the glomerular capillary wall of FHH rats were assessed. This was done with the tracer Ficoll, previously shown to be an ideal molecule for such studies. Two kidney FHH rats exhibited a defect for small to moderate-size molecules (20 - 42 Å range). Capillary restriction of albumin in these animals therefore depends relatively more on anionic charges in the filtration membrane than on size selectivity. Previous studies done by Kreisberg and Karnovsky in a related strain of fawn-hooded rats revealed a decreased density of these charges and a correlation between severity of loss of charge and the degree of proteinuria. Uninephrectomy in FHH rats induced a loss of size selectivity for large molecules and loss of charge selectivity. Treatment with an angiotensin I converting enzyme inhibitor (ACEI) repaired the latter defect. Analysis of all studied parameters showed a marked positive correlation between \bar{P}_{GC} and albuminuria, suggesting that high \bar{P}_{GC} might be responsible for the changes in permselectivity and charge.

Sieving data obtained in Experiment 8 and in an additional group of uninephrectomized FHH rats treated with a NO synthase inhibitor was analyzed in Chapter 9 in an attempt to calculate the transcapillary hydraulic pressure. Previously reported experiments were also included in these estimations. Various membrane models were used and data from FHH rats was processed for individual rats and for each treatment group. The currently available pore models were not advanced enough to allow differentiation between effects due to permselectivity and those from alterations in hemodynamics. Thus accurate estimation of $\Delta\bar{P}$ or directional changes in $\Delta\bar{P}$ from sieving data is not yet possible.

Initial ultrastructural studies were done in several FHH rats and presented in Chapter 10. The observed changes as detected by screening of glomeruli for lesions were summarized and discussed. Areas of interest for future studies were indicated.

Glomerular hypertension comprises a potent force in the progression of chronic renal disease. Not only well established models of induced chronic renal failure (CRF) such as diabetes and ablation nephropathy are characterized by this hemodynamic aberration, but as shown in this thesis, the fawn-hooded (FH) rats as well. Before extensive damage is present in young FH rats, mean glomerular capillary hydraulic pressure (\bar{P}_{GC}) is high and tightly linked with concomitant increases in proteinuria (U_pV) and albuminuria (U_aV), and subsequent progressive focal and segmental glomerulosclerosis (FSGS). The high \bar{P}_{GC} is a consequence of the transmission of systemic hypertension into the glomerular capillary tuft because of abnormalities in both the afferent and efferent resistance vessels. Preliminary results of a study assessing the NO system in the macula densa suggest an upregulated activity. Such dysregulation could explain the low inflow resistance. The NO system abnormality may be linked or associated with other vasoregulatory abnormalities. An important example of this is the recent finding of an immature pattern of renin expression in eight week old FHH rats with moderate systemic hypertension (SBP_{TC}: 140 ± 3 mm Hg) and mild U_pV (19 ± 2 mg/24h) (198). Plasma renin concentration was extremely high (95 ± 9.8 vs. $4 - 5$ ng AI/ml/h) and renal renin concentration was elevated (6.0 ± 0.4 vs. $1.6 - 1.7$ ng AI/mg protein/h) in these young FHH rats. Renal renin mRNA was upregulated in young FHH rats, and the distribution and immunostaining intensity of renin were indicative of an immature pattern. These observations further support the conclusion from Experiment 1 on the cause of the spontaneous glomerular hypertension and sclerosis, i.e. an exaggerated efferent arteriolar tone due to locally upregulated renin in the absence of afferent vasoconstriction. Aging of FHH rats is accompanied by a decline in renal and plasma renin, whereas renal immunostaining for angiotensin converting enzyme and angiotensinogen increase. These changes are accompanied by increments in U_pV and FSGS. The interaction between the NO system and the renin-angiotensin system (191, 311) was exemplified in Experiment 3, where the extremes of this interplay were revealed. Rats treated with NO synthase inhibition completely lost control over the efferent arteriole allowing the renin-angiotensin system to take over. These animals showed high values for \bar{P}_{GC} . Animals treated with an angiotensin I converting enzyme inhibitor (ACEI) opened the glomerular resistance vessels probably due to NO domination.

The dependence of U_pV (mainly albuminuria) in FHH rats on the level of systemic blood pressure as observed in Experiment 3 (Chapter 7) was recently investigated further (346). Four different ACEI's were used over a 15 week period. Regression analysis at various time intervals showed a significant correlation between SBP_{TC} and U_pV ($r = 0.77$

to 0.92). Morphologic examination of the kidneys showed that the incidence of FSGS was correlated with the final SBP_{TC} and U_pV (345). There were no notable alterations in glomerular tuft size among groups. When the ACEI's were withdrawn, hypertension and U_pV returned. A lag period of approximately one week was observed between the new level of blood pressure and U_pV . This latter finding may indicate that in addition to the direct hemodynamic effect of ACEI, a change occurs in the filtration membrane which affects renal protein excretion. This change may well be the charge of the filtration barrier, similar as reported in Experiment 4 of this thesis. A study with lisinopril (50 mg/l) in FHH rats revealed a similar biphasic response (432).

The elements of the filtration barrier are exposed to pressure and fluid fluxes as a result of both hemodynamic and oncotic forces. Pressure and flow act in an omnidirectional manner and causes various types of stress. Stress is an unidirectional feature, and basically four different types are recognized, i.e. tensile, compressive, shearing, and torsional. These stresses cause strain or deformities of the structure (225). It is thought that these deformities provide a signal to the various components of the glomerular capillary wall (80, 164, 260, 373). Signal processing includes the translation and integration of the information into cellular actions. For example, high \bar{P}_{GC} may result in focal failure of the anchorage of podocytes to the GBM (78) or in dimensional changes in the filtration slits (225). Mediated partially by integrins and the cytoskeleton, cell stress may lead to altered cell positioning (89), apoptosis (383) or other responses (264). The process of vascular remodeling is highly dynamic and is dependent upon and outlined by the available tools (144). These tools may differ for each individual, and are probably based on its genetic arsenal.

The variation in K_f among rat strains and models for CRF may perhaps serve to illustrate the above mentioned concept of the dynamic interaction between structure and function. Based on the Starling equation, we can envision the filtration process as a balance between the glomerular capillary ultrafiltration coefficient (K_f) and the net mean local ultrafiltration pressure (\bar{P}_{UF}). Increasing demand for filtration can be met by selectively modifying these variables. Rats unable to ideally regulate K_f and \bar{P}_{GC} , end up with high filtration pressures, develop proteinuria and die early. The Table below summarizes micropuncture data of euvolemic non-fasted male rats of several strains (24, 251), including some of the hemodynamic studies presented in this thesis. The SNGFR may reflect the demand for filtration. When values for this parameter are relatively low, filtration pressure and K_f can be low as well. Rats with the greatest susceptibility to sclerosis and U_pV have relatively low values for K_f in combination with a high $\Delta\bar{P}$. The \bar{P}_{UF} is separated in \bar{P}_{UF-A} and \bar{P}_{UF-E} to give an impression of the magnitude of forces to which

the capillaries are exposed over their length. In FHH rats for example, the \bar{P}_{UF} is not only high when blood just enters the glomerular units, but also when it is near the efferent arterioles. The whole capillary tufts are thus exposed to high stresses resulting from high hydraulic pressures and fluid fluxes. The level of \bar{P}_{GC} present within a glomerular capillary tuft is thought to be constant over the length of the capillary bed and thus independent of the site where this pressure is assessed in the network. This also applies to $\Delta\bar{P}$.

Hemodynamic data in euvolemic non-fasted male rats of various strains.

	\bar{P}_{GC}	$\Delta\bar{P}$	π_A	π_E	\bar{P}_{UF-A}	\bar{P}_{UF-E}	K_f	Q_A	SNGFR
	----- mm Hg -----						nl/(min-mm Hg)	- - nl/min - -	
MW	50	36	19	33	17	3	≥ 0.091	154	44
WKY	51	38	17	24	21	14	0.051	259	52
SD	55	40	18	32	22	8	0.050	140	42
FHH-Y	65	52	16	32	36	20	0.036	180	63
FHH	60	48	18	34	30	14	0.045	182	60
WAG	52	39	16	28	23	11	0.048	160	47

\bar{P}_{GC} , mean glomerular capillary hydraulic pressure as determined with direct puncture in Munich-Wistar rats and with the indirect stop-flow technique in the other rat strains; MW Munich-Wistar; WKY, Wistar Kyoto; SD, Sprague-Dawley; WAG, Wistar Albino Glaxo; $\Delta\bar{P}$, mean transcapillary hydraulic pressure difference; π_A and π_E , afferent and efferent arteriolar oncotic pressure, respectively; \bar{P}_{UF-A} and \bar{P}_{UF-E} , net mean local ultrafiltration pressure near the afferent and efferent arteriole, respectively; K_f , glomerular capillary ultrafiltration coefficient (Filtration disequilibrium was not present in MW rats and only minimal values for K_f are therefore provided, indicated by \geq); Q_A , initial glomerular plasma flow rate; SNGFR, single-nephron glomerular filtration rate. FHH (age 16 weeks) and FHH-Y (age 8 weeks) rats have highest susceptibility for early FSGS and CRF among the in the Table presented strains. The other strains do develop glomerular lesions but such damage is only observed after a considerable greater time span. The WKY rats have a remarkable resistance for FSGS and generally do not exhibit chronic renal failure.

The role for the above mentioned mechanism in progressive glomerular injury, low K_f and high \bar{P}_{GC} , is more easily appreciated in experimental models characterized by loss of nephrons by ablation. The model described by Bidani *et al.*, the normotensive remnant Wistar Kyoto (WKY) rat, is of particular interest in this respect (39). Most animals of this strain remained normotensive after 5/6 nephrectomy and showed only a modest elevation in

\bar{P}_{GC} . SNGFR was increased to a similar extent as observed in Munich-Wistar (MW) rats after such a procedure (179). Although values for K_f were not reported by Bidani *et al.*, the provided hemodynamic parameters suggested a substantial increase in this determinant of ultrafiltration. Intact WKY rats have a remarkable resistance to develop FSGS. Even after the extensive renal ablation none of the normotensive WKY rats developed glomerular injury. Only those WKY rats which became hypertensive after renal ablation showed FSGS. Hemodynamic assessment was not done in these latter animals. Dworkin and Feiner reported on the effects of uninephrectomy (NX) in WKY rats and the spontaneously hypertensive rat (SHR) (108). Compensatory hyperfiltration was observed in both strains after NX. WKY achieved this by increasing K_f , whereas SHR rats elevated \bar{P}_{GC} . Only NX SHR rats developed glomerulosclerosis. Electron micrographs were provided, and showed epithelial foot process obliteration, thickening of the glomerular basement membrane, and swelling of the endothelial cell cytoplasm and loss of fenestrae in NX SHR only. Increases in K_f have not been reported for MW rats after uninephrectomy or more extensive renal ablation (179). Glomerular injury invariably occurs in these animals after removal of nephrons, and the severity of the overall damage is paralleled by the rise in \bar{P}_{GC} .

Celsi *et al.* provided some additional insight into the hemodynamic response after NX, and K_f per se (67). These investigators showed that 20 days after NX of five day old Sprague-Dawley (SD) rats, no significant changes in the determinants of K_f were present. The increase in SNGFR resulted from elevated \bar{P}_{GC} . Sixty days after surgery, estimation of the effective hydraulic permeability of the glomerular capillary wall (k) in individual glomeruli and the surface area available for filtration per glomerulus (S) showed that NX rats had an increased S but a decrement of k . These alterations resulted in an unchanged value for K_f , the product of k and S . The authors stated that the significant lower k observed eight weeks after NX is probably an early sign of a pathological process in the glomerular membrane that leads to early development of glomerulosclerosis. Of note, the high \bar{P}_{GC} preceded the relative loss in k and therefore suggests a route of glomerular adaptation leading to injury, i.e. high \bar{P}_{GC} causing functional impairment of the filtration barrier. Treatment of the very young NX SD rats with a calcium channel blocker was associated with normalization of \bar{P}_{UF} , a concomitant rise in K_f because of increases in both k and S , and maintenance of glomerular hyperfiltration (68). Savin *et al.* assessed the components of K_f in individual glomeruli of the remnant MW rat (392). A biphasic response in k was observed, consisting of an increase seven weeks after surgery and a decrease at 28 weeks. Ablated rats on a restricted protein diet showed long-term preservation of k . These studies are of interest since assessment of K_f was done directly, independent of glomerular hemodynamic measurements. Combining glomerular

micropuncture with the morphometric estimation of S in individual glomeruli in order to assess k was done by Neuman *et al.* Measurements in the isolated perfused kidney of three month old Wistar rats four weeks after contralateral NX revealed an adaptive increase in k (304).

These various mentioned experiments suggest that the increase in glomerular tuft size, which occurs during normal maturation and is often observed after nephron loss, may represent a long-term glomerular adaptive response to maintain glomerular filtration. The increase in total glomerular filtration surface area (FSA) resulting from such growth may then limit increases in \bar{P}_{GC} . Microcirculatory studies performed in rats during the prenatal and infant periods indicate that the observed increases in total kidney GFR and SNGFR after birth are to some extent driven by increases in \bar{P}_{GC} , \bar{P}_{UP} , and k. The major determinant of the increases in GFR during this age period however is the absolute increase in glomerular capillary surface area (187, 407). When the combined elements of the glomerular barrier can not preserve or increase k, such glomerular size change may be associated with limitations in filtration capacity.

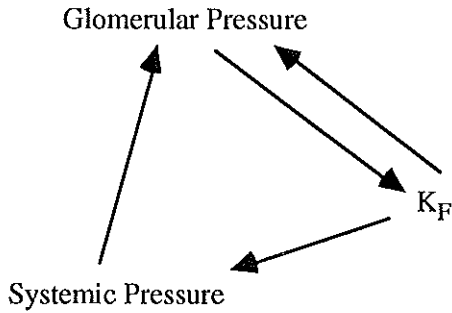
FHH rats have high values for SNGFR. The high filtration rate is the result of a high hydraulic filtration pressure, whereas K_f remains relatively low. These aberrations are present before major ultrastructural and light microscopic changes occur. FHH rats have a normal total amount of glomeruli and normal sizes of the glomerular tufts. An abnormally low FSA available for filtration is therefore unlikely to explain for the barrier defect. The inability of these animals to elevate K_f may reside in an intrinsic membrane defect, resulting in a low k. In response to reduction in renal mass, FHH rats do not increase K_f but augment \bar{P}_{GC} to maintain filtration. When treated with an ACEI, these NX rats exhibit an increase in K_f , normalization of \bar{P}_{GC} , and long-term protection from glomerulosclerosis. The increase in glomerular tuft size in untreated and ACEI treated NX FHH rats was not associated with FSGS in ACEI treated rats. These treated rats showed preservation of most foot processes despite the hypertrophic response. The absolute level of \bar{P}_{GC} was comparable with those observed in intact normal rats. It therefore appears conceivable that the adaptive growth response of glomeruli in FHH rats which occurs after nephron loss contributes to preservation of glomerular filtration. Only when high \bar{P}_{GC} becomes apparent, may the hypertrophic response act as a permissive factor for podocyte injury. Such a hypertrophic response is however not required for injury to occur. This was exemplified in our studies in the young 2K FHH rats and in NX FHH rats treated with a NO synthase inhibitor. In both cases, high \bar{P}_{GC} was associated with subsequent glomerular obsolescence and not accompanied by increases in the size of the glomerular tufts.

Although the information presented above is not conclusive, it appears that high \overline{P}_{GC} is associated with low K_f in several models in which FSGS develops relatively rapidly. Which elements of the filtration barrier are responsible for the apparent pathophysiologic link remains to be fully clarified. Some studies, including our preliminary findings in FHH rats, suggest that disturbances in the delicate architecture of the foot processes of the podocytes are associated with loss of filtration capability. The slit pores, formed by these highly differentiated cells are probably responsible for approximately 50% of the hydraulic pressure barrier (103). On the other hand, damage to the endothelium and the GBM is often seen in the various models of CRF. This was illustrated for the 2K FHH rat in Chapter 10. In that chapter, we also discussed the apparent association between level of \overline{P}_{GC} , the extent of foot process fusion, and adaptations in K_f among NX FHH rats. Furthermore, the possible association of proteinuria with morphological and hemodynamic changes was considered. Changes in hydraulic permeability are often encountered in proteinuric states and suggest that the structural alterations as observed in those diseases are tightly linked with protein conductivity. A mathematical model of an integrated filtration barrier, which includes the relative contributions of the separate layers of the glomerular membrane to the resistance to the filtration of water was recently presented by Drumond and Deen (103). The hydraulic permeability of the filtration barrier could be predicted from morphologic data in normal and injured glomeruli. Similarly, such estimations and models would be very relevant for the study of protein permeability and to possibly explain for proteinuria.

The question remains which layer of the membrane is responsible for protein restriction, what the contribution of anionic sites is in this respect, and what the typical morphological and functional changes are which result in proteinuria. Kanwar and Rosenzweig showed that firm attachment of the epithelial foot processes to the basement membrane play a vital role in determining the permselectivity to macromolecules (201). Focal detachments of the podocytes in neuraminidase treated animals and in puromycin aminonucleoside induced-nephrosis were identified as sites of increased convection of native ferritin, whereas areas with normal foot processes were not associated with such an increase. Changes in matrix, both structurally and in charge did occur but were not related with increased tracer trafficking. Podocyte anionic sites decreased, but did not result in increased tracer passage. These authors suggested that the focal disruptions in the podocyte-GBM interaction result in perturbations in local glomerular blood flow and increase in the $\Delta\overline{P}$ causing an accelerated bulk flow of proteins through these denuded areas. They concluded that the matrix-podocyte connection functionally couples the hemodynamic forces to permselectivity changes, allowing the charge and size selective properties of the GBM to act as fine discriminators precisely regulating the passage of macromolecules on the basis of their size, charge, and shape. Thus optimal interaction and

function of all compartments of the barrier is probably required for normal permselective function.

Reduction of the total kidney filtration surface area (FSA) as a major renal abnormality contributing to the initiation and maintenance of hypertension was proposed recently (55). Analysis of the pressure-natriuresis relationship and glomerular hemodynamics in conditions with a decreased FSA have revealed that sodium-sensitive essential hypertension and elevated \bar{P}_{GC} are the hallmarks of these low FSA states (160, 215). In single-nephron hemodynamics, K_f constitutes the product of the effective hydraulic conductivity (k) and the total surface area available for filtration in a single glomerulus (S) (97, 251). This parameter provides insight into the single-nephron characteristics of the filtration membrane as an *in vivo* determinant of hemofiltration (251). We can apply the microcirculatory term K_f to whole kidney ultrafiltration. The whole kidney K_f (K_F) is more comprehensive than FSA to explain renal responses to injury. This term allows us to understand that an alteration of K_F may represent changes in either nephron number, filtration surface area per glomerulus, the hydraulic permeability of the glomerular capillary walls, or a combination of these elements. When K_F is diminished by any cause, glomerular hypertension becomes evident, and leads to a syndrome of glomerular hyperfiltration, hypertension, progressive azotemia, proteinuria and eventually glomerulosclerosis (51, 56, 215). The regulation of K_F results from intimately linked structural and hemodynamic processes. The glomerular filtration barrier and the blood flowing through the capillaries operate in unity. *In vivo*, the glomerular tuft consists of a bowl of pulsating capillaries, constantly changing and adapting to the demands of the moment. The design of the glomerular filtration barrier, the product of genetic data and influenced by milieu factors, contributes to the regulation of \bar{P}_{GC} . Glomerular injury indicates endangerment of the various components of K_F . If in such an instance K_f can not be increased in the surviving glomeruli, \bar{P}_{GC} must rise in order to maintain filtration. This may or may not be accompanied by systemic blood pressure elevations. The elevated \bar{P}_{GC} initiates a cascade of progressive glomerular damage. Thus in those instances in which an important aberration in the control of blood filtration is present, the abnormal level of \bar{P}_{GC} dominates the process of hemofiltration and induces structural glomerular damage. Up to that moment, the process of glomerular filtration under normal conditions is the resultant of the optimal interaction of the elements of the filtration barrier and the precisely tuned exposure of this membrane to the hemodynamic forces. The illustration below summarizes these various concepts.



In summary, glomerular hypertension is both an injurious force in the progression of chronic renal disease and probably reflects an abnormality in the K_F of the kidney. Experimental work may provide a better understanding of the intricate relationships of the various elements of the glomerular capillary wall, the mechanisms by which these constituents define the hydraulic permeability and permselectivity of the filtration barrier and the numerous changes which occur in response to injury. The FHH rat, a unique spontaneous model of glomerular injury, should be further explored in this respect. The *in vivo* glomerular micropuncture techniques displayed in this thesis may continue to provide the hemodynamic fingerprint of pathophysiologic processes (7) and allow for correlations with cellular and biomolecular aberrations (214).

De fawn-hooded rat ontwikkelt spontaan chronisch nierfalen op relatief jonge leeftijd. Dit proces wordt gekenmerkt door verhoogde bloeddruk, proteinurie, albuminurie, en focale glomerulosclerose (FSGS). In dit proefschrift worden een aantal experimenten beschreven die tot doel hadden om deze veranderingen te verklaren. Deze studies zijn gebaseerd op vergelijkbaar experimenteel werk in andere diersmodellen van chronisch nierfalen, welke in Hoofdstuk 1 worden genoemd. Diverse aspecten van de fawn-hooded rat, zoals herkomst en ontwikkeling van de stam, details van eerder verrichtte pathologische studies van de glomeruli en een overzicht van andere gevonden afwijkingen worden besproken in Hoofdstuk 2. In Hoofdstuk 3 worden de gebruikte materialen en methoden beschreven en in Hoofdstuk 4 worden deze nader toegelicht.

In Hoofdstuk 5 wordt het experiment beschreven waarin de aanwezigheid van glomerulaire capillaire hypertensie in de fawn-hooded rat aangetoond wordt. Een verhoogde glomerulaire capillaire hydraulische druk (\bar{P}_{GC}) werd gemeten in jonge ratten, voorafgaand aan het ontstaan van belangrijke structurele veranderingen in de glomeruli. Het niveau van \bar{P}_{GC} was het hoogste in de FHH substam, die in tegenstelling tot de FHL substam, een progressief verloop van nierbeschadiging heeft. Een hoge weerstand in de efferente arteriolen en de afwezigheid van vasoconstrictie in de afferente arteriolen resulteerde in de transmissie van de verhoogde systemische bloeddruk in het glomerulaire capillaire netwerk. Meting van het glomerulaire volume liet geen verschil zien tussen de experimentele groepen. Zodoende werd geconcludeerd dat glomerulaire volumeveranderingen niet vereist zijn voor het spontane ontstaan van FSGS in de fawn-hooded rat.

De FHH substam werd gebruikt voor de verdere studies. De structurele en hemodynamische effecten van unilaterale nephrectomie (NX) werden onderzocht in Hoofdstuk 6. Het ontstaan van chronisch nierfalen en glomerulaire beschadiging werd versneld door deze ingreep. Dit was geassocieerd met een verdere verhoging van de \bar{P}_{GC} en glomerulaire hyperfiltratie. Daarnaast was het glomerulaire capillaire volume vergroot na NX. De morfologische en hemodynamische adaptaties na NX in de FHH rat werden vergeleken met eerder gerapporteerde gegevens voor andere rattendammen. De structurele aanpassing was vergelijkbaar. We concludeerden dat de hemodynamische veranderingen waarschijnlijk het meest bijdroegen tot het ontstaan van FSGS na NX in de FHH rat.

De relatieve bijdrage van glomerulaire capillaire hypertensie, hyperfiltratie en groei in het proces van FSGS werd nader onderzocht in Hoofdstuk 7. Drie groepen NX FHH ratten met een verschillende systemische bloeddruk werden onderzocht. Naast een onbehandelde controle groep werd een groep ratten behandeld met een remmer van de

aanmaak van angiotensine II ("angiotensin-converting enzyme inhibitor": ACEI), die een verlaging van de bloeddruk veroorzaakte. Een derde groep werd behandeld met een remmer van de aanmaak van stikstofoxide, waardoor de bloeddruk verder omhoog ging. Systemische bloeddruk en \bar{P}_{GC} correleerden sterk met elkaar, hetgeen het onvermogen illustreerde van de glomeruli in de FHH rat om de \bar{P}_{GC} optimaal te reguleren. Het niveau van \bar{P}_{GC} voorspelde het latere ontstaan van FSGS. Toename van het glomerulaire volume, zoals na verwijderen van nierweefsel optreedt, bleek geen onafhankelijke risicofactor voor het ontstaan van FSGS te zijn en niet noodzakelijk voor het ontstaan van FSGS. Indien glomerulaire capillaire hypertensie voorkomen wordt, zoals met een ACEI, ontstaat geen proteinurie en FSGS, terwijl de glomerulaire hyperfiltratie aanwezig blijft. Een literatuuroverzicht ondersteunde de conclusies van dit experiment.

In Hoofdstuk 8 werden de permselectieve eigenschappen van de glomerulaire filtratiebarriere van de FHH rat onderzocht met het tracer macromolecuul Ficoll. In vergelijking met eerder gepubliceerde gegevens in een normotensieve rattestam, hadden twee-nierige FHH ratten een filtratiedefect voor moleculen met een grootte van 20 - 42 Å. De capillaire restrictie van albumine (36 Å) was daarom relatief meer afhankelijk van de negatieve afstotende lading in de glomerulaire barriere. NX veroorzaakte een verminderde permselectiviteit voor grotere macromoleculen (> 42 Å) en een verlies van anion in de barriere. Behandeling met een ACEI voorkwam verlies van glomerulaire negatieve lading. De gevonden sterke correlatie tussen \bar{P}_{GC} en albuminurie suggereerde dat een hoge \bar{P}_{GC} verantwoordelijk kan zijn voor veranderingen in glomerulair anion.

In Hoofdstuk 9 werden de gegevens uit Hoofdstuk 8, aangevuld met nieuwe experimentele en literatuurgegevens, gebruikt om de \bar{P}_{GC} te berekenen uit de permselectiviteit. De zo verkregen \bar{P}_{GC} waarden bleken niet goed te correleren met de gemeten waarden. Geconcludeerd werd dat de verschillende glomerulaire membraanmodellen thans niet voldoende geavanceerd zijn om de hoogte van en verschillen in de \bar{P}_{GC} nauwkeurig te voorspellen.

De glomerulaire ultrastructuur van enkele ratten uit de voorafgaande experimenten werd met behulp van de electronenmicroscopie onderzocht. In Hoofdstuk 10 werden de gevonden afwijkingen samengevat en besproken in relatie met eerder gerapporteerde functionele en structurele parameters.

Na een Engelstalige samenvatting in Hoofdstuk 11 werden in Hoofdstuk 12 enige recente observaties besproken die de aanwezigheid van glomerulaire capillaire hypertensie in de fawn-hooded rat wellicht kunnen verklaren. Tevens werd de interactie van structuur en functie besproken aan de hand van de relatie tussen de glomerulaire hemodynamiek en de glomerulaire filtratiebarriere.

14 REFERENCES

1. SAS/STAT User's Guide. (4th edition ed.) Cary, NC, SAS Institute, Inc., 1990.
2. Abrams RL, Lipkin LE, Hennigar GR: A quantitative estimation of variation among human renal glomeruli. *Lab Invest* 12: 69-76, 1963.
3. Addis TB, Meyers BA, Oliver J: The regulation of renal activity: IX. The effect of unilateral nephrectomy on the function and structure of the remaining kidney. *Arch Intern Med* 34: 243, 1924.
4. Akima H: Interpolation and smooth curve fitting based on local procedures. *Comm ACM* 15: 914-918, 1972.
5. Alt JM, Hackbarth H, Deerberg F, Scholte H: Proteinuria in rats in relation to age-dependent renal changes. *Lab Anim* 14: 95, 1980.
6. Amato D, Tapia E, Bobadilla NA, Franco M, Calleja C, Garcia-Torres R, Lopez P, Alvarado JA, Herrera-Acosta J: Mechanisms involved in the progression to glomerular sclerosis induced by systemic hypertension during mild puromycin aminonucleoside nephrosis. *Am J Hypertens* 5: 629-636, 1992.
7. Anderson S: Relevance of single nephron studies to human glomerular function. *Kidney Int* 45: 384-389, 1994.
8. Anderson S, Brenner BM: Intraglomerular hypertension. *Annu Rev Med* 39: 243-253, 1988.
9. Anderson S, Diamond JR, Karnovsky MJ, Brenner BM: Mechanisms underlying transition from acute glomerular injury to late glomerular sclerosis in a rat model of nephrosis. *J Clin Invest* 82: 1757-1768, 1988.
10. Anderson S, Jung FF, Ingelfinger J: Renal renin-angiotensin system in diabetes: functional, immunohistochemical, and molecular biological correlations. *Am J Physiol* 265: F477-F486, 1993.
11. Anderson S, Meyer TW, Rennke HG, Brenner BM: Control of glomerular hypertension limits glomerular injury in rats with reduced renal mass. *J Clin Invest* 76: 612-619, 1985.
12. Anderson S, Rennke HG, BM BM Brenner: Nifedipine versus fosinopril in uninephrectomized diabetic rats. *Kidney Int* 41: 891-897, 1992.
13. Anderson S, Rennke HG, Brenner BM: Therapeutic advantage of converting enzyme inhibitors in arresting progressive renal disease associated with systemic hypertension in the rat. *J Clin Invest* 77: 1993-2000, 1986.
14. Anderson S, Rennke HG, Garcia DL, Brenner BM: Short and long term effects of antihypertensive therapy in the diabetic rat. *Kidney Int* 36: 526-536, 1989.
15. Andreucci VE, Herrera-Acosta J, Rector FC, Seldin DW: Effective glomerular filtration pressure and single nephron filtration rate during hydropenia, elevated ureteral pressure, and acute volume expansion with isotonic saline. *J Clin Invest* 50: 2230-2234, 1971.

16. Arendshorst WJ, Beierwaltes WH: Renal and nephron hemodynamics in spontaneously hypertensive rats. *Am J Physiol* 236: F246-F251, 1979.
17. Arora RC, Tong C, Jackman H, Stoff D, Meltzer HY: Serotonin uptake and imipramine binding in blood platelets and brain of Fawn-Hooded and Sprague-Dawley rats. *Life Sci* 33: 437-442, 1983.
18. Arturson G, Groth T, Grotte G: Human glomerular membrane porosity and filtration pressure: dextran clearance data analysed by theoretical models. *Clin Sci* 40: 137-158, 1971.
19. Ashmore RC, Rodman DM, Sato K, Webb SA, O'Brien RF, McMurtry IF, Stelzner TJ: Paradoxal constriction to platelets by arteries from rats with pulmonary hypertension. *Am J Physiol* 260: H1929-H1934, 1991.
20. Aukland K: Myogenic mechanisms in the kidney. *J Hypertens* 7: S71-S76, 1989.
21. Aulakh CS, Hill JL, Lesch KP, Murphy DL: Functional subsensitivity of 5-hydroxytryptamine_{1c} or alpha₂ adrenergic heteroreceptors mediating clonidine-induced growth hormone release in the Fawn-Hooded rat strain relative to the Wistar rat strain. *J Pharmacol Exp Ther* 262: 1038-1043, 1992.
22. Aulakh CS, Hill JL, Murphy DL: Attenuation of hypercortisolemia in fawn-hooded rats by antidepressant drugs. *Eur J Pharmacol* 240: 85-88, 1993.
23. Azar S, Johnson MA, Hertel B, Tobian L: Single-nephron pressures, flows, and resistances in hypertensive kidneys with nephrosclerosis. *Kidney Int* 12: 28-40, 1977.
24. Azar S, Johnson MA, Scheinman J, Bruno L, Tobian L: Regulation of glomerular capillary pressure and filtration rate in young Kyoto hypertensive rats. *Clin Sci* 56: 203-209, 1979.
25. Badr KF, Jacobson HR: Arachidonic acid metabolites and the kidney. In Brenner BM, Rector FC Jr (ed): *The Kidney*, 4th, 584-619. Philadelphia, W.B. Saunders Comp., 1991.
26. Baylis C: Immediate and long-term effects of pregnancy on glomerular function in the SHR. *Am J Physiol* 257: F1140-F1145, 1989.
27. Baylis C, Fredericks M, Leyboldt J, Frigon R, Wilson C, Henderson L: The mechanisms of proteinuria in aging rats. *Mech Ageing Developm* 45: 111-126, 1988.
28. Baylis C, Mitruka B, Deng A: Chronic blockade of nitric oxide synthesis in the rat produces systemic hypertension and glomerular damage. *J Clin Invest* 90: 278-281, 1992.
29. Bear PG, Navar LG, Guyton AC: Renal autoregulation, filtration rate and electrolyte excretion during vasodilation. *Am J Physiol* 219: 619-625, 1970.
30. Bell PD, Redington M, Ploth D, Navar LG: Tubuloglomerular feedback-mediated decreases in glomerular pressure in Munich-Wistar rats. *Am J Physiol* 247: F877-F880, 1984.
31. Bellin JS, Sorrentino JM: Kinetic characteristics of monoamine oxidase and serum cholinesterase in several related rat strains. *Biochem Genet* 11: 309-317, 1974.

32. Benabe JE, Wang S, Wilcox JN, Martinez-Maldonado M: Modulation of ANG II receptor and its mRNA in normal rat by low-protein feeding. *Am J Physiol* 265: F660-F669, 1993.
33. Benstein JA, Feiner HD, Parker M, Dworkin LD: Superiority of salt restriction over diuretics in reducing renal hypertrophy and injury in uninephrectomized SHR. *Am J Physiol* 258: F1675-F1681, 1990.
34. Berg BN, Simms HS: Nutrition and longevity in the rat: I. Longevity and onset of disease with different levels of food intake. *J Nutr* 71: 255-263, 1960.
35. Bergstein JM: Glomerular fibrin deposition and removal. *Pediatr Nephrol* 4: 78-87, 1990.
36. Bianchi G, Fox U, Francesco GF Di, Giovannetti AM, Pagetti D: Blood pressure changes produced by kidney cross-transplantation between spontaneously hypertensive rats and normotensive rats. *Clin Sci Mol Med* 47: 435, 1974.
37. Bick RL: Platelet function defects: a clinical review. *Semin Thromb Hemost* 18: 167-185, 1992.
38. Bidani AK, Griffin KA, Plott W, Schwartz MM: Genetic predisposition to hypertension and microvascular injury in the remnant kidney model. *J Lab Clin Med* 121: 284-291, 1993.
39. Bidani AK, Mitchell KD, Schwartz MM, Navar LG, Lewis EJ: Absence of glomerular injury or nephron loss in a normotensive rat remnant kidney model. *Kidney Int* 38: 28-38, 1990.
40. Blantz RC, Gabbai FB, Tucker BJ, Yamamoto T, Wilson CB: Role of mesangial cell in glomerular response to volume and angiotensin II. *Am J Physiol* 264: F158-F165, 1993.
41. Blatherwick NR, Medlar EM: Chronic nephritis in rats fed high protein diets. *Arch Intern Med* 59: 572, 1937.
42. Bohrer MP, Baylis C, Humes HD, Glasscock RJ, Robertson CR, Brenner BM: Permeability of the glomerular capillary wall. Facilitated filtration of circulating polycations. *J Clin Invest* 61: 72-78, 1978.
43. Bohrer MP, Baylis C, Robertson CR, Brenner BM: Mechanisms of the puromycin-induced defects in the transglomerular passages of water and macromolecules. *J Clin Invest* 60: 152-161, 1977.
44. Bohrer MP, Deen WM, Robertson CR, Brenner BM: Mechanisms of angiotensin II induced proteinuria in the rat. *Am J Physiol* 233: F13-F21, 1977.
45. Bohrer MP, Deen WM, Robertson CR, Troy JL, Brenner BM: Influence of macromolecular configuration on the passage of macromolecules across the glomerular capillary wall. *J Gen Physiol* 74: 583-593, 1979.
46. Bohrer MP, Patterson GD, Carroll PJ: Hindered diffusion of dextran and Ficoll in microporous membranes. *Macromolecules* 17: 1170-1173, 1984.

47. Bolton WK, Benton FR, Maclay JG, Sturgill BC: Spontaneous glomerular sclerosis in aging Sprague-Dawley rats. I. Lesions associated with mesangial IgM deposits. *Am J Pathol* 85: 277, 1976.
48. Braam B, Mitchell KD, Koomans H, Navar LG: Relevance of the tubuloglomerular feedback mechanism in pathophysiology. *J Am Soc Nephrol* 4: 1257-1274, 1993.
49. Bradley M, Schuman GB, Ward PCJ: Examination of urine. In Henry JB (ed): *Clinical Diagnosis and Management by Laboratory Methods.*, 604-605. Philadelphia, PA, WB Saunders, 1979.
50. Brandis A, Bianchi G, Reale E, Helmchen U, Kuhn K: Age-dependent glomerulosclerosis and proteinuria occurring in rats of the Milan normotensive strain and not in rats of the Milan hypertensive strain. *Lab Invest* 55: 234-243, 1986.
51. Brenner BM: Nephron adaptation to renal injury or ablation. *Am J Physiol* 249: F324-F337, 1985.
52. Brenner BM, Cohen RA, Milford EL: In renal transplantation, one size may not fit all. *J Am Soc Nephrol* 3: 162-169, 1992.
53. Brenner BM, Daugharty TM: The measurement of glomerular filtration rate in single nephrons of the rat kidney. *Yale J Biol Med* 45: 200-210, 1972.
54. Brenner BM, Daugharty TM, Ueki IF, Troy JL: Quantitative assessment of proximal tubule function in single nephrons of the rat kidney. *Am J Physiol* 220: 2058-2067, 1971.
55. Brenner BM, Garcia DL, Anderson S: Glomeruli and blood pressure: less of one, more the other? *Am J Hypertens* 1: 335-347, 1988.
56. Brenner BM, Meyer TW, Hostetter TH: Dietary protein intake and progressive nature of kidney disease: The role of hemodynamically mediated injury in the pathogenesis of progressive glomerular sclerosis in aging, renal ablation and intrinsic renal disease. *N Engl J Med* 307: 652-659, 1982.
57. Brenner BM, Milford EL: Nephron underdosing: a programmed cause of chronic allograft failure. *Am J Kidney Dis* 21: S66-S72, 1993.
58. Brenner BM, Troy JL, Daugharty TM: The dynamics of glomerular ultrafiltration in the rat. *J Clin Invest* 50: 1776-1780, 1971.
59. Brenner BM, Troy JL, Daugharty TM: Pressures in cortical structures of the rat kidney. *Am J Physiol* 222: 246-251, 1972.
60. Brenner BM, Troy JL, Daugharty TM, Deen WM: Dynamics of glomerular ultrafiltration in the rat. II. Plasma-flow dependence of GFR. *Am J Physiol* 223: 1184-1190, 1972.
61. Bricker NS, Klahr S, Rieselbach RE: The functional adaptation of the diseased kidney. I. Glomerular filtration rate. *J Clin Invest* 43: 1915-1921, 1964.
62. Briggs JP: Effect of loop of Henle flow on glomerular capillary pressure. *Renal Physiol* 7: 311-320, 1984.

63. Bright R: Tabular view of morbid appearance in 100 cases connected with albuminous urine. *Guy's Hosp Rep* 1: 380-410, 1836.
64. Cameron JS: Recurrent disease in renal allografts. *Kidney Int* 44: S91-S94, 1993.
65. Campese VM, Bigazzi R: The role of hypertension in the progression of renal diseases. *Am J Kidney Dis* 17: 43-47, 1991.
66. Cartwright ME, Jaenke RS: Effects of dietary protein and captopril on glomerular permselectivity in rats with unilateral nephrectomy. *Lab Invest* 59: 492-499, 1988.
67. Celsi G, Larsson L, Seri I, Savin V, Aperia A: Glomerular adaptation in uninephrectomized young rats. *Pediatr Nephrol* 3: 280-285, 1989.
68. Celsi G, Savin VJ, Henter JI, Sohtell M: The contribution of ultrafiltration pressure for glomerular hyperfiltration in young nephrectomized rats. *Acta Physiol Scand* 141: 483-487, 1991.
69. Chan AYM, Cheng MLL, Keil LC, Meyers BD: Functional response of healthy and diseased glomeruli to a large, protein-rich meal. *J Clin Invest* 81: 245-254, 1988.
70. Chang RLS: A model to study the dynamics of glomerular ultrafiltration and glomerular capillary permselectivity characteristics. *Microvasc Res* 16: 141-150, 1978.
71. Chang RLS, Deen WM, Robertson CR, Bennett CM, Glasscock RJ, Brenner BM: Permselectivity of the glomerular capillary wall. Studies of experimental glomerulonephritis in the rat using neutral dextran. *J Clin Invest* 57: 1272-1286, 1976.
72. Chang RLS, Deen WM, Robertson CR, Brenner BM: Permselectivity of the glomerular capillary wall. III. Restricted transport of polycations. *Kidney Int* 8: 212-218, 1975.
73. Chang RLS, Robertson CR, Deen WM, Brenner BM: Permselectivity of the glomerular capillary wall to macromolecules. I. Theoretical considerations. *Biophys J* 15: 861-886, 1975.
74. Chang RLS, Ueki IF, Troy JL, Deen WM, Robertson CR, Brenner BM: Permselectivity of the glomerular capillary wall to macromolecules. II. Experimental studies in rats using neutral dextran. *Biophys J* 15: 887-906, 1975.
75. Chanutin A, Ferris EB Jr: Experimental renal insufficiency produced by partial nephrectomy. I. Control diet. *Arch Intern Med* 49: 767-787, 1932.
76. Chasis H, Redish J, Goldring W, Ranges HA, Smith HW: Use of sodium p-aminohippurate for functional evaluation of human kidney. *J Clin Invest* 24: 583-591, 1945.
77. Cheigh JS, Mouradian J, Soliman M, Tapia L, Riggio RR, Stenzel KH, Rubin AL: Focal segmental glomerulosclerosis in renal transplants. *Am J Kidney Dis* 2: 449-455, 1983.
78. Cho CR, Lumsden CJ, Whiteside CI: Epithelial cell detachment in the nephrotic glomerulus: a receptor co-operativity model. *J Theoret Biol* 160: 407-426, 1993.

79. Coleman GL, Barthold SW, Osbaldiston GW, Foster SJ, Jonas AM: Pathological changes during aging in barrier-reared Fisher 344 male rats. *J Gerontol* 32: 258-278, 1977.
80. Cortes P, Riser BL, Zhao X, Narins RG: Glomerular volume expansion and mesangial cell mechanical strain: mediators of glomerular pressure injury. *Kidney Int* 45: S11-S16, 1994.
81. Couser WG, Stilmant MM: Mesangial lesions and focal glomerular sclerosis in the aging rat. *Lab Invest* 33: 491, 1975.
82. Cusi D, Tripodi G, Casari G, Robba C, Bollini P, Merati G, Bianchi G: Onset and development of renal damage in hypertension: genetics of renal damage in primary hypertension. *Am J Kidney Dis* 21: 2-9, 1993.
83. Damme B Van, Koudstaal J: Measuring glomerular diameters in tissue sections. *Virchows Arch* 369: 283-291, 1976.
84. Daniels BS, Deen WM, Mayer G, Meyer T, Hostetter TH: Glomerular permeability barrier in the rat: functional assessment by *in vitro* methods. *J Clin Invest* 92: 929-936, 1993.
85. Daniels BS, Hostetter TH: Adverse effects of growth in the glomerular microcirculation. *Am J Physiol* 258: F1409-F1416, 1990.
86. Daoust M, Compagnon P, Legrand E, Boucly P: Ethanol intake and 3H-serotonin uptake: a study in fawn-hooded rats. *Life Sci* 48: 1969-1976, 1991.
87. Davidson MG, Deen WM: Hindered diffusion of water-soluble macromolecules in membranes. *Macromolecules* 21: 3474-3481, 1988.
88. Davidson WD, Sackner MA: Simplification of the anthrone method for the determination of inulin in clearance studies. *J Lab Clin Med* 62: 351-356, 1963.
89. Davies PF, Robotewskyj A, Griem ML: Quantitative studies of endothelial cell adhesion: directional remodeling of focal adhesion sites in response to flow forces. *J Clin Invest* 93: 2031-2038, 1994.
90. Deen WM, Bridges CR, Brenner BM: Biophysical basis of glomerular permselectivity. *J Membr Biol* 71: 1-10, 1983.
91. Deen WM, Bridges CR, Brenner BM, Meyers BD: Heteroporous model of glomerular size selectivity: application to normal and nephrotic humans. *Am J Physiol* 249: F374-F389, 1985.
92. Deen WM, Maddox DA, Robertson CR, Brenner BM: Dynamics of glomerular ultrafiltration in the rat. VII. Response to reduced renal mass. *Am J Physiol* 227: 556-562, 1974.
93. Deen WM, Robertson CR, Brenner BM: A model of glomerular ultrafiltration in the rat. *Am J Physiol* 223: 1178-1183, 1972.
94. Deen WM, Robertson CR, Brenner BM: Concentration polarization in an ultrafiltering capillary. *Biophys J* 14: 412-431, 1974.

95. Deen WM, Satvat B: Determinants of the glomerular filtration of proteins. *Am J Physiol* 241: F162-F170, 1981.
96. Deen WM, Satvat B, Jamieson JM: Theoretical model for glomerular filtration of charged solutes. *Am J Physiol* 238: F126-F139, 1980.
97. Deen WM, Troy JL, Robertson CR, Brenner BM: Dynamics of glomerular ultrafiltration in the rat. IV. Determination of the ultrafiltration coefficient. *J Clin Invest* 52: 1500-1508, 1973.
98. Diamond JR: Analogous pathobiologic mechanisms in glomerulosclerosis and atherosclerosis. *Kidney Int* 39: S29-S34, 1991.
99. Diamond JR, Anderson S: Irreversible tubulointerstitial damage associated with chronic aminonucleoside nephrosis. *Am J Pathol* 137: 1323-32, 1990.
100. DiBona GF, Rios LL: Mechanisms of exaggerated diuresis in spontaneously hypertensive rats. *Am J Physiol* 235: F409-F416, 1979.
101. Dilley JR, Schrier CT, Arendshorst WJ: Abnormalities in glomerular function in rats developing spontaneous hypertension. *Am J Physiol* 246: F12-F20, 1984.
102. Drumond MC, Deen WM: Analysis of pulsatile pressures and flows on glomerular filtration. *Am J Physiol* 261: F409-F419, 1991.
103. Drumond MC, Deen WM: Structural determinants of glomerular hydraulic permeability. *Am J Physiol* 266: F1-F12, 1994.
104. DuBois R, Decoodt P, Gasse JP, Verniory A, Lambert PP: Determination of glomerular intracapillary and transcapillary pressure gradients from sieving data. I. A mathematical model. *Pflugers Arch* 356: 299-316, 1975.
105. DuBois R, Stoupel E: Permeability of artificial membranes to a pluridisperse solution of 125I-polyvinylpyrrolidone. *Biophys J* 16: 1427-1445, 1976.
106. Dumbrille-Ross A, Tang SW: Absence of high-affinity [3H]imipramine binding in platelets and cerebral cortex of fawn-hooded rats. *Eur J Pharmacol* 72: 137-138, 1981.
107. Dworkin LD, Benstein JA, Parker M, Tolbert E, Feiner HD: Calcium antagonists and converting enzyme inhibitors reduce renal injury by different mechanisms. *Kidney Int* 43: 808-814, 1993.
108. Dworkin LD, Feiner HD: Glomerular injury in uninephrectomized spontaneously hypertensive rats: a consequence of glomerular hypertension. *J Clin Invest* 77: 796-809, 1986.
109. Dworkin LD, Feiner HD, Parker M, Tolbert E: Effects of nifedipine and enalapril on glomerular structure and function in uninephrectomized SHR. *Kidney Int* 39: 1112-1117, 1991.
110. Dworkin LD, Feiner HD, Randazzo J: Glomerular hypertension and injury in desoxycorticosterone-salt rats on antihypertensive therapy. *Kidney Int* 31: 718-724, 1987.
111. Dworkin LD, Grosser M, Feiner HD, Ullian M, Parker M: Renal vascular effects of antihypertensive therapy in uninephrectomized SHR. *Kidney Int* 35: 790-798, 1989.

112. Dworkin LD, Hostetter TH, Rennke HG, Brenner BM: Hemodynamic basis for glomerular injury in rats with desoxycorticosterone-salt hypertension. *J Clin Invest* 73: 1448-1452, 1984.
113. Eddy AA, Michael AF: Immunopathogenic mechanisms of glomerular injury. In Tisher CC, Brenner BM (ed): *Renal Pathology*, 2nd, 162-221. Philadelphia, Lippincott Comp., 1994.
114. Elema JD, Arends A: Focal and segmental glomerular hyalinosis and sclerosis in the rat. *Lab Invest* 33: 554-561, 1975.
115. Elias H, Hennig A: Stereology of the human renal glomerulus. In Weibel ER, Elias H (ed): *Quantitative Methods in Morphology*, 130-166. Heidelberg, Springer, 1967.
116. Elias H, Hennig A, Schwartz DE: Stereology: applications to biomedical research. *Physiol Rev* 51: 158-200, 1971.
117. Emery JL, Macdonald MS: Involuting and scarred glomeruli in the kidneys of infants. *Am J Pathol* 36: 713-723, 1960.
118. Fahr T: Pathologische Anatomie des Morbus Brightii. In Henke F, Lubarsch O (ed): *Handbuch der Speziellen Pathologischen Anatomie und Histologie.*, 222-236. Berlin, Springer-Verlag, 1925.
119. Falk SA, Buric V, Hammond WS, Conger JD: Serial glomerular and tubular dynamics in thyroidectomized rats with remnant kidneys. *Am J Kidney Dis* 17: 218-227, 1991.
120. Farr LE, Smadel JE: The effect of dietary protein on the course of nephrotoxic nephritis in the rat. *J Exp Med* 70: 615-627, 1939.
121. Feld LG, Liew JB Van, Brentjens JR, Boylan JW: Renal lesions and proteinuria in the spontaneously hypertensive rat made normotensive by treatment. *Kidney Int* 20: 606-614, 1981.
122. Feld LG, Liew JB Van, Galaske RG, Boyland JW: Selectivity of renal injury and proteinuria in the spontaneously hypertensive rat. *Kidney Int* 12: 332-343, 1977.
123. Feldman HI, Klag MJ, Chiapella AP, Whelton PK: End-stage renal disease in US minority groups. *Am J Kidney Dis* 14: 397-410, 1992.
124. Floege J, Alpers CE, Burns MW, Pritzl P, Gordon K, Couser WG, Johnson RJ: Glomerular cells, extracellular matrix accumulation, and the development of glomerulosclerosis in the remnant kidney model. *Lab Invest* 66: 485-497, 1992.
125. Floege J, Burns MW, Alpers CE, Yoshimura A, Pritzl P, Gordon K, Seifert RA, Bowen-Pope DF, Couser WG, Johnson RJ: Glomerular cell proliferation and PDGF expression precede glomerulosclerosis in the remnant kidney model. *Kidney Int* 41: 297-309, 1992.
126. Floege J, Eng E, Young BA, Alpers CE, Barrett TB, Bowen-Pope DF, Johnson RJ: Infusion of platelet-derived growth factor or basic fibroblast growth factor induces selective glomerular mesangial cell proliferation and matrix accumulation in rats. *J Clin Invest* 92: 2952-2962, 1993.

127. Fogo A, Ichikawa I: Evidence for the central role of glomerular growth promoters in the development of sclerosis. *Semin Nephrol* 9: 329-342, 1989.
128. Fogo A, Ichikawa I: Glomerular growth promoter: the common channel to glomerulosclerosis. In Mitch W, Stein J (ed): *The Progressive Nature of Renal Disease*, 2nd, 23-54. New York, Churchill Livingstone, 1992.
129. Fox U, Bianchi G: The primary role of the kidney in causing the blood pressure difference between the Milan hypertensive strain (MHS) and normotensive rats. *Clin Exp Pharmacol Physiol* 3: S71, 1976.
130. Fransen R. Tubular lithium handling in the rat. [Ph.D.]. Utrecht, 1994.
131. Freytag JW, Dalrymple PN, Maguire MH, Strickland DK, Carraway KL, Hudson BG: Glomerular basement membrane. Study on its structure and interaction with platelets. *J Biol Chem* 253: 9069-9074, 1978.
132. Fries JW, Sandstrom DJ, Meyer TW, Rennke HG: Glomerular hypertrophy and epithelial cell injury modulate progressive glomerulosclerosis in the rat. *Lab Invest* 60: 205-218, 1989.
133. Fuhr J, Kaemarczyk J, Kruttgen CD: Eine einfache colorimetrische Methode zur Inulinbestimmung für Nieren-clearance Untersuchungen bei Stoffwechselfgesunden und diabetikern. *Klin Wochenschr* 33: 729-730, 1955.
134. Fujihara CK, Michelazzo SM, Santos MM, Nucci G De, Zatz R. Chronic nitric oxide inhibition worsens glomerular injury in the remnant kidney (abstract). XIIth Int Congress Nephrol., Jerusalem 1993: 52.
135. Fujihara CK, Michelazzo SM, Sena CR, Padilha RM, Santos MM, Nucci G De, Zatz R. Massive albuminuria and renal parenchymal injury by chronic nitric oxide inhibition and salt overload (abstract). XIIth Int Congress Nephrol., Jerusalem 1993: 52.
136. Galaske RG, Liew JB Van, Feld LG: Filtration and reabsorption of endogenous low-molecular-weight protein in the rat kidney. *Kidney Int* 16: 394-403, 1979.
137. Garcia DL, Anderson S, Rennke HG, Brenner BM: Anemia lessens and its prevention with recombinant human erythropoietin worsens glomerular injury and hypertension in rats with reduced renal mass. *Proc Natl Acad Sci USA* 85: 6142-6146, 1988.
138. Garcia DL, Rennke HG, Brenner BM, Anderson S: Chronic glucocorticoid therapy amplifies glomerular injury in rats with renal ablation. *J Clin Invest* 80: 867-874, 1987.
139. Garcia DL, Rennke HG, Brenner BM, Anderson S: Glucocorticoids amplify glomerular injury in rats with renal ablation. *Am J Hypertension* 1: 54-57, 1988.
140. Gasse JP: Effects of acetylcholine on glomerular sieving of macromolecules. *Pflugers Arch* 342: 239-254, 1973.
141. Gasse JP, Decoodt P, Verniory A, Lambert PP: Autoregulation of effective glomerular filtration pressure. *Am J Physiol* 266: 616-623, 1974.

142. Gasse JP, DuBois R, Staroukine M, Lambert PP: Determination of glomerular intracapillary and transcapillary pressure gradients from sieving data. III. The effect of angiotensin II. *Pflugers Arch* 367: 15-24, 1976.
143. Gertz KH, Mangos JA, Braun G, Pagel HD: Pressure in the glomerular capillaries of the rat kidney and its relation to arterial blood pressure. *Pflugers Arch* 288: 369-374, 1966.
144. Gibbons GH, Dzau VJ: The emerging concept of vascular remodeling. *N Engl J Med* 330: 1431-1438, 1994.
145. Gilboa N, Rudofsky U, Magro A: Urinary and renal kallikrein in hypertensive fawn-hooded (FH/Wjd) rats. *Lab Invest* 50: 72-78, 1984.
146. Gilboa N, Rudofsky UH, Phillips MI, Magro AM: Modulation of urinary kallikrein and plasma renin activities does not affect established hypertension in the fawn-hooded rat. *Nephron* 51: 61-66, 1989.
147. Golbetz H, Black V, Shemesh O, Meyers BD: Mechanisms of the antiproteinuric effect of indomethacin in nephrotic humans. *Am J Physiol* 256: F44-F51, 1989.
148. Goor H Van, Diamond JR, Grond J: Renal disease induced in rats by puromycin aminonucleoside. In Gretz N, Strauch M (ed): *Experimental and Genetic Rat Models of Chronic Renal Failure*, 68-81. Basel, Karger, 1993.
149. Goor H Van, Fidler V, Weening JJ, Grond J: Determinants of focal and segmental glomerulosclerosis in the rat after renal ablation: evidence for involvement of macrophages and lipids. *Lab Invest* 64: 754-765, 1991.
150. Gottschalk CW: Function of the chronically diseased kidney. The adaptive nephron. *Circ Res* 28(Suppl. II): 1-13, 1971.
151. Gray JE: Chronic progressive nephrosis in the albino rat. *CRC Crit Rev Toxicol* 5: 115, 1977.
152. Gray JE, Zwieten MJ Van, Hollander CF: Early light microscopic changes of chronic progressive nephrosis in several strains of aging laboratory rats. *J Gerontol* 37: 142-150, 1982.
153. Gretz N, Strauch M: The adriamycin model. In Gretz N, Strauch M (ed): *Experimental and Genetic Rat Models of Chronic Renal Failure*, 82-89. Basel, Karger, 1993.
154. Gretz N, Waldherr R, Strauch M: The remnant kidney model. In Gretz N, Strauch M (ed): *Experimental and Genetic Rat Models of Chronic Renal Failure*, 1-28. Basel, Karger, 1993.
155. Grond J, Beukers JJB, Schilthuis MS, Weening JJ, Elema JD: Analysis of renal structural and functional features in two rat strains with a different susceptibility to glomerular sclerosis. *Lab Invest* 54: 77-83, 1986.
156. Guasch A, Deen WM, Meyers BD: Charge selectivity of the glomerular filtration barrier in healthy and nephrotic humans. *J Clin Invest* 92: 2274-2282, 1993.

157. Gutmann PH, Andersen AC: Progressive intercapillary glomerulosclerosis in aging and irradiated beagles. *Radiol Res* 35: 45-60, 1968.
158. Guyton AC: *Arterial Pressure and Hypertension*. Philadelphia, WB Saunders, 1980.
159. Guyton AC: Renal function curve-a key to understanding the pathogenesis of hypertension. *Hypertension* 10: 1-6, 1987.
160. Guyton AC, Coleman PJ, Cowley AW: A systems analysis approach to understanding long range arterial blood pressure control and hypertension. *Circ Res* 35: 159-176, 1974.
161. Haberle DA, Konigbauer B, Davis JM, Kawata T, Mast C, Metz C, Dahlheim H: Autoregulation of the glomerular filtration rate and the single-nephron glomerular filtration rate despite inhibition of tubuloglomerular feedback in rats chronically volume-expanded by deoxycorticosterone acetate. *Pflugers Arch* 416: 548-553, 1990.
162. Hakim RM, Goldszer RC, Brenner BM: Hypertension and proteinuria: long-term sequelae of uninephrectomy in humans. *Kidney Int* 1984: 930-936, 1984.
163. Halbach GR, Alt JM, Brunkhorst R, Frei U, Kuhn K, Scholte H: Single nephron hyperfiltration and proteinuria in a newly selected rat strain with superficial glomeruli. *Renal Physiol* 9: 317-325, 1986.
164. Harris RC, Akai Y, Yasuda T, Homma T: The role of physical forces in alterations of mesangial cell function. *Kidney Int* 45: S17-S21, 1994.
165. Hayman JM Jr, Martin J Jr, Miller M: Renal function and the number of glomeruli in the human kidney. *Ach Int Med* 64: 69-83, 1939.
166. Hayslett JP: Functional adaptation to reduction in renal mass. *Physiol Rev* 59: 137-164, 1979.
167. Hayslett JP, Kashgarian M, Epstein FH: Functional correlates of compensatory renal hypertrophy. *J Clin Invest* 47: 774-782, 1968.
168. Hayslett JP, Krassner LS, Bensch KG, al. et: Progression of "lipoid nephrosis" to renal insufficiency. *N Engl J Med* 281: 181-187, 1969.
169. Heptinstall RH: End-stage renal disease. In Heptinstall RH (ed): *Pathology of the Kidney*, 4th, 713-777. Boston, Little Brown Comp., 1992.
170. Heptinstall RH, Hill GS: Steroid-induced hypertension in the rat. *Lab Invest* 16: 751-767, 1967.
171. Herrera-Acosta J, Gabbai F, Tapia E, al. et: Effect of captopril and hydrochlorothiazide on glomerular haemodynamics and histological damage in Goldblatt hypertension with partial renal ablation. *J Hypertension* 4: S275-S278, 1986.
172. Herxheimer G: Uber hyaline glomeruli der Neugeborenen und Sauglinge. *Z Pathol* 2: 138-152, 1909.

173. Heudes D, Chevalier MJ, Schalbert E, Ezan E, Bariety J, Zimmerman A, Corman B: Effect of chronic ANG I-converting enzyme inhibition on aging processes. I. Kidney structure and function. *Am J Physiol* 266: R1038-R1051, 1994.
174. Hirose K, Osterby R, Nozawa M, Gundersen HJG: Development of glomerular lesions in experimental long-term diabetes in the rat. *Kidney Int* 21: 689-695, 1982.
175. Holmsen H, Weiss HJ: Hereditary defect in the platelet release reaction caused by a deficiency in the storage pool of platelet adenine nucleotides. *Brit J Haemat* 19: 643-649, 1970.
176. Holmsen H, Weiss HJ: Further evidence for a deficient storage pool of adenine nucleotides in platelets from some patients with thrombocytopathia "storage pool disease". *Blood* 39: 197-209, 1972.
177. Holstein-Rathlou NH: Oscillations and chaos in renal blood flow control. *J Am Soc Nephrol* 4: 1275-1287, 1993.
178. Hostetter TH, Meyer TW, Rennke HG, Brenner BM: Chronic effects of dietary protein in the rat with intact and reduced renal mass. *Kidney Int* 30: 509-517, 1986.
179. Hostetter TH, Olson JL, Rennke HG, Venkatachalam MA, Brenner BM: Hyperfiltration in remnant nephrons: a potentially adverse response to renal ablation. *Am J Physiol* 241: F85-F93, 1981.
180. Hostetter TH, Troy JL, Brenner BM: Glomerular hemodynamics in experimental diabetes mellitus. *Kidney Int* 19: 410-415, 1981.
181. Howell TH, Piggot AP: The kidney in old age. *J Gerontol* 3: 124-128, 1948.
182. Hulihan-Giblin BA, Park YD, Aulakh CS, Goldman D: Regional analysis of 5-HT_{1A} and 5-HT₂ receptors in the fawn-hooded rat. *Neuropharmacology* 31: 1095-1099, 1992.
183. Hulihan-Giblin BA, Park YD, Goldman D, Aulakh CS: Analysis of the 5-HT_{1c} receptor and the serotonin uptake site in fawn-hooded rat brain. *Eur J Pharmacol* 239: 99-102, 1993.
184. Hutchison FN, Webster SK: Effect of ANG II receptor antagonist on albuminuria and renal function in passive Heyman nephritis. *Am J Physiol* 263: F311-F318, 1992.
185. Ichikawa I, Brenner BM: Mechanisms of action of histamine and histamine antagonists on the glomerular microcirculation in the rat. *Circ Res* 45: 737-745, 1979.
186. Ichikawa I, Harris RC: Angiotensin actions in the kidney: renewed insight into the old hormone. *Kidney Int* 40: 583-596, 1991.
187. Ichikawa I, Maddox DA, Brenner BM: Maturation development of glomerular ultrafiltration in the rat. *Am J Physiol* 236: F465-F471, 1979.
188. Ichikawa I, Maddox DA, Cogan MG, Brenner BM: Dynamics of glomerular ultrafiltration in euvolemic Munich-Wistar rats. *Renal Physiol, Basel* 1: 121-131, 1978.
189. Ichikawa I, Miele JF, Brenner BM: Reversal of renal cortical actions of angiotensin II by verapamil and manganese. *Kidney Int* 16: 137-147, 1979.

190. Isaka Y, Fujiwara Y, Ueda N, Kaneda Y, Kamada T, Imai E: Glomerulosclerosis induced by *in vivo* transfection of transforming growth factor- β or platelet-derived growth factor gene into the rat kidney. *J Clin Invest* 92: 2597-2601, 1993.
191. Ito S, Arima S, Ren YL, Juncos LA, Carretero OA: Endothelium-derived relaxing factor/nitric oxide modulates angiotensin II action in the isolated microperfused rabbit afferent but not efferent arteriole. *J Clin Invest* 91: 2012-2019, 1993.
192. Jacob HJ, Lindpaintner K, Lincoln SE, Kusumi K, Bunker RK, Mao YP, Ganten D, Dzau VJ, Lander ES: Genetic mapping of a gene causing hypertension in the stroke-prone spontaneously hypertensive rat. *Cell* 67: 213-224, 1991.
193. Jaremko G, Larsson L, Bohman SO: Angiotensin-induced structural changes in the rat glomerulus (abstract). *J Ultrastruct Mol Struct Res* 100: 300-301A, 1989.
194. Jobe MI: Mechanisms of coagulation and fibrinolysis. In Lotspeich-Steiniger CA, Stiene-Martin EA, Koepke JA (ed): *Clinical Hematology*, 1st, 579-598. Philadelphia, PA, Lippincott Comp., 1992.
195. Johnson JE, Barrows CH: Effects of age and dietary restriction on the kidney glomeruli of mice: Observations by scanning electron microscopy. *Anat Rec* 196: 145-151, 1980.
196. Jones DB: Arterial and glomerular lesions associated with severe hypertension: light and electron microscopic studies. *Lab Invest* 31: 303, 1974.
197. Joseph MH: Brain tryptophan metabolism on the 5-hydroxytryptamine and kynurenine pathways in a strain of rats with a deficiency in platelet 5-HT. *Br J Pharmac* 63: 529-533, 1978.
198. Jung F, Provoost AP, Bouyounes B, Ingelfinger JR: Persistence of immature pattern of renin expression in young fawn-hooded rats (abstract). *J Am Soc Nephrol* 4: 773, 1993.
199. Kanfer A: Glomerular coagulation system in renal diseases. *Renal Failure* 14: 407-412, 1992.
200. Kanwar YS: Biology of disease: biophysiology of glomerular filtration and proteinuria. *Lab Invest* 51: 7-21, 1984.
201. Kanwar YS, Rosenzweig LJ: Altered glomerular permeability as a result of focal detachment of the visceral epithelium. *Kidney Int* 21: 565-574, 1982.
202. Kaplan C, Pasternack B, Shah H: Age-related incidence of sclerotic glomeruli in human kidneys. *Am J Pathol* 80: 227-234, 1975.
203. Kappel B, Olsen S: Cortical interstitial tissue and sclerosed glomeruli in the normal human kidney, related to age and sex. A quantitative study. *Virchows Arch (Pathol Anat)* 387: 271-277, 1980.
204. Kasiske BL, O'Donnell MP, Cleary MP, Keane WF: Treatment of hyperlipidemia reduces glomerular injury in obese Zucker rats. *Kidney Int* 33: 667-672, 1988.

205. Katsumata H, Suzuki H, Ohishi A, Nakamoto H, Saruta T, Sakaguchi H: Effects of antihypertensive agents on blood pressure and the progress of renal failure in partially nephrectomized Spontaneously Hypertensive Rats. *Lab Invest* 62: 474-480, 1990.
206. Kaufman JM, Siegel NJ, Hayslett JP: Functional and hemodynamic adaptation to progressive renal ablation. *Circ Res* 36: 286-293, 1975.
207. Keijzer MH De, Provoost AP: Effects of dietary protein on the progression of renal failure in the fawn-hooded rat. *Nephron* 55: 203-209, 1990.
208. Keijzer MH De, Provoost AP: Renal deterioration after uninephrectomy in adult fawn-hooded rats (abstract). *Kidney Int* 38: 359, 1990.
209. Keijzer MH De, Provoost AP, Molenaar JC: Glomerular hyperfiltration in hypertensive fawn-hooded rats. *Renal Physiol Biochem* 11: 103-108, 1988.
210. Keijzer MH De, Provoost AP, Molenaar JC: Proteinuria is an early marker in the development of progressive renal failure in hypertensive fawn-hooded rats. *J Hypertens* 7: 525-528, 1989.
211. Keijzer MH De, Provoost AP, Zijlstra FJ: Enhanced urinary excretion of eicosanoids in fawn-hooded rats. *Nephron* 62: 454-458, 1992.
212. Kempfer AC, Frontroth JP, Farias C, Bermejo E, Lazzari MA: A simple enzyme-immunoassay test for von Willebrand factor binding in human arterial subendothelium. *Thromb Res* 68: 131-136, 1992.
213. Kentera D, Susi D, Veljkovic V, Tucakovic G, Koko V: Pulmonary artery pressure in rats with hereditary platelet function defect. *Respiration* 54: 110-114, 1988.
214. Kerjaschki D: Dysfunctions of cell biological mechanisms of visceral epithelial cell (podocytes) in glomerular diseases. *Kidney Int* 45: 300-313, 1994.
215. Kimura G, Brenner BM: A method for distinguishing salt-sensitive from non-salt sensitive forms of human and experimental hypertension. *Curr Opin Nephrol Hypertens* 2: 341-349, 1993.
216. Kiprov DD, Colvin RB, McCluskey: Focal and segmental glomerulosclerosis and proteinuria associated with unilateral renal agenesis. *Lab Invest* 46: 275-281, 1982.
217. Kirchmaier CM, Meyer M, Spangenberg P, Heller R, Haroske D, Breddin HK, Till U: Platelet membrane defects in the fawn hooded bleeder rats. *Thromb Res* 57: 353-360, 1990.
218. Klahr S, Levey AS, Beck GJ, Caggiula AW, Hunsicker L, Kusek JW, Striker G, Group For the Modification of Diet in Renal Disease Study: The effects of dietary protein restriction and blood-pressure control on the progression of chronic renal disease. *N Engl J Med* 330: 877-84, 1994.
219. Klahr S, Schreiner G, Ichikawa I: The progression of renal disease. *N Engl J Med* 318: 1657-1666, 1988.
220. Kleinbaum DG, Kupper LL, Muller KE: Applied Regression Analysis and other Multivariable methods. Boston, MA, PWS-Kent Publishing Co., 1988.

221. Kopf D, Waldherr R, Rettig R: Source of kidney determines blood pressure in young renal transplanted rats. *Am J Physiol* 265: F104-F111, 1993.
222. Kreisberg JJ, Karnovsky MJ: Focal glomerular sclerosis in the fawn-hooded rat. *Am J Pathol* 92: 637-652, 1978.
223. Kriz W, Elger M, Lemley KV, Sakai T: Mesangial cell-glomerular basement membrane connections counteract glomerular capillary and mesangium expansion. *Am J Nephrol* 10(S1): 4-13, 1990.
224. Kriz W, Elger M, Nagata M, Kretzler M, Uiker S, Koeppen-Hagemann I, Tenschert S, Lemley KV: The role of podocytes in the development of glomerular sclerosis. *Kidney Int* 45: S64-S72, 1994.
225. Kriz W, Hackenthal E, Nobiling R, Sakai T, Elger M: A role for podocytes to counteract capillary wall distension. *Kidney Int* 45: 369-376, 1994.
226. Kuijpers MHM. Hypertension in the fawn-hooded rat. [PhD]. University of Utrecht, 1986.
227. Kuijpers MHM, Gruys E: Nephrosclerosis and hypertension in the fawn-hooded rat. *Berl Munch Tierarztl Wochenschr* 94: 39, 1981.
228. Kuijpers MHM, Gruys E: Spontaneous hypertension and hypertensive renal disease in the fawn-hooded rat. *Br J Exp Pathol* 65: 181-190, 1984.
229. Kuijpers MHM, Jong W De: Spontaneous hypertension in the fawn-hooded rat: a cardiovascular disease model. *J Hypert* 4: S41-S44, 1986.
230. Kuijpers MHM, Jong W De: Relationship between blood pressure level, renal histopathological lesions and plasma renin activity in fawn-hooded rats. *Br J Exp Pathol* 68: 179-187, 1987.
231. Kuijpers MHM, Provoost AP, Jong W De: Development of hypertension and proteinuria with age in fawn-hooded rats. *Clin Exp Pharmacol Physiol* 13: 201-209, 1986.
232. Kurnick NB, Lindsey PA: Compensatory renal hypertrophy in parabiotic mice. *Lab Invest* 10: 45-48, 1968.
233. Ladefaged J: Renal failure 22 years after kidney donation. *Lancet* 339: 128, 1992.
234. Lafayette RA, Mayer G, Park SK, Meyer TW: Angiotensin II receptor blockade limits glomerular injury in rats with reduced renal mass. *J Clin Invest* 90: 766-771, 1992.
235. Lafferty HM, Anderson S, Brenner BM: Anemia: a potent modulator of renal hemodynamics in models of progressive renal disease. *Am J Kidney Dis* 17: 2-7, 1991.
236. Lafferty HM, Brenner BM: Are glomerular hypertension and "hypertrophy" independent risk factors for progression of renal disease? *Semin Nephrol* 10: 294-304, 1990.
237. Lambert PP, DuBois R, Decoodt P, Gasse JP, Verniory A: Determination of glomerular intracapillary and transcapillary pressure gradients from sieving data. II. A physiological study in the normal dog. *Pflugers Arch* 359: 1-22, 1975.

238. Lambert PP, Gasse JP, Verniory A, Ficherouille P: Measurement of the glomerular filtration pressure from sieving data for macromolecules. *Pflugers Arch* 329: 34-58, 1971.
239. Lambert PP, Gasse JP, Verniory A, Ficherouille P, DuPont E: The measurement of glomerular filtration pressure from sieving data for macromolecules. *Adv Nephrol* 1: 113-124, 1971.
240. Lambert PP, Verniory A, Gasse JP, Ficherouille P: Sieving equations and effective glomerular filtration pressure. *Kidney Int* 2: 131-146, 1972.
241. Laouari D, Kleinknecht C, Gubler MC, Broyer M: Adverse effect of proteins on remnant kidney: dissociation from that of other nutrients. *Kidney Int* 24: S248-S253, 1983.
242. Larson M, Hermansson K, Wolgast M: Hydraulic permeability of the glomerular capillary membranes in the rat kidney. *Acta Physiol Scand* 117: 251-261, 1983.
243. LaVail MM: Fawn-hooded rats, the fawn mutation and interaction of pink-eyed and red-eyed dilution genes. *J Hered* 72: 286-287, 1981.
244. Lee ML, Purkerson ML, Agate FJ, Dempsey EW: Ultrastructural changes in renal glomeruli of rats during experimentally induced hypertension and uremia. *Am J Anat* 135: 191-204, 1972.
245. Lewis E: Recurrent focal sclerosis after renal transplantation. *Kidney Int* 22: 315-323, 1982.
246. Lewis EJ, Hunsicker LG, Bain RP, Rohde RD, Group For the Collaborative Study: The effect of angiotensin-converting-enzyme inhibition on diabetic nephropathy. *N Engl J Med* 329: 1456-62, 1993.
247. Lombet JR, Adler SG, Anderson PS, Nast CC, Olson DR, Glassock RJ: Sex vulnerability in the subtotal nephrectomy model of glomerulosclerosis in the rat. *J Lab Clin Med* 114: 66-74, 1989.
248. Lommel A Van, Lauweryns JM: Neuroepithelial bodies in the fawn hooded rat lung: morphological and neuroanatomical evidence for a sensory innervation. *J Anat* 183: 553-566, 1993.
249. Maddox DA, Bennett CM, Deen WM, Glassock RJ, Knutson D, Daugharty TM, Brenner BM: Determinants of glomerular filtration in experimental glomerulonephritis in the rat. *J Clin Invest* 55: 305-318, 1975.
250. Maddox DA, Brenner BM: Glomerular Ultrafiltration. In Brenner BM, Rector FC Jr (ed): *The Kidney*, 4th ed., 205-244. Philadelphia, WB Saunders Comp., 1991.
251. Maddox DA, Deen WM, Brenner BM: Glomerular filtration. In Windhager EE (ed): *Handbook of Physiology*, Section 8: Renal Physiology, Chapter 13., 545-638. Bethesda, American Physiological Society, 1992.
252. Maddox DA, Price DC, Rector FC: Effects of surgery on plasma volume and salt and water excretion in rats. *Am J Physiol* 233: F600-F606, 1977.
253. Maddox DA, Troy JL, Brenner BM: Autoregulation of filtration rate in the absence of macula densa-glomerulus feedback. *Am J Physiol* 227: 123-131, 1974.

254. Magro AM: Histamine release from fawn-hooded rat mast cells is not potentiated by phosphatidylserine. *Immunol* 44: 1-10, 1981.
255. Magro A, Bizios R, Catalfamo J, Blumenstock F, Rudofsky U: Collagen-induced rat platelet reactivity is enhanced in whole blood in both the presence and absence of dense granule secretion. *Thromb Res* 68: 345-356, 1992.
256. Magro A, Gilboa N, Rudofsky U: The fawn-hooded rat as a genetic hypertensive animal model. In Magro A, Osswald W, Reis D, Vanhoutte P (ed): *Central and Peripheral Mechanisms of Cardiovascular Regulation.*, 219-267. New York, Plenum, 1986.
257. Magro AM, Rudofsky UH: Plasma renin activity decrease precedes spontaneous focal glomerular sclerosis in aging rats. *Nephron* 31: 245-253, 1982.
258. Magro AM, Rudofsky UH, Gilboa N, Seegal R: Increased catecholamine output in the hypertensive fawn-hooded rat. *Lab Anim Sci* 36: 646-649, 1986.
259. Mahomed FA: On the sphygmographic evidence of arteriocapillary fibrosis. *Trans Pathol Soc* 28: 394, 1877.
260. Malek AM, Gibbons GH, Dzau VJ, Izumo S: Fluid shear stress differentially modulates expression of genes encoding basic fibroblast growth factor and platelet-derived growth factor B chain in vascular endothelium. *J Clin Invest* 92: 2013-2021, 1993.
261. Mancini G, Carnonara AO, Hermans OF: Immunochemical quantitation of antigens by single radial immunodiffusion. *Immunochemistry* 2: 235-254, 1965.
262. Mann JFE, Luft FC: Hypertension-induced models of nephrosclerosis in the rat. In Gretz N, Strauch M (ed): *Experimental and Genetic Rat Models of Chronic Renal Failure*, 141-147. Basel, Karger, 1993.
263. Mario U Di, Bacci S, Morano S, Pugliese G, Pietravalle P, Andreani D, Morabito S, Simonetti B, Pierucci A: Selective decrement of anionic immunoglobulin clearance after induced renal hemodynamic changes in diabetic patients. *Am J Physiol* 262: F381-F388, 1992.
264. Marx M, Sterzel RB, Sorokin L: Renal matrix and adhesion in injury and inflammation. *Curr Opin Nephrol Hypertens* 2: 527-535, 1993.
265. Matsuyama M, Ogiu T, Kontani K, Yamada C, Kawai M, Hiai H, Nakamura T, Shimizu F, Toyokawa T, Kinoshita Y: Genetic regulation of the development of glomerular sclerotic lesions in the BUF/Mna rat. *Nephron* 54: 334-347, 1990.
266. Mauer SM, Steffes MW, Azar S, Sandberg SK, Brown DM: The effects of Goldblatt hypertension on development of the glomerular lesions of diabetes mellitus in the rat. *Diabetes* 27: 738-744, 1978.
267. Maunsbach AB: The influence of different fixatives and fixation methods on the ultrastructure of rat kidney proximal tubule cells. I. Comparison of different perfusion fixation methods and of glutaraldehyde, formaldehyde and osmium tetroxide fixatives. *J Ultrastruct Res* 15: 242-282, 1966.
268. Maunsbach AB: The influence of different fixatives and fixation methods on the ultrastructure of the rat kidney proximal tubule cells. II. Effects of varying osmolality, ionic

strength, buffer system and fixative concentration of glutaraldehyde solutions. *J Ultrastruct Res* 15: 283-309, 1966.

269. Mayer G, Lafayette RA, Oliver J, Deen WM, Myers BD, Meyer TW: Effects of angiotensin II receptor blockade on remnant glomerular permselectivity. *Kidney Int* 43: 346-353, 1993.

270. McCrary RF, Pitts TJ, Puschett JB: Diabetic nephropathy: natural course, survivorship and treatment. *Am J Nephrol* 1: 206-218, 1981.

271. McGraw M, Poucell S, Sweet J, Baumal R: The significance of focal segmental glomerulosclerosis in oligomeganephronia. *Int J Pediatr Nephrol* 5: 67-72, 1984.

272. McGregor L: Histological changes in the renal glomerulus in essential (primary) hypertension. A study of fifty-one cases. *Am J Pathol* 6: 347-366, 1930.

273. McLachlan MSF, Guthrie JC, Anderson CK, Fulker MJ: Vascular and glomerular changes in the ageing kidney. *J Pathol* 121: 65-78, 1977.

274. Medlar EM, Blatherwick NR: The pathogenesis of dietary nephritis in the rat. *Am J Pathol* 13: 881, 1937.

275. Mehls O, Irzyniec T, Ritz E, Eden S, Kovacs G, Klaus G, Floege J, Mall G: Effects of rhGH and rhGF-1 on renal growth and morphology. *Kidney Int* 44: 1251-1258, 1993.

276. Meyer TW, Anderson S, Rennke HG, Brenner BM: Reversing glomerular hypertension stabilizes established glomerular injury. *Kidney Int* 31: 752-759, 1987.

277. Meyer TW, Lawrence WE, Brenner BM: Dietary protein and the progression of renal disease. *Kidney Int* 24: S243-S247, 1983.

278. Meyer TW, Rennke HG: Progressive glomerular injury after limited renal infarction in the rat. *Am J Physiol* 254: F856-F862, 1988.

279. Meyers BD: What is cyclosporine nephrotoxicity? *Transplant Proc* 21: 1430-1432, 1989.

280. Meyers BD, Deen WM, Robertson CR, Brenner BM: Dynamics of glomerular ultrafiltration in the rat. VIII. Effects of hematocrit. *Circ Res* 36: 425-435, 1975.

281. Meyers BD, Peterson C, Molina C, Tomlanovich SJ, Newton LD, Nitkin R, Sandler H, Murad F: Role of cardiac atria in the human renal response to changing plasma volume. *Am J Physiol* 254: F562-573, 1988.

282. Meyers KM, Hopkins G, Holmsen H, Benson K, Prieur DJ: Ultrastructure of resting and activated storage pool deficient platelets from animals with the Chediak-Higashi syndrome. *Am J Pathol* 106: 364-377, 1982.

283. Michel JB, Dussaule JC, Choudat L, al. et: Effects of antihypertensive treatment in one-clip, two kidney hypertension in rats. *Kidney Int* 29: 1011-1020, 1986.

284. Michels LD, Davidman M, Keane WF: The effects of chronic mesangial immune injury on glomerular function. *J Lab Clin Med* 96: 396-407, 1980.

285. Michels LD, Davidman M, Keane WF: Determinants of glomerular filtration and plasma flow in experimental diabetic rats. *J Lab Clin Med* 98: 869-885, 1981.
286. Michels LD, Davidman M, Keane WF: Glomerular permeability to neutral and anionic dextrans in experimental diabetes. *Kidney Int* 21: 699-705, 1982.
287. Miller PL, Meyer TW: Effects of tissue preparation on glomerular volume and capillary structure in the rat. *Lab Invest* 63: 862-866, 1990.
288. Miller PL, Rennke HG, Meyer TW: Hypertension and progressive glomerular injury caused by focal glomerular ischemia. *Am J Physiol* 259: F239-F245, 1990.
289. Miller PL, Rennke HG, Meyer TW: Glomerular hypertrophy accelerates hypertensive glomerular injury in rats. *Am J Physiol* 261: F459-F465, 1991.
290. Moise TS, Smith AH: The effect of high protein diet on the kidneys. *Arch Pathol* 4: 530-542, 1927.
291. Molitoris BA: The potential role of ischemia in renal disease progression. *Kidney Int* 41: S21-S25, 1992.
292. Moore LC, Mason J: Tubuloglomerular feedback control of distal fluid delivery: effect of extracellular volume. *Am J Physiol* 250: F1024-F1032, 1986.
293. Morrison AB: Experimentally induced chronic renal insufficiency in the rat. *Lab Invest* 11: 321-332, 1962.
294. Morrison AB, Howard RM: The functional capacity of hypertrophied nephrons: effect of partial nephrectomy on the clearance of inulin and PAH in the rat. *J Exp Med* 123: 829-844, 1966.
295. Motulsky HJ, Ransnas LA: Fitting curves to data using nonlinear regression: a practical and nonmathematical review. *FASEB J* 1: 365-374, 1987.
296. Munger K, Baylis C: Sex differences in renal hemodynamics in rats. *Am J Physiol* 254: F223-F231, 1988.
297. Nadasdy T, Silva FG, Hogg RJ: Minimal change nephrotic syndrome-Focal sclerosing complex (including IgM nephropathy and diffuse mesangial hypercellularity). In Tisher C, Brenner B (ed): *Renal Pathology*, 330-389. Philadelphia, JB Lippincott Comp., 1994.
298. Nagata M, Kriz W: Glomerular damage after uninephrectomy in young rats. II. Mechanical stress on podocytes as a pathway to sclerosis. *Kidney Int* 42: 148-160, 1992.
299. Nagata M, Scharer K, Kriz W: Glomerular damage after uninephrectomy in young rats. I. Hypertrophy and distortion of tuft architecture. *Kidney Int* 42: 136-147, 1992.
300. Nakamura T, Ebihara I, Tomino Y, Koide H, Kikuchi K, Koiso K: Gene expression of growth-related proteins and ECM constituents in response to unilateral nephrectomy. *Am J Physiol* 262: F389-F396, 1992.
301. Nath KA, Chmielewski DH, Hostetter TH: Regulatory role of prostanoids in glomerular microcirculation of remnant nephrons. *Am J Physiol* 252: F829-F837, 1987.

302. Nemes Z, Dietz R, Mann JFE, Lueth JB, Gross F: Vasoconstriction and increased blood pressure in the development of accelerated vascular disease. *Virchows Arch [A]* 386: 161-73, 1980.
303. Neugarten J, Kozin A, Cook K: Effect of indomethacin on glomerular permselectivity and hemodynamics in nephrotoxic serum nephritis. *Kidney Int* 36: 51-56, 1989.
304. Neumann KH, Schurek HJ, Kellner C, Kuhn K, Acikens B: Effective hydraulic permeability of the glomerular capillary wall in rats after uninephrectomy. *Renal Physiol* 9: 270-278, 1986.
305. Neuringer JR, Anderson S, Brenner BM: The role of systemic and intraglomerular hypertension. In Mitch WE, Stein JH (ed): *The Progressive Nature of Renal Disease*, 2nd, 1-21. New York, Churchill Livingstone, 1992.
306. Neuringer JR, Brenner BM: Hemodynamic theory of progressive renal disease: a 10-year update in brief review. *Am J Kidney Dis* 22: 98-104, 1992.
307. Newburgh LH, Curtis AC: Introduction of renal injury in the white rat by the protein of the diet: dependence of the injury on the duration of feeding, and on the amount and kind of protein. *Arch Intern Med* 1928: 801-821, 1928.
308. Nicolson GL: A rapid method for determining the topological distribution of anionic sites on membrane surfaces. *J Supramol Struct* 1: 159-164, 1972.
309. Nyengaard JR: Number and dimensions of rat glomerular capillaries in normal development and after nephrectomy. *Kidney Int* 43: 1049-1057, 1993.
310. Nyengaard JR, Bendtsen TF: Glomerular number and size in relation to age, kidney weight, and body surface in normal man. *Anat Rec* 232: 194-201, 1992.
311. Ohishi K, Carmines PK, Inscho EW, Navar LG: EDRF-angiotensin II interactions in rat juxtamedullary afferent and efferent arterioles. *Am J Physiol* 263: F900-F906, 1992.
312. Oken DE: Does the ultrafiltration coefficient play a key role in regulating glomerular filtration in the rat. *Am J Physiol* 256: F505-F515, 1989.
313. Oliver JD, Simons JL, Troy JL, Provoost AP, Brenner BM, Deen WM: Glomerular hypertension reduces charge selectivity in fawn-hooded rats (abstract). *J Am Soc Nephrol* 3: 746, 1992.
314. Oliver JD III, Analysis of glomerular permselectivity in the rat using theoretical models of hindered transport [Health Sciences and Technology]. Massachusetts Institute of Technology, 1992.
315. Oliver JD III, Anderson S, Troy JL, Brenner BM, Deen WM: Determination of glomerular size-selectivity in the normal rat using Ficoll. *J Am Soc Nephrol* 3: 214-228, 1992.
316. Oliver JD III, Simons JL, Troy JL, Provoost AP, Brenner BM, Deen WM: Proteinuria and impaired glomerular permselectivity in uninephrectomized fawn-hooded rats. *Am J Physiol* submitted: , 1994.

317. Olivetti G, Giacomelli F, Wiener J: Morphometry of superficial glomeruli in acute hypertension in the rat. *Kidney Int* 27: 31-38, 1985.
318. Olson JL: The nephrotic syndrome. In Heptinstall R (ed): *Pathology of the Kidney*, 4th, 779-869. Boston, Little Brown, 1992.
319. Olson JL, Hostetter TH, Rennke HG, Brenner BM, Venkatachalam MA: Altered glomerular permselectivity and progressive sclerosis following extreme ablation of renal mass. *Kidney Int* 22: 112-126, 1982.
320. Olson JL, Wilson SK, Heptinstall RH: Relation of glomerular injury to preglomerular resistance in experimental hypertension. *Kidney Int* 29: 849-857, 1986.
321. Ong ACM, Fine LG: Loss of glomerular function and tubulointerstitial fibrosis: cause or effect? *Kidney Int* 45: 345-351, 1994.
322. Ono T, Kanatsu K, Doi T, Sekita K, Onoe C, Nagai H, Muso E, Yoshida H, Tamura T, Kawai C: Relationship of intraglomerular coagulation and platelet aggregation to glomerular sclerosis. *Nephron* 58: 429-436, 1991.
323. Overstreet DH, Kampov-Polevoy AB, Rezvani AH, Murrelle L: Saccharin intake predicts ethanol intake in genetically heterogenous rats as well as different rat strains. *Alcohol Clin Exp Res* 17: 366-369, 1993.
324. Overstreet DH, Rezvani AH, Janowsky DS: Genetic animal models of depression and ethanol preference provide support for cholinergic and serotonergic involvement in depression and alcoholism. *Biol Psychiatry* 31: 919-936, 1992.
325. Pappenheimer JR: Passage of molecules through capillary walls. *Physiol Rev* 33: 384-423, 1953.
326. Pappenheimer JR, Renkin EM, Borrero LM: Filtration, diffusion, and molecular sieving through peripheral capillary membranes. A contribution to the pore theory of capillary permeability. *Am J Physiol* 167: 13-46, 1951.
327. Parfrey PS, Hollomby DJ, Gilmore NJ, Knaack J, Schur PH, Guttmann RD: Glomerular sclerosis in a renal isograft and identical twin donor: a family study. *Transplantation* 38: 343-346, 1984.
328. Pelayo JC, Quan AH, Shanley PF: Angiotensin II control of the renal microcirculation in rats with reduced renal mass. *Am J Physiol* 258: F414-F422, 1990.
329. Pelayo JC, Westcott JY: Impaired autoregulation of glomerular capillary hydrostatic pressure in the rat remnant nephron. *J Clin Invest* 88: 101-105, 1991.
330. Persson AEG, Bianchi G, Boberg U: Tubuloglomerular feedback in hypertensive rats of the Milan strain. *Acta Physiol Scand* 123: 139-146, 1985.
331. Persson AEG, Gushwa LC, Blantz RC: Feedback pressure-flow responses in normal and angiotensin-blocked rats. *Am J Physiol* 247: F925-F931, 1984.
332. Peterson C, Madsen B, Perlman A, Chan AYM, Meyers BD: Atrial natriuretic peptide and the renal response to hypovolemia in nephrotic humans. *Kidney Int* 34: 825-831, 1988.

333. Pickering TG, Laragh JH: Renovascular hypertension. In Brenner B, Rector F (ed): *The Kidney*, 1940-1967. Philadelphia, WB Saunders Comp, 1991.
334. Pinto J, Lacerda G, Cameron JS, Turner DR, Bewick M, Ogg SG: Recurrence of focal segmental glomerulosclerosis in renal allografts. *Transplantation* 32: 83-89, 1981.
335. Platt R, Roscoe MH, Smith FW: Experimental renal failure. *Clin Sci* 11: 217-231, 1952.
336. Press WH, Flannery BP, Teukolsky SA, Vetterling WT: *Numerical Recipes: The Art of Scientific Computing*. New York, Cambridge University Press, 1986.
337. Prieur DJ, Meyers KM: Genetics of the fawn-hooded rat strain. *J Hered* 75: 349-352, 1984.
338. Provoost AP: Spontaneous glomerulosclerosis: insights from the fawn-hooded rat. *Kidney Int* 45: S2-S5, 1994.
339. Provoost AP, Baudoin P, Keijzer MH De, Aken M Van, Molenaar JC: The role of nephron loss in the progression of renal failure: Experimental evidence. *Am J Kidney Dis* 5(Suppl 1): 27-32, 1991.
340. Provoost AP, Keijzer MH DE: Kidney function and volume homeostasis during the development of hypertension in the fawn-hooded rat. In Nijkamp FP, Wied D De (ed): *Hypertension, Brain Catecholamines and Peptides*, 45-50. Amsterdam, Elsevier Science Publishers B.V. (Biomedical Division), 1989.
341. Provoost AP, Keijzer MH De: The fawn-hooded rat: a model for chronic renal failure. In Gretz N, Strauch M (ed): *Experimental and genetic rat models of chronic renal failure*, 100-114. Basel, Karger, 1993.
342. Provoost AP, Keijzer MH De, Molenaar JC: Effect of protein intake on life long changes in renal function of rats unilaterally nephrectomized at young age. *J Lab Clin Med* 114: 19-26, 1989.
343. Provoost AP, Keijzer MH De, Wolff ED, Molenaar JC: Development of renal function in the rat. The measurement of GFR and ERPF and correlation to body and kidney weight. *Renal Physiol* 6: 1-9, 1983.
344. Provoost AP, Molenaar JC: Changes in the glomerular filtration rate after unilateral nephrectomy in rats. *Pflüger Arch* 385: 161-165, 1980.
345. Provoost AP, Sterk LT, Weening JJ: Chronic ACE-inhibition in hypertensive and proteinuric fawn-hooded (FHH) rats (abstract). *J Am Soc Nephrol* 4: 781, 1993.
346. Provoost AP, Verseput GH. Temporal dissociation of the antihypertensive and anti-proteinuric effects of ACE-inhibition in fawn-hooded (FHH) rats (abstract). *International Society of Nephrol.*, Jerusalem 1993.
347. Purkerson ML, Hoffsten PE, Klahr S: Pathogenesis of the glomerulopathy associated with renal infarction in rats. *Kidney Int* 9: 407-417, 1976.
348. Raij L: Nitric oxide and the kidney. *Circ (Suppl V)* 87: V26-V29, 1993.

349. Raij L, Azar S, Keane W: Mesangial immune injury, hypertension, and progressive glomerular damage in Dahl rats. *Kidney Int* 25: 137-143, 1984.
350. Raymond SL, Dodds WJ: Characterization of the fawn-hooded rat as a model for hemostatic studies. *Thrombos Diathes haemorrh.* (Stuttg.) 33: 361-369, 1975.
351. Rector FC, Andreucci VE, Herrera-Acosta J, Seldin DW: Potential sources of error in measuring single-nephron glomerular filtration rate. *Yale J Biol Med* 45: 193-199, 1972.
352. Remuzzi A, Battaglia C, Rossi L, Zoja C, Remuzzi G: Glomerular size selectivity in nephrotic rats exposed to diets with different protein content. *Am J Physiol* 253: F318-F327, 1987.
353. Remuzzi A, Brenner BM, Vittorino P, Tebaldi G, Mariano R, Belloro A, Remuzzi G: Three-dimensional reconstructed glomerular capillary network: blood flow distribution and local filtration. *Am J Physiol* 263: F562-F572, 1992.
354. Remuzzi A, Deen WM: Theoretical effects of a distribution of capillary dimensions on glomerular ultrafiltration. *Microvasc Res* 32: 131-144, 1986.
355. Remuzzi A, Deen WM: Theoretical effects of network structure on glomerular filtration of macromolecules. *Am J Physiol* 257: F152-F158, 1989.
356. Remuzzi A, Pergolizzi R, Mauer MS, Bertani T: Three-dimensional morphometric analysis of segmental glomerulosclerosis in the rat. *Kidney Int* 38: 851-856, 1990.
357. Remuzzi A, Perico N, Amuchastegui CS, Malanchini B, Mazerska M, Battaglia C, Bertani T, Remuzzi G: Short- and long-term effects of angiotensin II receptor blockade in rats with experimental diabetes. *J Am Soc Nephrol* 4: 40-49, 1993.
358. Remuzzi A, Puntorieri S, Battaglia C, Bertani T, Remuzzi G: Angiotensin converting enzyme inhibition ameliorates glomerular filtration of macromolecules and water and lessens glomerular injury in the rat. *J Clin Invest* 85: 541-549, 1990.
359. Remuzzi A, Puntorieri S, Mazzoleni A, Remuzzi G: Sex related differences in glomerular ultrafiltration and proteinuria in Munich-Wistar rats. *Kidney Int* 34: 481-486, 1988.
360. Remuzzi G, Bertani T: Is glomerulosclerosis a consequence of altered glomerular permeability to macromolecules? *Kidney Int* 38: 284-294, 1990.
361. Renkin EM: Filtration, diffusion, and molecular sieving through porous cellulose membranes. *J Gen Physiol* 38: 225-243, 1954.
362. Rennke HG: Structural alterations associated with glomerular hyperfiltration. In Mitch WE, Brenner BM, Stein JH (ed): *Contemporary issues in nephrology. The progressive nature of kidney disease.*, 1st, 111-131. New York, Churchill Livingstone Inc, 1986.
363. Rennke HG: How does glomerular epithelial cell injury contribute to progressive glomerular damage? *Kidney Int* 45: S58-S63, 1994.
364. Rennke HG, Anderson S, Brenner BM: The progression of renal disease: structural and functional correlations. In Tisher CC, Brenner BM (ed): *Renal Pathology*, 116-139. Philadelphia, JB Lippincott Comp., 1994.

365. Rennke HG, Klein PS: Pathogenesis and significance of nonprimary focal and segmental glomerulosclerosis. *Am J Kidney Dis* 13: 443-456, 1989.
366. Rennke HG, Patel Y, Venkatachalam MA: Glomerular filtration of proteins: Clearance of anionic, neutral, and cationic horseradish peroxidase in the rat. *Kidney Int* 13: 278-288, 1978.
367. Rennke HG, Venkatachalam MA: Glomerular permeability of macromolecules. Effect of molecular configuration on the fractional clearance of uncharged dextrans and neutral horseradish peroxidase in the rat. *J Clin Invest* 63: 713-717, 1979.
368. Rettig R, Folberth C, Strauss H, Kopf D, Waldherr R, Unger T: Role of the kidney in primary hypertension: a renal transplantation study in rats. *Am J Physiol* 258: F606-F611, 1990.
369. Rettig R, Strauss H, Folberth C, Ganten D, Waldherr R, Unger T: Hypertension transmitted by kidneys from stroke-prone spontaneously hypertensive rats. *Am J Physiol* 257: F197-F203, 1989.
370. Rezvani AH, Garges PL, Miller DB, Gordon CJ: Attenuation of alcohol consumption by MDMA (ecstasy) in two strains of alcohol-preferring rats. *Pharmacol Biochem Behav* 43: 103-110, 1992.
371. Rezvani AH, Overstreet DH, Janowsky DS: Drug-induced reductions in ethanol intake in alcohol preferring and fawn-hooded rats. *Alcohol Alcohol* 1: S433-S437, 1991.
372. Rich AR: A hitherto undescribed vulnerability of the juxtamedullary glomeruli in lipoid nephrosis. *Bull Johns Hopkins Hosp* 100: 173-186, 1957.
373. Riser BL, Cortes P, Zhao X, Bernstein J, Dumler F, Narins RG: Intraglomerular pressure and mesangial stretching stimulate extracellular matrix formation in the rat. *J Clin Invest* 90: 1932-1943, 1992.
374. Ritz E, Fliser D: Hypertension and the Kidney-An overview. *Am J Kidney Dis* 21: 3-9, 1993.
375. Robitalille P, Lortie L, Mongeau JG, Sinnassamy P: Long-term follow-up of patients who underwent unilateral nephrectomy in childhood. 1: 1297-1299, 1985.
376. Rojo-Ortega JM, Genest J: A method for production of experimental hypertension in rats. *Can J Physiol Pharmacol* 46: 883-885, 1968.
377. Rosen RM, Tolbert E, Dworkin LD: Development of glomerular hypertension with aging in spontaneously hypertensive rats (abstract). *J Am Soc Nephrol* 2: 689, 1991.
378. Rosenberg ME, Chmielewski D, Hostetter TH: Effect of dietary protein on rat renin and angiotensinogen gene expression. *J Clin Invest* 85: 1144-1149, 1990.
379. Rosenberg ME, Smith Lj, Correa-Rotter R, Hostetter TH: The paradox of the renin-angiotensin system in chronic renal disease. *Kidney Int* 45: 403-410, 1994.
380. Royer P, Habib R, Leclerc F: L'hypoplasie renale bilaterale avec oligomeganephronie. In Schreiner GE (ed): *Proceedings of the 3rd International Congress of Nephrology*, 251-275. Basel, Karger-Verlag, 1967.

381. Rudofsky UH, Magro AM: Spontaneous hypertension in fawn-hooded rats. *Lab Anim Sci* 32: 389-391, 1982.
382. Ruedin P, Mougnot B, Ruedin D, Rondeau E, Sraer JD, Lacave R, Kanfer A: Fibrin deposition and adaptive changes in glomerular procoagulant and fibrinolytic activities in rat renoprival nephropathy. *J Exp Path* 71: 269-278, 1990.
383. Ruoslahti E, Reed JC: Anchorage dependence, integrins, and apoptosis. *Cell* 77: 477-478, 1994.
384. Ryan GB, Karnovsky MJ: Ultrastructural study of the mechanisms of proteinuria in aminonucleoside nephrosis. *Kidney Int* 3: 219-232, 1975.
385. Rybak ME, Renzulli LA: A liposome based platelet substitute, the plateletsome, with hemostatic efficacy. *Biomater Artif Cells Immobilization Biotechnol* 21: 101-118, 1993.
386. Sakariassen KS, Bolhuis PA, Blomback M, Thorell L, Blomback B, Sixma JJ: DDAVP enhances platelet adherence and platelet aggregate growth on human artery subendothelium. *Blood* 64: 229-236, 1984.
387. Sakemi T, Baba N: Castration attenuates proteinuria and glomerular injury in unilaterally nephrectomized male Sprague-Dawley rats. *Lab Invest* 69: 51-57, 1993.
388. Salmond R, Seney FD: Reset tubuloglomerular feedback permits and sustains glomerular hyperfunction after extensive ablation. *Am J Physiol* 260: F395-F401, 1991.
389. Samani NJ, Lodwick D, Vincent M, Dubay C, Kaiser MA, Kelly MP, Lo M, Harris J, Sassard J, Lathrop M, Swales JD: A gene differentially expressed in the kidney of the spontaneously hypertensive rat cosegregates with increased blood pressure. *J Clin Invest* 92: 1099-1103, 1993.
390. Sato K, Tucker A, O'Brien RF, McMurtry IF, Stelzner TJ: The fawn hooded rat: a model of spontaneous pulmonary hypertension (abstract). *Am Rev Respir Dis* 139: 167, 1989.
391. Sato K, Webb S, Tucker A, Rabinovitch M: Factors influencing the idiopathic development of pulmonary hypertension in the fawn hooded rat. *Am Rev Respir Dis* 145: 793-797, 1992.
392. Savin VJ, Seaton RD, Richardson WP, Duncan KA, Beason-Griffin C, Ahnemann J: Dietary protein and glomerular response to subtotal nephrectomy in the rat. *J Lab Clin Med* 113: 41-49, 1989.
393. Saxton JA, Kimball JC: Relation of nephrosis and diseases of albino rats to age and to modifications of diet. *Arch Pathol* 32: 951, 1941.
394. Schechter MD, Meehan SM: Ethanol discrimination in fawn-hooded rats is compromised when compared to other strains. *Alcohol* 10: 77-81, 1993.
395. Schechter MD, Meehan SM, Gordon TL, McBurney DM: The NMDA receptor antagonist MK-801 produces ethanol-like discrimination in the rat. *Alcohol* 10: 197-201, 1993.

396. Schmitz PG, O'Donnell MP, Kasiske BL, Katz SA, Keane WF: Renal injury in obese Zucker rats: glomerular hemodynamic alterations and effects of enalapril. *Am J Physiol* 263: F496-F502, 1992.
397. Schwartz MM, Korbet SM: Primary focal segmental glomerulosclerosis: pathology, histological variants, and pathogenesis. *Am J Kidney Dis* 22: 874-883, 1993.
398. Schwietzer G, Gertz KH: Changes of hemodynamics and glomerular ultrafiltration in renal hypertension of rats. *Kidney Int* 15: 134-143, 1979.
399. Seien G, Muller-Suur R, Persson AE: Activation of the tubuloglomerular feedback mechanism in dehydrated rats. *Acta Physiol Scand* 117: 83-89, 1983.
400. Shannon JA, Jolliffe N, Smith HW: The excretion of urine in the dog. IV. The effect of maintenance diet, feeding, etc. upon the quantity of glomerular filtrate. *Am J Physiol* 101: 625-638, 1932.
401. Shimamura T, Morrison AB: A progressive glomerulosclerosis occurring in partial five-sixths nephrectomized rats. *Am J Pathol* 79: 95-106, 1975.
402. Shirley DG, Walter SJ: Acute and chronic changes in renal function following unilateral nephrectomy. *Kidney Int* 40: 62-68, 1991.
403. Simons JL, Provoost AP, Anderson S, Rennke HG, Troy JL, Brenner BM: Modulation of glomerular hypertension defines susceptibility to progressive glomerular injury. *Kidney Int* :in press, 1994.
404. Simons JL, Provoost AP, Anderson S, Troy JL, Rennke HG, Sandstrom DJ, Brenner BM: Pathogenesis of glomerular injury in the fawn-hooded rat: Early glomerular capillary hypertension predicts glomerular sclerosis. *J Am Soc Nephrol* 3: 1775-1782, 1993.
405. Simons JL, Provoost AP, Keijzer MH De, Anderson S, Rennke HG, Brenner BM: Pathogenesis of glomerular injury in the fawn-hooded rat: Effect of unilateral nephrectomy. *J Am Soc Nephrol* 4: 1362-1370, 1993.
406. Smith LJ, Rosenberg ME, Correa-Rotter R, Hostetter TH: The renin-angiotensin system in chronic renal disease. In Mitch W (ed): *The Progressive Nature of Renal Disease*, 2nd, 55-76. New York, Churchill Livingstone, 1992.
407. Spitzer A, Schwartz GJ: The kidney during development. In Windhager E (ed): *Handbook of Physiology. Section 8: Renal Physiology, Chapter 12.*, 475-544. Bethesda, American Physiological Society, 1992.
408. Steiner RW, Tucker BJ, Gushwa LC, Gifford J, Wilson CB, Blantz RC: Glomerular hemodynamics in moderate Goldblatt hypertension in the rat. *Hypertension* 4: 51-57, 1982.
409. Stelzner TJ, O'Brien RF, Yanagisawa M, Sakurai T, Sato K, Webb S, Zamora M, McMurtry IF, Fisher JH: Increased lung endothelin-1 production in rats with idiopathic pulmonary hypertension. *Am J Physiol* 262: L614-L620, 1992.
410. Sterzel RB, Luft FC, Gao Y, Schnermann J, Briggs JP, Ganten D, Waldherr R, Schnabel E, Kriz W: Renal disease and the development of hypertension in salt-sensitive rats. *Kidney Int* 33: 1119-1129, 1988.

411. Stewart RM, Gershon S, Baldessarini RJ, Tobach RJ, Krieger DT: Discordance of serotonin uptake in brain and platelets of the Fawn-Hooded rat: A model for Chediak-Hihashi syndrome. *Pharmacol Ther* 13: 219-247, 1981.
412. Stewart RJ, Marsden PA: Vascular endothelial cell activation in models of vascular and glomerular injury. *Kidney Int* 45(Suppl 45): S37-S44, 1994.
413. Striker GE, Nagle RB, Kohnen PW, Smuckler GA: Response to unilateral nephrectomy in old rats. *Arch Pathol* 87: 434-442, 1969.
414. Sweeney TK, Needleman P: Mechanisms underlying the defect in storage pool deficient platelets from fawn-hooded rats (abstract). *Fed Proc* 38: 419, 1979.
415. Tanaka R, Kon V, Yoshioka T, Ichikawa I, Fogo A: Angiotensin converting enzyme inhibition modulates glomerular function and structure by distinct mechanisms. *Kidney Int* 45: 537-543, 1994.
416. Thomas DM, Coles GA, Griffiths DFR, Williams JD: Permselectivity in thin membrane nephropathy. *J Clin Invest* 93: 1881-1884, 1994.
417. Tierney WM, Clement MJ, Luft FC: Renal disease in hypertensive adults: effect of race and type II diabetes mellitus. *Am J Kidney Dis* 13: 485-493, 1989.
418. Tischer CC, Alexander RW: Focal glomerular sclerosis. In Brenner B, Stein J (ed): *Contemporary issues in nephrology.*, 173-197. New York, Livingstone, 1982.
419. Tobach E, Santis JL De, Zucker MB: Platelet storage pool disease in hybrid rats. *J Hered* 75: 15-18, 1984.
420. Tolins JP, Raj L: Comparison of converting enzyme inhibitor and calcium channel blocker in hypertensive glomerular injury. *Hypertension* 16: 452-461, 1990.
421. Toynebee J: On the intimate structure of the human kidney and on the changes which its several components undergo in "Bright's disease". *Med Chir Trans* 29: 303, 1846.
422. Trachtman H, Futterweit S, Schwob N, Maesaka J, Valderrama E: Recombinant human growth hormone exacerbates chronic aminonucleoside nephropathy in rats. *Kidney Int* 44: 1281-1288, 1993.
423. Tschopp TB, Baumgartner HR: Defective platelet adhesion and aggregation on subendothelium exposed in vivo or in vitro to flowing blood of fawn-hooded rats with storage pool disease. *Thrombos Haemostas* 38: 620-629, 1977.
424. Tschopp TB, Weiss HJ: Decreased ATP, ADP and serotonin in young platelets of fawn-hooded rats with storage pool disease. *Thrombos Diathes haemorrh* 32: 670-677, 1974.
425. Tschopp TB, Zucker MB: Hereditary defect in platelet function in rats. *Blood* 40: 217-226, 1972.
426. Tufro-McReddie A, Arrizurieta EE, Brocca S, Gomez RA: Dietary protein modulates intrarenal distribution of renin and its mRNA during development. *Am J Physiol* 263: F427-F435, 1992.

427. Uchida K, Uchida S, Nitta K, Yumura W, Marumo F, Nihei H: Glomerular endothelial cells in culture express and secrete vascular endothelial growth factor. *Am J Physiol* 266: F81-F88, 1994.
428. Urizar RE, Cerda J, Dodds WJ, Raymond SL, Largent JA, Simon R, Gilboa N: Age-related renal, hematologic, and hemostatic abnormalities in FH/Wjd rats. *Am J Vet Res* 45: 1624-1631, 1984.
429. Vancura P, Miller WL, Little JW, Malt RA: Contribution of glomerular and tubular RNA synthesis to compensatory renal growth. *Am J Physiol* 219: 78-83, 1970.
430. Vanholder RC, Lambert PP, Lameire NH: PVP-sieving curves as an estimate of glomerular hemodynamics in HgCl₂ acute renal failure in the dog. *Circ Res* 61: 311-317, 1987.
431. Verniory A, Dubois R, DeCoodt P, Gasse JP, Lambert PP: Measurement of the permeability of biological membranes. Application to the glomerular wall. *J Gen Physiol* 62: 489-507, 1973.
432. Verseput GH, Provoost AP, Koomans HA: Reductions of proteinuria and systolic blood pressure (SBP) by lisinopril are temporarily dissociated in the fawn-hooded (FH) rat (abstract). *J Am Soc Nephrol* 4: 786, 1993.
433. Viets JW, Deen WM, Troy JL, Brenner BM: Determination of serum protein concentration in nanoliter blood samples using fluorescamine or o-phthalaldehyde. *Anal Biochem* 88: 513-521, 1978.
434. Vogel S: *Life's Devices: The Physical World of Animals and Plants*. (1st ed.) :1-367. Princeton, NJ, Princeton University Press, 1988.
435. Volhard F, Fahr T: *Die Brightsche Nierenkrankheit*. Berlin, Springer-Verlag, 1914.
436. Vurek GC, Pegram SE: Fluorometric method for the determination of nanogram quantities of inulin. *Anal Biochem* 16: 409-419, 1966.
437. Wainwright SA: *Axis and Circumference: The Cylindrical Shape of Plants and Animals*. (1st ed.) :1-132. ; vol 1) Cambridge, MA, Harvard University Press, 1988.
438. Walker AM, Bott P, Oliver J, MacDowell M: The collection and analysis of fluid from single nephrons of the mammalian kidney. *Am J Physiol* 134: 580-595, 1941.
439. Watanabe N, Kamei S, Ohkubo A, Yamanaka M, Ohsawa S, Makino K, Tokuda K: Urinary protein as measured with Pyrogallol Red Molybdate Complex. *Clin Chem* 32: 1551-1554, 1986.
440. Weening JJ, Beukers JJB, Grond J, Elema JD: Genetic factors in focal and segmental glomerulosclerosis. *Kidney Int* 29: 789-798, 1986.
441. Weening JJ, Rennke HG: Glomerular permeability and polyanion in Adriamycin nephrosis in the rat. *Kidney Int* 24: 152-159, 1983.
442. Weening JJ, Westenend PJ, Beukers JJB, Grond J: Experimental models of glomerulosclerosis. *Contrib Nephrol (Basel, Karger)* 77: 65-76, 1990.

443. Weening JJ, Westenend PJ, Nooyen YA, Brummelen P Van: Monotherapy with captopril (CAP) prevents progressive sclerosis (GS) in fawn-hooded rats, but ketanserin (K) is ineffective (abstract). *Kidney Int* 37: 523, 1990.
444. Weibel ER: Stereological principles for morphometry in electron microscopic cytology. *Int Rev Cytol* 26: 235-302, 1969.
445. Weibel ER: Practical Methods for Biological Morphometry. *Stereological Methods; vol 1*) London, Academic Press, 1979.
446. Weibel ER: Theoretical Foundations. *Stereological Methods; vol 2*) London, Academic Press, 1980.
447. Weibel ER, Elias H: Quantitative methods in morphology. Berlin, Springer, 1967.
448. Westenend PJ, Grond J, Weening JJ: Strain and species differences in experimental models of progressive glomerulosclerosis. In Gretz N, Strauch M (ed): *Experimental and genetic rat models of chronic renal failure*, 236-249. Karger, 1993.
449. Westenend PJ, Nooyen JA, Krogt JA Van Der, Brummelen P Van, Weening JJ: The effect of a converting enzyme inhibitor upon renal damage in spontaneously hypertensive fawn-hooded rats. *J Hypertens* 10: 417-422, 1992.
450. Westenend PJ, Nooyen JA, Krogt JA Van der, Brummelen P Van, Weening JJ: Functional and structural determinants of glomerulosclerosis in the fawn-hooded rat. *Eur J Clin Invest* 22: 391-395, 1992.
451. Westenend PJ, Nooyen YA, Brummelen P Van, Weening JJ: Intrinsic vasodilatation protects Wistar Kyoto rats from progressive glomerulosclerosis after unilateral nephrectomy. *J Lab Clin Med* 117: 25-32, 1991.
452. Wey H, Gallon L, Subbiah MTR: Prostaglandin synthesis in aorta and platelets of fawn-hooded rats with platelet storage pool disease and its response to cholesterol feeding. *Thromb Haemostas (Stuttgart)* 48: 94-97, 1982.
453. Whiteside CI, Cameron R, Munk S, Levy J: Podocyte cytoskeletal disaggregation and basement-membrane detachment in puromycin aminonucleoside nephrosis. *Am J Pathol* 142: 1641-1653, 1993.
454. Wiederhielm CA, Woodbury JW, Kirk S, Rushmer RF: Pulsatile pressures in the microcirculation of frog's mesentery. *Am J Physiol* 207: 173-176, 1964.
455. Williams JD, Coles GA: Proteinuria--A direct cause of renal morbidity? *Kidney Int* 45: 443-450, 1994.
456. Wilson C, Byrom FB: Renal changes in malignant hypertension: experimental evidence. *Lancet* 1: 136-139, 1939.
457. Woods LL: Mechanisms of renal hemodynamic regulation in response to protein feeding. *Kidney Int* 44: 659-675, 1993.
458. Yang CW, Striker LJ, Pesce C, Chen WY, Peten EP, Elliot S, Doi T, Kopchick JJ, Striker GE: Glomerulosclerosis and body growth are mediated by different portions of bovine growth hormone. *Lab Invest* 68: 62-70, 1993.

459. Yoshida Y, Kawamura T, Ikoma M, Fogo A, Ichikawa I: Effects of antihypertensive drugs on glomerular morphology. *Kidney Int* 36: 626-635, 1989.
460. Yoshioka T, Ichikawa I, Fogo A: Reactive oxygen metabolites cause massive, reversible proteinuria and glomerular sieving defect without apparent ultrastructural abnormality. *J Am Soc Nephrol* 2: 902-912, 1991.
461. Yoshioka T, Mitarai T, Kon V, Deen WM, Rennke HG, Ichikawa I: Role for angiotensin II in an overt functional proteinuria. *Kidney Int* 30: 538-545, 1986.
462. Yoshioka T, Rennke HG, Salant DJ, Deen WM, Ichikawa I: Role of abnormally high transmural pressure in the permselectivity defect of glomerular capillary wall: a study in early passive Heymann nephritis. *Circ Res* 61: 531-538, 1987.
463. Yoshioka T, Shiraga H, Yoshida Y, Fogo A, Glick AD, Deen WM, Hoyer JR, Ichikawa I: "Intact nephrons" as the primary origin of proteinuria in chronic renal disease: study in the rat model of subtotal nephrectomy. *J Clin Invest* 82: 1614-1623, 1988.
464. Zatz R, Dunn BR, Meyer TW, Anderson S, Rennke HG, Brenner BM: Prevention of diabetic glomerulopathy by pharmacological amelioration of glomerular capillary hypertension. *J Clin Invest* 77: 1925-1930, 1986.
465. Zatz R, Fujihara CK: Glomerular hypertrophy and progressive glomerulopathy. Is there a definite pathogenetic correlation? *Kidney Int* 45: S27-S29, 1994.
466. Zatz R, Meyer TW, Rennke HG, Brenner BM: Predominance of hemodynamic rather than metabolic factors in the pathogenesis of diabetic glomerulopathy. *Proc Natl Acad Sci USA* 82: 5963-5967, 1985.
467. Zeier M, Gretz N: The influence of gender on the progression of renal failure. In Gretz N, Strauch M (ed): *Experimental and Genetic Rat Models of Chronic Renal Failure*, 250-7. Basel, Karger, 1993.
468. Zoja C, Perico N, Remuzzi G: Antiplatelet agents: effects on the progressive renal disease. *Am J Kidney Dis* 17(Suppl 1): 98-102, 1991.
469. Zuchelli P, Cagnoli L, Casanova S, Donini U, Pasquali S: Focal glomerulosclerosis in patients with unilateral nephrectomy. *Kidney Int* 4: 649-655, 1983.
470. Zusman RM: Effects of converting-enzyme inhibitors on the renin-angiotensin-aldosterone, bradykinin, and arachidonic acid-prostaglandin systems: correlation with chemical structure and biologic activity. *Am J Kidney Dis* 10: 13-23, 1987.

DANKWOORD

Dank aan Prof. Dr. J.C. Molenaar voor het vertrouwen, de interesse, inspanning en tijd. Ik ben erg trots dat U mijn promotor bent. Ik hoop dat dit werk wellicht enige antwoorden bevat op de vragen die U mij stelde toen ik door U geïnterviewd werd in het voorjaar van 1990.

Dank aan Dr. A.P. Provoost. Bedankt Bram voor de bijzondere vriendschap, steun en hulp gedurende de laatste jaren. Nooit echt haast maar altijd alles af en ruim tijd. Het was een project waarin je me vrij liet zodat ik kon experimenteren naar harte lust. Je gaf de grenzen aan waar binnen dit kon geschieden, je was zo flexibel en gaf volop discussie. Je bent vele malen overgekomen naar de V.S. en moest vaak belangrijke aanpassingen in je drukke reis schema's maken om bij mij langs te kunnen komen. Ik hoop dat dit proefschrift een blijvende stimulus zal zijn. Ik ben dankbaar voor je vertrouwen en heb veel plezier gehad met jou en aan dit werk.

Dank aan Prof. Dr. M.A.D.H. Schalekamp voor de beoordeling van het manuscript en zitting te nemen als secretaris in de commissie.

Dank aan Prof. Dr. H.A. Koomans voor het beoordelen van het manuscript en zitting te nemen in de commissie. Ik ben blij dat het micropunctie-onderzoek in de fawnhooded rat in Utrecht voorgezet kon worden.

Dank aan Prof. Dr. J.J. Weening voor het beoordelen van het manuscript en zitting te nemen in de commissie. Ik ben dankbaar voor Uw steun en optimisme.

I am grateful to Dr. Barry M. Brenner. Dear Dr. Brenner, thank you for your friendship, hospitality, inspiration, contribution to the papers, and the support of the fawnhooded rat project. I hope we did learn something after all.

I am grateful to Julia L. Troy and all the technicians of Dr. Brenner's Laboratory for Kidney and Electrolyte Physiology. Dear Julia, thank you for the tremendous laboratory support.

I am grateful to Dr. Helmut G. Rennke and Debbie J. Sandstrom for all the morphometric work, the electron microscopic study, the friendship, discussions and for introducing me to the realm of pathology.

I am grateful to Dr. Sharon Anderson for teaching me the micropuncture skills and the optimal use of time, for the valuable contributions to the papers, the friendship and the numerous discussions.

I am grateful to Dr. Bill Deen and Dr. James D. Oliver III for the sieving studies, the generous support and friendship.

Dank aan de Nier Stichting Nederland voor de financiële ondersteuning van dit project.

Dank aan Dr. Wil Kort voor de gastvrijheid, vriendschap, en de adviezen voor de experimenten en de omgang met de proefdieren.

Dank aan Dr. Ries de Keijzer voor de ondersteuning aan het begin van de stage in het Laboratorium voor Chirurgie, en al het experimentele werk dat vooraf ging aan dit project.

Dank aan de medewerkers van het Laboratorium voor Chirurgie en het Centraal Proefdieren Bedrijf, met name Thijs van Aken, Ed Lansbergen en John Mahabier.

Dank aan de ratten. Zonder deze knaagdieren geen experiment. Ik hoop dat ik jullie niet nodeloos heb gepijnigd, en hoop jullie niet weer te ontmoeten, maar het blijft een zaak van het geheugen.

CURRICULUM VITAE

Jacob (Jaap) Levie Simons werd geboren op 21 december 1963 te Rotterdam. Hij volgde het voortgezet onderwijs aan het Rotterdamsch Lyceum, waar het eindexamen Atheneum B in juni 1983 werd behaald. De Universitaire opleiding werd begonnen in augustus 1983 met de studie Biologie aan de Landbouw Hogeschool te Wageningen. Het daarop volgende jaar werd van studie richting veranderd en begon hij met de studie Geneeskunde aan de Erasmus Universiteit Rotterdam. Gedurende het tweede en derde jaar van deze studie (1985-1987) was hij als student-assistent verbonden aan de afdeling Anatomie. Tijdens de studie werden verscheidene wetenschappelijke onderzoeken verricht aan de afdeling Algemene Heelkunde en het Laboratorium voor Chirurgie onder leiding van Dr. W.R. Schouten. Enkele maanden vóór het behalen van het artsexamen in januari 1991 startte hij het in dit proefschrift beschreven en door de Nier Stichting Nederland gesubsidiëerde onderzoek. Onder leiding van Dr. A.P. Provoost was hij als wetenschappelijk onderzoeker in dienst van het Instituut Kinderheelkunde (Hoofd, Prof. Dr. J.C. Molenaar) werkzaam in het Laboratorium voor Chirurgie. Als research-fellow in medicine voerde hij het micropunctie-onderzoek vanaf eind januari 1991 uit in het Laboratory for Kidney and Electrolyte Physiology in het Brigham and Women's Hospital te Boston, Massachusetts, onder supervisie van Prof. Dr. B.M. Brenner, Dr. S. Anderson en J.L. Troy. Histologische, stereologische en ultrastructurele studies van de glomeruli werden verricht door en in samenwerking met Prof. Dr. H.G. Renke en D.J. Sandstrom van de afdeling Pathologie van dit ziekenhuis. Met Prof. Dr. W.M. Deen en Dr. J.D. Oliver III verbonden aan het Massachusetts Institute of Technology te Boston werden de studies verricht naar de glomerulaire permselectiviteit voor macromoleculen. De experimenten werd afgerond in april 1992. Van juli 1992 tot juni 1993 werkte hij als arts-assistent Algemene Heelkunde aan de State University of New York te Stony Brook, New York. Na dit klinische jaar werd op 1 oktober 1993 de basis opleiding Pathologie gestart aan de Vanderbilt University Medical Center en Medical School te Nashville, Tennessee.

